Influence of mixing and curing conditions on the characteristics and durability of soils stabilised by deep mixing

Antoine Guimond-Barrett

Thèse de Doctorat

en vue de l'obtention du titre de

Docteur de l'Université du Havre

Spécialité : Génie Civil

présentée par

Antoine Guimond-Barrett

Ecole Doctorale SPMII: Sciences Physiques, Mathématiques et de l'Information pour l'Ingénieur

Influence of mixing and curing conditions on the characteristics and durability of soils stabilised by deep mixing

Yu-Jun CUI	*Rapporteur*
Hussein MROUEH	*Rapporteur*
Abir AL-TABBAA	*Examinatrice*
Sabine DARSON-BALLEUR	*Examinatrice*
Nicolas DENIES	*Examinateur*
Alain LE KOUBY	*Examinateur*
Anne PANTET	*Directrice de thèse*
Philippe REIFFSTECK	*Directeur de thèse*
Jean-François MOSSER	*Invité*

Date de soutenance: 19-09-2013

Remerciements

Je voudrais tout d'abord remercier M. Hussein MROUEH et M. Yu-Jun CUI de m'avoir fait l'honneur d'accepter d'évaluer ce travail de thèse en tant que rapporteurs.

Je remercie également Mme Abir AL-TABBAA et M. Nicolas DENIES d'avoir accepté de participer au jury de thèse en tant qu'examinateurs.

Je tiens à adresser mes sincères remerciements à Mme Anne PANTET et M. Philippe REIFFSTECK, directeurs de cette thèse, pour leur immense soutien, leur encadrement, leur disponibilité, leurs conseils. Je remercie également M. Alain LE KOUBY de son suivi continu tout au long de ce doctorat.

Ce travail est le fruit d'une étroite collaboration entre l'Ifsttar et Soletanche Bachy dans le cadre du projet de recherche Rufex. Je tiens à remercier tout particulièrement Mme Sabine DARSON-BALLEUR et M. Jean-Fançois MOSSER pour leur suivi, leur soutien, leur aide et leurs conseils pendant toute la durée de ce projet qui ont grandement contribué à améliorer ce travail.

Je voudrais également remercier l'ensemble des partenaires de Rufex pour leurs commentaires pertinents et constructifs lors des réunions de projet.

Au sein de l'Ifsttar, je tiens à remercier M. Franck GUIRADO, Mme Sonia FANELLI et M. Jean-Louis TACITA pour leur participation à la réalisation des essais en laboratoire et sur le terrain. Je remercie Mme Myriam DUC et Mme Aurélie MALOULA pour leur contribution à la partie microstructure de ce travail. Je remercie également M. Christophe CHEVALIER et M. Sébastien BURLON.

Je tiens à saluer les autres doctorant(e)s de l'Ifsttar avec qui j'ai partagé trois années intenses: Chi-Wei CHEN, Jerôme CHRISTIN, Iman HAGHIGHI, Elodie NAULEAU, Mamadou NGOM et Fabien SZYMKIEWICZ. Merci à tous !

Enfin, je ne pourrais pas finir ces remerciements sans penser à Mathilde, mes parents et ma sœur pour leur présence, leur patience et leurs encouragements qui m'ont permis de passer ces trois années dans le bonheur et la bonne humeur !

Abstract

Deep mixing is a ground improvement technique used in various offshore and on-land applications. In this method, soils are mechanically mixed in situ with a hydraulic binder using specifically designed mixing tools. Although deep mixing is used as an economical alternative with a minimum environmental impact in many projects compared to other types of foundations, the uncertainties regarding the characteristics of the soil-cement materials ("soil-mix materials") frequently limit the application of the process. Indeed, the mechanical properties (essentially compressive strength and stiffness) of soils stabilised by deep mixing are still poorly understood and particularly difficult to control. Many factors influence the characteristics of treated soils. These factors are essentially related to the type and amount of binder, the soil conditions (soil type, moisture content), the mixing conditions and the curing conditions. The durability or long-term behaviour of soils stabilised with cement is also an important concern for the design of permanent deep mixing structures.

The aim of this research, part of the French RUFEX research project, is to reach a better understanding of the properties of soil-mix materials produced in situ by wet deep mixing. Two main objectives are defined. The first objective is to evaluate and compare the strength and deformation characteristics of soils treated in the laboratory and in situ. Different soils were mixed with cement in the laboratory and tested. Additionally, the characteristics of soils treated in situ were determined on specimens taken from four different test sites where soil-cement columns were installed by Soletanche Bachy. The second objective is to analyse potential factors impacting the durability of treated soils. The presence of potential deleterious chemical compounds (calcium sulfate, sodium chloride and diesel) and the effects of drying are the two potential degradation mechanisms studied in order to assess the durability of cement-mixed soils.

Despite relatively large scatter, the results from this study highlight distinctive trends in terms of relations between strength (compressive and tensile) and stiffness (static and dynamic) which are specific to soil-mix materials. The effects of different mixing and curing conditions on the characteristics of treated soils are identified. The data gathered in this research shows that it is possible to define a standardised framework for the assessment of the durability of soils stabilised by deep mixing based on potential durability indicators. The direct correlation between potential indicators and controllable factors (such as binder and water contents) point to the possibility of optimising the durability related properties of soil-mix materials within the boundaries imposed by the soil conditions on site. Potential durability classes based on porosity accessible to water are proposed to compare different soil-cement mixtures.

Keywords: deep mixing; soil treatment; cement; strength; stiffness; durability.

Résumé

Le deep mixing est une technique d'amélioration de sols utilisée dans diverses applications sur terre et en mer. La méthode consiste à mélanger mécaniquement les sols en place avec un liant hydraulique à l'aide d'outils de malaxage spécifiques. Dans de nombreux projets, le deep mixing est utilisé comme une alternative économique avec un impact minimal sur l'environnement comparée à d'autres solutions de fondations. Cependant, les incertitudes concernant les caractéristiques des matériaux produits ("matériaux soil-mix") pénalisent fortement le procédé. En effet, les propriétés mécaniques (en particulier la résistance à la compression et le module de déformation) des sols traités par deep mixing sont encore mal connues et particulièrement difficiles à contrôler. De nombreux facteurs influencent les caractéristiques des sols traités. Ces facteurs sont essentiellement liés à la nature et à la quantité de liant, aux caractéristiques du sol (type de sol, la teneur en eau), aux conditions de mélange et aux conditions de cure. La durabilité ou le comportement à long-terme des sols traités avec du ciment est également une préoccupation importante pour la conception d'ouvrages permanents.

Les principaux objectifs de ce travail, qui s'intègre dans le projet de recherche RUFEX, sont de parvenir à une meilleure connaissance des propriétés mécaniques des matériaux sol-ciment produits in situ par deep mixing. Deux axes principaux sont définis. Le premier objectif est de comparer les caractéristiques de résistance et de déformation des sols traités en laboratoire et in situ. Différents sols ont été mélangés avec du ciment en laboratoire. Les caractéristiques de sols traités in situ ont été déterminées sur des éprouvettes prélevées sur quatre sites expérimentaux où des colonnes de sol-ciment ont été installées par Soletanche Bachy. Le second objectif est d'évaluer l'impact de certains facteurs susceptibles d'influer sur la durabilité des sols traités. La présence de composés chimiques potentiellement perturbateurs (sulfate de calcium, chlorure de sodium et diesel) et les effets du séchage sont les deux mécanismes de dégradation potentiels étudiés afin d'évaluer la durabilité des sols traités.

Malgré une certaine dispersion, les résultats de cette étude mettent clairement en évidence des relations entre la résistance (en compression et en traction) et la rigidité (modules statique et dynamique) spécifiques aux matériaux soil-mix. Les effets de différentes conditions de mélange et de cure sur les caractéristiques des sols traités sont identifiés. Les données accumulées dans cette recherche montrent qu'il est possible de définir, à partir de différents indicateurs, un cadre général pour l'évaluation de la durabilité des sols traités par deep mixing. La corrélation directe entre certains indicateurs potentiels et les paramètres de mise en oeuvre (tels que le dosage en ciment et la teneur en eau) suggère qu'il est possible d'optimiser les propriétés des matériaux soil-mix dans les limites imposées par les conditions géologiques du site. Des classes de durabilité potentielle basées sur la porosité accessible à l'eau sont proposées pour comparer différents mélanges sol-ciment.

Mots clés: deep mixing; traitement de sol; ciment; résistance; rigidité; durabilité.

Table of contents

Nomenclature

C	cement content (% and kg/m^3)
c	cohesion (kPa)
Cu	Undrained shear strength (kPa)
C/W	cement-water ratio
E_0	dynamic modulus (MPa)
$E_{0,t}$	dynamic modulus at curing time t (MPa)
E_{50}	static secant deformation modulus at 50% of maximum stress (MPa)
F_s	safety factor
$f_{c,d}$	strength used for the design
f_p	resonant frequency for compression waves (Hz)
f_s	resonant frequency for shear waves (Hz)
G_0	small strain shear modulus (MPa)
$G_{0,t}$	small strain shear modulus at curing time t (MPa)
i	hydraulic gradient
k	permeability (m/s)
k_7	empirical parameter used to predict the shear modulus growth based on 7-day data
L	length (m)
M	number of mixing blades
N_d	rotation speed of the mixing tool during penetration (rev/min)
N_u	rotation speed of the mixing tool during retrieval (rev/min)
PI	plasticity index (%)
pl*	Menard pressuremeter limit pressure (MPa)
q_7	empirical parameter used to predict modulus growth based on 7-day data
q_{28}	empirical parameter used to predict modulus growth based on 28-day data
q_d	dynamic penetration resistance (MPa)
q_{it}	indirect tensile strength (MPa)
q_u	unconfined compressive strength (MPa)
$q_{u,t}$	unconfined compressive strength at curing time t (MPa)
s_7	empirical parameter used to predict strength growth based on 7-day data
s_{28}	empirical parameter used to predict strength growth based on 28-day data
T	blade rotation number (rotation/m)
t	curing time (days) or travel time (s)
V	wave velocity (m/s)
V_d	penetration velocity (m/min)
V_p	compression wave velocity (m/s)
V_s	shear wave velocity (m/s)
V_u	speed during withdrawal (m/min)
w	moisture content (%)
w_L	liquid limit (%)
α	empirical parameter used to calculate the design strength
β	empirical factor used to predict strength and modulus growth
ϕ	angle of friction (rad/°)
ν	Poisson's ratio
τ_0	yield stress (Pa)
η	viscosity (Pa.s)
ρ	density (kg/m^3)

General Introduction

The foundations of many old railway lines in Europe need to be reinforced as they no longer meet the requirements of modern traffic. Deterioration of the platform is often linked to insufficient drainage causing a reduction in the mechanical properties of the subgrade. Railway structures lying on damaged platforms may present problems such as reduced stability, settlements, and extensive vibrations (Eurosoilstab, 2002). In all these cases, remediation works most often involve increasing the stiffness of the subsoil.

Classic platform reinforcement works are time-consuming and require the temporary removal of the tracks with ensuing traffic interruptions. Moreover, these types of works are expensive and their production rates are low. Optimising track maintenance operations and reducing the impact on traffic is an important issue in railway network management.

Jet grouting, a ground improvement process in which high speed jets of grout are used to cut the soil and form columns or panels (Chu et al., 2009), has been tested to reinforce railway platforms while keeping the tracks and sleepers in place. This method has its advantages in terms of stiffness increase but has proved to be unsuitable due to the generation of significant amounts of spoil which pollute the ballast with cement.

There is currently no platform foundation reinforcement method compatible with the requirements of maintaining traffic (working under low catenaries without removing the tracks and with minimal impact on the ballast).

Deep mixing is a general term for a large number of techniques in which binding agents are dispersed within the soil either in powder (dry method) or slurry form (wet method) using specially designed mixing tools. The hydraulic binders are injected at low pressures and mechanically mixed with the soil thus limiting the volume of spoil. Hence, deep mixing could be used to reinforce the foundations of existing railway platforms.

The dry soil mixing method was tested in Scandinavia on many new railway construction projects in soft soils (Baker, 2000; Holm et al., 2002; Alen et al., 2005; Olsson et al., 2008). In the United Kingdom, the wet method was tested on an existing railway line (Konstantelias et al., 2002).
In France, the first field trial carried out to assess the effects of vertical soil-cement columns constructed with the wet soil mixing method was undertaken in the European research project Innotrack (INNOvative TRACK systems; Ekberg and Paulsson, 2010; Le Kouby et al., 2008). Field tests were conducted on an existing LGV railway in the Picardie region. Preliminary results from these tests were promising as they showed that the wet mixing method could meet the requirements for traffic maintenance.

Following Innotrack, the French RUFEX research project, launched in 2010, focuses on the reinforcement and re-use of existing railway track and building foundations by deep soil mixing. Its main objectives are to increase knowledge and understanding of the behaviour of such structures by working on both technological (tools and materials) and design aspects of wet deep soil mixing.
As part of RUFEX, the present experimental work focuses on the properties of the soil-cement materials ("soil-mix materials") produced in situ by deep mixing.

Originally, the primary application of deep mixing was ground improvement to enhance the stability and reduce the settlements of embankments on very soft cohesive soils. The objective was to produce stabilised soils that have higher strength, lower permeability and lower compressibility than the original soils. Nowadays, there is increasing interest in the use of this technique not only for soil stabilisation but also to construct temporary and permanent foundation/structural (load bearing) elements and excavation retaining walls (Denies et al., 2012a; Shao et al., 2005). The properties and types of soils encountered for these new applications of deep mixing differ greatly from those found in soft soil stabilisation projects. For this reason, the results from previous research may not necessarily apply to these new materials.
The scope of this research extends beyond the reinforcement of railway platforms. This study on the properties of deep-mixed soils covers general geotechnical works such as foundations and retaining walls.

The mechanical properties of soil-cement mixtures produced by deep mixing lie between those of soil and concrete. The parameters required for design vary depending on the projects and proposed applications. In general, strength but also reliable stiffness characteristics are essential as they significantly affect the distribution of loads between soil mixing elements and the surrounding soil, thus controlling the settlements. Stiffness values are the main input parameters in numerical analyses carried out to design soil mixing structures.
Many factors influence the strength and compressibility characteristics of treated soils. These factors are essentially related to the type and amount of binder, the soil conditions, the mixing conditions and the curing conditions. The engineering properties are highly variable and difficult to control.

Soils are stabilised in the laboratory to evaluate the effects of different binder contents, binder types and water/binder ratios on the mechanical properties of treated soils. Previous research carried out at IFSTTAR focused mainly on the mechanical properties of soils treated in the laboratory (Szymkiewicz, 2011). A large number of soils were mixed with different quantities of cement and water. The results provide interesting information regarding the influence of particle size distribution, clay content and dosage on the strength of soil-mix materials. However, the relation between field and laboratory properties remains unclear. The mixing conditions on site are different from laboratory procedures. The strength and deformation properties determined in situ may differ considerably from those measured on laboratory samples. In addition, the methods used to sample soils treated in situ may influence the results.

The durability or long-term behaviour of soils stabilised with cement is also an important concern for the design of permanent deep mixing structures. In the field, the cement hydration process and hardening of the material take place in various environmental conditions that may modify the effects of the binder. Depending on the application, treated soils may be subjected to different curing conditions which could considerably alter the mechanical properties.

Although deep mixing is often used as an economical alternative with a minimum environmental impact in many projects compared to other types of foundations, the uncertainties regarding the characteristics of the material often seriously penalise the process. These uncertainties are usually compensated by preliminary trials and conservative designs which ultimately (and often unnecessarily) increase the construction costs.

The aim of this research is to contribute to the reduction of some uncertainties regarding in situ soil-mix materials. The objectives are to:

- to reach a better understanding of the engineering properties required for design. The general approach followed consists in analysing the mechanical properties of different soils stabilised in the laboratory and to compare the results with the characteristics of soils treated in situ by deep mixing.
- to assess the impact of some potential degradation mechanisms on the durability of treated soils. Artificial soils treated in controlled laboratory conditions are preferred to field specimens of potentially variable characteristics to study factors related to durability.

Organisation of the thesis

The thesis is organised in five chapters.

The first chapter provides a non-exhaustive overview of previously published work on soil-mix materials. Firstly, the different techniques used to construct soil mixing elements are presented. The engineering parameters required for design and the methods used in practice to determine these parameters are outlined. Current knowledge of the engineering properties of soil-mix materials is reviewed and the factors affecting the characteristics of treated soils are examined. Finally, the durability of treated soils is addressed with emphasis on the long-term behaviour of existing structures and potential degradation mechanisms. Research needs are highlighted and precise objectives are defined.

The second chapter details the different materials, experimental techniques and experimental programs followed in this research. The characteristics of the soils and binders used in this study are given. The procedures used to prepare specimens of treated soils in the laboratory are explained. The sampling methods employed to obtain specimens of soils mixed in situ by deep mixing are described. The various laboratory testing procedures utilised to determine the properties of soil-mix materials are presented. The experimental programs followed to assess the properties and durability of soils treated in the laboratory are specified.

The results of tests carried out to evaluate the mechanical behaviour of soils mixed in the laboratory with cement are presented in the third chapter. The study is performed on soil-mix materials in the fresh state immediately after mixing and in the hardened state. Special attention is paid to the relations between strength and stiffness.

The properties of soils stabilised in the laboratory are compared with those of soils treated in situ in the fourth chapter. The soils mixed in situ were taken from test sites where soil-cement columns were installed by Soletanche Bachy. The effects of mixing conditions and sampling method are examined. The similarities and discrepancies between laboratory and field samples are highlighted. The results are discussed with respect to the design of soil mixing elements.

In the fifth chapter, the durability of soil-mix materials against different potential degradation mechanisms is assessed through tests performed on specimens treated in the laboratory. The long-term effects of these degradation mechanisms on the physical and mechanical properties are studied for curing times of up to 360 days.

The thesis closes on a general discussion on the possibility of optimising the durability-related properties of soil-mix materials. General conclusions are drawn in an attempt to provide useful recommendations for future deep mixing projects.

Chapter 1. The Deep Mixing Method – overview

1.1 Introduction

This chapter is a non-exhaustive overview of previously published work on the deep mixing method and soil-mix materials. The purpose of this review is to identifiy research needs in order to specify the objectives of this research. The chapter is organised in 3 main sections:

- In section 1.2, the different construction techniques, equipment and various applications of deep mixing are presented.
- The engineering properties and some factors affecting the characteristics of treated soils are examined in section 1.3.
- Finally, the durability of treated soils is addressed in section 1.4. Reported long-term behaviour of existing structures and potential degradation mechanisms are reviewed.

1.2 The Deep Mixing Method

1.2.1 Classification

Laboratory and field research started on deep mixing technology using dry and wet binders in the mid-1960s in Sweden at the Swedish Geotechnical Institute and in Japan at the Port and Harbour Research Institute. The aim of this research was to develop a new method to improve the properties of soft soils (Holm, 2000). The classification adopted by the Ground Improvement Technical Committee 211 of the International Society for Soil Mechanics and Geotechnical Engineering defines deep mixing as a ground improvement method with grouting type admixtures (Table 1-1 after Chu et al., 2009).

Ground improvement with grouting type admixtures	1. Particulate grouting	Grout granular soil or cavities or fissures in soil or rock by injecting cement or other particulate grouts to either increase the strength or reduce the permeability of soil or ground.
	2. Chemical grouting	Solutions of two or more chemicals react in soil pores to form a gel or a solid precipitate to either increase the strength or reduce the permeability of soil or ground.
	3. Mixing methods (including premixing or deep mixing)	**Treat the weak soil by mixing it with cement, lime, or other binders in-situ using a mixing machine or before placement**
	4. Jet grouting	High speed jets at depth erode the soil and inject grout to form columns or panels
	5. Compaction grouting	Very stiff, mortar-like grout is injected into discrete soil zones and remains in a homogeneous mass so as to densify loose soil or lift settled ground.
	6. Compensation grouting	Medium to high viscosity particulate suspension is injected into the ground between a subsurface excavation and a structure in order to negate or reduce settlement of the structure due to on-going excavation.

Table 1-1 Classification of ground improvement methods adopted by TC211, formerly TC 17 (Chu et al., 2009).

Several classification systems for the different technologies and equipments used in deep mixing have been proposed (FHWA, 2000; CDIT, 2002 and AFNOR, 2005). The classification by Topolnicki (2004) is based on three parameters (Figure 1-1):

- the form in which the binder is introduced into the soil (either wet or dry),
- the method used to mix the binder (by mechanical mixing with the tool, by high pressure injection (jet) or both (mechanical + jet),
- the location where mixing occurs (at the end or along the shaft).

The large number of techniques identified in Figure 1-1 can be explained in part by the necessity to adapt to local geological conditions and by the variety of projects and applications.

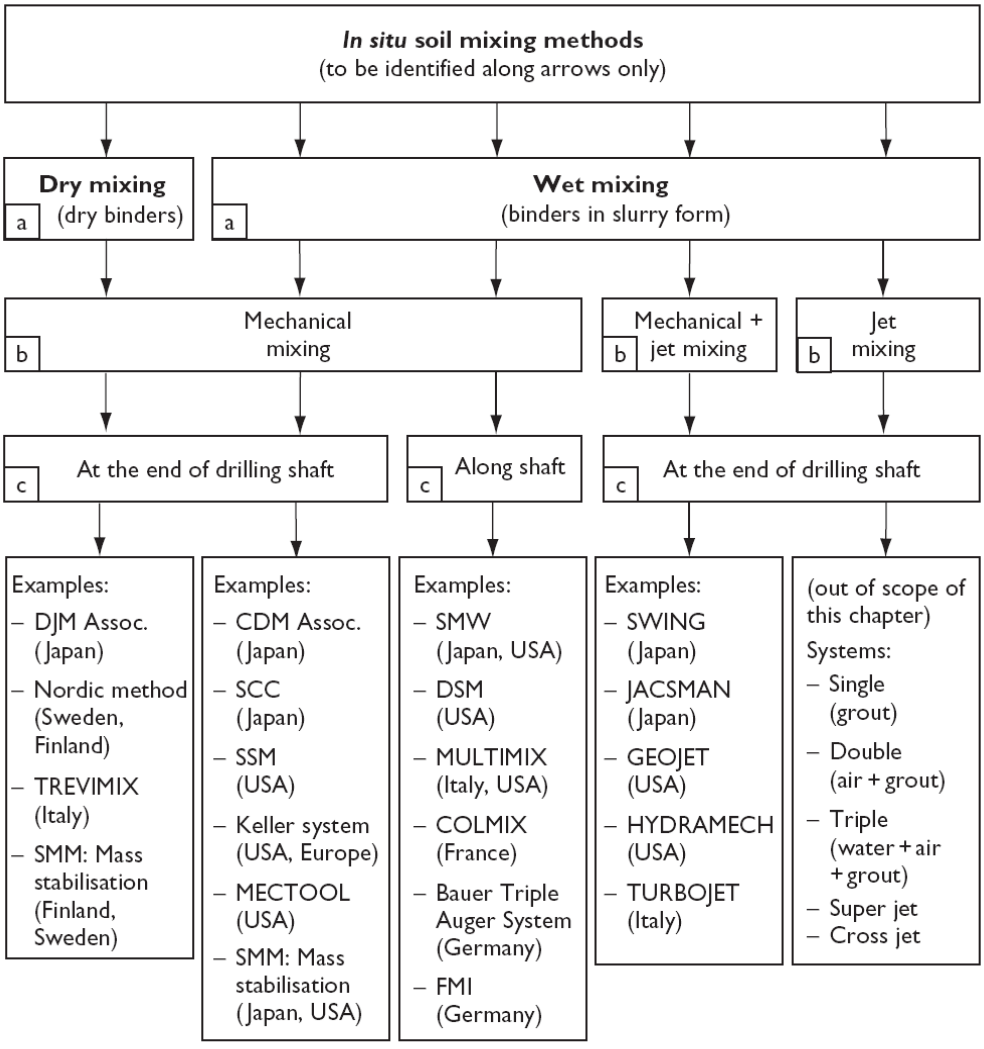

Figure 1-1 General classification of in situ soil mixing based on (a) binder form, (b) mixing principle and (c) location of mixing action, with selected examples of methods developed in various countries (Topolnicki, 2004).

The main differences between deep mixing and soil treatment for the construction of fills and capping layers are summarised in Table 1-2. No compaction is performed during the

construction of deep mixing elements; the soil-binder mixtures must be sufficiently fluid to be self-compacting.

	Deep mixing	Soil treatment for earthworks
Excavation	Mixing is performed in situ on intact soils, No previous excavation	Soil are excavated before treatment, Mixing is performed on remoulded soils
Depth	Mixing is carried out at depth	Mixing is carried out at the surface
Form of binder	Dry powder or slurry	Dry powder
Dosage	The quantities of binder used in deep mixing projects are generally higher than for fills and capping layers (usually more than 10 % by mass)	Usually between 1 and 7 % by mass
Compaction	No compaction is performed, the soil-binder mixtures must be sufficiently fluid to be self-compacting	Treatment is carried out on soils of relatively low moisture content to facilitate compaction

Table 1-2 Main differences between deep mixing and soil treatment for earthworks.

Currently, the majority of soil mixing works involve the construction of column-type elements. However, other techniques are used to construct blocks or panels. The following paragraphs describe the equipment and execution processes used in the main types of column-construction techniques. The equipment used to install blocks or panels are also briefly presented.

1.2.2 Equipment and execution

1.2.2.1 Dry mixing methods

For the dry mixing method, column construction usually starts by penetrating the mixing tool down to the target depth. The mixing tool is then lifted back up to the surface. The binder in powder form is injected during the withdrawal phase. The rotation of the mixing tool destructures the soil during penetration and mixes the soil and binder during withdrawal (Eurosoilstab, 2002).

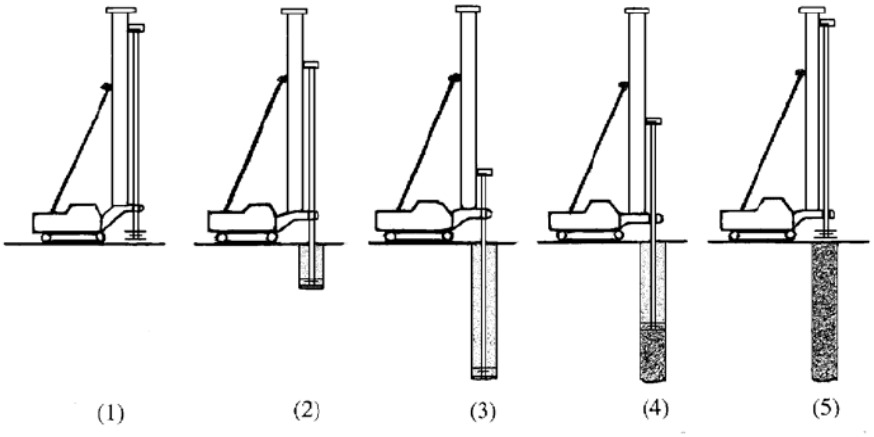

Figure 1-2 Execution process for the installation of soil mixing columns using the dry mixing method (AFNOR, 2005).

The two main dry mixing techniques are the Scandinavian method (lime-cement columns) and the Japanese method (Dry Jet Mixing).

1.2.2.1.1 Scandinavian method: lime-cement columns

Lime and lime-cement columns are commonly used in Scandinavia to stabilise clays and silts as well as organic soils (Broms, 2004). The mixing machines generally have only one mixing shaft. The Scandinavian dry mixing method is mostly carried out in soft to very soft soils with undrained shear strengths lower than approximately 50 kPa. Typical mixing tools are shown in Figure 1-3. The injection outlet hole is located on the central shaft above the lower mixing blades to allow mixing during the lifting of the tool (Topolnicki, 2004). Columns can be installed to depths of about 25 m. The diameter of the columns is typically between 0.6 and 1.0 m. Columns can be inclined at an angle of up to 70° (AFNOR, 2005). The tool rotation speeds and withdrawal rates vary depending on geological conditions and projects. The penetration speed is in general close to 2 to 3 m per minute. Withdrawal of the tool is often carried out at 15 to 25 mm per rotation with 150 to 180 rotations per minute (FHWA, 2000).

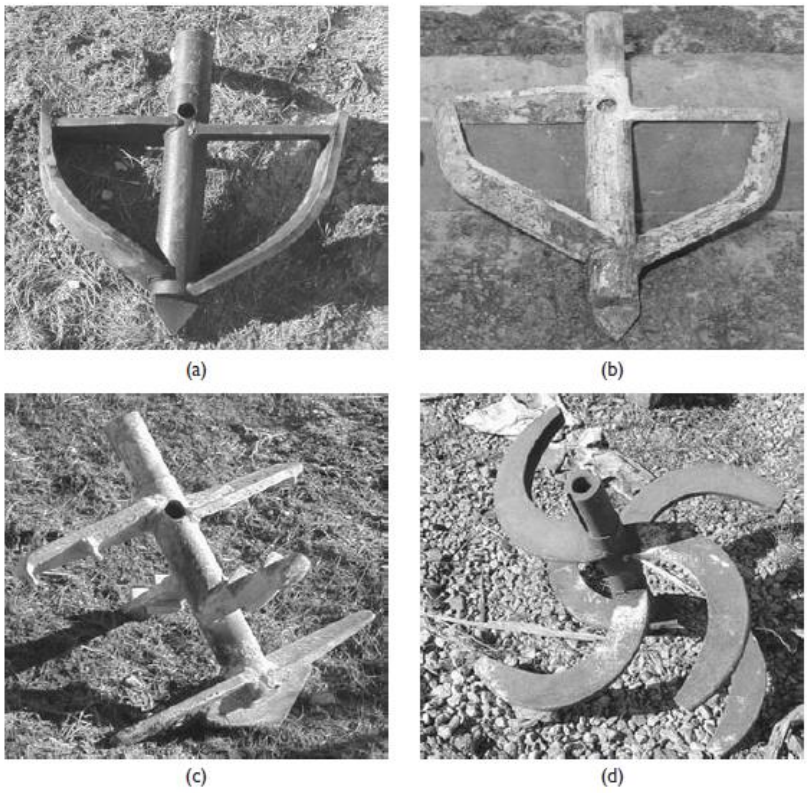

Figure 1-3 Typical mixing tools used for the Scandinavian dry mixing method (Topolnicki, 2004).

Initially, lime was the most frequently used binder. Currently, columns are constructed using mixtures of lime and cement (Åhnberg and Johansson, 2005). The mixing energy required for the production of a column depends on the types of soil and binder, and the amount of binder. It has been noticed that the use of cement requires more energy than mixing lime alone (AFNOR, 2005). Lime contents used to treat inorganic soft clays vary between 70 to 90 kg/m^3

(Broms, 2004). More generally, 80 to 150 kg of binder per cubic meter of soil are injected into the columns. The compressive strength of treated soils by the Scandinavian method is often between 0.2 and 0.5 MPa (FHWA, 2000).
Stabilised soil columns constructed by the Scandinavian method are semi-rigid. They interact with the surrounding untreated soil to form a composite system of improved ground (Holm, 1999). The permeability of the treated soils is often substantially greater than that of the initial clayey ground (Broms, 1999). Therefore the columns may also act as vertical drains.

1.2.2.1.2 Japanese method: Dry Jet Mixing (DJM)

In Japan, many techniques have been developed for the treatment of soils by the dry mixing method. The main technique is named Dry Jet Mixing (DJM). DJM rigs can be equipped with one or two shafts. The diameter of the mixing tools can reach up to 1 m. Stabilised soil columns may be installed down to depths of 16 to 33 m. The binder is injected during the withdrawal of the tool as in the Scandinavian method, but the injection can also be carried out during the penetration phase (AFNOR, 2005). The standard mixing tool is generally composed of two levels of horizontal blades (Figure 1-4). The binder outlet holes are located above and below these blades. DJM is used in soft clays with maximum shear strengths of 70 kPa and in sands with SPT blow counts below 15 (Terashi, 2003). The tool penetration speeds are typically between 1 and 1.5 m per minute. The uplift rate is usually slower from 0.7 to 0.9 m/min (Topolnicki, 2004). The rotational speed of the tool is relatively low between 24 and 32 rpm.

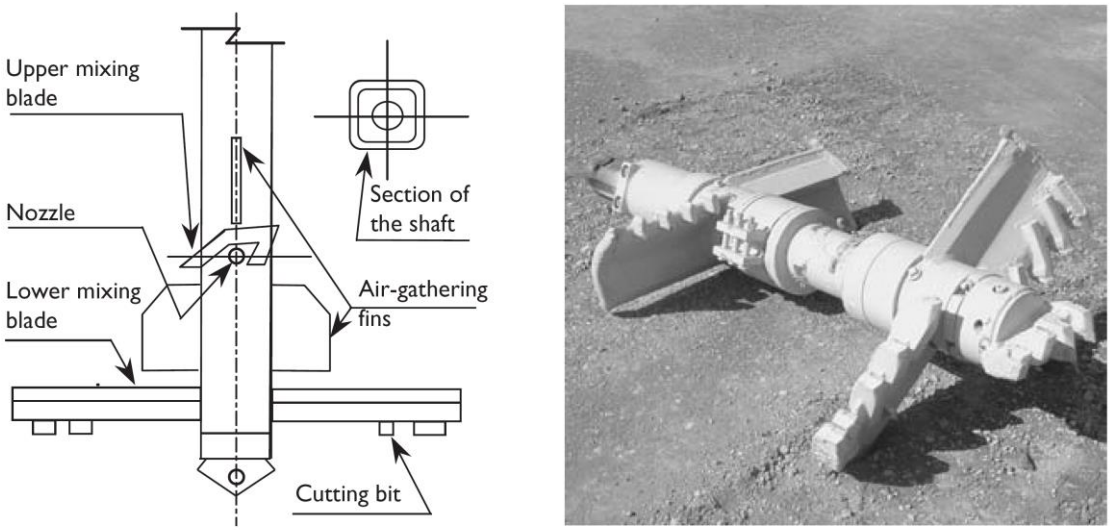

Figure 1-4 Typical mixing tool used for DJM (Topolnicki, 2004).

The binder used in DJM is mainly Portland cement (Porbaha, 1998) with dosages ranging from 100 to 400 kg/m^3 (Bruce et al., 1999). The compressive strengths of treated soils by the Japanese method greatly vary depending on soil type but are generally close to 1 MPa (FHWA, 2000).

1.2.2.1.3 Comparison

The following table summarises and compares the main features of Scandinavian and Japanese methods of dry soil mixing.

Larger diameter columns can be executed to greater depths with the DJM equipment. The amount of binder injected in the columns is higher for DJM. The column installation parameters (penetration, withdrawal and rotation speeds) are approximately 2 to 3 times faster for the Scandinavian technique. However, by combining these parameters, both methods have comparable uplift rates (in mm per rotation). Blade rotation numbers (tool rotations per meter of column) are similar for both techniques.

The main difference between the Scandinavian technique and the Japanese technique is related to the parameter which is assumed to be most important to control the mixing process. In the Scandinavian method, rotation speed of the tool is seen as the major controlling factor whereas for DJM, the (relatively slow) translational speed of the mixing tool is deemed to be most important in the mixing process.

	Scandinavian method	**Japanese method**
Number of columns	1	1 or 2
Diameter of mixing tool	0.4 m to 1.0 m	0.8 m to 1.3 m
Maximum depth of mixing	25 m	33 m
Position of binder outlet hole	Above mixing blades	Below mixing blades
Penetration rate	2.0 m/min to 6.0 m/min	1.0 m/min to 1.5 m/min
Withdrawal rate	1.5 m/min to 6.0 m/min	0.7 m/min to 0.9 m/min
Rotation speed of mixing blades	150 to 180 rpm	24 to 32 rpm
Blade rotation number	150 to 500 per m	$\geq$ 274 per m
Quantity of binder	180 to 150 kg/m^3	100 to 400 kg/m^3
Withdrawal rate per tool rotation	10 to 30 mm/rotation	10 to 35 mm/rotation
Binder Injection	Generally during withdrawal	Penetration and/or withdrawal

Table 1-3 Main features of the Scandinavian and Japanese methods of dry soil mixing (modified after AFNOR, 2005).

1.2.2.2 Wet mixing methods

In the wet mixing method, the hydraulic binder is mixed with water to form a slurry before it is injected into the soil. The slurry is delivered during penetration and/or withdrawal of the mixing tool. The hydraulic binder used is generally cement. The grouts are characterised by a cement-water ratio (C/W), i.e. the ratio between the mass of dry cement C and the mass of water W. The C/W ratio can be between 0.5 and 2.5, but it generally varies between 0.8 and 1.2 for most soil mixing techniques. The values of C/W are in general lower for the treatment of clays and silts than for sands and gravel because larger amounts of water are necessary to treat fine grained soils (FHWA, 2000). The addition of grout into soil normally causes the production of spoil which returns to the surface (Eurosoilstab, 2002).

1.2.2.2.1 Japanese method: Cement Deep Mixing (CDM)

In Japan, the wet soil mixing method is used both on land and offshore (CDIT, 2002). The main technique is called Cement Deep Mixing (CDM). On land, the machines are equipped with 1 to 4 shafts. The mixing tools consist of several levels of blades (Figure 1-5).

The diameter of the mixing tool is generally close to 1 m. Columns can be installed down to approximately 40 meters (Yano et al., 1996). The binder is usually cement (FHWA, 2000). Slurries have W/C ratios between 0.6 and 1.3 for binder contents between 70 and 300 kg per cubic meter of soil (Topolnicki, 2004). The tool penetration speed generally lies between 0.5 and 2 m per minute and the withdrawal speed between 1 and 2 m per minute. The compressive strengths obtained on soils treated by CDM are generally between 0.5 and 4 MPa (FHWA, 2000).

Figure 1-5 Equipment used for CDM (Topolnicki, 2004).

1.2.2.2.2 European methods

The binder used in European methods of deep mixing is generally cement. An example of a wet mixing method used in Europe is the CVR C-mix® from Belgium. The tool rotation speed is about 100 rpm. Depending on the soil conditions, the slurry (W/C ratios between 0.6 and 0.8) is injected to add approximately 350 and 450 kg of dry binder per cubic meter of soil. As in most wet mixing techniques, the binder partly (between 0 and 30 %) returns to the surface as spoil. The resulting columns have diameters between 0.43 and 1.03 m (Denies et al., 2012a). The strengths of soils treated with this method are relatively high, in general between 2 and 10 MPa (Ganne et al., 2010).

As mentioned in the introduction, the first field trial carried out to evaluate the effects of vertical soil-cement columns constructed using the wet soil mixing method to reinforce an existing railway platform was undertaken in the European research project Innotrack (INNOvative TRACK systems) (Ekberg and Paulsson, 2010; Le Kouby et al., 2008). Field tests were conducted on an existing LGV railway using a spreadable mixing tool named Springsol developed by Soletanche Bachy.

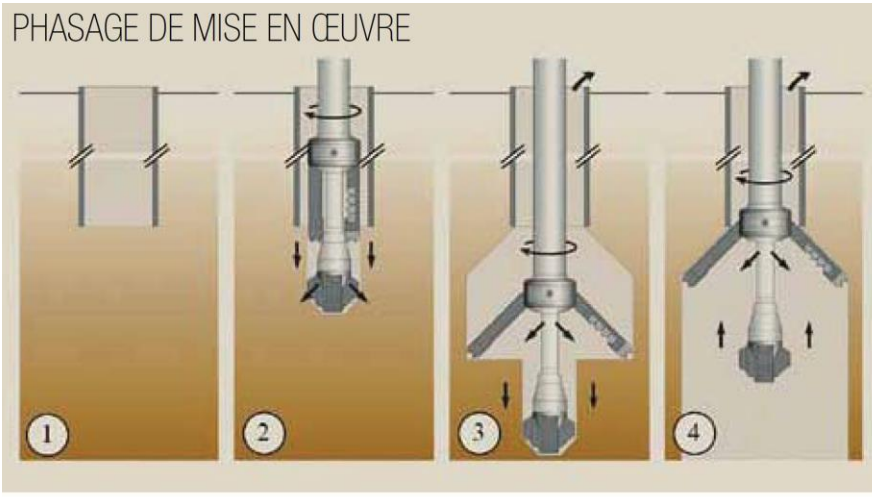

Figure 1-6 Installation procedure for columns using the Springsol tool developed by Soletanche Bachy (Mosser and Mathieu, 2011).

The installation procedure for columns constructed under existing tracks using the Springsol tool is as follows (Figure 1-6):

- a steel casing placed between the sleepers is driven through the ballast to the desired depth (n°1),
- the Springsol tool is lodged inside the casing (n°2). Once it reaches the end of the casing and penetrates the underlying soil, the blades spread out under the action of springs,
- the column is installed to the desired depth by mixing the soil with cement grout (n°3),
- finally, the steel casing is withdrawn (n°4).

The injected slurries have W/C ratios between 0.5 and 1.5. Tool rotation speeds are generally between 50 and 100 rpm. Typical compressive strengths of soils treated with the Springsol tool are between 2 and 8 MPa. The Springsol tool can also be used to construct columns near existing structures or under concrete slabs (Mosser and Mathieu, 2011).

1.2.2.2.3 Comparison

The following table summarises and compares the main features of European and Japanese methods of wet soil mixing for on land applications.

Soil mixing in Japan is used to install columns with large diameters to great depths. The amounts of binder injected in the columns are generally higher in Europe than in Japan. Consequently, the strength of the soil-mix material is also higher. The tool penetration speed is similar for both Japanese and European techniques. In contrast, the withdrawal rate and tool rotation speed are superior in European methods. The approach used in Japan for wet mixing is similar to the method described for DJM: mixing is carried out by slowly withdrawing the mixing tool with low rotation speeds.

	Europe	Japan
Number of columns	1 to 3	1 to 4
Diameter of mixing tool	0.4 m to 0.9 m	1.0 m to 1.6 m
Maximum depth of mixing	25 m	48 m
Position of binder outlet hole	shaft	shaft and blades
Injection pressure	500 kPa to 1 000 kPa	300 kPa to 600 kPa
Penetration rate	0.5 m/min to 1.5 m/min	0.5 to 2.0 m/min.
Withdrawal rate	3.0 m/min to 5.0 m/min	1.0 m/min to 2.0 m/min
Rotation speed of mixing blades	50 to 100 rpm	20 to 40 rpm
Blade rotation number	Often continuous mixing along shaft	350 per metre
Quantity of binder	80 to 450 kg/m^3	70 to 300 kg/m^3
Binder Injection	Penetration and/or withdrawal	Penetration and/or withdrawal

Table 1-4 Main features of the European and Japanese methods of wet soil mixing (modified after AFNOR, 2005).

1.2.2.3 Other methods

Many other techniques of treatment by soil mixing exist and can be used to construct blocks and panels or stabilise large volumes of soil. The main techniques include shallow mass treatment, Cutter Soil Mixing and Trenchmix. These methods are briefly described in the following paragraphs.

1.2.2.3.1 Shallow soil mixing – mass treatment

General mass treatment is used in very unfavourable geological conditions with soils of very low strength, for example in the case of peats and soft organic clay deposits. The machines used for mass stabilisation by soil mixing are in general conventional excavators equipped with specially designed mixing tools (Figure 1-7). The binder is injected while the mixing tool rotates and simultaneously moves vertically and horizontally. Mass stabilisation can also be carried out by constructing overlapping columns (Eurosoilstab, 2002). Mass treatment is generally limited to shallow depths between 2 and 3 m (maximum depth of 5 m) (AFNOR, 2005).

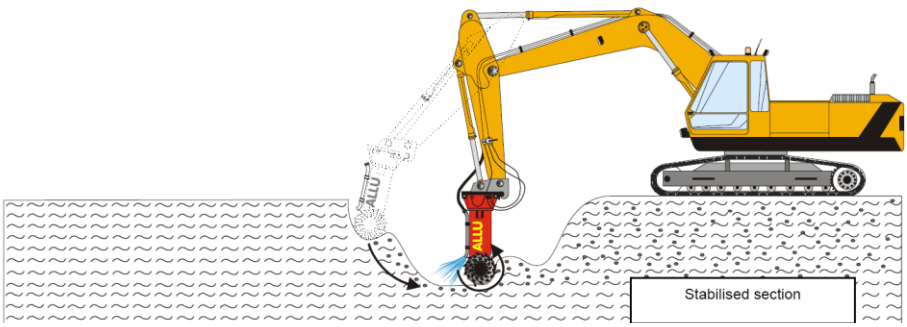

Figure 1-7 Equipment used for mass stabilisation (Eurosoilstab, 2002).

1.2.2.3.2 Cutter Soil Mixing

Cutter soil mixing is based on the technique used to construct diaphragm walls (hydrofraise). It enables the construction of rectangular soil mixing panels. The mixing tools are cutter head wheels with vertical cutting teeth. The construction principle is shown in Figure 1-8. First, the tool penetrates the soil to the target depth with outward rotation of the drums and injection of a drilling fluid. Once the target depth is reached, the drum rotation is reversed. The tool is withdrawn as cement grout is continuously injected (Lebon, 2005).

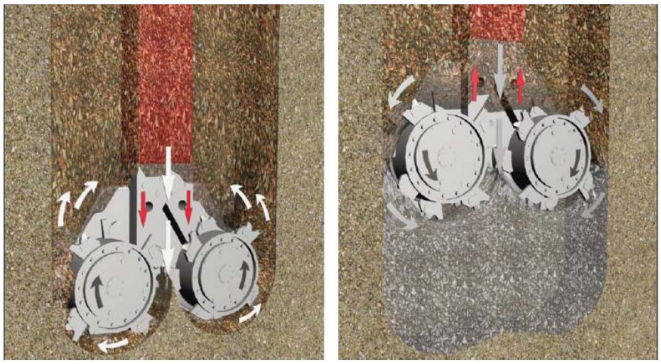

Figure 1-8 Construction process for cutter soil mixing (Benhamou and Mathieu, 2012).

1.2.2.3.3 Trenchmix

Continuous trenches of soil mixed with a binder can be produced using the Trenchmix ® method. The equipment consists of a specifically designed toothed chainsaw-type blade adapted on the arm of a trencher (Figure 1-9). The binder can be introduced either in powder (dry) or slurry (wet) form (Lebon, 2005). The blade is introduced in the soil to the desired depth of treatment (maximum depth of 10 m). The trencher then moves horizontally, creating a continuous wall of mixed soil. The width of the wall is generally between 0.40 and 0.85 m.

Figure 1-9 Insertion of the mixing blade and operation of the Trenchmix method (Lebon, 2005).

1.2.2.4 Conclusions

Although the overall principles of soil mixing are the same for the various techniques, the strength of the soil-mix material produced by wet mixing is generally higher than the strength obtained by dry mixing. Compressive strengths are greater than 2 MPa for the wet method, around 1 MPa for DJM and close to 250 kPa for the Scandinavian method. These differences are mainly due to the characteristics of the soils that are treated and to the binders used.

The differences in the properties of the treated soils result in significant variations in the overall behaviour of the treated soil masses. For example, columns installed by the Scandinavian method are of relatively low strength and assumed to act as vertical drains whereas Japanese columns are assumed virtually impermeable. These discrepancies result in different intended applications for soil mixing structures (CDIT, 2002).

1.2.3 Applications, advantages and limitations of deep mixing

1.2.3.1 Applications

Many authors have listed various applications of soil mixing (Porbaha et al., 1998; FHWA, 2000; CDIT, 2002; AFNOR, 2005; Topolnicki, 2004). The main applications are as follows:

- ground improvement (Broms, 2004; Stewart et al., 2004),
- foundation support (Taki and Yang, 1991; Bahner and Naguib, 2000; Cavey et al., 2004, Kasali and Taki 2003),
- retaining walls (Andromalos and Bahner 2003, Denies et al., 2012a, Topolnicki, 2004),
- liquefaction mitigation (Benhamou and Mathieu, 2012; Ryan and Jasperse, 1989),
- hydraulic cut-off walls,
- environmental remediation (Al-Tabbaa, 2005; Al-Tabbaa et al., 2009).

Originally, the primary application of deep soil mixing was ground improvement to enhance the stability and reduce the settlements of structures on soft soils of low shear strength and very high moisture contents using the dry mixing method. Nowadays, improving the strength and deformation properties as well as the permeability of very soft soils by deep soil mixing is a commonly used stabilisation process. Liquefaction mitigation, hydraulic cut-off walls and environmental remediation are more recent applications which have been used successfully on many sites. There is increasing interest in the use of the wet mixing technique to construct temporary and permanent foundation/structural (load bearing) elements and excavation retaining walls.

1.2.3.2 Patterns

Depending on the purpose of the soil mixing works and the site conditions, soil mixing elements are installed in various patterns (Figure 1-10) by combining spaced or overlapping columns.

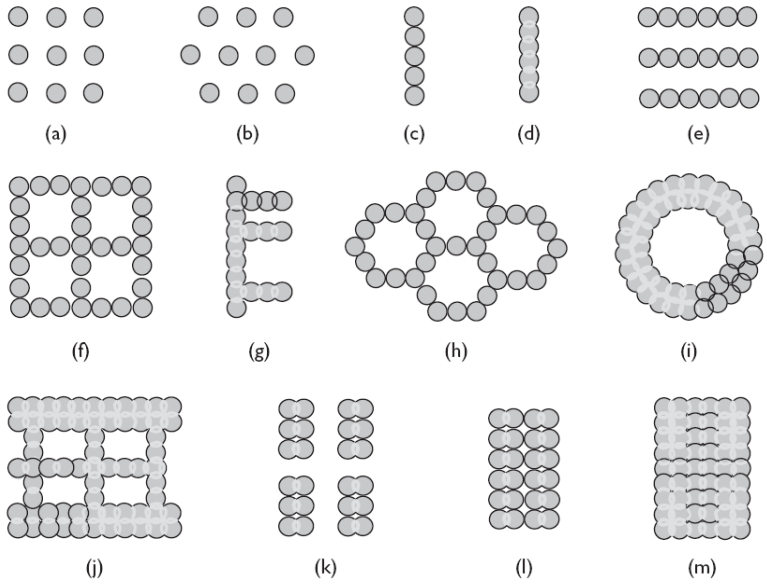

Figure 1-10 Examples of deep soil mixing patterns: (a), (b) column-type (square and triangular arrangement); (c) tangent wall; (d) overlapped wall; (e) tangent walls; (f) tangent grid; (g) overlapped wall with buttresses; (h) tangent cells; (i) ring; (j) lattice; (k) group columns; (l) group columns in-contact;(m) block (Topolnicki, 2004).

Isolated columns (Figure 1-10 (a) and (b)) are generally installed in square or triangular arrangements for ground improvement purposes. Tangent or overlapping columns are often constructed to serve as cut-off or retaining walls (Figure 1-10 (c) and (d)). Grids and cells (Figure 1-10 (f) and (h)) can be used to isolate contaminants but they have also been found effective for liquefaction mitigation.

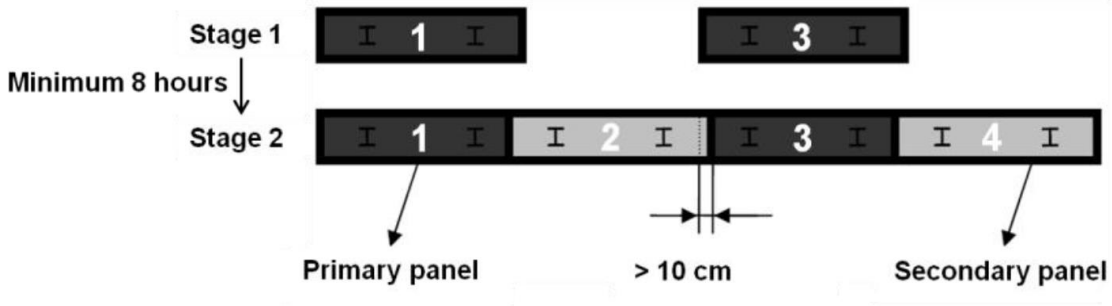

Figure 1-11 Execution sequence for soil mixing panels (Denies et al, 2012a).

Continuous walls executed by cutter soil mixing are generally constructed by overlapping primary and secondary panels. Steel reinforcements (H or I-beams) can be inserted into the fresh soil-mix material to counter shear forces and bending moments (Denies et al, 2012a).

1.2.3.3 Advantages and limitations

Although the advantages and limitations of deep mixing methods vary depending on the projects, the following table summarises the general benefits and disadvantages (FHWA, 2000 and Topolnicki, 2004):

Main advantages	Main limitations
- High productivity usually possible, hence economical for large scale projects - Column spacing and patterns highly variable, arrangements tailored to specific needs - Causes minimal lateral or vertical stress that could potentially damage adjacent structures - No vibration, medium–low noise - Can be used for on-land, waterfront and marine projects - Quality of treatment verifiable during construction - Minimum environmental impact construction	- Depth limitations (depending on the method applied) - Not applicable in soils that are very dense, very stiff, or contain boulders - Uniformity and quality of mixed soil may vary considerably in certain conditions - Significant spoil produced with the wet method - Weight of the equipment may be problematic for weak soils (depending on the method) - Limited ability to treat isolated strata at depth - Lack of definitive quality assurance and control (QA/QC) methods and procedures

Table 1-5 Main advantages and limitations for the use of deep mixing (Topolnicki, 2004).

1.2.4 Conclusions

Deep mixing is a general term for different techniques in which binders are mechanically mixed with the soil. The binder, introduced in dry or slurry form, is mixed using specially designed mixing tools. Deep mixing is used for various applications. The choice of the mixing method depends on ground conditions and application. Deep mixing was initially developed to improve the properties of very soft soils and is now used for structural elements such as foundations and retaining walls.

In Europe, deep mixing is generally carried out by the wet method using cement grouts. The engineering parameters required for design and the methods used in practice to determine these parameters are outlined in the following section. Current knowledge of the engineering properties of soil-mix materials is reviewed and the factors affecting the characteristics of treated soils are examined.

1.3 Engineering properties of soils stabilised with cement

1.3.1 Parameters required for design

The parameters used for design and the testing methods used to obtain these parameters depend on the requirements and objectives of the projects. For example, if soil mixing elements are installed to reduce settlements, values of the static deformation modulus of the soil mixing columns are essential. In projects carried out to improve stability and eliminate the risk of rupture, strength parameters are important. Permeability is crucial in environmental remediation projects (AFNOR, 2005). The investigation of small strain stiffness (E_0 and G_0) may be of interest in projects associated with vibration problems such as liquefaction mitigation but also to verify that satisfactory design strengths have been reached after treatment.

1.3.2 Methods used to determine the properties of stabilised soils

Quality assurance and quality control are important in deep mixing works as it is necessary to confirm that the assumed strength and deformation properties have been reached. Quality

assurance and quality control involve laboratory and in situ testing methods. Quality assessment may also refer to controlling and monitoring the execution parameters during construction (Larsson, 2005).

1.3.2.1 Sampling and laboratory testing

Laboratory tests are performed on:

- specimens of soil stabilised in the laboratory,
- cored specimens,
- wet-grab specimens.

1.3.2.1.1 Specimens prepared in the laboratory

Field studies are difficult and expensive to perform. Specimens prepared in the laboratory are used to evaluate the effects of different binder contents, binder types and water/binder ratios on the mechanical properties of treated soils. Standard procedures for specimen preparation are given in many soil mixing reference guides (AFNOR, 2005; EuroSoilStab, 2002; Kitazume et al., 2009). These laboratory tests are normally conducted before the beginning of construction.

Many authors have attempted to establish empirical relations between the strengths achieved in the laboratory and those achieved in the field based on past experiences. However, the specimen preparation procedures have been found to have a significant influence on the strength of specimens of soil mixed in the laboratory with cement (Hirabayashi et al., 2005). Hence, different laboratories may obtain different results when mixing the same soil with the same binder. It is an established opinion that the field mixing process cannot be simulated in the laboratory (Terashi, 1997; Bruce et al., 1998; Larsson, 2005). The strength and deformation properties determined in situ may differ considerably from those measured on laboratory samples (Larsson, 2005). Therefore, it is important to verify the mechanical properties of specimens taken in situ (wet-grab or cored).

1.3.2.1.2 Wet-grab specimens

Wet-grab samples are taken immediately after the execution of deep mixing elements by the wet method. A sampling device is used to extract the fresh soil-binder mixture from the desired depth. The fresh mix is generally poured into cylindrical moulds for laboratory tests (Larsson, 2005). Wet-grab samples are frequently used especially in Europe and in the USA. Generally, at least one sample is taken for every 500 m^3 of treated soil or one sample per day (AFNOR, 2005). Significant scatter of data from wet-grab samples have been observed due to the heterogeneity of the treated soils, the sampling and curing processes (Bruce and Bruce, 2004). The main uncertainty lies in the representativity of the wet-grab specimens as discussed by Bruce et al. (2000) and Denies et al. (2012b). Some reports state that strengths measured from wet-grab samples are lower than strengths obtained from cored samples. The opposite result has been reported in other studies (Larsson, 2005).

1.3.2.1.3 Cored specimens

Specimens cored from deep mixing elements are used to study the strength and compressibility characteristics as well as the homogeneity of treated soils. The choice of the coring technique and diameter is highly dependent on strength and type of soil. The number of cores depends on the project. A minimum of three cores is recommended in European standards (AFNOR, 2005).

1.3.2.1.4 Laboratory testing

In current practice, strength characteristics and the static modulus of stabilised soils are generally determined from unconfined compression tests on cylindrical specimens (AFNOR, 2005). Triaxial tests can also be used to obtain the shear strength parameters and stiffness of treated soils (Ajorloo et al., 2011).

In addition to these tests, non-destructive geophysical methods may be used. Seismic-based testing procedures have been utilised to assess the dynamic modulus of laboratory specimens (Nazarian et al., 1999; Ryden et al., 2006; Hilbrich and Scullion, 2007; Åhnberg and Holmen, 2008; Hoyos et al., 2004; Puppala et al., 2006; Rabbi et al., 2011) and offer promising perspectives in terms of quality assessment and quality control of stabilised soils (Madhyannapu et al., 2010). In order to estimate strength properties based on measured dynamic parameters, empirical relations with unconfined compressive strength are necessary. Bender elements are often used to measure small strain properties.
Different studies have been published relative to the use of free-free resonance testing (FFR testing) on homogeneous laboratory specimens of rather low strengths. Åhnberg and Holmen (2011) have investigated the use of resonant column free-free testing on different types of soils of high moisture contents (over 40%) stabilised in the laboratory with cement and lime. They demonstrated the usefulness of this method by proposing empirical correlations between compression wave velocity, shear wave velocity and unconfined compressive strength. Toohey and Mooney (2012) analysed the growth in seismic modulus with curing time up to 28 days for soils stabilised with lime in the laboratory. One of the main advantages of FFR tests is that they can be executed very rapidly on specimens of different dimensions.

1.3.2.2 In situ testing

An international survey concerning quality control in deep mixing projects by Puppala and Porbaha (2004) showed that in situ testing methods are more frequently used than laboratory tests and that strength is the most important parameter to control. Many existing geotechnical testing techniques have been adapted for deep mixing elements (Table 1-6) and are primarily used to estimate the undrained shear strength of stabilised soils (Bruce et al., 2001).

Method	Countries	Notes
Conventional Column Penetration (KPS)	Nordic countries	Used in columns of strength less than 200 to 300 kPa. Depth limit 6 to 8 m, aided by predrilling.
Inverted Column Penetrometer (FOPS)	Nordic countries	For strengths up to 600 to 800 kPa and to depths of 20 m.
Pressuremeter	Sweden/U.S.	Especially for stronger columns.
Dynamic Penetrometer	France/U.K.	
Standard Penetration Test	Japan	Widespread, simple test, well known.
Cone Penetrometer (CPT)	Norway and Finland (since 1970s) less in Sweden	Can provide data in columns of strengths up to 1000 kPa, 20 m depth.
Modified Vane Test	Norway	For strength less than 200 kPa.
Tube Sampler	Norway	Promising development but gives low strengths in heterogeneous columns.
Screw Plate Test	Scandinavia	Developed in early 1970s and is a very precise but expensive test.
Measurement While Drilling (MWD)	Japan, Finland	Real time monitoring of drilling parameters.

Table 1-6 Modified geotechnical testing methods (Bruce et al., 2001).

1.3.2.3 Execution parameters

According to AFNOR (2005), the execution process should be supervised by continuous monitoring and recording of the following parameters:

- penetration and retrieval speeds of the mixing tool,
- rotation speed of the mixing tool,
- air/slurry injection pressure,
- delivery rate of binder/slurry.

1.3.3 Types of cement and basic mechanisms involved in soil treatment

The main binder used in Europe for deep mixing is cement. The different types of cement are divided in five categories based on their composition in the current European standard NF EN 197-1 (AFNOR, 2001):

- CEM I: Portland cement,
- CEM II: Portland-composite cement,
- CEM III: Blast furnace cement,
- CEM IV: Pozzolanic cement,
- CEM V: Composite cement.

The most widely used types of cement in deep mixing are Portland cement and Blast furnace cement (CDIT, 2002).

Portland cement is composed of clinker (more than 90%), a limited quantity of calcium sulfate and a small amount of minor constituents (up to 5%).
Portland cement clinker is made by heating in a kiln a homogeneous mixture of limestone and alumino-silicates (clay). Clinker is composed of the following mineral:

- tricalcium silicate (C_3S),
- dicalcium silicate (C_2S),
- tricalcium aluminate (C_3A),
- tetracalcium aluminoferrite (C_4AF).

The hydration of clinker forms calcium silicate hydrates (C-S-H), calcium aluminate hydrates (C-A-H) and calcium hydroxide (C-H). The hydration reactions of tricalcium silicate and dicalcium silicate with water are largely responsible for the cementing action of Portland cement. The hydration products progressively fill the spaces between soil particles to give a continuous matrix, thereby generating a relatively high strength impermeable material (Hewlett, 2003).

In the case of clayey soils, the calcium hydroxide may dissolve in pore water and react with dissolved silica and aluminium from the clay particles to produce water-insoluble gels of calcium-silicate and/or aluminium-silicate. This pozzolanic reaction also contributes to strength increase in soils treated with cement (CDIT, 2002).

Blast furnace slag is a by-product of the iron production industry. The chemical composition of slag depends on the composition of the raw materials in the iron production process. Blast furnace slag produces pozzolanic reaction products under high alkaline conditions. The high alkaline conditions are created by the presence of clinker in blast furnace cements. Blast furnace slag cements are often used for the construction of foundations as the resistance to chemical attack is improved and corrosion in aggressive environments is inhibited.

1.3.4 Mechanical characteristics and engineering properties of soil-mix materials

As illustrated in Figure 1-12, the composition and strength of soil-cement mixtures lie between those of soil and concrete.

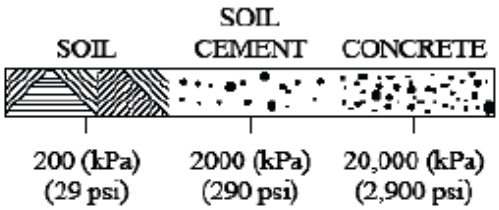

Figure 1-12 Examples of typical values of the strengths of soil, soil-cement and concrete (Rutherford, 2004).

The most frequently required engineering parameters of the soil-mix material for the design of deep mixing structures are the compressive and tensile strengths, modulus of elasticity, density and permeability (Topolnicki, 2004). Typical values measured on specimens of soil treated by wet mixing have been summarised by Bruce and Bruce (2003; Table 1-7).

Property	Typical range
Compressive strength q_u (typically at 28 days)	0.2 - 5.0 MPa (0.5 - 5 MPa in granular soils) (0.2 - 2 MPa in cohesive soils)
Permeability K	1×10^{-6} to 1×10^{-9} m/s (lower if bentonite is used)
Modulus of elasticity	350 to 1000 times q_u for lab samples and 150 to 500 times q_u for field samples
Tensile strength	Typically 8 - 14% q_u

Table 1-7 Typical values for soils treated by wet deep mixing (Bruce and Bruce, 2003).

1.3.4.1 Density

Figure 1-13 shows that the density of soils stabilised by the dry method slightly increases whereas the density of soils treated by the wet method remains unchanged irrespective of the cement content.

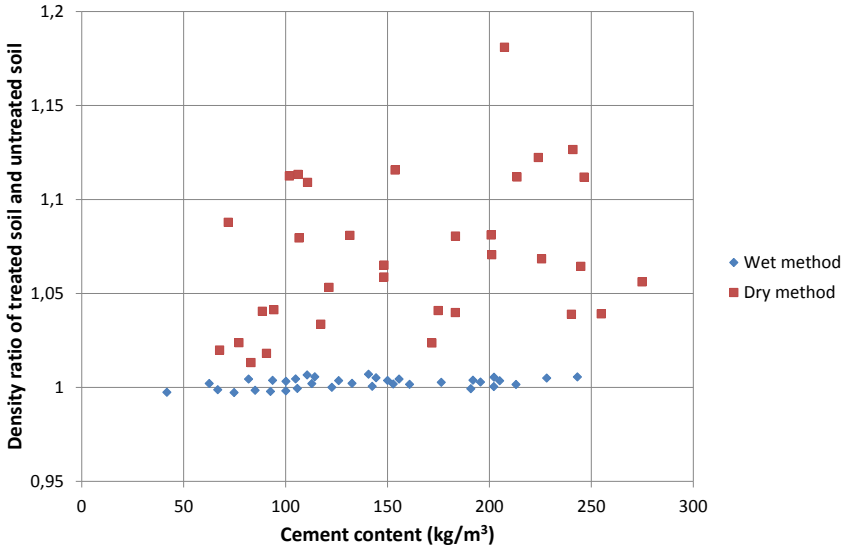

Figure 1-13 Change in density of soils treated by soil mixing (CDIT, 2002).

1.3.4.2 Unconfined compression strength

Even for low dosages, the addition of cement increases the strength of soils (Larsson, 2003; Broms, 2004; FHWA, 2000). The following table (Table 1-8) gives orders of magnitude of typical unconfined compressive strengths which can be obtained after 28 days (Topolnicki, 2004). The values vary depending on soil type and are much lower than typical strengths obtained on concretes after 28 days.

Soil type	Cement factor (kg/m^3)	28-day q_u (MPa)	Permeability, k (m/s)
Sludge	250 - 400	0.1 - 0.4	$1x10^{-8}$
Peat, organic silts/clays	150 - 350	0.2 - 1.2	$5x10^{-9}$
Soft clays	150 - 300	0.5 - 1.7	$5x10^{-9}$
Medium/hard clays	120 - 300	0.7 - 2.5	$5x10^{-9}$
Silts and silty sands	120 - 300	1.0 - 3.0	$1x10^{-8}$
Fine-medium sands	120 - 300	1.5 - 5.0	$5x10^{-8}$
Coarse sands and gravels	120 - 250	3.0 - 7.0	$1x10^{-7}$

Table 1-8 Typical field strengths and permeabilities for different types of soil stabilised by the wet method (Topolnicki, 2004).

Soil mixing elements contain inclusions of intact soil due to the mixing process. Because of the heterogeneous nature of soils stabilised by deep mixing, variability of the measured properties is rather high. Figure 1-14 presents data from tests on field samples compiled by Larsson (2005). The results show that the coefficients of variation of strength (ratio of the standard deviation to the mean) evaluated from unconfined compression tests are relatively high and vary considerably between different studies. This variability is important as it has to be taken into account in probabilistic design methods. Furthermore, it also has an impact on quality assessment because variability affects the choice of sample size and laboratory tests. The main factors affecting strength variability are related to the heterogeneity of the material in relation with the specific installation process for deep mixing. However, part of the variability displayed in Figure 1-14 can also be attributed to sampling and testing conditions (Larsson, 2005).

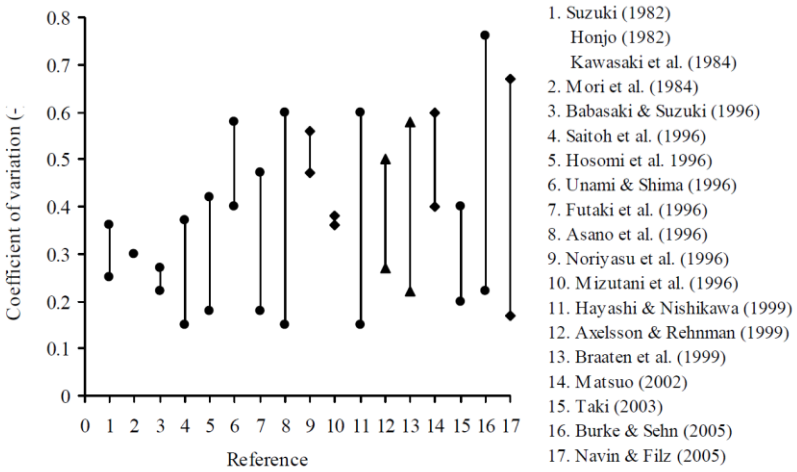

Figure 1-14 Coefficient of variation evaluated from compression tests in a number of reported studies (Larsson, 2005).

The strength of soils treated with cement increases with curing time. Many authors have published empirical relations to estimate the increase in strength (Table 1-9). Many researchers have found that strength increase is proportional to the logarithm of curing time in days.

References	Proposed relations
Porbaha et al., 2000	$q_{u,28}$ = (1.49 to 1.56) $q_{u,7}$ $q_{u,91}$ = (1.85 to 1.97) $q_{u,7}$ $q_{u,91}$ = (1.20 to 1.33) $q_{u,28}$
Bruce and Bruce, 2003	$q_{u,60} = 1.5\ q_{u,28}$ $q_{u,15\text{-years}} = 3\ q_{u,60}$
Nagaraj et al., 1998	$\frac{q_{u,t}}{q_{u,14}} = a + b \times Ln(t)$ t time in days; a and b constants
Horpibulsuk et al., 2003	$\frac{q_{u,t}}{q_{u,28}} = c + d \times Ln(t)$ t time in days; c and d constants
Szymkiewicz et al., 2012	$q_{u,t} = \frac{w_f}{w_i} \times q_{u,7} \times (Ln(t) - 1)$ t time in days; W_f final water content ; W_i initial water content

Table 1-9 Empirical relations to estimate the increase in strength of stabilised soils with time.

Strength and stiffness increase in time of materials mixed with cementing agents has been widely studied in concrete research. Empirical relations given in current standards in Europe (Eurocode 2, 2005) are used in practice for concretes. However these correlations are rarely applied to stabilised soils (Denies et al., 2012b).
In Eurocode 2 (2005), the proposed empirical relations are based on 28-day measurements and use an empirical factor β to calculate the strength or stiffness at a certain time:

$$\beta = \exp\left[s_{28} \times \left(1 - \sqrt{\frac{28}{t}} \right) \right]$$

where t is the curing time in days and s_{28} is the empirical parameter used to predict the strength based on 28-day data.

The unconfined compressive strength growth is calculated using the following relationship:

$$q_{u,t} = q_{u,28} \times \beta = q_{u,28} \times \exp\left[s_{28} \times \left(1 - \sqrt{\frac{28}{t}} \right) \right]$$

$q_{u,t}$ is the unconfined compressive strength after t days and $q_{u,28}$ is the unconfined compressive strength after 28 days.
For concrete, the values of s_{28} depend on the type of cement and vary between 0.20 and 0.38.

1.3.4.3 Tensile strength

The tensile strength of cement-treated soils is often determined indirectly by Brazilian tests (indirect tensile strength tests). Tests performed on specimens prepared in the laboratory show a linear relationship with unconfined compressive strength for strengths lower than 2 MPa

(Terashi et al., 1980 cited by CDIT, 2002). The tensile strength was found to be approximately 0.15 times the unconfined compressive strength (Figure 1-15).

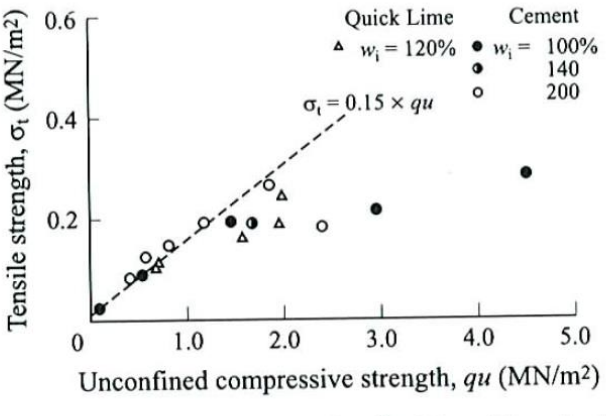

Figure 1-15 Tensile strength of laboratory treated soils (Terashi et al., 1980 cited by CDIT, 2002).

Denies et al. (2012b) also found a more or less linear relation between tensile and compressive strength for field specimens as shown in Figure 1-16.

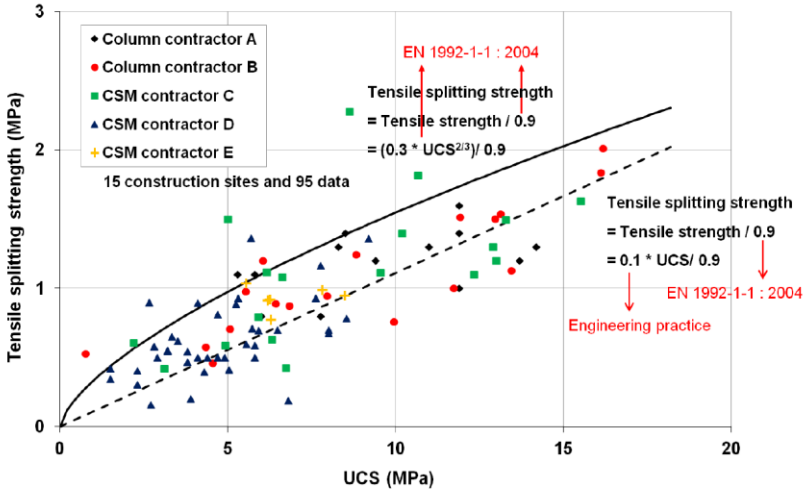

Figure 1-16 Tensile strength of soils treated in situ by deep mixing (Denies et al., 2012b).

1.3.4.4 Deformation modulus

Stiffness characteristics are essential for design as they significantly affect the distribution of loads between the treated soil and the surrounding ground. Static modulus values are used as input parameters in numerical models to evaluate the settlements of structures founded on soil mixing elements.

Different deformation moduli for stabilised soils can be determined from stress-strain curves. The most commonly used moduli are:

- E_{ini} or E_{max}: initial slope of the stress strain curve (tangent modulus);
- E_{50}: secant modulus at a stress equal to half the maximum strength.

It is common in the engineering practice of deep mixing projects to determine the static modulus E_{50} from correlations with unconfined compressive strength q_u. In general, linear relations are assumed. However, significant disparities in the proposed correlations can be found in the literature. This is demonstrated in Table 1-10.

Reference	Relationship	Note
Saitoh et al. (1996)	$350\ q_u < E_{50} < 1000\ q_u$	/
Eurosoilstab (2002)	$100\ q_u < E_{50} < 200\ q_u$	/
Asano et al. (1996)	$50\ q_u < E_{50} < 500\ q_u$	In situ samples
Futaki et al. (1996)	$140\ q_u < E_{50} < 200\ q_u$	Cored samples
Tan et al. (2002)	$350\ q_u < E_{50} < 800\ q_u$	Lab samples samples – Local strain measurement
Tatsuoka et al. (1996)	$E_{max} < 1000\ q_u$	Local strain measurement - E_{max} stiffness at small strain levels

Table 1-10 Relationships between modulus and unconfined compressive strength.

It is generally acknowledged that the methods used to measure strains during testing significantly affect the values of stiffness. However, many studies on soil-mix materials do not explicitly specify the equipment used to measure strains. In tests on materials such as concrete and steel, the issue of bedding errors is well understood, and measuring displacements externally between end plates during compression tests is rarely done.

Reliable measurement of soil stiffness over the full range of loading from very small strain to failure requires the use of local strain gauges attached directly to the sample (Jardine et al., 1984). Few studies have addressed this issue for stabilised soils. Tatsuoka et al. (1996) and Tan et al. (2002) have shown that external measurements of strains between end-platens often considerably underestimated the stiffness (Figure 1-17).

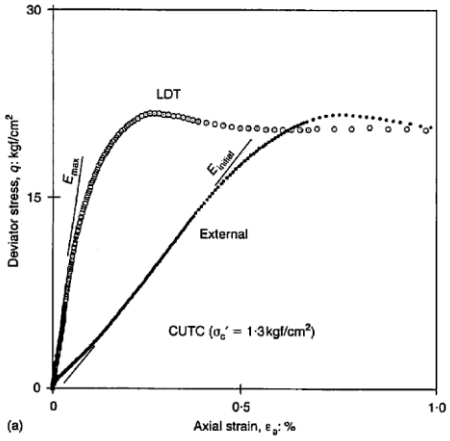

Figure 1-17 Comparison of stress-strain curves of cement-treated sand in triaxial tests obtained with local and external strain measurements (Tatsuoka et al., 1997).

For Singapore marine clay improved in the laboratory with cement, Tan et al. (2002) found E_{50}/q_u ratios between 150 and 400 by external strain measurements. Using local strain

measurements consisting of Hall's effect transducers, E_{50}/q_u ratios between 350 and 800 were calculated (Figure 1-18). These results suggest that strains are overestimated by a factor of 2 when using external measurements. Results from other studies given in Figure 1-19 and Figure 1-20 suggest higher ratios between 2 (for sand) and more than 6 (for silt).

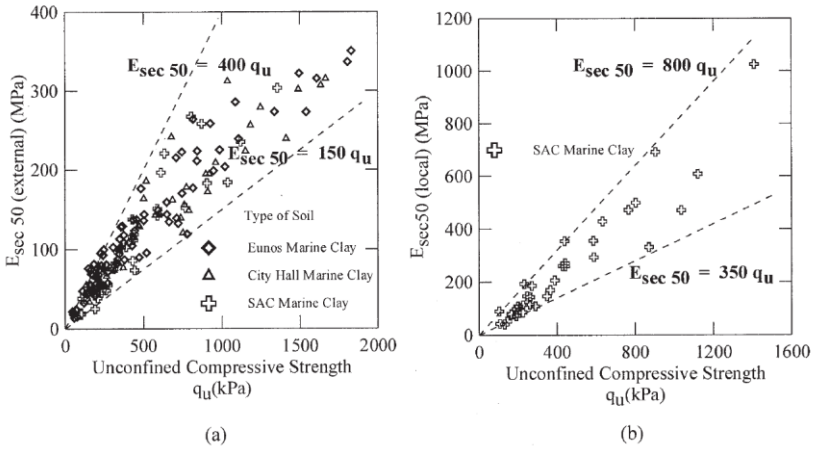

Figure 1-18 Correlation between E_{50} and q_u derived using: (a) external strain measurement method; (b) local strain measurement method (Tan et al., 2002).

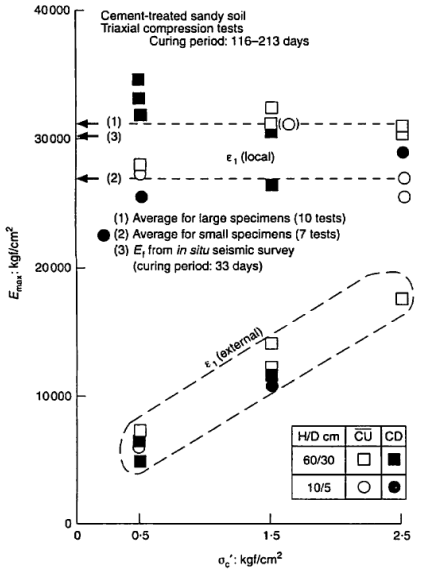

Figure 1-19 Comparison of stiffness E_{max} obtained with local and external strain measurements (Tatsuoka et al., 1997).

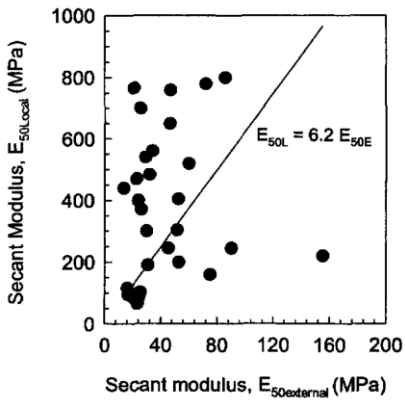

Figure 1-20 Comparison between E_{50} obtained with local and external strain measurements on cement-treated silt specimens (Bouazza et al., 2004).

Denies et al. (2012b) calculate the tangent elastic modulus E of cored field specimens from strains measured locally between applied loads of 10 % and 30 % of the estimated unconfined compressive strength (Figure 1-21). The results show a non-linear relation between E and q_u. Power laws are fitted to the data. No information on soil type is given in the figure.

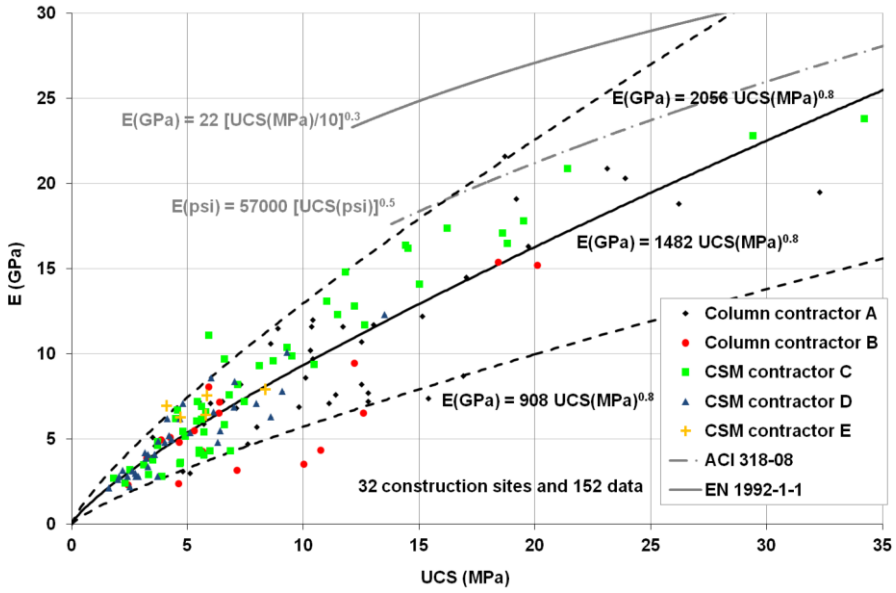

Figure 1-21 Elastic modulus of soils treated in situ by deep mixing (Denies et al., 2012b).

Non-linear relations between strength and stiffness have also been proposed for concretes and are given in various standards. The following relation is recommended in Eurocode 2 (2005):

$$E = 22 \times \left(\frac{q_u}{10} \right)^{0.3}$$

with E in GPa and q_u in MPa.

The equation linking compressive strength to modulus given in ACI-318 (2005) depends on the unit weight of the concrete (between 1500 and 2400 kg/m^3):

$$E = 0.043 \times \rho^{1.5} \times \sqrt{q_u}$$

with E in MPa, ρ in kg/m^3 and q_u in MPa.

The method used to measure strain during testing of treated soils has a significant influence on the calculated values of the static modulus. Reliable estimates of stiffness require the use of local strain measurements. However, external strain measurements are still widely used and have been reported to underestimate the modulus by a factor between 2 and 6. The use of modulus values obtained from external measurements for design may result in significant overestimations of settlements. Consequently, unnecessary increases in dosage or modifications of installation patterns may be adopted.
The procedures used to measure and calculate the modulus of treated soils are of great importance because they directly impact the construction and cost of soil mixing projects.

1.3.4.5 Permeability

Stabilisation by deep mixing can significantly affect the permeability of soils. The permeability of clays may increase up to 100 or 1000 times (Eurosoilstab, 2002). On the other hand, the permeability of coarse grained soils such as sand is considerably reduced by the addition of cement (Tokunaga et al., 2005). Curing time does not seem to notably affect permeability (Eurosoilstab, 2002). Typical values for different types of soil are given in Table 1-8. Denies et al. (2012b) measured permeabilities between 10^{-8} and 10^{-12} m/s on specimens with porosities between 30 % and 65 % (Figure 1-22).

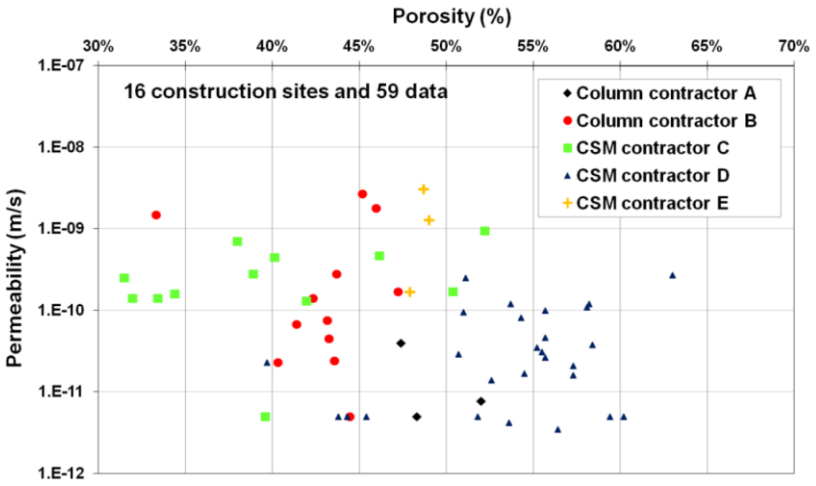

Figure 1-22 Permeability of soils treated in situ by deep mixing (Denies et al., 2012b).

1.3.5 Important factors affecting the characteristics of stabilised soils

Many factors influence the characteristics of soils treated by soil mixing. Terashi (1997) classifies these factors into four main groups (Table 1-11).

I	Characteristics of hardening agent	1. Type of hardening agent 2. Quality 3. Mixing water and additives
II	Characteristics and conditions of soil (especially important for clays)	1. Physical, chemical and mineralogical properties of soil 2. Organic content 3. pH of pore water 4. Water content
III	Mixing conditions	1. Degree of mixing 2. Time of mixing/re-mixing 3. Quality of hardening agent
IV	Curing conditions	1. Temperature 2. Curing time 3. Humidity 4. Wetting and drying; freezing and thawing, etc.

Table 1-11 Factors affecting the characteristics of soils treated by soil mixing (Terashi, 1997).

Topolnicki (2004) proposes a similar classification but adds the effects of sampling and testing procedures.

1.3.5.1 Factors related to the binder

The type, quality and quantity of binder affect the development of strength in cement-treated soils (Porbaha et al., 2000).

1.3.5.1.1 Effect of dosage

Binder content has a significant effect on the strength of treated soils. Many studies are devoted to the analysis of changes in compressive strength as a function of binder content. According to Janz and Johansson (2002), a minimum dosage (threshold) is required to increase the strength of soils (Figure 1-23).

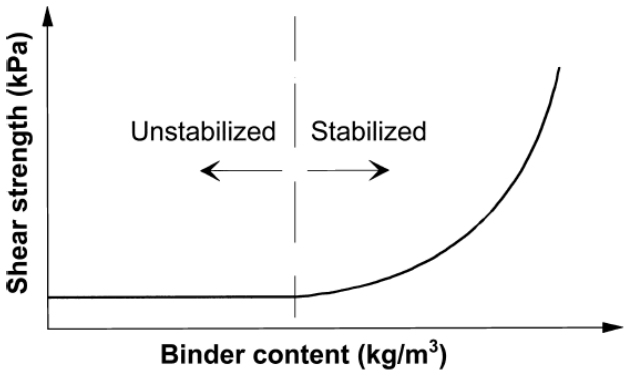

Figure 1-23 Relation between binder content and shear strength of treated soils (Janz and Johansson, 2002).

Above this threshold, strength increases with increasing binder content as illustrated in Figure 1-24.

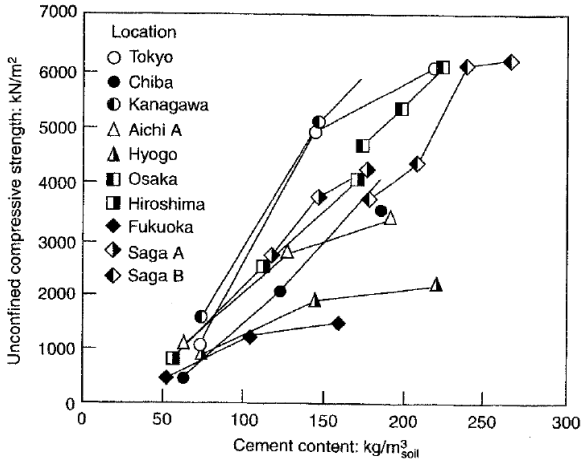

Figure 1-24 Effect of cement content on the strength of Japanese soils (Porbaha et al., 2000).

The strength of soil-cement mixtures also depends on the water-cement ratio W/C (Figure 1-25). Strength decreases as the ratio increases.

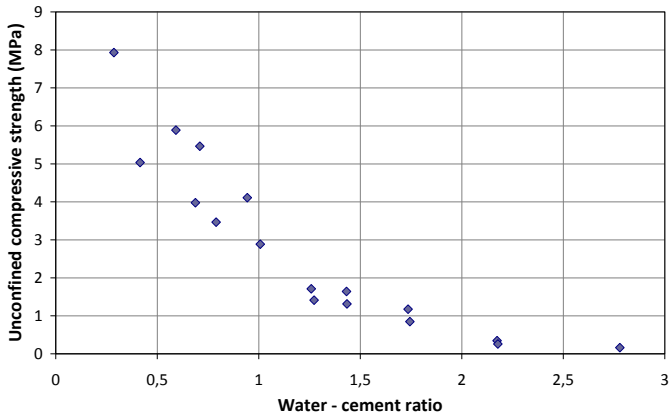

Figure 1-25 Effect of water-cement ratio on the strength of stabilised soils (after Asano et al., 1996).

1.3.5.1.2 Effect of the type of binder

Åhnberg et al. (1995, cited by Porbaha et al., 2000) found that the strength of stabilised clays depends on the type of binder (Figure 1-26). The figure shows than higher strengths are generally measured on soils treated with cement. Furthermore, the same binder can have different effects depending on the soil (Figure 1-27).

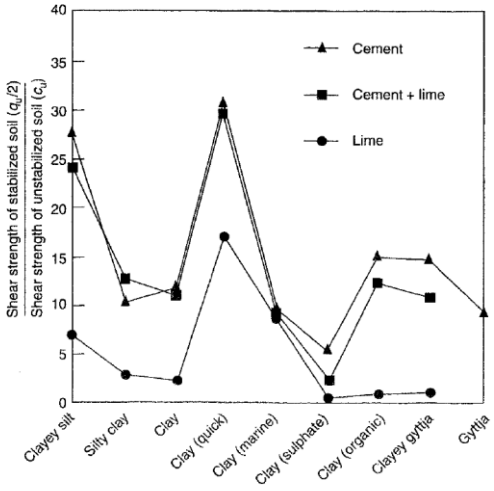

Figure 1-26 Effects of the type of binder on the strength of different soils (Åhnberg et al., 1995).

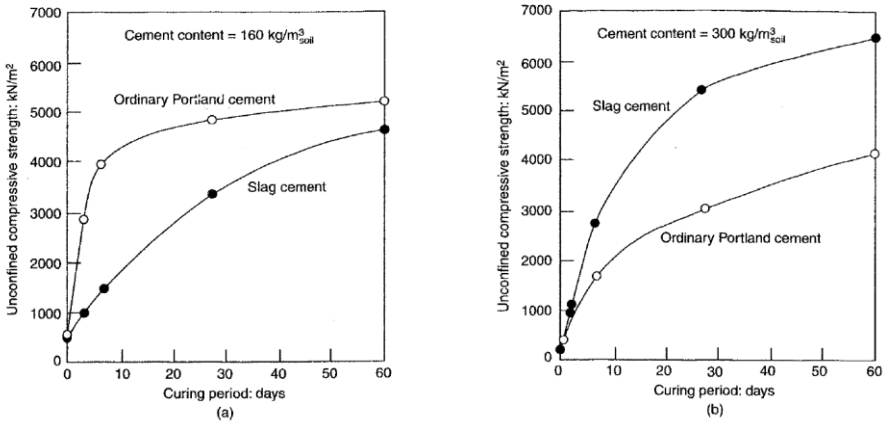

Figure 1-27 Effects of the type of binder on the strength of different soils (a) soil from Kanawaga (b) soil from Saga, Japan (Porbaha et al., 2000).

1.3.5.2 Factors related to soil characteristics

1.3.5.2.1 Influence of soil type

The type of soil has a major impact on the characteristics after treatment. Figure 1-28 shows the compressive strength of different soils (clay - silt - sand) treated with cement. In general, for the same cement content, the compressive strength of sandy soils is higher than the strength of silts and clays. It is worth noting that this figure does not take into account the initial moisture content.

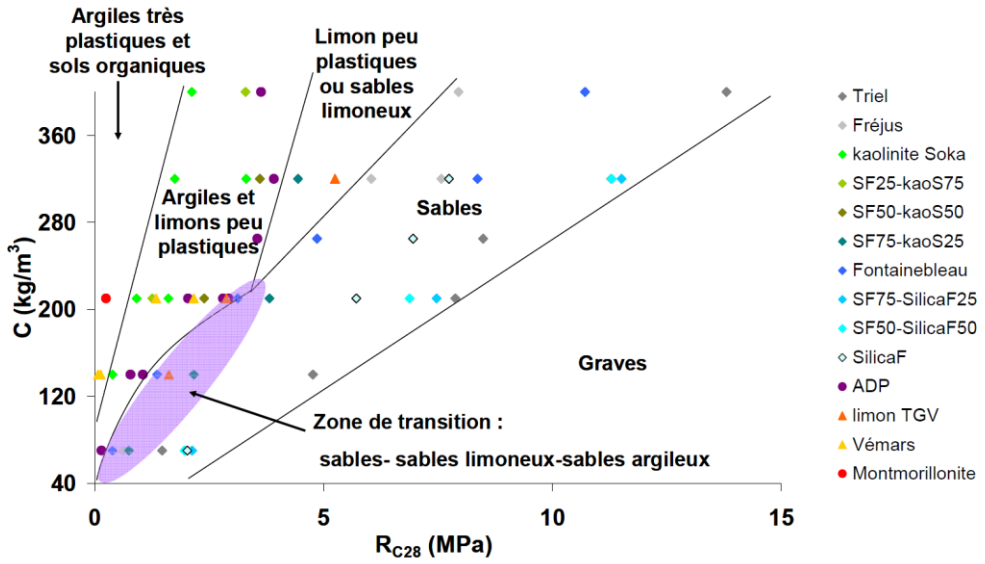

Figure 1-28 Effect of soil type on the strength of stabilised soils (Szymkiewicz, 2011).

1.3.5.2.2 Effect of moisture content

The compressive strength of cement-treated soils also varies with the initial water content. The compressive strength is lower for higher initial moisture contents (Figure 1-29).

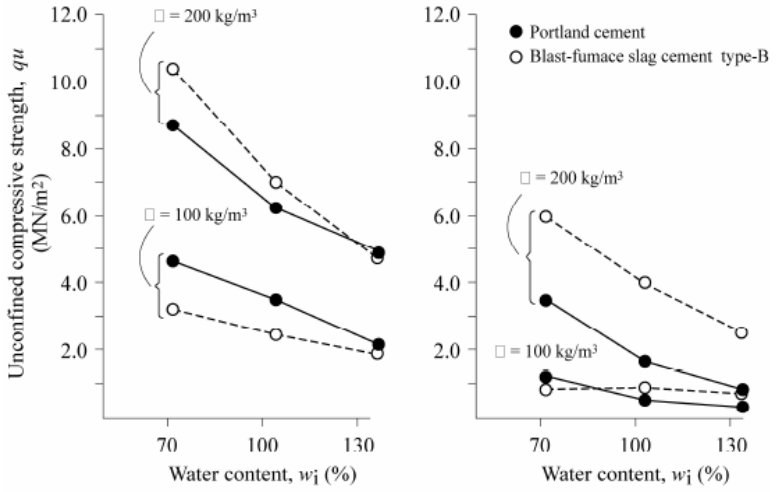

Figure 1-29 Influence of initial water content on strength (a) Yokohama Port clay, (b) Imari Port clay (CDIT, 2002).

1.3.5.2.3 Effect of grain size distribution

Grain size distribution, especially the sand fraction, influences the compressive strength of cement-treated soils (Figure 1-30). Many authors have studied the strength of treated soils composed of mixtures of sand and finer particles. Generally, an optimum strength is measured for sand contents between 50 and 75 %. These contents correspond to the most favourable particle packing arrangement which can be reached (Lade et al., 1998; Reiffsteck, 2007). Szymkiewicz et al. (2012) showed that treated uniform sand exhibits the same hardening trend with time for varying cement contents. On the contrary, the hardening process for treated sandy soils with larger spread grain size distributions depends on cement content. Sand content also has an effect on the strength-stiffness ratio (Figure 1-31). Stiffness is higher compared to strength for higher sand contents.

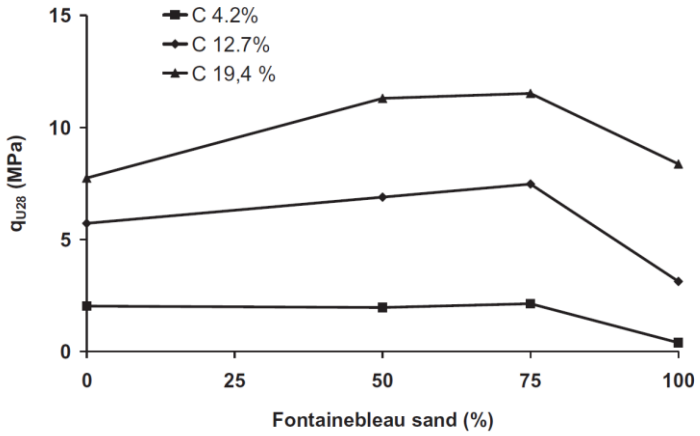

Figure 1-30 Influence of sand content on the strength of treated soils (Szymkiewicz et al., 2012).

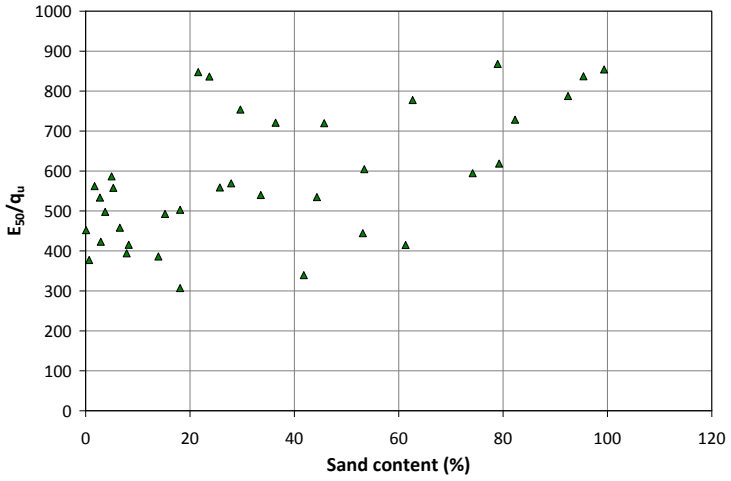

Figure 1-31 Influence of sand content on strength-stiffness ratio E_{50}/q_u (after Saitoh et al., 1996).

1.3.5.3 Factors associated with the mixing conditions

1.3.5.3.1 Rheology of clays and cement pastes

The aim of the installation process in deep soil mixing is to inject and spread a binder in dry or slurry form into the soil in order to produce a homogeneous soil-binder mixture. The

execution process is very complex compared to other ground improvement methods. The mixing mechanisms that occur during deep mixing are difficult to monitor and present engineering challenges (Larsson, 2003). The homogeneity and strength of soils stabilised by deep mixing largely depend on the mixing conditions and mechanisms that occur during construction (degree of mixing, mixing tool). It has been observed that the mixing of fine grained soils with binders is particularly difficult in extremely cohesive soils of high moisture contents. The addition of water facilitates mixing in the wet method. Soil type and rheological characteristics have a significant effect on the mixing process.

The mixing mechanisms in deep mixing are directly related to the rheological properties of the materials being mixed (Larsson, 2003). Therefore, rheology is the starting point in understanding the processes involved in deep soil mixing. However, knowledge of the rheological characteristics of stabilised soils is very limited (Larsson, 2005).

Few detailed studies have been conducted on the effects of soil rheology in the mixing process of deep mixing. In current practice, certain simple tests are performed on site to rank and compare flow properties of grouts, concrete and soil-binder mixtures using empirical parameters (Marsh cone, Abrams cone). These tests can be very useful in the field for rapid assessments of rheological characteristics but are limited to comparisons of the effects of different dosages on flow properties. They do not enable a quantitative assessment of rheological parameters or the understanding of fundamental physical and chemical interactions between the different constituents in the mixtures.

The use of rheometry offers a more quantitative study of the impacts of the addition of binders on the flow properties of soils. The type of soil and its rheological behaviour have a considerable impact on the efficiency of the mixing process. Many authors (Coussot and Ancey, 1999; Lagaly, 1989; Roussel, 2005) have reported that cement slurries and clay–water suspensions could be described in the liquid state as shear-thinning yield stress fluids (Figure 1-32). The viscosity of shear-thinning fluids decreases as the shear rate increases.

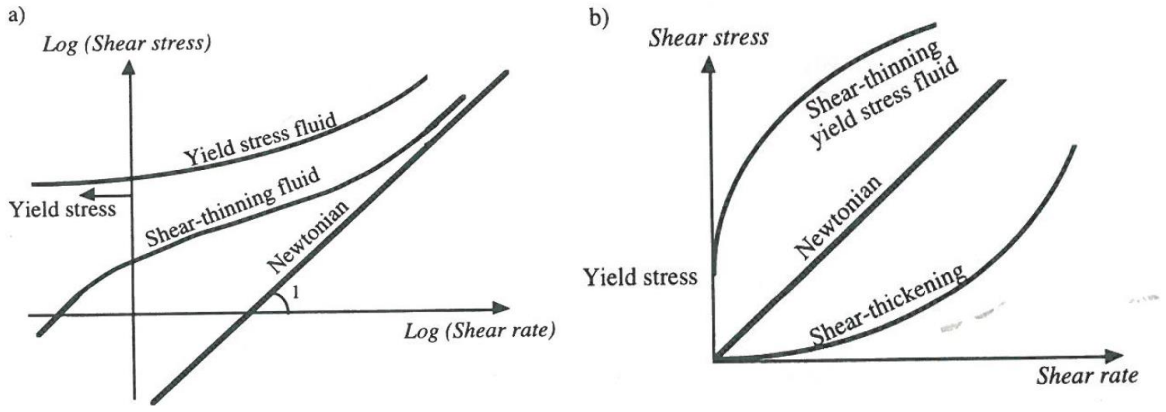

Figure 1-32 Main steady state behaviour types a) logarithmic diagram b) linear diagram (Coussot, 1997).

The simplest theoretical model for yield stress fluids is the Bingham model:

$$\tau = \tau_0 + \eta \dot{\gamma}$$

where τ_0 = yield stress (Pa), η = viscosity (Pa.s).

It is possible to fit this model to experimental data in a narrow range of large shear rates. However, key material properties may be disregarded using this model. Consequently, the Herschel–Bulkley model (Herschel and Bulkley, 1926) is often fitted to experimental data:

$$\tau = \tau_0 + K\dot{\gamma}^n$$

where K and n are experimental parameters; (n < 1 for shear shinning fluids).

Usually, the yield stress represents the strength resulting from interparticle interaction forces under shear displacement. It corresponds to a critical value of shear stress below which it is not possible to have flow. However, the concept of yield stress is still widely discussed (Tattersal and Banfill, 1983; Barnes and Walters, 1995; Coussot et al., 1996; Barnes, 1999). Indeed, depending on the test procedure, many different values of yield stress can be defined. Even during a single test, different yield stresses can be measured or calculated. This is especially the case for fluids that exhibit a minimum in flow curves. This phenomenon is related to flocculation and deflocculation processes that depend on the hydration of the particles (clay and cement particles are particularly reactive in terms of swelling, phase modification and crystallisation).

1.3.5.3.2 Degree of mixing and mixing energy

Nakamura et al. (1982) carried out compression tests on specimens of clay treated with Portland cement. The specimens were prepared in the laboratory with different mixing times. The results show that compressive strength increases with mixing time (Figure 1-33).

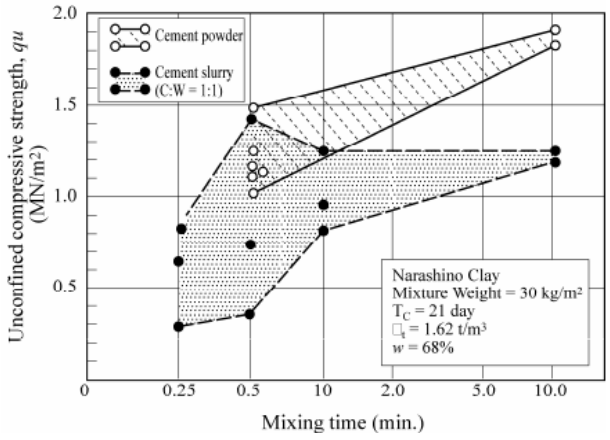

Figure 1-33 Effect of mixing time on strength (Nakamura et al., 1982).

Mixing time is an index that quantifies the degree of mixing between the ground and the binder. The degree of mixing also depends on the mixing equipment used and the soil characteristics (Kitazume, 2005).
Mixing work in deep mixing projects is evaluated using the tool penetration rate (m/min), rotation speed (rpm) and withdrawal rate (m/min). These parameters are combined to calculate the blade rotation number T (Yoshizawa et al., 1997):

$$T = \sum M \times \left[\left(\frac{N_d}{V_d} \right) + \left(\frac{N_u}{V_u} \right) \right]$$

where M is the number of mixing blades, N_d is the rotation speed of the mixing tool during penetration (rev/min), V_d is the penetration velocity (m/min), N_u is the rotation speed of the mixing tool during retrieval (rev/min), V_u is the speed during withdrawal (m/min).

The mixing work (quantified by the blade rotation number) has a significant effect on the magnitude and variability of strength in soil-mix materials. A power law or logarithmic relationship between blade rotation number and strength of the material has been reported (Figure 1-34). The data provided by Topolnicki (2009) illustrates the non-linear relation between blade rotation number and coefficient of variation of strength (Figure 1-35).

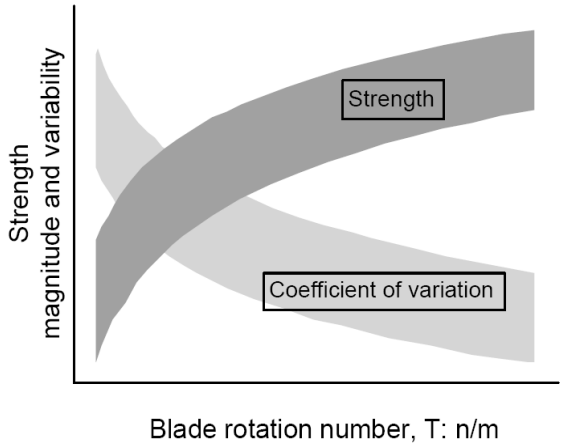

Figure 1-34 Variations in magnitude and variability of strength versus blade rotation number T (Larsson, 2005).

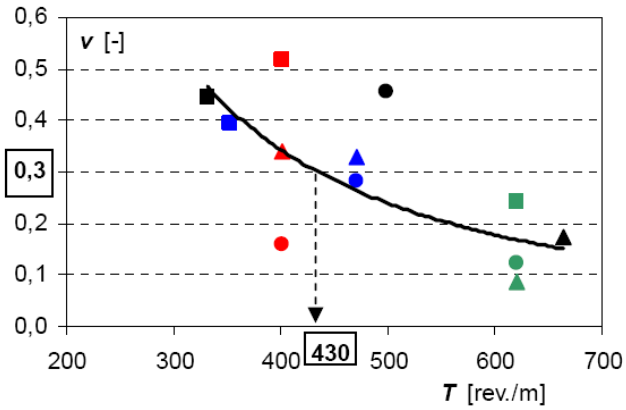

Figure 1-35 Coefficient of variation of strength v obtained on field specimens versus blade rotation number T (Topolnicki, 2009).

However, Larsson (2005) deems it is impossible to estimate the strength of treated soils only as a function of the blade rotation number because many other factors are involved. For example, the coefficient of variation of strength also depends on dosage (Figure 1-36).

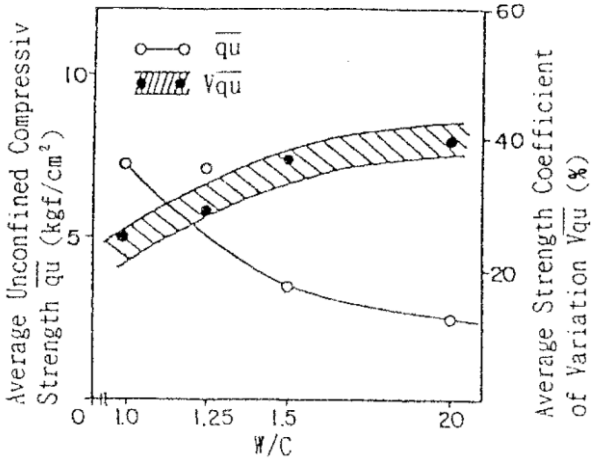

Figure 1-36 Effect of water-cement ratio W/C on average strength and coefficient of variation of strength obtained on field specimens (Nishibayashi et al., 1988 cited by Yoshizawa et al., 1997).

1.3.5.3.3 Difference between field and laboratory samples

Many authors (Terashi 1997; Bruce et al., 1998; Larsson, 2005) agree that soil mixing in the laboratory should be performed to investigate the effect of different binders on different soils but that the inconsistencies between the strength of laboratory mixed samples and the strength of deep mixed columns in the field have to be considered. Results concerning the relationship between the strength of laboratory mixed samples (q_{ul}) and field samples (q_{uf}) are shown in Figure 1-37 (Kamon, 1996 cited by Holm, 2000). The strength of in situ specimens is usually lower than the strength of laboratory mixed samples (the ratio is generally close to 0.5).

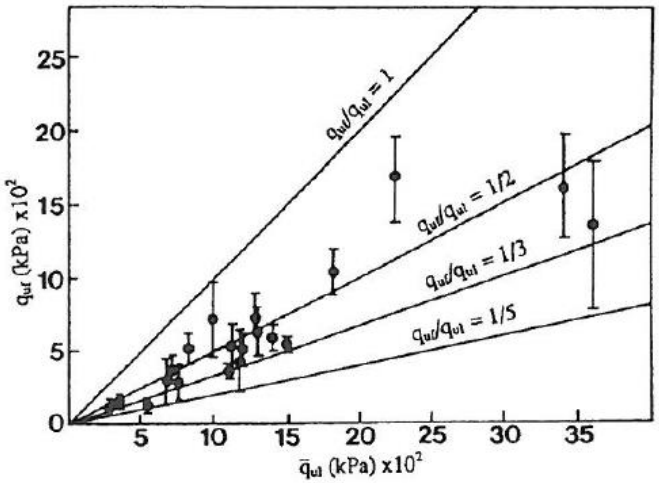

Figure 1-37 Strength in field and laboratory samples (Holm, 2000).

Results of laboratory tests on specimens of treated silt (Figure 1-38) show that strength gain between 7 and 14 days is the same for treated soils mixed in the laboratory and in situ if the curing conditions are similar (field samples were cured in the lab).

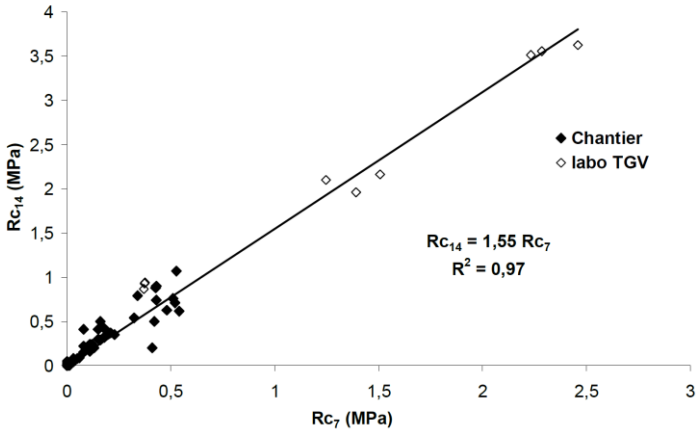

Figure 1-38 Relationship between strengths measured after 7 and 14 days for field and laboratory samples (Szymkiewicz, 2011).

1.3.5.4 Factors related to the curing conditions

1.3.5.4.1 Effect of curing time

As previously mentioned, the strength of cement-treated soils increases with time. Figure 1-39 shows the increase in compressive strength for different soils treated with different cement contents (Kawasaki et al., 1981).

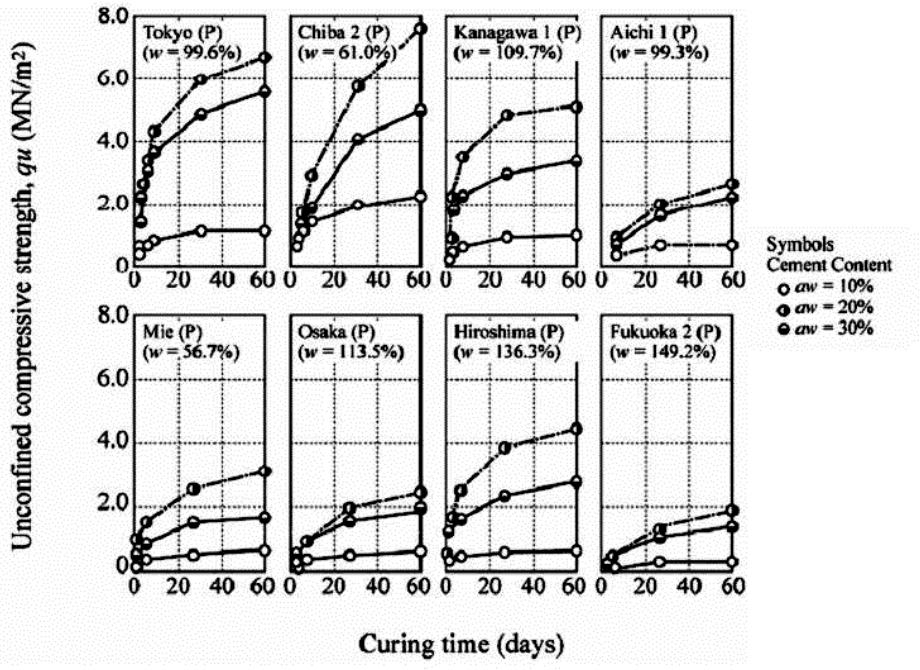

Figure 1-39 Compressive strength versus time for different soils treated with cement (Kawasaki et al., 1981).

1.3.5.4.2 Effect of confining pressure during curing

The stress–strain relation of treated soils strongly depends on effective confining pressure (Figure 1-40, Ajorloo et al., 2011). Tests carried out by Åhnberg (2006a) showed that the shear strength of cement and lime-treated soils increases if a confining stress is applied to the specimens during curing.

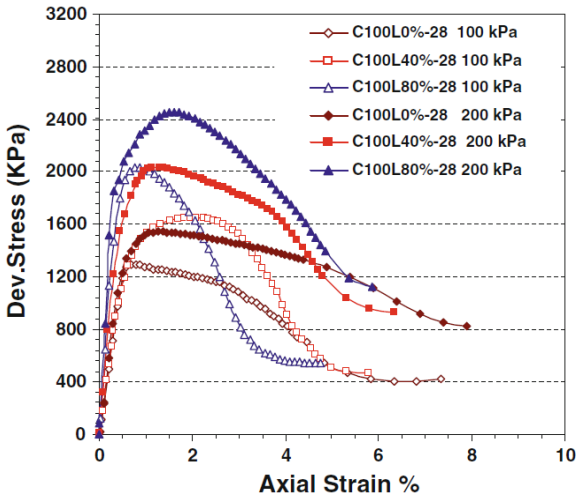

Figure 1-40 Effect of confining stress on stress-strain response of treated soils (Ajorloo et al., 2011).

1.3.5.4.3 Effect of curing temperature

The effect of temperature on compressive strength has been studied by Hirabayashi et al. (2009). An increase in curing temperature accelerates the cement hydration process and thus the development of strength in cement stabilised soils (Figure 1-41).

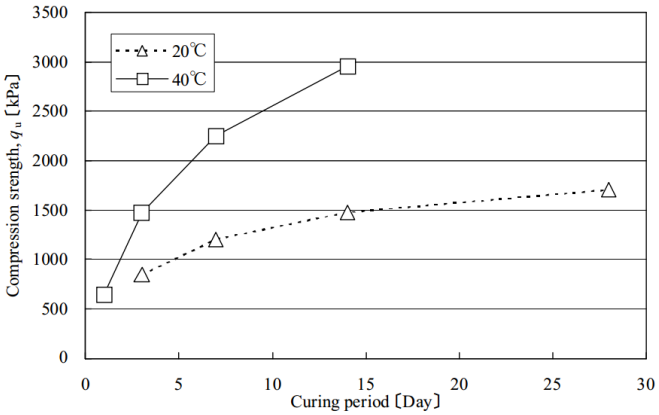

Figure 1-41 Effect of curing temperature on compressive strength (Hirabayashi et al., 2009).

1.3.6 Parameters used for design

Currently, there is no commonly accepted method for determining characteristic values of parameters used for design in soil mixing projects. Characteristic strength parameters for example depend on the type of soil, but also on the mixing technique, dosage and type of binder. The characteristic strength can be calculated as a certain fractile directly from a

sufficient number of measured values (Denies et al. (2012b) suggest a minimum of 20 values) or by assuming a certain distribution function applies to the data. Researchers found that characteristic strength values obtained assuming a normal distribution are very pessimistic. They are generally much lower than the fractiles calculated from the measured data and can in some cases lead to negative values (Denie et al., 2012b; Topolnicki and Pandrea, 2012). The use of a lognormal distribution seems more appropriate for the determination of characteristic strength values. The fractile used is generally taken at 5 %. Another approach to determine characteristic strength values consists in multiplying the average measured strength by a reduction coefficient. This method, described by Topolnicki and Pandrea (2012), is used in Japan and Germany. In Japan, the characteristic strength value f_c is given by:

$$f_c = \alpha \times q_{u,average}$$

where $q_{u,\,average}$: average strength and α : reduction coefficient ($\alpha<1$).

In Germany, the characteristic strength value f_c is defined as the minimum of three values:

$$f_c = \min \begin{cases} q_{u,\min} \\ \alpha \times q_{u,average} \\ 12 N.mm^{-2} \end{cases}$$

where $q_{u,min}$ is the minimum measured value, $q_{u,average}$ is the average strength determined from at least four specimens.

The value of α depends on the coefficient of variation of measured strengths, the reliability of overlapping of the columns, the characteristics of the untreated soil between the columns, the difference between the strength of specimens mixed in the laboratory and in situ. To obtain the value used for the design of deep mixing structures, both German and Japanese approaches divide the characteristic strength by a factor of safety:

$$f_{c,d} = \frac{f_c}{F_s}$$

where $f_{c,d}$ is the strength used for the design and F_s is a safety factor.

1.3.7 Conclusions

The properties of soil-cement mixtures produced by deep mixing lie between those of soil and concrete. The strength and deformation characteristics of treated soils are highly variable and difficult to control since they are influenced but many factors. These factors are essentially related to the type and amount of binder, the soil conditions (soil type, moisture content), the mixing conditions (degree of mixing) and the curing conditions. The parameters required for design and the tests performed to obtain these parameters also depend on the requirements and objectives of the projects. The variability of the material is responsible for the absence of a commonly accepted method for determining characteristic values of parameters used for the design of soil mixing projects.

In addition to the issues regarding the engineering properties, the durability and long-term behaviour of soils stabilised with cement is an important concern because of increasing ambition to use deep mixing to construct permanent structures.

1.4 Durability of stabilised soils

In the field, cement hydration and hardening of the material take place in different environmental conditions that may modify the effects of the treatment. This is especially the case in certain curing conditions or when the soils are polluted or contain significant amounts of chemical compounds that may alter the stabilisation process. The durability of treated soils is a function of many parameters. It depends on the properties of the binder, the soil, the execution of treatment and environmental conditions. Stabilisation techniques such as deep mixing are becoming increasingly used on sites of contaminated land (Perera et al., 2005). However, most of these applications were generally carried out based on treatability studies conducted for short curing times (usually 28 days). As a result, there are concerns regarding the long-term efficiency of the treatment.

Section 1.4.1 presents a summary of some available data on the long-term performance of soil mixing structures. Mechanisms which may affect the durability of soils treated with cement and the methods used to assess their impact are presented in section 1.4.2.

1.4.1 Long-term performance of soil mixing structures

Many researchers have published findings related to the long-term behaviour of soil mixing structures. Two aspects of the long-term performance of in situ soil-cement elements have been reported: an increase in strength after long curing times but also some degradation (loss in strength) of the materials.

1.4.1.1 Increase in mechanical properties over time

The design of soil mixing structures is generally based on the compressive strength measured after 28 days. However, the strength of soil-mix materials can continue to increase after longer curing times. Many authors have reported increases many years and even decades after construction (Terashi, 2003). According to Terashi (2005), this provides additional safety for the design of soil-cement elements.

Butcher (2005) studied the long-term behaviour of treated soils by excavating soil mixing columns four years after installation. The columns had been installed by the wet method in organic silty clay. The grout was composed of blast furnace slag (25 %) and Portland cement (75 %) with a water-cement ratio W/C of 0.50. The binder content was of 350 kg/m^3. Despite acidic groundwater and high sulfate content of the organic soil, the columns showed little signs of deterioration. However, the columns appeared quite heterogeneous. The results of X-ray diffraction analyses showed only minor attacks caused by sulfates.

Contaminated coarse grained soils were stabilised by deep mixing in West Drayton, in the south of England (Al-Tabbaa and Evans, 2003). The site was contaminated with heavy metals and organic compounds with concentrations of up to 3000 mg/kg of lead and copper, 2000 mg/kg of mineral oil and 9000 mg/kg of total petroleum hydrocarbons. Treatment was carried out by the wet method using a binder composed of fly ash cement, lime and bentonite. Cored samples were tested in compression up to five years after treatment. Permeability measurements were also performed. The results show an increase in strength during five years and a slight decrease in permeability (Figure 1-42 and Figure 1-43).

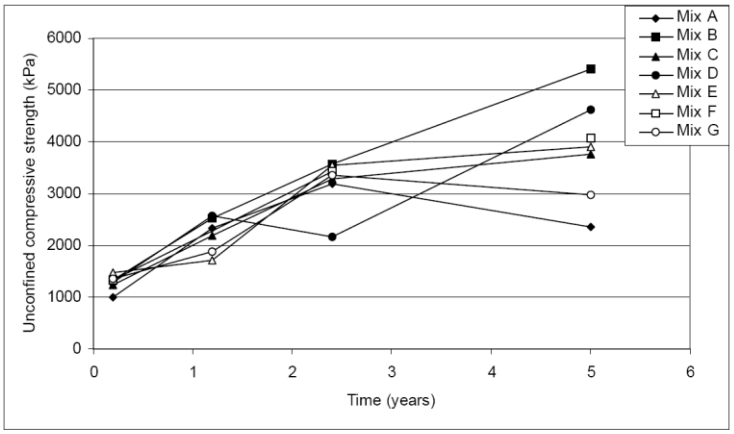

Figure 1-42 Unconfined compressive strength versus time up to five years (Al-Tabbaa and Evans, 2003).

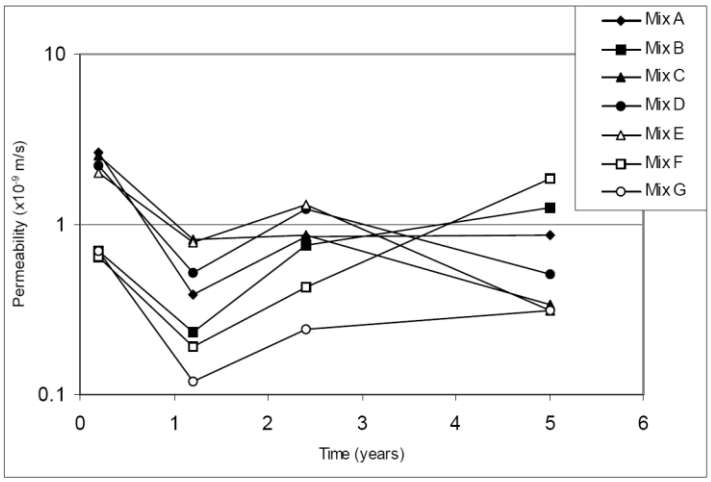

Figure 1-43 Permeability versus time up to five years (Al-Tabbaa and Evans, 2003).

Onimaru et al. (2009) studied the strength of specimens cored in soil-cement columns 8.5 years after construction. Alluvial sands had been stabilised with 200 kg/m^3 of cement. The average compressive strength of specimens from the inner axial part of the columns was 1.5 to 2 times higher after 8.5 years than the strengths measured after 28 and 60 days (Figure 1-44).

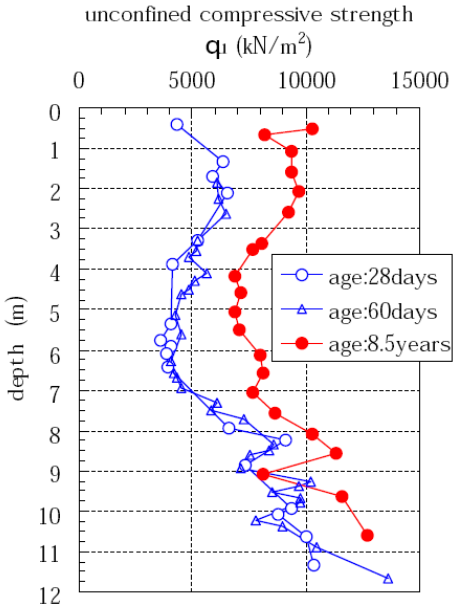

Figure 1-44 Increase in strength between 28 days et 8.5 years (Onimaru et al., 2009).

Hayashi et al. (2003) observed an increase in strength in the central part of soil mixing columns 17 years after construction.

Undisturbed samples of treated alluvial clay were cored at the port of Yokohama in Japan 20 years after mixing with cement was performed by the wet method with a dosage of 160 kg/m^3 (Ikegami et al., 2005). The compressive strengths obtained 3 months and 20 years after treatment are compared in Figure 1-45. The average strength after 3 months was 6.3 MPa with a coefficient of variation of 0.40. Twenty years later, the average strength had doubled (13.2 MPa with a coefficient of variation of 0.39).

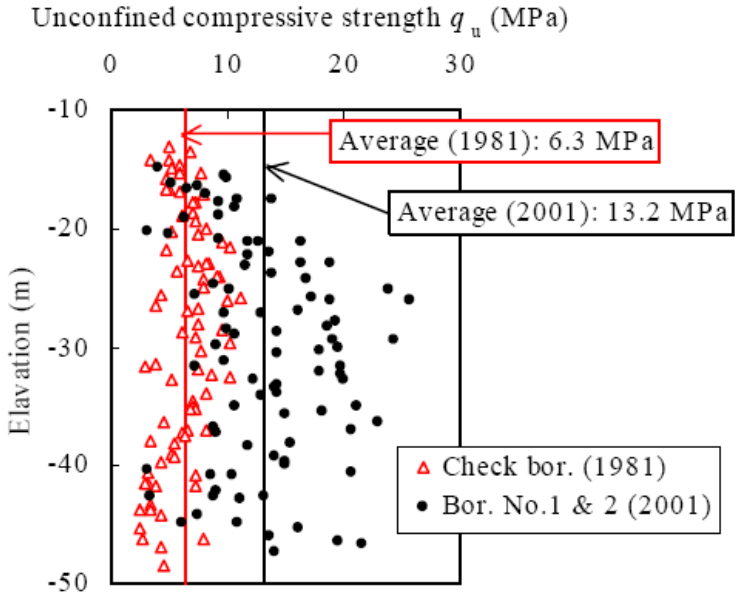

Figure 1-45 Increase in strength between 3 months and 20 years (Ikegami et al., 2005).

Many other Japanese studies report similar trends of long-term increases in strength in soil mixing elements (Figure 1-46).

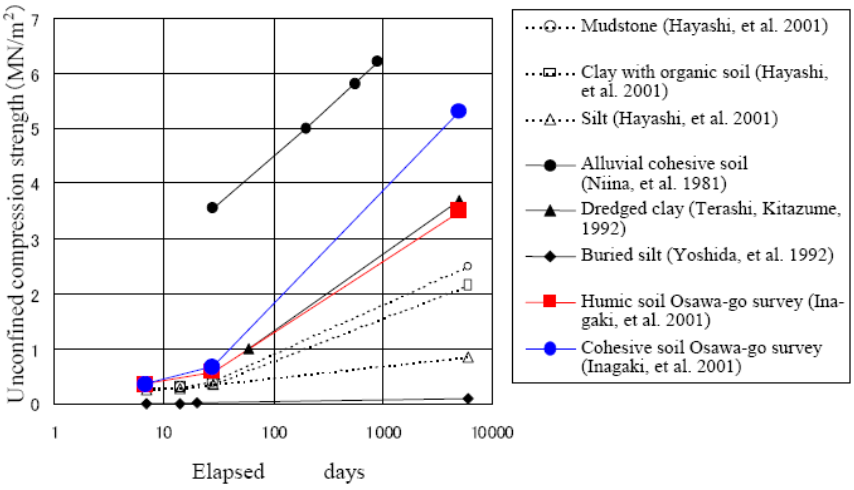

Figure 1-46 Long-term increase in strength compiled from various studies (Shinkawa et al., 2009).

In general, an increase of 2 to 3 times the initial strength can be expected 10 to 20 years after treatment. High W/C ratios can alter the long-term strength increase (Topolnicki, 2004). In general, little variation in density and water content are observed in the long-term (Shinkawa et al., 2009; Ikegami et al., 2005).

1.4.1.2 Long-term deterioration of stabilised soils

Some authors have also noted deterioration in soil mixing works over time (Kitazume et al., 2003; Hayashi et al., 2003; Terashi, 2005).

Several published articles have pointed out that the degradations are often related to environmental conditions and attributed to the outward diffusion of Ca^{2+} ions from the treated soil to the surrounding ground.

Laboratory tests performed by Kitazume et al. (2003) showed that degradation usually starts at the boundary between the treated and untreated soil and progresses inwards towards the central part of the soil mixing elements. Åhnberg et al. (1995) and Larsson et al. (2009) also confirmed these observations on the leaching of calcium in the laboratory.

Figure 1-47 shows the distributions of strength and calcium concentration as a function of the horizontal distance from the edge of a cement-treated soil element (Ikegami et al., 2005). A reduction in strength towards the boundary is clearly visible in this figure. In a 30 to 50 mm thick zone from the side boundary, the strength of the treated soil is much lower than in the rest of the soil mixing element. This drop in strength is clearly related to the reduction of the calcium content.

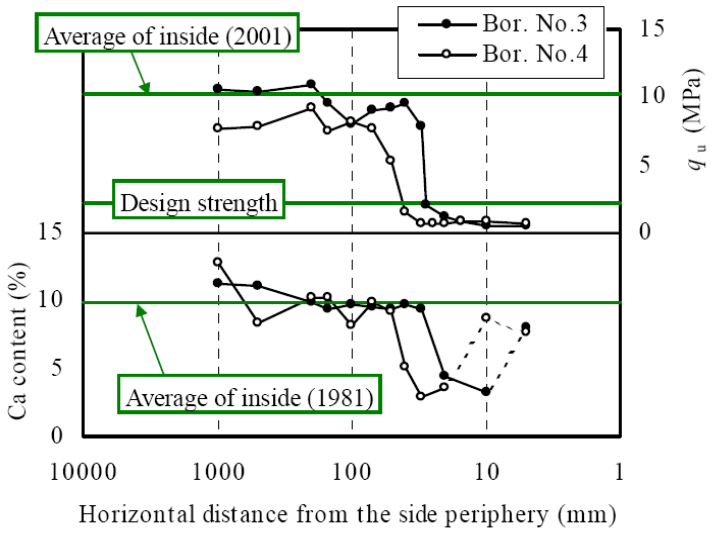

Figure 1-47 Strength and Ca content versus horizontal distance from the side periphery (Ikegami et al., 2005).

Similar observations were made by Löfroth (2005). An altered zone about 50 mm thick was observed around a column of soil-cement 10 years after treatment (Figure 1-48).

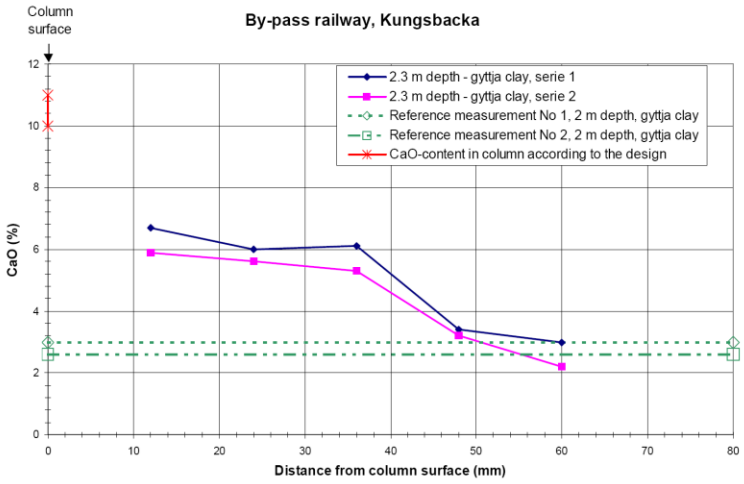

Figure 1-48 Ca content versus horizontal distance from column surface (Löfroth, 2005).

The results of several studies on the depth of degradation in treated soil elements over time have been compiled by Ikegami et al. (2005). Deterioration caused by the diffusion of calcium ions appears to be a slow process roughly proportional to the square root or logarithm of time. The extent of damage is often limited, between 10 and 100 mm after 10 to 20 years (Terashi and Kitazume, 2009, Topolnicki, 2004).

According to Topolnicki (2004), the deterioration caused by leaching of Ca is compensated by the long-term increase in strength and therefore does not significantly impact the overall durability of the structures.

However, there are other mechanisms which may affect the durability of soil-mix materials. Details on selected potential degradation mechanisms are given in the following paragraph.

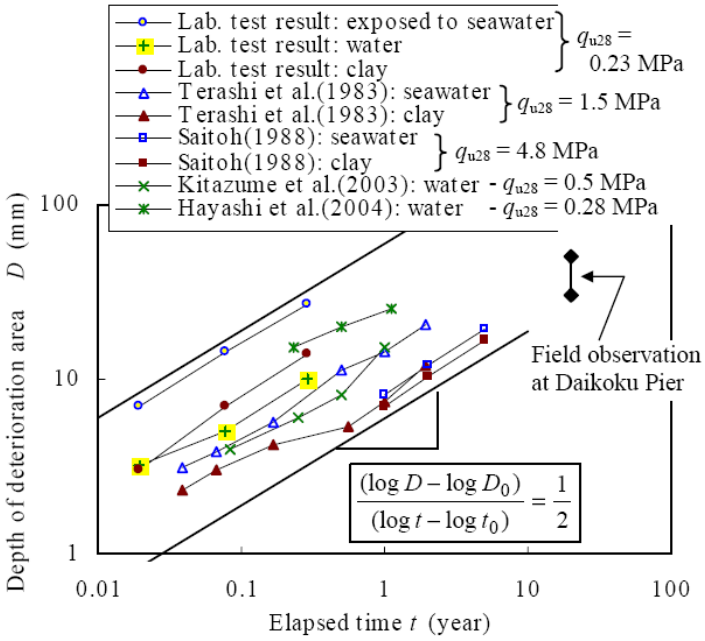

Figure 1-49 Depth of deterioration versus elapsed time (Ikegami et al., 2005).

1.4.2 Potential degradation mechanisms

1.4.2.1 Drying and wet/dry cycles

Many studies have focused on the mechanical properties of soils stabilised with cement and/or lime cured in a humid environment (Åhnberg, 2006b; Åhnberg and Johanson, 2005; Åhnberg et al., 2003; Ajorloo et al., 2012; Consoli et al., 2007; Consoli et al., 2010; Horpibulsuk et al., 2006; Miura et al., 2001; Porbaha et al., 2000; Szymkiewicz et al., 2012). However, there is very limited information available on the impact of desiccation (air drying) on the strength and stiffness of cement stabilised soils. For retaining walls, the changes in curing conditions caused by excavation adjacent to soil-cement elements (often carried out shortly after construction) may produce alterations in the mechanical properties of the stabilised soils and affect the durability of such structures. Wetting and drying cycles may be due to seasonal variations in groundwater levels or contact with rain water.

In a study on stiffness development in cemented paste backfill (an engineered mine backfill material having significantly higher void ratio and lower binder content than conventional mortars and concretes), Galaa et al. (2011) measured a significant reduction of compression wave velocities in specimens subjected to air-drying (Figure 1-50). The authors of this study indicate that, in some cases, the curing conditions (humidity and saturation) can be significantly more important than the binder content in controlling V_p.

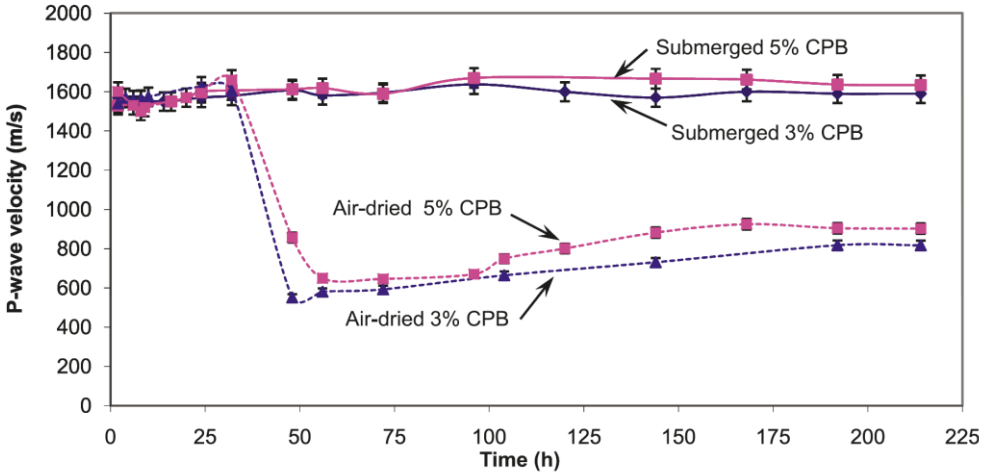

Figure 1-50 Development of P-wave velocity with time for drying and submerged CPB samples containing 3% and 5% binder (Galaa et al., 2005).

Resistance to wetting and drying cycles depends primarily on permeability according to Perera et al. (2005). A standard test (ASTM D559, 2005) has been developed to evaluate the durability of compacted specimens of cement-treated soils. The test evaluates the loss in mass after brushing of specimens subjected to 12 cycles of wetting and drying.

Wetting–drying durability tests following the ASTM standard performed on silty clay treated with Portland cement showed that the water–cement ratio has a dominant influence on the test results (Zhang and Tao, 2008). Lower mass losses (higher durability) were measured for soil-cement mixes with higher cement contents and lower water-cement ratios (Figure 1-51). Good correlations were found between the 7-day unconfined compressive strength and the soil-cement mass loss after cyclic wetting–drying.
Shihata and Baghdadi (2001) also assert that the compressive strength is an efficient indicator of durability in addition to the conventional mass loss.

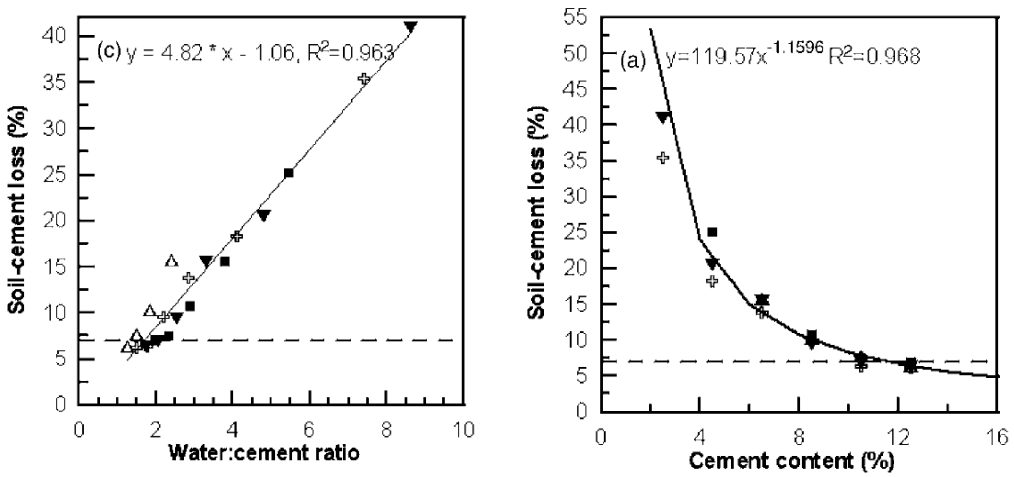

Figure 1-51 Results of wetting–drying durability tests: (a) soil–cement loss versus cement content; (b) soil–cement loss versus water–cement ratio (Zhang and Tao, 2008).

1.4.2.2 Carbonation

Carbonation is caused by the reaction of CO_2 with the cement hydration products: the C-S-H and calcium hydroxide are converted into calcium carbonate $CaCO_3$. The pH of the pore water is reduced by carbonation. The speed at which carbonation occurs depends on many factors such as CO_2 concentration, water content, permeability, type of binder, and temperature. Carbonation can have significant effects on the microstructure of stabilised soils. Volume changes associated with the precipitation of $CaCO_3$ can create cracking which increase the permeability and lead to a reduction in strength. However, the precipitation of $CaCO_3$ can also have the opposite effect and act as a cementing agent, increasing permeability and strength (Perera et al., 2005).

1.4.2.3 Sulfate attack

Sulfates are the most widely known compounds to affect soil stabilisation with lime and cement (Mitchell, 1986; Hunter, 1988; Mitchell and Dermatas, 1992; Rajasekaran et al., 1997; Wild et al., 1999).

The action of sulfates on cement depends on many parameters (concentration and type of sulfate, type of cement and dosage). Sulfates may have different origins. They can come from (Escadeillas and Hornain, 2008):

- additives in the cement,
- the external natural environment (in natural soils, for example),
- polluted groundwater infiltrations in industrial and urban environments.

Calcium components of stabilisers are known to react with free alumina and soluble sulfates in treated soils to form ettringite. The formation of minerals such as ettringite can cause swelling, cracking and loss of mechanical properties (Perera et al., 2005). The expansion mechanism is linked to the high crystallization pressures that develop in confined micropores (Escadeillas and Hornain, 2008). Experimental analyses on the swelling produced by ettringite in treated soils showed that ettringite or sulfate-induced swelling was higher in clays than in sands under similar chemistry and environmental conditions because of the crystallisation of ettringite in voids of different sizes in the different soil types (Puppala et al., 2005).

The curing conditions also have an impact on the behaviour of treated soils containing sulfates as shown by Cuisinier et al. (2011). In the case of lime, substantial variations in swelling have been observed by Wang et al. (2003) and Harris et al. (2004) in different humidity and temperature conditions.

Osman and Al-Tabbaa (2009) studied the durability of clay mixed in the laboratory with cement-bentonite and cement-zeolite grouts (zeolites are alumino-silicates with rigid hollow structures). The results show that the addition of bentonite in cement grouts reduces the resistance of stabilised clays to sulfate attack. The authors attribute this result to the high shrink-swell potential of bentonite which causes cracking when subjected to sulfate attack.

Shihata and Baghdadi (2001) studied the compressive strength of compacted silty sand-cement mixtures after wetting/drying cycles with saline ground water containing sulfates. They observed that the strength of soil-cement mixtures continues to increase up to 90 days despite the exposure to saline water. The strength then deteriorates to a residual value reached after 270 days (Figure 1-52).

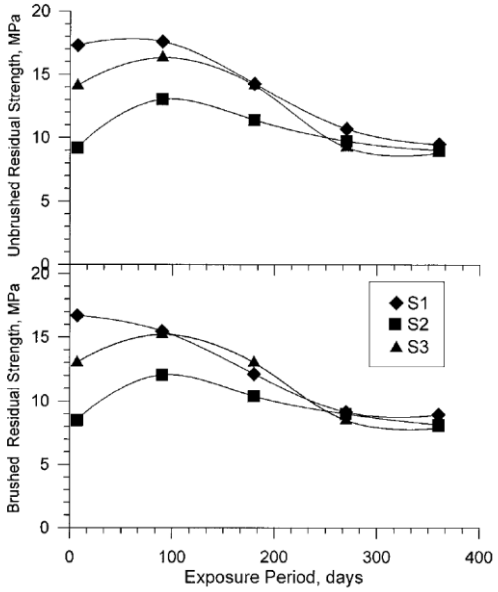

Figure 1-52 Variations of strength of different soils (S1-S2-S3) with exposure period to saline water (Shihata and Baghdadi, 2001).

The small strain shear modulus of cement-treated natural and artificial clays containing sulfates increases with curing time (up to 100 hours in Figure 1-53). However, the increase depends on sulfate content and curing conditions. Puppala et al. (2006) found that improvements in shear modulus were lower for soil specimens containing sulfates continuously soaked under water compared to those cured in a humidity room.

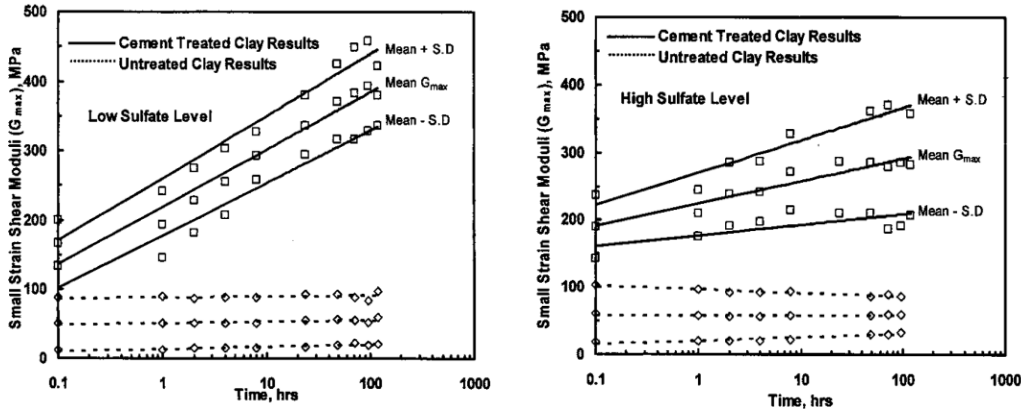

Figure 1-53 Small strain shear moduli of untreated and cement-treated clays (Puppala et al., 2006).

Cements with improved sulfate resistance properties have been developed by reducing the amount of tricalcium aluminate (C_3A) in Portland cements (CEM I) since this is the

compound which is specifically attacked by sulfates, and also by replacing Portland cement by a suitable granulated blastfurnace slag (CEM III) (Hewlett, 2003) .

Puppala et al. (2004) investigated the effectiveness of sulfate resistant cements (ASTM Types I/II and V) for the treatment of sulfate-rich soils. They found that the tested cements improved the physical properties and engineering characteristics of sulfate-rich soils and decreased the swelling potential. The unconfined compressive strength and small strain shear modulus (Figure 1-54) were enhanced by treatment.

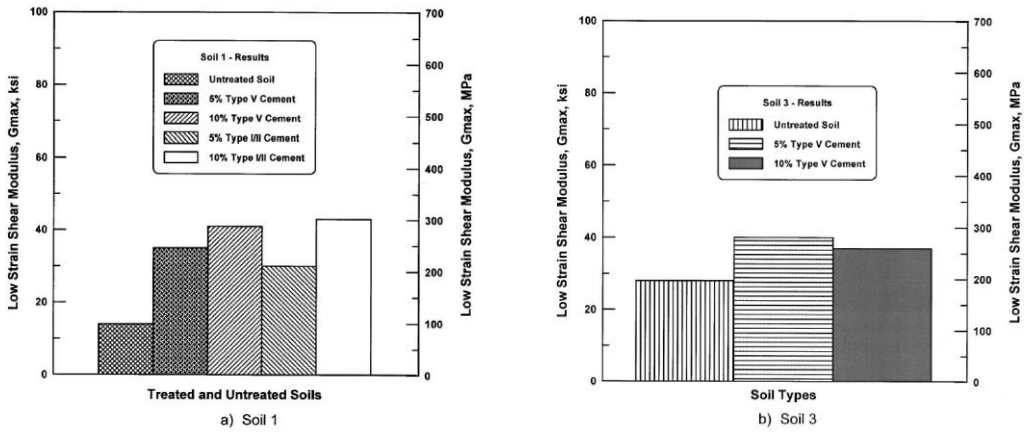

Figure 1-54 Influence of cement treatment with sulphate-resistant cements on small strain shear modulus of sulfate rich soils (Puppala et al. 2004).

The long-term effects of sulfates on the stiffness of soils stabilised with cement are not well known. An experiment carried out by Dupas and Pecker (1979) showed that the small strain stiffness of 6 month old specimens percolated for 15 days with a sodium sulfate solution drops by a factor of 2 to 4.

1.4.2.4 Effects of exposure to chlorides

Data on the effects of chlorides on the engineering properties of cement-treated soils is very limited.

For concretes, the main issue related to exposure to chlorides is the corrosion of steel reinforcements but chlorides also interact with the cement hydration products (Perera et al., 2005). Two mechanisms are involved in the action of sodium chloride on cement:

1 - Consumption of calcium ions from portlandite (CH) and calcium silicate hydrates (C-S-H) to produce soluble calcium chloride:

$Ca(OH)_2 + 2NaCl \leftrightarrow CaCl_2 + 2NaOH$

2 - Formation of Friedel's salt, by reaction between chlorides and tricalcium aluminate C_3A:

$C_3A + CaCl_2 + 10H_2O \leftrightarrow C_3A.CaCl_2.10H_2O$ (Friedel's salt)

It is generally accepted that the penetration of chlorides does not cause expansion or cracking in cement-based materials. Calcium chloride ($CaCl_2$) is used as an accelerating admixture for cement (Hewlett, 2003). Modmoltin and Voottipruex (2009) observed beneficial effects of chlorides on the strength of cement-treated kaolinite and bentonite.

Xing et al. (2009) studied the effect of different concentrations of Cl^- and SO_4^{2-} on the compressive strength of clay stabilised with Portland cement at different curing times. Figure 1-55 shows the effects on the stress-strain relationship 28 days after treatment. They found that increasing concentrations of Cl^- and SO_4^{2-} have deleterious effects on compressive strength. Horpibulsuk et al. (2012) also observed that the strength of clay treated with Portland cement decreases as the NaCl content increases (Figure 1-56).

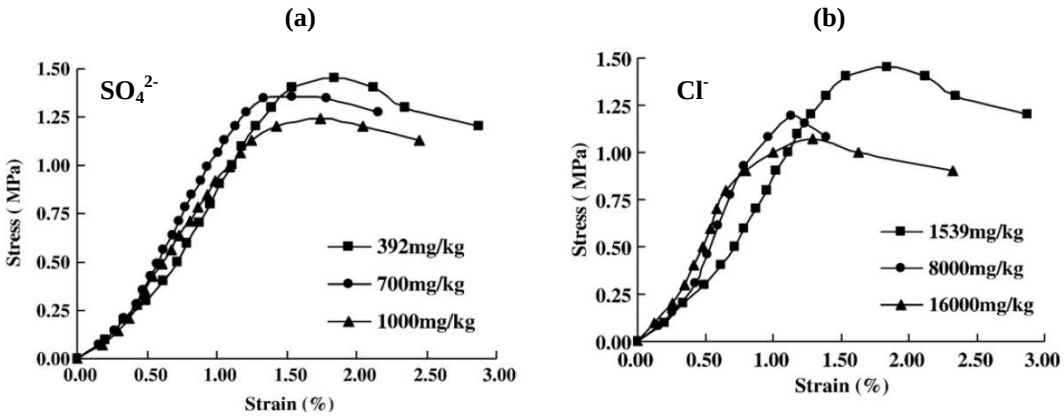

Figure 1-55 Effects of changing Cl^- (a) and SO_4^{2-} (b) content on the stress–strain behaviour of soil–cement (Xing et al., 2009).

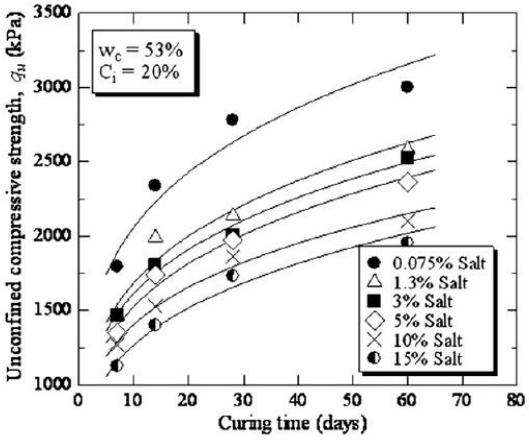

Figure 1-56 Strength development with time of saline clay for various salt contents (Horpibulsuk et al., 2012).

Al-Tabbaa and King (1998) studied the durability to wet-dry cycles and the permeability of sand mixed in the laboratory with slurry composed of a mixture of Portland cement, PFA and bentonite. The sand was contaminated with sodium chloride (NaCl) and two other pollutants. The results showed that the behaviour of stabilised contaminated soils depends on the type of pollutant but also on the concentration. In the case of NaCl, permeability changes were

attributed to the fact that sodium chloride promotes flocculation of clay minerals and hence increases the permeability of the material.

1.4.2.5 Effects of organic contaminants

According to the Basol database from the French Ministry of Ecology, Sustainable Development and Energy (http://basol.ecologie.gouv.fr), hydrocarbons are present in 36.7 % of the 2617 identified contaminated sites in France. Data on the mechanical properties of stabilised soils containing organic contaminants such as diesel oil is very limited in the literature. Diesel oil presents a non-volatile behaviour and is not miscible with water. Cruz et al. (2004) observed a reduction of unconfined compressive strength and a slight decrease in permeability with increasing diesel oil content (Figure 1-57 and Figure 1-58).

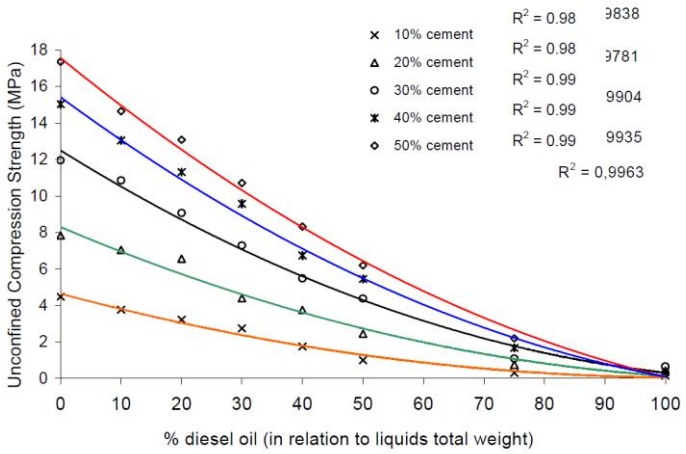

Figure 1-57 Effects of diesel on the unconfined compressive strength of silty sand treated with Portland cement after seven days of curing (Cruz et al., 2004).

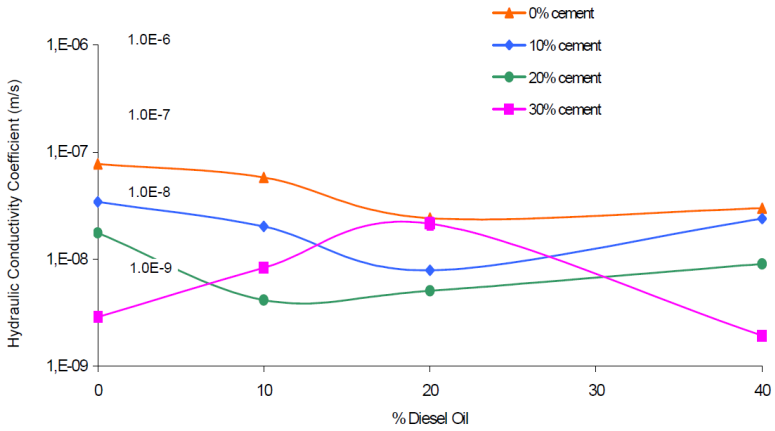

Figure 1-58 Effects of diesel on the permeability of silty sand treated with Portland cement after seven days of curing (Cruz et al., 2004).

1.4.3 Conclusions

Many published studies have reported long-term strength increases in deep mixing elements. In some cases, deterioration related to environmental conditions and attributed to the outward diffusion of Ca^{2+} ions from the treated soil to the surrounding ground have also been

observed. However, this deterioration is believed to be compensated by the long-term increase in strength and therefore does not significantly impact the durability of soil mixing structures.
Other mechanisms which may impact the durability of soil-mix materials have been identified. These include the effects of certain chemical compounds and curing conditions. There is very limited information available on the impact of desiccation (air drying) on the strength and stiffness of cement stabilised soils although drying may occur during excavation for retaining walls constructed using soil-cement elements. The deleterious effects of sulfates on concrete and stabilised soils have been widely studied although the impact on the long-term properties remains unclear, especially on stiffness. Contradictory results can be found in the literature concerning the effects of NaCl on the strength of cement-treated soils. Although hydrocarbons are largely present in contaminated sites, data on the long-term properties of stabilised soils containing organic contaminants such as diesel oil is very limited.

1.5 Summary and objectives of this study

Published information on different deep mixing construction techniques and data concerning the engineering properties and durability of treated soils were presented in this chapter.
The literature review highlights the following research needs:

- The deep mixing mechanisms are directly related to the rheological properties of the materials being mixed. However, knowledge of the rheological characteristics of stabilised soils in the fresh state is very limited.
- Strength and modulus are essential parameters for the design of soil-mix structures. Reliable estimates of static stiffness require the use of local strain measurements yet external strain measurements are still widely used. There is a lack of information on the effects of soil type and dosage on the relations between strength and stiffness obtained with local strain measurements.
- The characteristics and homogeneity of in situ soil-mix materials depend on many factors. The relation between the properties of field and laboratory samples remains unclear. The mixing conditions on site are considerably different from laboratory procedures. Some authors have attempted to establish empirical relations between strengths achieved in the laboratory and in the field. Very limited information is available on the influence of mixing conditions on stiffness.
- The sampling method also influences the characteristics of treated soils. Contradictory effects on measured properties of treated soils have been reported.
- Non-destructive geophysical methods are used to assess the dynamic modulus of laboratory specimens and offer promising perspectives in terms of quality assessment and quality control of stabilised soils. To estimate mechanical properties based on measured dynamic parameters, empirical relations with strength are necessary. Few studies have verified the relevance of such correlations to field samples.
- Many published studies have reported long-term strength increases in deep mixing elements. Some mechanisms which may affect the durability of soils treated with cement are identified (effects of chemicals compounds such as sulfates and chlorides,

curing conditions involving drying or wet-dry cycles). Further research is required to assess the effects of these mechanisms on the medium to long-term strength and stiffness properties of soils stabilised with cement.

This research focuses on the properties of soil-cement mixtures produced in the laboratory and in situ by wet deep mixing. Given the aforementioned research needs, the three main objectives of the present study are:

1) to examine the mechanical properties of soils stabilised in the laboratory in fresh and hardened states:

- For fresh soil-cement mixtures, the aim of this research is to investigate the effects of the addition of cement on the rheological characteristics of soils.
- For hardened soil-cement mixtures, the objectives are:
  - to assess long-term growth in strength and stiffness with time for different soils treated with varying quantities of cement and cured in the laboratory,
  - to examine the relationship between strength and static modulus obtained with local strain measurements,
  - to study possible correlations between properties measured by non-destructive techniques and mechanical parameters determined by destructive tests.

2) to compare the results from soils mixed in the laboratory with soils treated in situ by deep mixing using the wet method. The purpose is:

- to evaluate the strength and stiffness of in situ deep mixed soils,
- to determine the effects of sampling and mixing conditions on the properties of treated soils.

3) to study the durability of soil-cement mixtures against potential degradation mechanisms:

- by assessing the effectiveness of blastfurnace cement to counter the potential effects of certain chemical compounds on long-term strength and stiffness,
- by considering the influence of drying on the properties of treated soils.

Each of these three objectives is addressed in a separate chapter. Details on the different materials, experimental techniques and testing programs followed in this research are given in Chapter 2.

Chapter 2. Materials, methods and experimental programs

2.1 Introduction

In this chapter, the characteristics of the soils and binders used in this study are presented.
The specimen preparation methods and the experimental programs followed to examine the properties of treated soils in fresh and hardened states are explained.
Finally, the laboratory testing procedures used to determine the characteristics of soil-mix materials are presented.

2.2 Soils and binders

Three artificial soils and two natural soils were mixed in the laboratory with cement. The natural soils were taken from a test site on which soil-cement columns were installed by Soletanche Bachy.

2.2.1 Artificial soils

The artificial soils used in this study are Fontainebleau sand (FS), which is a silica sand from the south of the Parisian basin, and an artificial silt (AS) composed of a mixture of silica flour (crushed silica sand) and Speswhite kaolin. The proportions of silica flour and kaolin in the silt are of 70 % and 30 % by weight respectively. Fontainebleau sand has a uniform distribution of sub-rounded quartz grains (Figure 2-2 (a)) whereas the quartz grains in the artificial silt are angular (Figure 2-2 (c)). The silt has a liquid limit W_L of 27 % and a plasticity index PI of 11 %. In addition, Speswhite kaolin (SK) alone was mixed with cement to study the properties of soil-cement materials in the fresh state. Speswhite kaolin has a liquid limit W_L of 55 % and a plasticity index PI of 25 %.

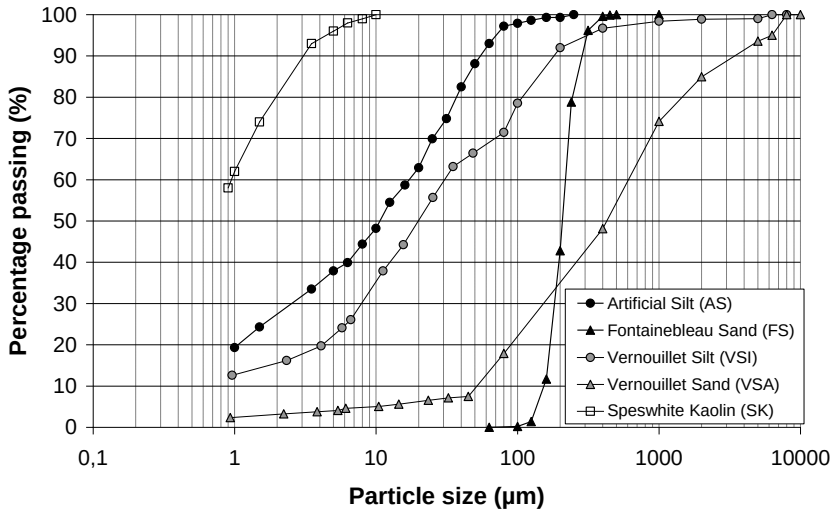

Figure 2-1 Grain-size distribution curves of soils mixed in the laboratory with cement.

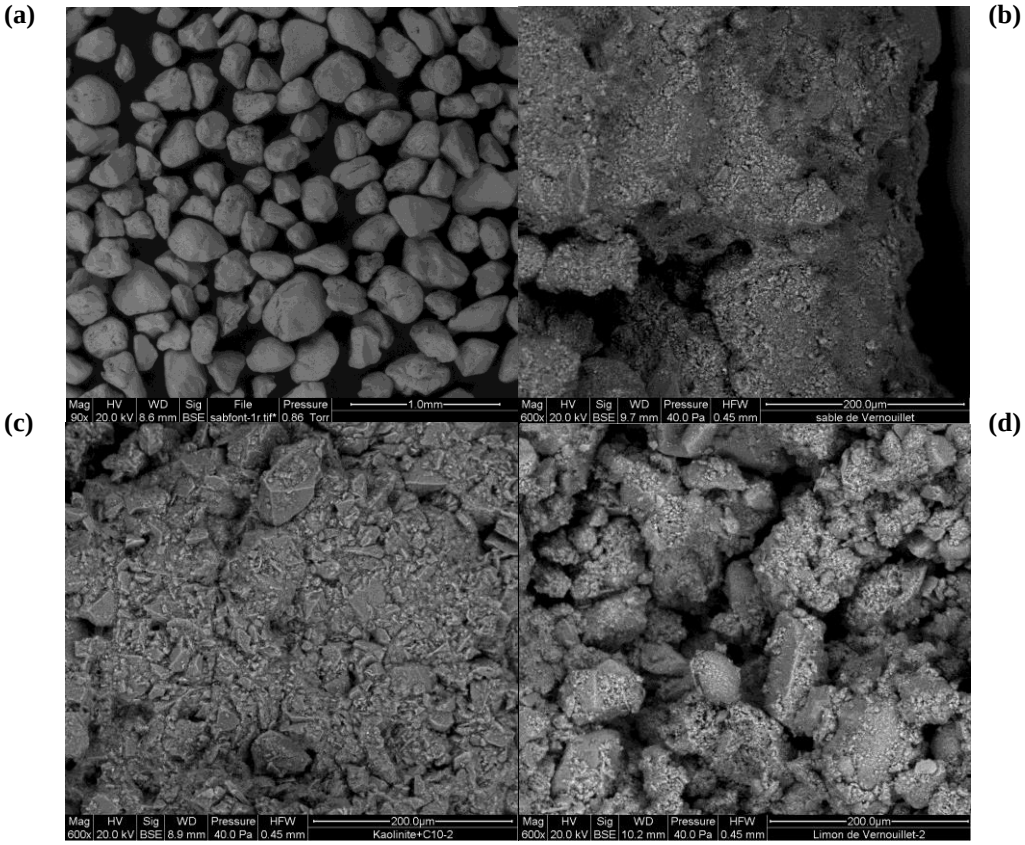

Figure 2-2 Scanning electron microscope images of untreated soils (a) Fontainebleau sand; (b) Vernouillet sand (c) Artificial silt; (d) Vernouillet silt.

2.2.2 Natural soils

Soil-cement columns were installed by deep mixing at the RUFEX test site in Vernouillet (Yvelines), France. A preliminary site investigation was carried out to determine the ground conditions. The ground investigation revealed that the site was covered by a 3 m thick layer of brownish beige silt. Underlying the silt is a layer of dense brownish orange gravely sand. Disturbed samples of the silt (VSI) and sand (VSA) were taken from trial pits. The geotechnical properties of the soils used in this study are summarised in Table 2-1. Grain size distributions and SEM images and are presented in Figure 2-1 and Figure 2-2 respectively.

Soil		Artificial silt (AS)	Speswhite kaolin (SK)	Fontainebleau Sand (FS)	Vernouillet Silt (VSI)	Vernouillet Sand (VSA)
In situ moisture content w (%) (CEN, 2005a)		/	/	/	11.9 to 19.7	5 to 7.6
% passing 80 µm (CEN, 2005b)		97.2	100	0	72.5	17.9
Methylene Bleu Value MBV (AFNOR, 1998)		/	/	0.1	1.38	0.71
Atterberg Limits (CEN, 2005d)	w_L (%)	27	55	/	30	/
	PI (%)	11	25	/	10	/

Table 2-1 Summary of soil characteristics.

2.2.3 Binders

Two cements were used in this study.

The main binder is blast furnace cement manufactured by Calcia (Rombas factory) containing 85 % granulated ground blast furnace slag (European classification: CEM III/C 32.5 N CE PM-ES NF "HRC"). This cement is widely used in France for foundation works. It presents a slow strength development with an initial setting time of 4 hours after hydration. It is resistant to sulfates and chlorides.

In addition, Portland cement produced by Calcia in the Gargenville factory (European classification: CEM I/A 52.5 L) was also used.

The cement contents C (%), moisture contents W (%) and the cement-water ratios C/W (or water-cement ratios W/C) are defined as follows:

- C: ratio of the mass of dry cement to the mass of dry soil,
- W: ratio of the mass of water to the mass of dry soil + cement,
- C/W: ratio of the mass of dry cement to the mass of water.

2.3 Specimen preparation procedures and experimental program for fresh materials

For fresh soil-cement mixtures, the aim of this research is to investigate the effects of the addition of cement on the rheological characteristics of soils in relation to the installation process of deep mixing elements.

2.3.1 Specimen preparation

Speswhite kaolin, cement slurries and kaolin-cement mixes were prepared to investigate the properties of mixtures in the fresh state immediately after mixing. For the preparation of the Speswhite-cement samples, the appropriate amount of tap water to reach the target water content was added to the dry soil. Dry cement was then added to the humidified clay and mixed using a laboratory mixer with a 4-bladed propeller for 5 to 10 minutes at a rotation speed of 2000 rpm. The time between sample preparation and testing was less than 15 minutes. For the cement slurries, dry cement was mixed with tap water for 10 minutes also at a speed of 2000 rpm.

2.3.2 Experimental program for fresh material

The experimental program for fresh mixtures is presented in Table 2-2, Table 2-3 and Table 2-4. Kaolin alone was tested at 3 different moisture contents. Flow curves of cement slurries were established for 5 different water-cement ratios. In total, 7 kaolin-cement mixes were tested. The cement contents C (weight of dry cement / weight of dry clay) varied between 5 and 20 % and the total moisture contents between 43 % and 174 %. To study the effects of an increase in cement content, 4 kaolin-cement mixtures were prepared with a water/clay ratio

equal to 100 % and with varying cement contents between 5 % and 20 % (Table 2-4). The 3 other kaolin-cement mixes were prepared with a cement content of 15 % and different water contents.

	Moisture content W (%) = weight of water/weight of dry solids				
Kaolin	200 %	150 %	100 %	-	-

Table 2-2 Characteristics of the kaolin suspensions.

	Water-Cement ratio W/C = weight of water/weight of dry cement				
Cement	0.60	0.55	0.50	0.45	0.42

Table 2-3 Characteristics of the cement slurries.

Mix	Cement content C (%)	Moisture content W (%)	weight of water/weight of dry clay (%)
SK5W95	5 %	95 %	100 %
SK10W91	10 %	91 %	100 %
SK15W87	15 %	87 %	100 %
SK20W83	20 %	83 %	100 %
SK15W74	15 %	74 %	200 %
SK15W130	15 %	13 0 %	150 %
SK15W43	15 %	43 %	50 %

Table 2-4 Characteristics of the kaolin-cement suspensions.

2.3.3 Testing apparatus and procedure

Tests on fresh mixtures were carried out using a MCR 501 rheometer manufactured by Anton Paar equipped with parallel plates and the ball measuring system.

The parallel plates geometry consists of two coaxial disks. The material placed between the disks is sheared by their relative rotation. The parallel plates used in this study were of 50 mm in diameter. The gap between the plates was 1 mm.

The ball measuring system consists of a 12 mm diameter sphere that is dragged through a sample volume of approximately 0.5 L (Figure 2-3) implemented in a standard rheometer (Schatzmann et al., 2009). The rotating speed was controlled and torque measurements were recorded by a computer. The shear stress and the shear rate were then calculated.

Figure 2-3 The BMS of Müller et al. (1999) implemented in a standard rheometer (Schatzmann et al., 2009).

It is well known that clay–water suspensions are thixotropic materials (Coussot, 1997). To obtain consistent and reproducible measurements, specific rheometric procedures must be executed. The procedure used is similar to the method described by Pantet and Monnet (2007). In order to define a structural reference state, measurements with the parallel plate geometry started with an initial shearing phase (constant shearing at a rate of 300 s^{-1} during 60 s), followed by a rest period of 120 s. Then, the material was subjected to increasing and decreasing shear rates. The difference between the increasing and decreasing values gives indications about the thixotropic properties (i.e. structural evolution) of the material. Flow curves were established for shear rates between 0.01 and 300 s^{-1} with the parallel plates geometry and between 0.01 and 50 s^{-1} with the ball measuring system.

2.4 Specimen preparation procedures and experimental programs for hardened materials

The properties of hardened soil-cement mixtures were examined on specimens of soils treated in the laboratory and in situ by wet deep mixing.

2.4.1 Specimen preparation and sampling

2.4.1.1 Specimen preparation for soils mixed in the laboratory

Mixing trials were carried out in the laboratory using two artificial soils and two natural soils from Vernouillet to assess long-term growth in strength and stiffness with curing time and to examine the relations between strength, static modulus and dynamic modulus. Soil–cement mixing in the laboratory was performed using a mortar mixer. The sample preparation method used is similar to the procedures recommended in many soil mixing reference guides (AFNOR, 2005, EuroSoilStab 2002). Firstly, the appropriate amounts of soil, then dry cement and finally dry bentonite (if any) were placed in the mixer and tap water was added. The constituents were mixed for ten minutes. The fresh mixtures were then poured in cylindrical moulds of 52 mm internal diameter. To reduce the amount of trapped air bubbles, the soil–cement pastes were compacted in three layers by lightly tapping the moulds on a horizontal surface. To ensure endogenous curing conditions, the moulds were sealed and placed in hermetic bags containing a wet textile to preserve the humidity during curing. They were stored at a constant curing temperature of 20 °C. Their extremities were cut and smoothed to a height to diameter ratio of 2 (approximately 100 x 50 mm). The specimens were then precisely measured, weighted and tested after different curing times.

2.4.1.2 Sampling and specimen preparation for soils mixed in situ

Block samples (Figure 2-4) were taken at different depths from eight soil-cement columns excavated in Vernouillet to determine the mechanical properties of the soil-mix material. Cylindrical specimens of approximately 100 by 50 mm (height to diameter ratio of 2) were cored from these blocks in the laboratory (Figure 2-5).

Figure 2-4 Coring of soil-cement specimens from block samples.

Figure 2-5 Cored specimens from block samples.

In addition, wet-grab samples were taken during column installation in Vernouillet and three other sites. The fresh soil-cement mixtures were sampled directly from the surface or using a sampling tube pushed into the fresh column down to the desired depth (Figure 2-6). The fresh spoil was placed in cylindrical moulds of 100 by 50 mm and 220 by 110 mm (height to diameter ratios of 2). Tapping of the moulds on a horizontal surface was performed to compact the fresh soil-cement mixtures.

Figure 2-6 Spoil return to surface and sampling tube used for wet-grab samples.

The cored and wet-grab specimens were stored in tap water at a constant curing temperature of 20 °C. Their extremities were cut and smoothed. The specimens were then measured, weighted and tested.

2.4.2 Experimental programs for soils mixed in the laboratory

Three distinct experimental programs were followed to study the mechanical properties and the durability of soils treated in the laboratory. These programs were carried out:

- to examine the long-term mechanical characteristics of hardened soil-cement specimens (section 2.4.2.1),
- to assess the effectiveness of blast furnace cement to counter the potential effects of certain chemical compounds on long-term strength and stiffness (section 2.4.2.2),
- to study the influence of drying on the properties of treated soils (section 2.4.2.3).

2.4.2.1 Experimental program to investigate the properties of soils stabilised in the laboratory

The characteristics of the soil-cement mixes prepared to investigate the mechanical properties of soils stabilised in the laboratory are given in Table A-1 (artificial soils) and Table A-2 (natural soils) of Appendix A. The cement and moisture contents tested in this study were chosen to simulate those used in wet deep mixing projects carried out in France.

Mixtures are referenced in the tables, figures and text as follows:

- the first letters stand for the type of soil ("FS" for Fontainebleau sand and "VSI" for Vernouillet silt for example),
- the following numbers refer to the cement content in kg/m^3,
- the reference continues with the letter W and the value of the moisture content in %,
- finally, if bentonite is added in the mixture, the reference ends with B50.

Two mixes were prepared with the artificial silt (AS) and CEM III cement (Table A-1). Both mixes had the same cement-water ratio C/W but different cement and moisture contents.
Five mixes were made with Fontainebleau sand (FS): three contained CEM III while CEM I was used for the other two (CEM I is indicated as "-I-" in the mix references). The cement contents in kg/m^3 are calculated assuming dry unit weights of 1450 kg/m^3 for the artificial silt and 1680 kg/m^3 for the Fontainebleau sand. All the Fontainebleau sand mixes had cement contents of 200 kg/m^3. The moisture contents were selected to ensure a sufficient fluidity of the fresh soil-cement mixtures. The mixes with the artificial silt had moisture contents of 40 % and 57 %. Water contents of 15 %, 20 % and 35 % were tested for the Fontainebleau sand. Bentonite was required to stabilise the mixture with a moisture content of 35 % (FS200W35B50). The effects of bentonite on the characteristics of treated Fontainebleau sand were investigated by adding the equivalent of 50 kg of bentonite per cubic meter of sand in mix FS200W20B50.

For the natural soils from Vernouillet (Table A-2), cement contents in kg/m^3 were calculated based on assumed in situ unit weights of 1750 kg/m^3 for the silt (VSI) and 2000 kg/m^3 for the sand (VSA). Mix VSI300W57 was prepared with the same cement and moisture contents as

AS300W57. The cement and moisture contents of the other mixes with the natural silt and sand were chosen to simulate those used in three columns installed in Vernouillet.
It is important to note that the mass of bentonite was not taken into account for the calculation of the moisture contents as the quantities used were small.

Tests performed on specimens of soil-cement mixes prepared in the laboratory are given in Table A-3 (Appendix A). Details on the testing equipment and procedures are given in section 2.5. The results of this program are presented in Chapter 3.

2.4.2.2 Experimental program to investigate the effects of chemical compounds

Assessing the individual effects of a given chemical compound on soil stabilisation with natural soils can be difficult. Artificial soils (artificial silt and Fontainebleau sand) were preferred to assess the impact of chemical compounds on the long-term properties because their mineralogical composition is known and controlled. Quartz and kaolin are widely present in natural soils.

Sodium chloride was selected given the contradictory data found in the literature concerning the effects of NaCl on the properties of treated soils. Calcium sulfate ($CaSO_4$, 2 H_2O) was also considered in this study although the negative effects on concretes and treated soils have already been demonstrated. The objective is to assess the usefulness of blastfurnace cement (CEM III) to counter the potential effects of these two compounds on the long-term strength and stiffness of treated soils.

A crucial factor in investigating the effects of chemical compounds is the amount of each chemical compound that should be added to the soil samples. The selected concentrations are given in Table 2-5. The concentrations of sulfates and chlorides were chosen slightly above the maximum concentrations reported in France (Cuisinier et al., 2011). The concentration of sodium chloride is similar to the concentrations found in soils near the sea coast. Similar concentrations of calcium sulfate can be found in soils in the northern parts of France.
In addition to NaCl and $CaSO_4$, diesel oil was also added in soil-cement mixes. The chosen concentration was reported by Namkoong et al. (2002).

The compositions of the tested mixes are given in Table A-4 (Appendix A). The soil-cement specimens were prepared as described in section 2.4.1. The required amounts of chemical compounds were mixed with water before they were added to the dry soil-cement mixture. The mixes of Fontainebleau sand treated with CEM I which contain $CaSO_4$ (FS-I-200W15-CaSO4-endo and FS-I-200W20-CaSO4-endo) serve as references to verify the well-known negative effects of sulfates on Portland cement. The other mixes of Fontainebleau sand and artificial silt treated with CEM III all had the same cement-water ratio of 0.30. The curing conditions were endogenous for all mixes except FS200W35B50-Imm, FS200W35B50-CaSO4-Imm and FS200W35B50-Imm-CaSO4. The specimens from those batches were stored in water (tap water for FS200W35B50-Imm, tap water in which 1g of $CaSO_4$ / L was

dissolved in the case of mixes FS200W35B50-CaSO4-Imm and FS200W35B50-Imm-CaSO4).

Chemical compounds	Concentration	
	Internal exposure (added to the soil cement mixtures)	External exposure (specimens immersed in water containing chemical compound)
Calcium sulfate ($CaSO_4$, $2H_2O$)	10 g per kg of dry soil	1g/L
Sodium chloride (NaCl)	2 g per kg of dry soil	/
Diesel oil	10 g per kg of dry soil	/

Table 2-5 Concentration of the chemical compounds.

Tests performed on specimens of soil-cement mixes prepared to investigate the effects of chemical compounds are given in Table A-5 (Appendix A). In addition, microstructural investigations were also carried out (mercury intrusion porosimetry, x-ray diffraction analyses and scanning electron microscopy).
Details on the testing equipment and procedures are given in section 2.5. The results of this program are presented in Chapter 5 (section 5.1).

2.4.2.3 Experimental program to investigate the effects of drying and wetting/drying cycles

For retaining walls constructed using soil-cement elements, drying may occur during excavation (often carried out shortly after construction) as the material is exposed to air. Wetting and drying cycles may be due to seasonal variations in groundwater levels or contact with rain water. The purpose of this program is to investigate the effects of different curing conditions (immersion in water, cycles of wetting and drying, air curing) on the mechanical properties of specimens of soil treated with blast furnace cement in the laboratory.
The effects of drying and wetting-drying cycles were examined on three artificial soil-cement mixes: FS200W20, AS300W57 and AS200W40 (Table A-1).

Laboratory tests carried out on the soil-cement specimens included free-free resonance (FFR) testing and unconfined compression tests. FFR testing was used to determine the small strain shear modulus G_0 whereas the compression tests were performed to evaluate the unconfined compressive strength q_u and static stiffness E_{50}. Details on the testing procedures are given in section 2.5. The small strain shear modulus was chosen to investigate the effects of drying on the solid fraction of soil-cement specimens as G_0 is not significantly affected by changes in moisture content (shear waves do not propagate in water).

Preliminary compression tests were carried out on specimens from both mixes of artificial silt treated with CEM III cement placed in a climatic chamber at a temperature of 20°C and a relative humidity of 65 % after 28 days of curing in endogenous conditions (mixes AS200W40-ac and AS300W57-ac). Unconfined compression tests were performed on these specimens after 90 and 180 days.

In addition, 45 soil-cement specimens of mixes FS200W20, AS300W57 and AS200W40 (15 per mix) were prepared and immediately placed in water. For each soil-cement mix, the unconfined compressive strength q_u and the small strain shear modulus G_0 of 3 specimens were determined after 7 days of curing in water. The shear moduli G_0 of 9 other specimens of each mix were also determined 7 days after moulding. These 9 specimens were divided into 3 groups and placed in different curing conditions:

- Condition 1: specimens remained immersed in water at a temperature of 20°C.
- Condition 2: specimens were subjected to cycles of wetting and drying by alternating periods of soaking in water and periods of drying in a climatic chamber at a temperature of 20 °C and a relative humidity of 65 %.
- Condition 3: specimens were placed in a climatic chamber at a temperature of 20 °C and a relative humidity of 65 %.

The ASTM standard procedure for wetting-drying cycles (ASTM D559, 2005) was not followed because of the temperature used for drying (60 °C), which accelerates the cement hydration process (Figure 1-41) and may alter the effects of the cycles.
It is important to note that the specimens were placed in the different curing conditions at an early age before the cement hydration process was complete. The shear modulus G_0 of the specimens was monitored every 1 to 4 days between 7 and 30 days. During curing, the moisture content of the specimens W was followed by measuring the changes in mass (m) using the following equation (assuming the amount of solid particles lost during testing was negligible):

$w = (1 + w_i) \times (m / m_i) - 1$

where w_i and m_i are respectively the initial water content and the initial mass of the soil specimen after 7 days.

For the specimens subjected to successive periods of wetting and drying (curing condition 2) after the initial 7 days of curing in water, the phases of soaking lasted between 1 and 4 days. The specimens were submitted to periods of drying of 24 hours (except between 20 and 22 days where two successive 24 hours drying periods were applied). Details of the applied cycles of wetting and drying are given in Table 2-6.

Curing time (days)	**0 -7**	**7-8**	**8-11**	**11-12**	**12-13**	**13-14**	**14-18**	**18-19**	**19-20**	**20-22**	**22-25**	**25-26**	**26-30**
Wetting	x		x		x		x		x		x		x
Drying		x		x		x		x		x		x	

Table 2-6 Details of applied cycles of wetting and drying.

The variations in moisture content between curing times during cycles give an indication on the curing conditions: an increase in moisture content indicates soaking whereas a decrease points to drying.

After 30 days of curing, unconfined compressive strength tests were performed on the specimens from all three curing conditions.
To study the effects of prolonged curing in water on the resistance to desiccation, the remaining 3 specimens (of each mix), which stayed in water for 30 days, were placed in curing condition 3 (continuous drying). The shear moduli G_0 of these specimens were monitored for 17 days (between 30 and 47 days). The experimental program is summarised in Figure 2-7. The results of this program are presented in Chapter 5.

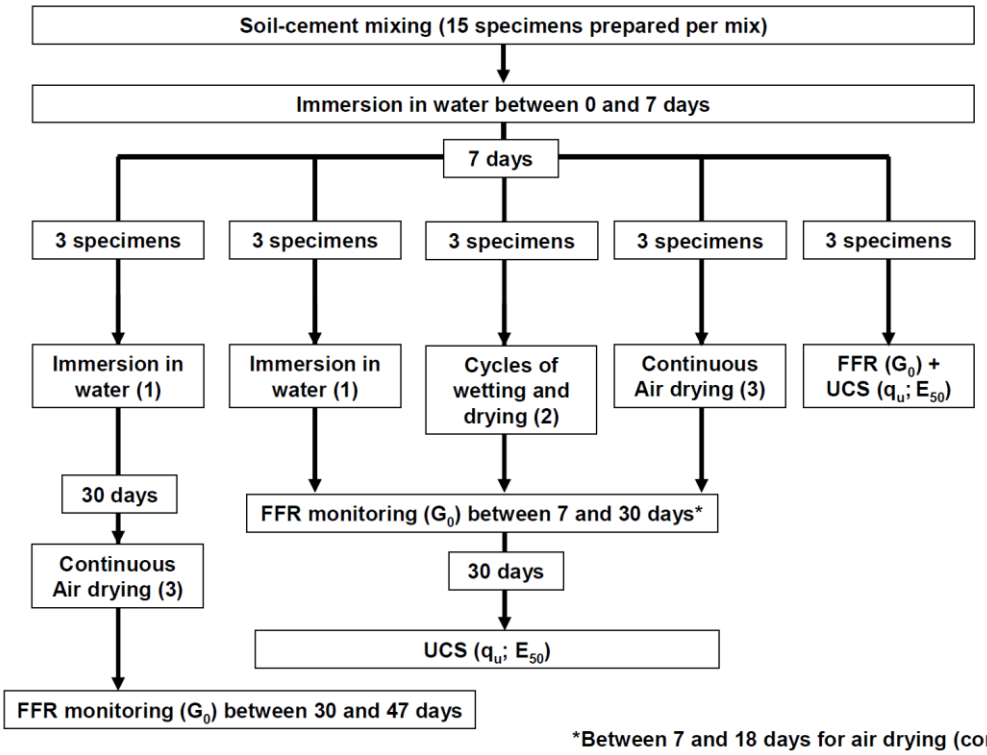

Figure 2-7 Experimental program to investigate the effects of drying and wetting/drying cycles.

2.5 Laboratory testing procedures

Laboratory tests carried out to determine the mechanical properties of treated soils include:

- destructive testing methods (unconfined compression tests and Brazilian tests),
- non-destructive techniques (ultrasonic wave velocity and resonance testing).

In addition, measurements of hydraulic properties (porosity accessible to water and permeability measurements) and microstructural investigations (x-ray diffraction analyses, scanning electron microscopy and mercury intrusion porosimetry) were performed.

2.5.1 Mechanical parameters derived from destructive tests

Destructive tests were executed on specimens of soil treated in the laboratory and in situ to measure the unconfined compressive strength q_u, the static deformation modulus E_{50} and the indirect tensile strength q_{it}.

2.5.1.1 Unconfined compressive strength tests and static deformation modulus measurements

Unconfined compression tests were preferred to triaxial tests to evaluate the strength and stiffness of treated soils for the following reasons:

- unconfined compression testing is extensively used on treated soils in current engineering practice,
- the test is rapid and reliable which enabled a large number of laboratory and field specimens to be studied,
- the test is widely used for concretes, hence made possible comparisons between treated soils and other cimentitious materials.

Compression tests performed on specimens with a height to diameter ratio of 2 to evaluate their strength (q_u). The tests were conducted in accordance with standard EN 13286-41 (AFNOR, 2003a). The vertical load was statically applied at a constant displacement rate of 1.5 %/min. The longitudinal strains were measured locally in the central part of the specimens by three LVDTs offset by 120° supported by two rigid rings (Figure 2-8). Each ring was attached on the wall of the specimen by three screws as described in standard EN 13286-43 (AFNOR, 2003c). The stress-strain curves are plotted using the average strain from the 3 LVDTs (Figure 2-9).

Figure 2-8 Set up for unconfined compression tests with local strain measurements.

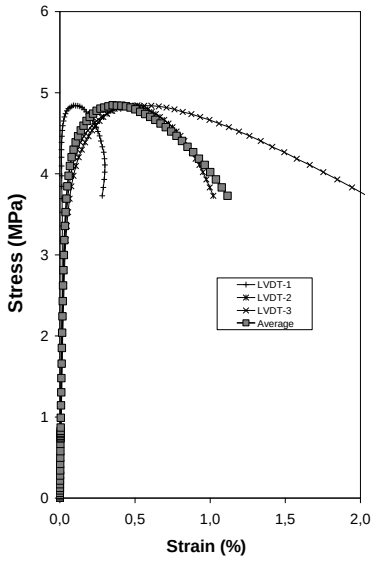

Figure 2-9 Example of stress-strain curves obtained using local strain measurements.

2.5.1.2 Splitting tensile strength tests

Splitting tensile strength tests were performed as per EN 13286-42 (AFNOR, 2003b) on specimens of approximately 50 by 50 mm (height to diameter ratio of 1) to evaluate their indirect tensile strength (q_{it}) (Figure 2-10). The vertical load was statically applied at a constant displacement rate of 3 mm/min and the maximum load was recorded.

Figure 2-10 Set up for splitting tensile strength tests.

2.5.2 Mechanical parameters derived from non-destructive tests

Non-destructive tests were used to measure parameters related to the small strain stiffness of treated soils. The dynamic modulus E_0 and the small strain shear modulus G_0 were obtained by ultrasonic wave velocity measurements and free-free resonance testing.

2.5.2.1 Ultrasonic wave velocity measurements

Ultrasonic wave velocity measurements were carried out on the soil-cement specimens. The ultrasonic equipment used in this study consisted of a pulser/receiver device (Figure 2-11).

Figure 2-11 Set up for ultrasonic pulse wave velocity measurements.

The device generates and receives ultrasonic waves with a digital display of the results. Measurements were conducted according to the procedure described in ASTM C597-02

(2005). The device can be used with different testing methods: direct transmission, semi-direct transmission, and indirect transmission. The direct transmission method with 54 or 150 kHz transducers (depending on specimen size as ASTM C597 states that the smallest dimension of the specimen must exceed the wavelength of the ultrasonic vibrations) was used throughout this study. The transducers were pressed against the specimens by hand in order to ensure a uniform and constant pressure between transducers and specimen surfaces.

Vaseline was used as couplant. The device served to read the time required for ultrasonic waves to propagate from the pulser through the specimen to the receiver. The distance between the transducers, which is equal to the specimen height, was divided by the measured time to calculate the wave velocity. Three readings were performed on each specimen.
Preliminary tests were performed on 50 mm diameter specimens of in situ stabilised soils to compare the wave velocities obtained using different transducer frequencies. It is interesting to note that, although the maximum pulse velocity to obtain a wavelength of 50 mm is 2700 m/s with a frequency of 54 kHz, a good agreement is found between the velocities measured using 54 kHz and 150 kHz transducers (Figure 2-12).

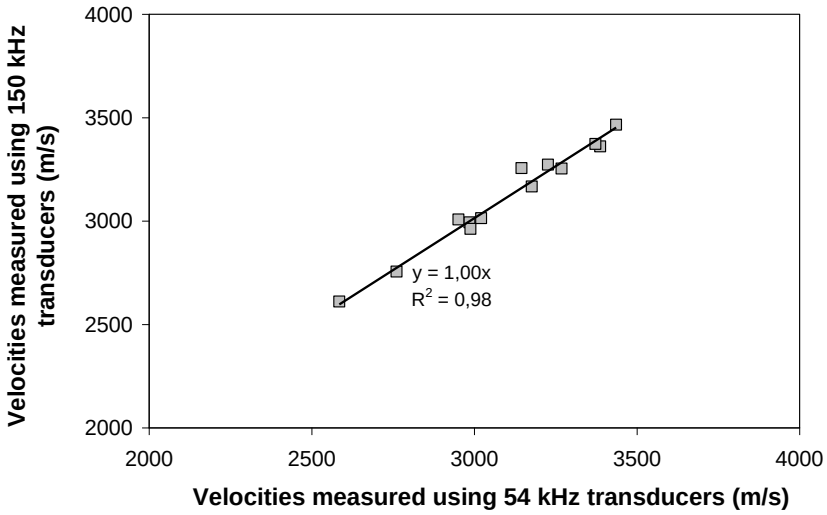

Figure 2-12 Ultrasonic wave velocities measured using 54 kHz and 150 kHz transducers.

The dynamic elastic modulus based on ultrasonic wave velocity measurements is calculated using the following equation (ASTM, 2005):

$$E_0 = \rho \times \frac{(1+\nu)\times(1-2\nu)}{(1-\nu)} \times V_p{}^2$$

where E_0 is the dynamic elastic modulus (Pa), ρ is the density (kg/m^3), ν is the dynamic Poisson's ratio and V_p is the ultrasonic wave velocity (m/s).

2.5.2.2 Free-free resonance tests (FFR tests)

The aim of FFR testing is to measure the natural frequency of free vibration of the tested specimen. To perform the free-free resonant column tests, compression and flexural signals were measured by two 6 mm diameter accelerometers with a frequency range of 1 to 17 kHz. Three different methods of excitation and recording were considered (Figure 2-13). Details on these methods are given in Appendix B.

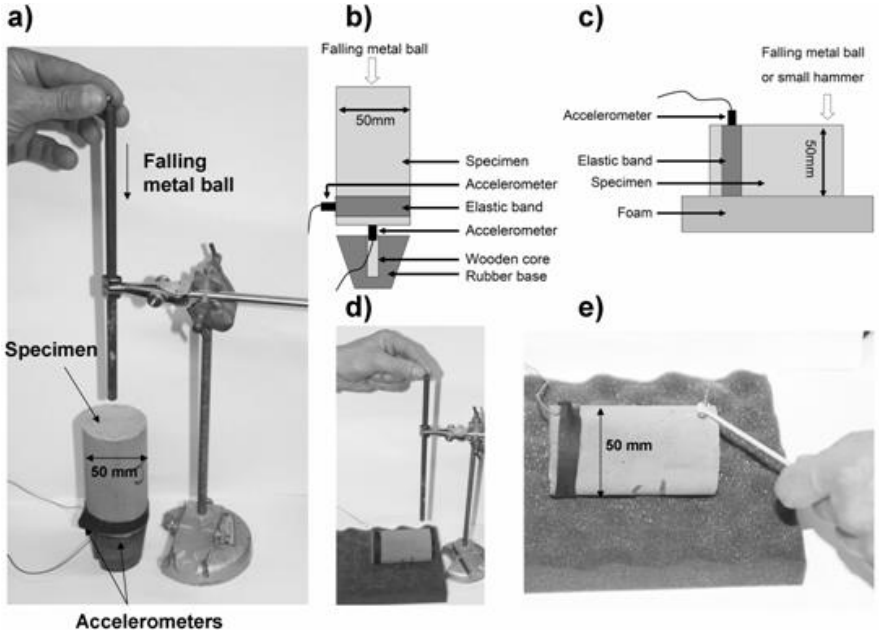

Figure 2-13 FFR testing: (a) set up for longitudinal excitation / longitudinal and flexural recording with impulses produced by a falling metal ball; (b): schematic drawing of the set up for longitudinal excitation / longitudinal and flexural recording; (c): schematic drawing of the set up for flexural excitation and recording; flexural excitation and recording with impulses produced by (d) a falling metal ball and (e) a small hammer.

The following relationships are used to determine the shear wave and compression wave velocities from the resonant column free-free tests:

$$V_s = 2 \times L \times f_s$$

$$V_p = 2 \times L \times f_p$$

where V_s is the shear wave velocity, V_p is the compression wave velocity, L is the specimen length, f_s and f_p are the resonant frequencies for shear waves and compression waves respectively.

The wavelength is assumed to be equal to twice the length of the specimen during free vibration for specimens with free ends and with a length-to-diameter ratio of about two or more (Ryden et al., 2006).

The small strain shear (G_0) modulus can be calculated from the wave velocities knowing the specimen's mass density (ρ) using the following equations (Nazarian et al., 1999):

$$G_0 = \rho \times V_s^{\,2}$$

Assuming homogeneous, isotropic, linear elasticity, the Poisson's ratio can be determined from the computed values of E_0 and G_0 by the following relation:

$$\nu = \frac{E_0}{2G_0} - 1$$

2.5.3 Measurements of hydraulic properties

Porosity accessible to water and permeability are the hydraulic properties measured on specimens of stabilised soil.

2.5.3.1 Porosity accessible to water

The total porosity of some specimens was determined by hydrostatic weighing after saturation under vacuum for 24 hours and by the measurement of the loss of water under controlled drying by heating to 105°C.

2.5.3.2 Permeability

The cells used to measure the permeability of 40 mm diameter specimens were composed of two aluminium plates and a steel cylinder (Figure 2-14). A lateral confining pressure was applied to the specimens. Water flowed from the lower base to the upper side of the sample in order to avoid trapped air bubbles. The fluid circulation was done with a constant hydraulic head of 8 m (80 kPa). Permeability k of the specimens was determined based on Darcy's law from the quantity of water collected for a given time of percolation:

V = ki

In laminar flow conditions, the velocity V is proportional to the hydraulic gradient i.

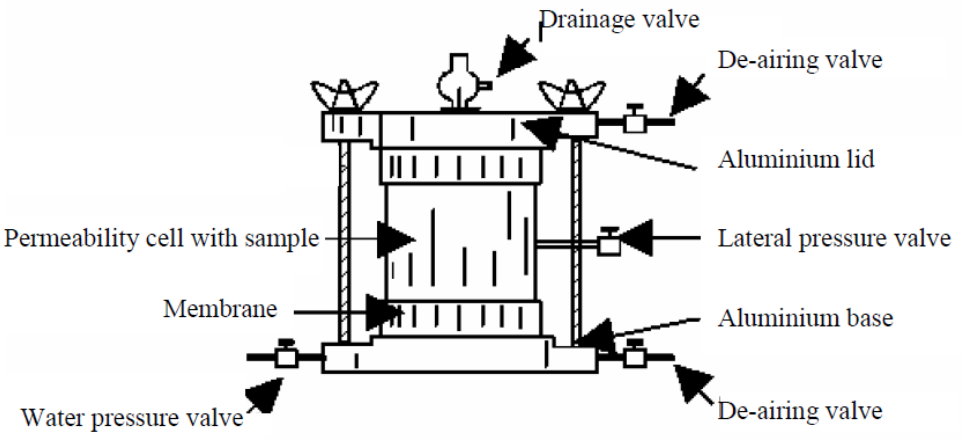

Figure 2-14 Schematic diagram of permeability cell.

2.5.4 Microstructural investigations

The microstructure of treated soils was examined by means of x-ray diffraction analyses, scanning electron microscopy and mercury intrusion porosimetry.

2.5.4.1 X-Ray diffraction analysis

X-ray diffraction (XRD) analyses were carried out using a D8 Advance x-ray diffractometer from Bruker. XRD patterns were obtained using a Cu Kα (λ=1.5148 Å) x-ray tube with input voltage of 40 kV and current of 40 mA. Scanning was performed every 0.02° between 3.5 and 70° with a scan rate of 2.4°/min.

The analyses were performed on cryodesiccated fragments of treated soil specimens which had been ground and sieved to obtain particles with sizes less than 80 µm. Minerals were identified using the PDF-2 mineralogical database.

2.5.4.2 Scanning electron microscopy

A Zeiss/LEO 1530 microscope was employed to produce magnified images by scanning electron microscopy. A maximum magnification of 25000 times was adopted.

The specimens were coated with platinum palladium and scanned using secondary electrons.

2.5.4.3 Pore size distribution by mercury intrusion porosimetry (MIP)

Mercury intrusion porosimetry (MIP) was used to examine the microstructure of cement-treated soils. The porosimeter used in this study was an AutoPore IV 9500 manufactured by Micromeritics.

MIP consists in forcing the intrusion of mercury in a dry porous media by increasing mercury pressure. The entrance radius of a pore space penetrated by mercury is inversely proportional to the applied pressure according to Washburn's equation:

$$r = \frac{2 \times \sigma \times \cos\theta}{P}$$

where r is the pore radius, σ the surface tension (0.48 $N.m^{-1}$ for mercury), θ the solid/liquid contact angle, and P applied pressure (Pa).

In the data analysis, a mercury contact angle of 141.3° and surface tension of 485 dyn/cm were assumed. The maximum mercury pressure applied was 200 MPa.

In order to conduct MIP measurements, the tested samples must be dry. Fragments of treated soil specimens were quick-frozen using liquid nitrogen then cryodesiccated. The range of pressure used allowed only measurements of entrance radii varying from 0.004 µm and 220 µm.

Chapter 3. Mechanical properties of soils stabilised with cement in the laboratory

3.1 Introduction

The results of tests carried out to evaluate the mechanical behaviour of soils mixed in the laboratory with cement are presented in this chapter. The study is performed on soil-mix materials in the fresh state immediately after mixing (section 3.2) and in the hardened state (section 3.3).

Speswhite kaolin, cement slurries and kaolin-cement mixes in the fresh state were tested using a rheometer equipped with parallel plates and the ball measuring system. The aim of these tests is to investigate the effects of the addition of cement on the rheological characteristics of soils in relation to the installation process of deep mixing elements.

Laboratory tests were performed on hardened samples of two silts and two sands treated with cement to assess long-term growth in strength and stiffness with curing time and to examine the relations between strength, static modulus and dynamic modulus.

3.2 Experimental results and analyses on fresh materials

3.2.1 Flow curves of kaolin

The flow curves obtained using the parallel plates and the ball measuring system for Speswhite kaolin at different moisture contents are presented in Figure 3-1. For both geometries, the shear stresses measured increase as the moisture content decreases. This can be explained by the increasing interaction between the clay particles as their concentration increases.

The yield stresses obtained for the two geometries, taken as the shear stress at a shear rate of 1 s^{-1}, are compared in Table 3-1. An acceptable agreement is found between the yield stresses obtained using the parallel plates and the ball measuring system.

No thixotropic effects (time-dependent behaviour under shear) were observed for the Speswhite kaolin. Thixotropic behaviour exhibited by other clay minerals such as smectites is related to high reactivities and modifications in particle size and surface properties caused by the hydration process (Lagaly, 1989; Besq et al., 2003; Pantet and Monnet, 2007).

Geometry	Yield stress (Pa)		
	W = 100 %	W = 150 %	W = 200 %
Parallel plates (average)	300	55	7.5
Ball Measuring system	300	43	14

Table 3-1 Yield stress of kaolin at different moisture contents.

3.2.2 Flow curves of cement slurries

The flow curves obtained using the ball measuring system for cement slurries with different concentrations are plotted in Figure 3-2. The yield stresses, taken as the shear stress at a shear rate of 1 s^{-1}, are given in Table 3-2.

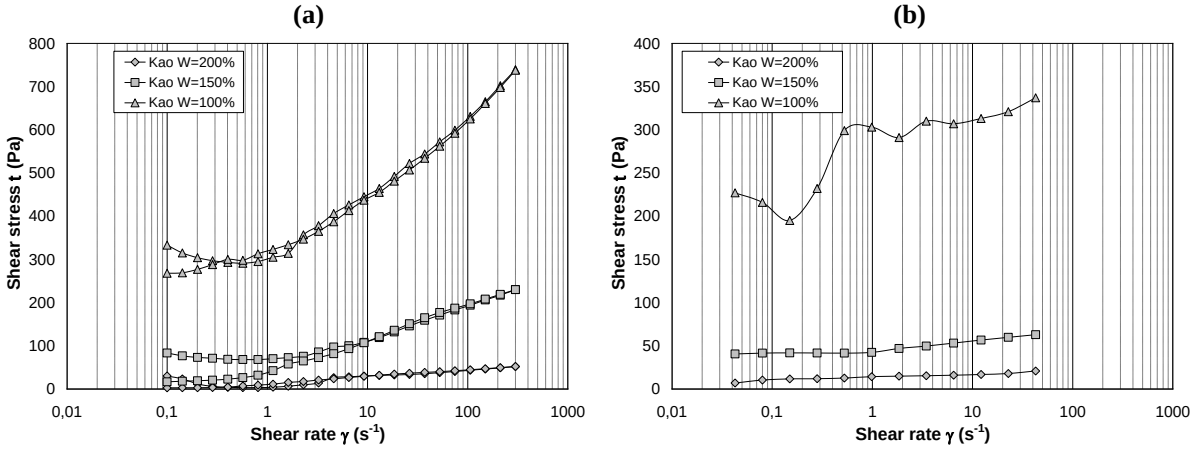

Figure 3-1 Flow curves for kaolin using a) the parallel plates b) the ball measuring system.

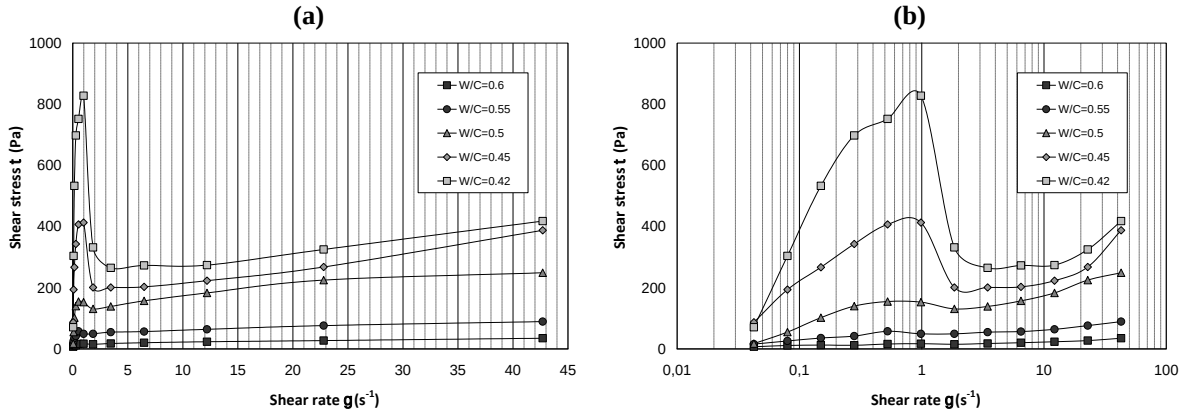

Figure 3-2 Flow curves for cement slurries a) linear scale b) logarithmic scale.

Geometry	Yield stress (Pa)				
	W/C = 0.6	W/C = 0.55	W/C = 0.50	W/C = 0.45	W/C = 0.42
Ball Measuring system	17	50	153	415	830

Table 3-2 Yield stresses of cement slurries at different concentrations.

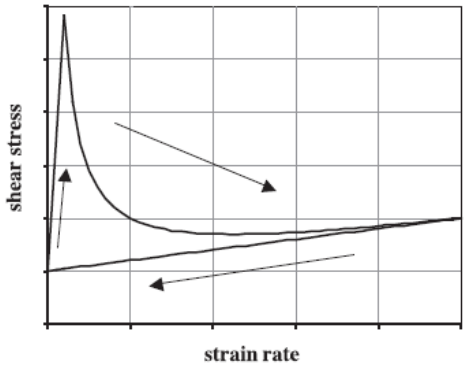

Figure 3-3 Cement paste flow curve: short cycle test; steady state not reached (Roussel, 2005).

The measured flow curves are above the equilibrium state flow curves. These results demonstrate that the deflocculation process was insufficient to bring the structure to its equilibrium state. This type of flow curve is directly related to the duration of the experimental measuring cycle as reported by Roussel (2005, Figure 3-3).

3.2.3 Flow curves of clay-cement mixes

The flow curves obtained for clay-cement mixtures using the ball measuring system are plotted in Figure 3-4 and Figure 3-5. The flow curves are similar to those obtained for the cement slurries. The behaviour, once the minimum is reached, is rheopetic and can be related to the hydration process. Figure 3-4 shows that the addition of dry cement affects the measured shear stresses in as much as it causes an increase in particle concentration. The effect of moisture content on the rheological behaviour of cement-kaolin mixes is clearly visible in Figure 3-5 as the measured shear stresses drastically increase for moisture contents lower than 100 %. The yield stresses (shear stress at a shear rate of 1 s^{-1}) are summarised in Table 3-3.

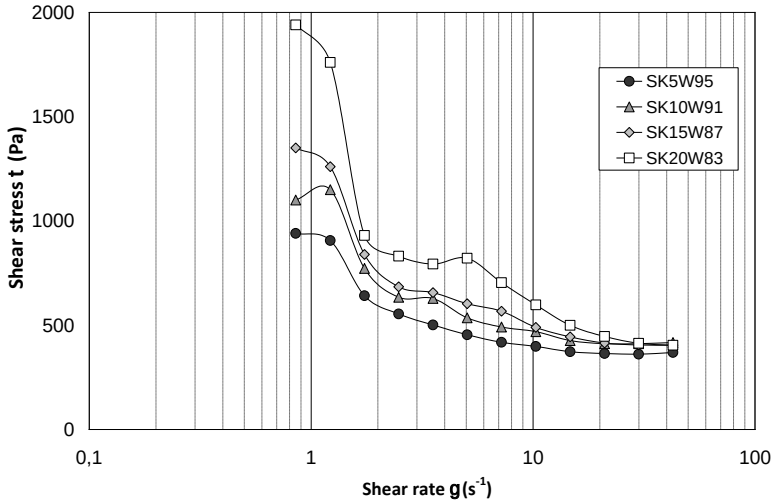

Figure 3-4 Flow curves for clay-cement mixes with increasing cement contents using the BMS.

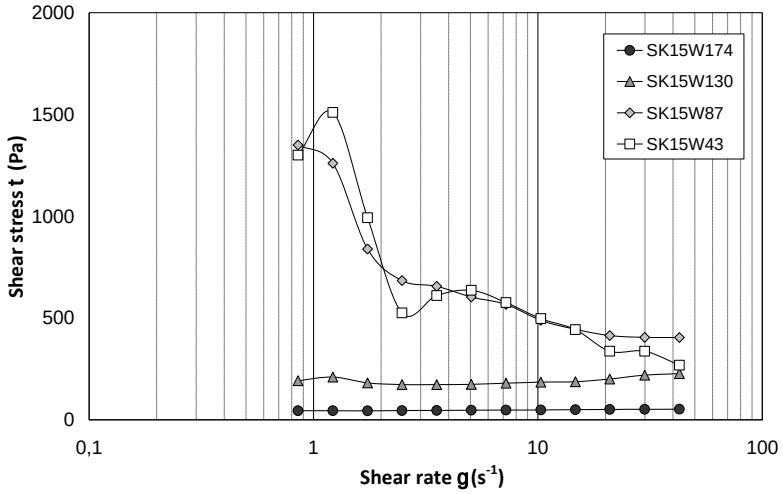

Figure 3-5 Flow curves for clay-cement mixes with different water contents using the BMS.

Mix	SK5W95	SK10W91	SK15W87	SK20W83	SK15W174	SK15W130	SK15W43
Cement content	5 %	10 %	15 %	20 %	15 %	15 %	15 %
Moisture content	95 %	91 %	87 %	83 %	174 %	130 %	43.5 %
Yield stress (Pa)	906	1150	1260	1760	45	210	1510

Table 3-3 Yield stresses of kaolin-cement mixes measured with the BMS.

3.2.4 Discussion

Observations made in the field regarding the installation process of soil mixing elements can be related to the rheological properties of soils. Many others have reported that faster tool rotation speeds increase the homogeneity and strength of treated soils (CDIT, 2002). In the case of fine grained soils, this can be explained by the shear-thinning behaviour of clays discussed in section 1.3.5.3.1 (i.e. lower viscosity at higher shear rates). As the blade rotation speed increases, the soil is subjected to increasing shear rates. Assuming that homogenising low viscosity fluids or suspensions is easier than mixing viscous fluids, the efficiency of the mixing process is improved at higher shear rates (blade rotation speeds). The clay-binder mixture produced is more homogeneous and therefore of higher strength after curing. These results explain the preference for high tool rotation speeds in the Scandinavian dry mixing method (Table 1-3) for the treatment of soft (probably shear-thinning) clays.

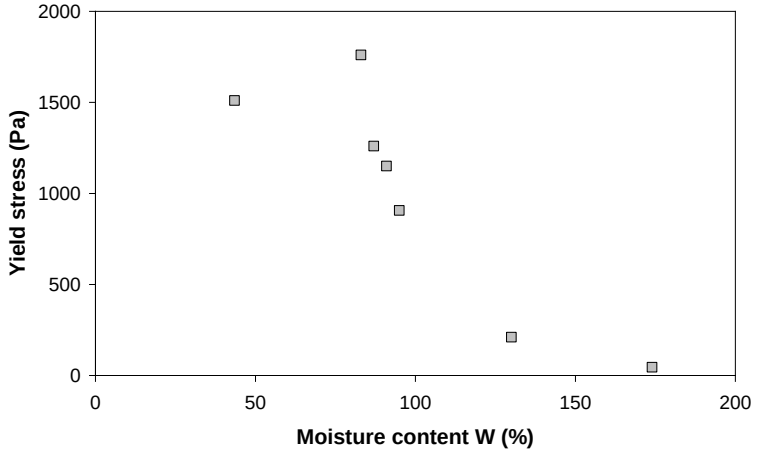

Figure 3-6 Yield stress versus moisture content for kaolin-cement mixes.

The effects of yield stress on the mixing process in deep mixing are less straightforward as the stresses produced by the rotation of the mixing tool are much higher than the yield stresses of clay suspensions. The yield stress may be related to the workability of soil-cement mixtures. In general, no compaction is performed during the installation of soil mixing columns. The soil-cement mixtures must therefore be sufficiently fluid to be self-compacting. This implies that the mixes should have a yield stress which is low enough to allow the mixture to flow under its own weight and fill the voids created by the passing of the mixing tool. The results obtained on kaolin-cement mixtures clearly show the predominant effect of moisture content on yield stress (Figure 3-6). Further research and experiments are needed in this direction as it may be possible to determine, for a particular soil-cement mixture, an optimum moisture

content which does not significantly alter the strength of treated soils after curing but at which the yield stress in the fresh state is sufficiently low for the mixtures to be self-compacting. Further field experiments could allow the determination of yield stress thresholds for the workability of soil-cement mixtures.

3.2.5 Conclusions

The flow properties of kaolin, cement slurries and kaolin–cement mixtures at various moisture contents were measured using a rheometer with two different geometries: the parallel plates and the ball measuring system. For all mixtures tested, the yield stress decreases as the moisture content increases. A good agreement is found between the stresses measured using the parallel plates and the ball measuring system for kaolin suspensions.
Observations made in the field on the relation between blade rotation speed and strength and homogeneity of treated soils could be explained by the shear-thinning behaviour of clays. The yield stress may be a relevant tool to study the workability of soil-cement mixtures.

3.3 Experimental results and analyses on hardened materials

Unconfined compression strength tests, splitting tensile strength tests, porosity and ultrasonic wave velocity measurements were performed after different curing times on two silts and two sands mixed with cement to investigate the long-term properties of soils stabilised in the laboratory. The dosages used for the soil-cement mixes are given in Table A-1 and Table A-2 (Appendix A). The testing program is shown in Table A-3.

For hardened soil-cement mixtures, the objectives are:

- to assess long-term growth in strength and stiffness with time for soils treated with cement and cured in the laboratory,
- to examine the relationship between strength and static modulus obtained using local strain measurements,
- to study possible correlations between parameters measured by non-destructive techniques and mechanical properties determined by destructive tests.

3.3.1 Density, moisture content and porosity accessible to water

Variations in wet density with curing time for specimens prepared in the laboratory and cured in endogenous conditions are presented in Figure 3-7 and Figure 3-8. The moisture contents are plotted in Figure 3-9 and Figure 3-10.

The wet densities of the sand-cement mixes are higher than the densities of the silt-cement mixes. The densities of the silt mixes are between 1600 and 1900 kg/m^3 (Figure 3-7) whereas the densities of the sand-cement mixes are between 1900 and 2200 kg/m^3 (Figure 3-8).

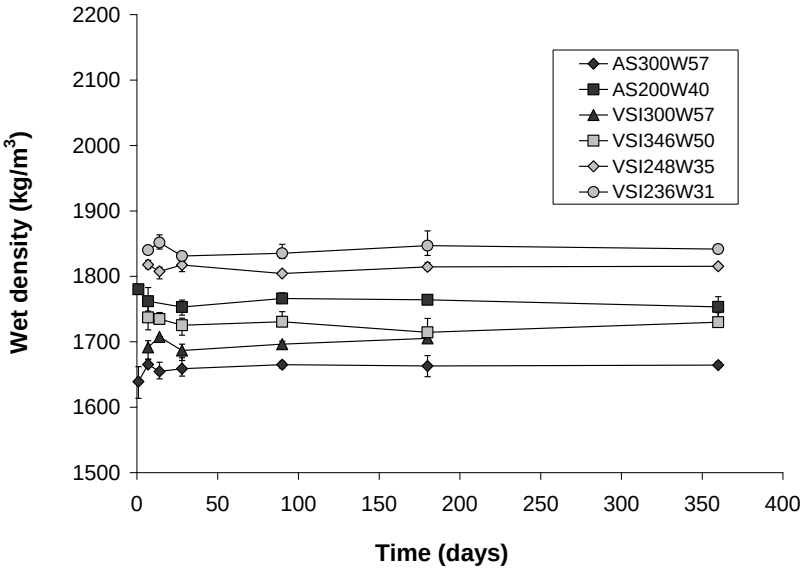

Figure 3-7 Evolution of wet density with curing time for specimens of silt mixed in the laboratory with cement.

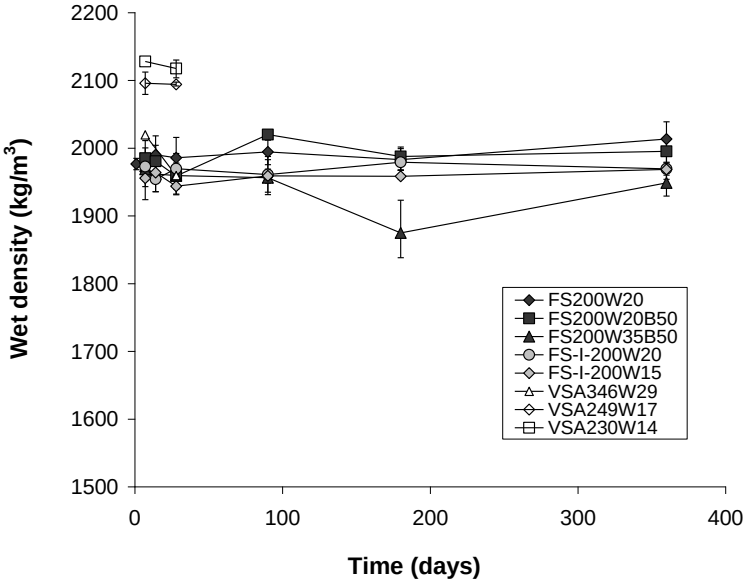

Figure 3-8 Evolution of wet density with curing time for specimens of sand mixed in the laboratory with cement.

A noticeable decrease in water content occurs during the first 7 to 14 days after treatment (Figure 3-9 and Figure 3-10). This reduction in moisture content reflects the consumption of water caused by the hydration of the cement (Åhnberg, 2003). Both wet density and moisture content remain generally constant for longer curing times. This confirms that the specimens were sealed in hermetic conditions and that no hydric exchange (loss or gain of water) occurred between the specimens and the exterior environment.

The average densities and total porosities after 28 days are given in Table 3-4. The wet densities of the mixes prepared with the soils from Vernouillet (VSI and VSA) and the artificial silt (AS) clearly decrease as the moulding moisture contents increase (Figure 3-11). The density of the specimens prepared with Fontainebleau sand appears to be relatively

constant for moulding moisture contents between 15 and 35 %. The total porosity of the specimens increases approximately linearly with moulding moisture content (Figure 3-12).

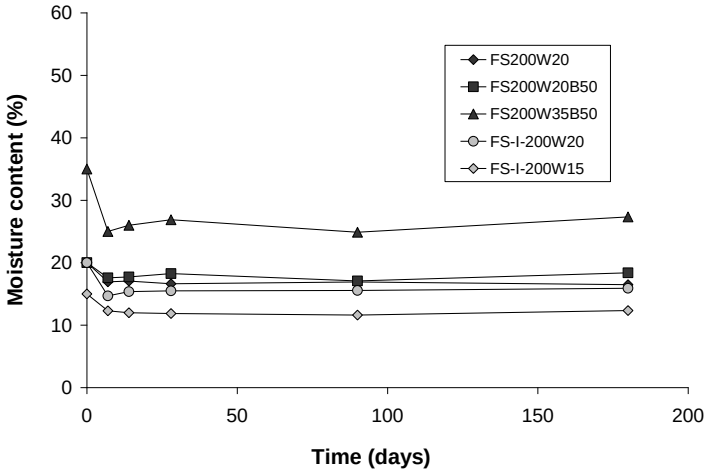

Figure 3-9 Evolution of moisture content with curing time for specimens of sand mixed in the laboratory with cement.

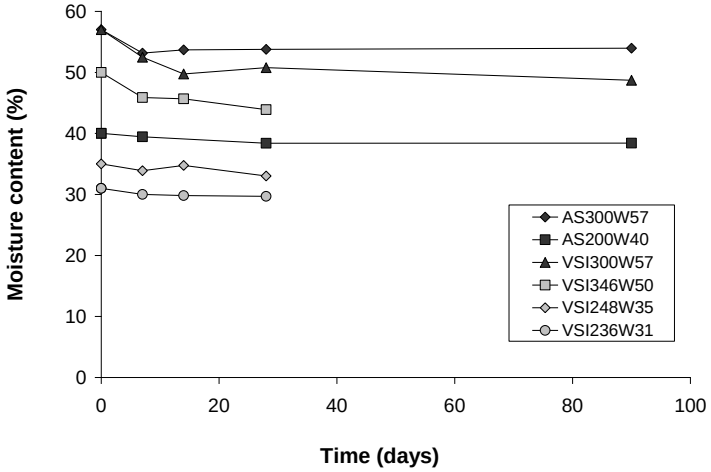

Figure 3-10 Evolution of moisture content with curing time for specimens of silt mixed in the laboratory with cement.

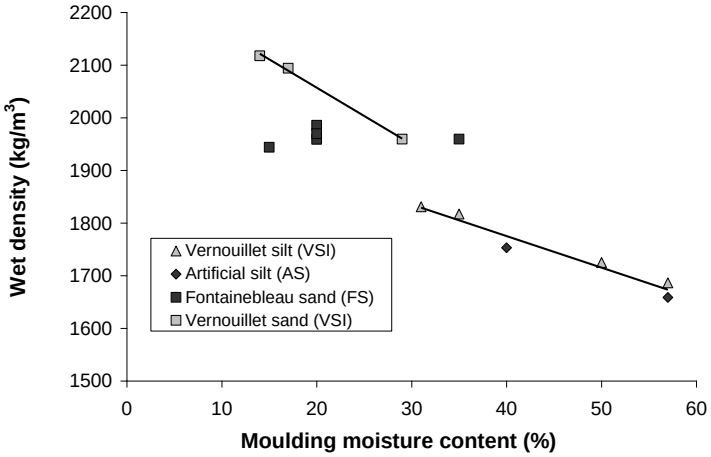

Figure 3-11 Wet density after 28 days of curing versus moulding moisture content for specimens prepared in the laboratory.

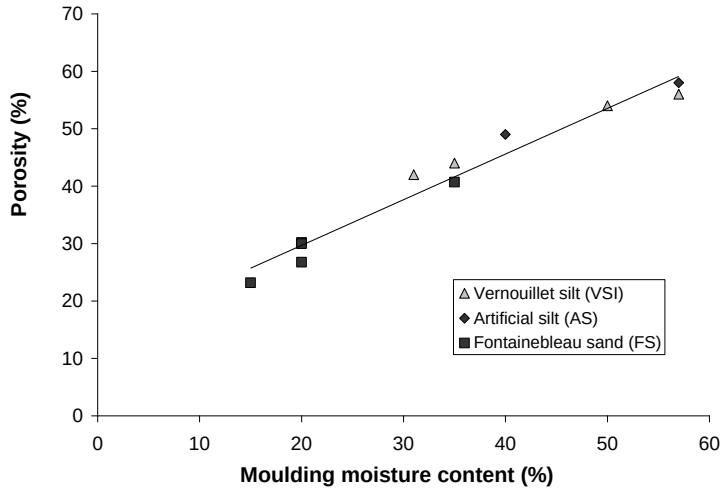

Figure 3-12 Porosity accessible to water after 28 days of curing versus moulding moisture content for specimens prepared in the laboratory.

Mix	Wet density (kg/m^3)	Porosity accessible to water (%)
AS300W57	1659	58
AS200W40	1753	49
VSI300W57	1687	56
VSI346W50	1725	54
VSI248W35	1817	44
VSI236W31	1831	42
FS200W20B50	1986	30
FS200W20	1959	30
FS200W35B50	1959	41
FS-I-200W20	1970	27
FS-I-200W15	1944	23

Table 3-4 Porosity accessible to water and density after 28 days.

3.3.2 Unconfined compressive strength

3.3.2.1 Development of unconfined compressive strength with time

Typical stress-strain curves obtained from unconfined compressive strength tests performed after different curing times for artificial silt (AS200W40) and Fontainebleau sand (FS200W20) are shown in Figure 3-13. These graphs indicate that the sand-cement specimens of mix FS200W20 exhibit ductile behaviour whereas the behaviour of the artificial silt-cement specimens is more brittle.

The mixes have similar cement contents (200 kg/m^3) but very different moisture contents. Figure 3-13 shows that the strength of treated artificial silt is higher than strength of stabilised Fontainebleau sand of same age. The relatively low strengths of the sand-cement specimens can be explained by the uniform grain size distribution of the untreated Fontainebleau sand (Figure 2-1) which has an adverse effect on packing arrangement (section 1.3.5.2.3). The large difference in strength may also be due to porosity. Although the total porosity of the treated silt mixes are higher because of the higher initial water content (Figure 3-12), mercury

intrusion porosimetry measurements (the results are given in Chapter 5) show that the pores in specimens of treated Fontainebleau sand are much larger than in treated artificial silt.
Figure 3-13 also clearly shows that the strength of both soil-cement mixes increases with curing time.

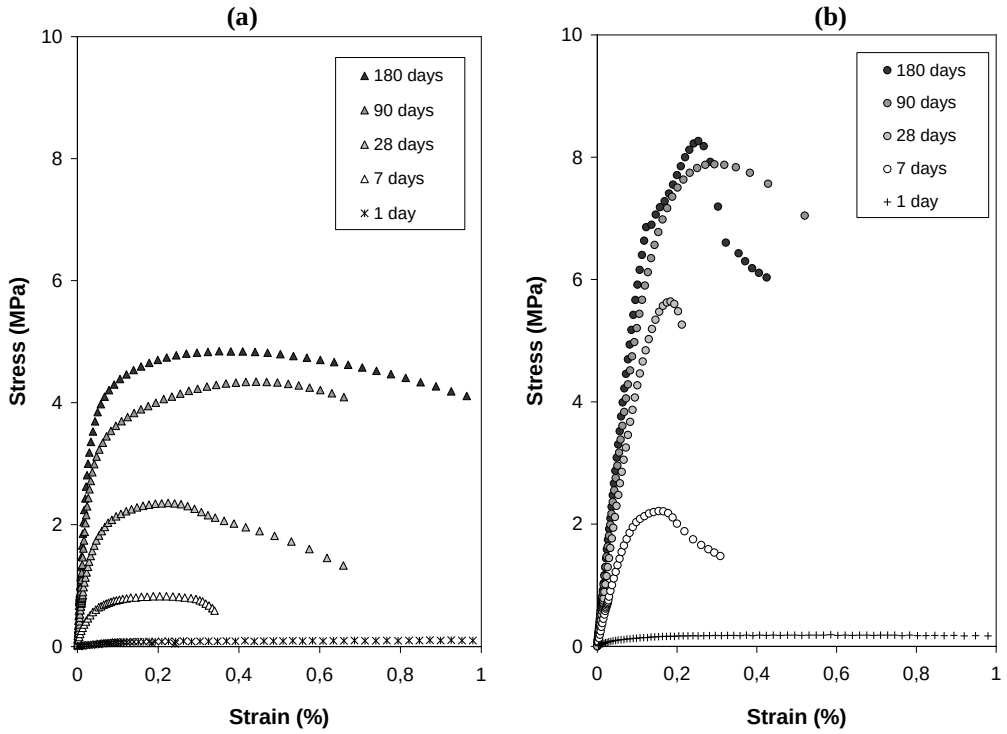

Figure 3-13 Typical stress-strain curves for (a) specimens of stabilised Fontainebleau sand (FS200W20) and (b) specimens of stabilised artificial silt (AS200W40).

3.3.2.1.1 Strength growth in treated silts

The stress-strain curves for the different silt-cement mixes are shown in Figure 3-14. The unconfined compressive strength increases with curing time for all silt mixes (Figure 3-15 and Figure 3-16). Throughout this study, results on graphs of strength or stiffness versus time correspond to the average values measured on 3 specimens for each curing time; the error bars represent the minimum and maximum values. Measured strengths and strength gains between different curing times are given in Table 3-5.

After 1 day of curing, an average compressive strength of 70 kPa is measured on specimens of mix AS300W57. The average compressive strength for the specimens of mix AS200W40 is of 200 kPa. After 28 days, strengths of 4.23 MPa and 5.59 MPa are determined for mixes AS300W57 and AS200W40 respectively. The specimens of mix AS200W40 remain of higher strength than the specimens of mix AS300W57 after 360 days despite the lower cement content.

The cement-water ratios C/W of mixes AS200W40, AS300W57 and VSI300W57 are equal to 0.30 (Table A-1 and Table A-2, Appendix A). The strengths measured for these mixes are

higher than the strength of the corresponding CEM III cement paste with the same C/W ratio (Figure 3-15**)**.

For equal cement and moisture contents, the specimens prepared with Vernouillet silt (VSI300W57) have slightly lower compressive strengths than the specimens prepared with artificial silt (AS300W57; Table 3-5).

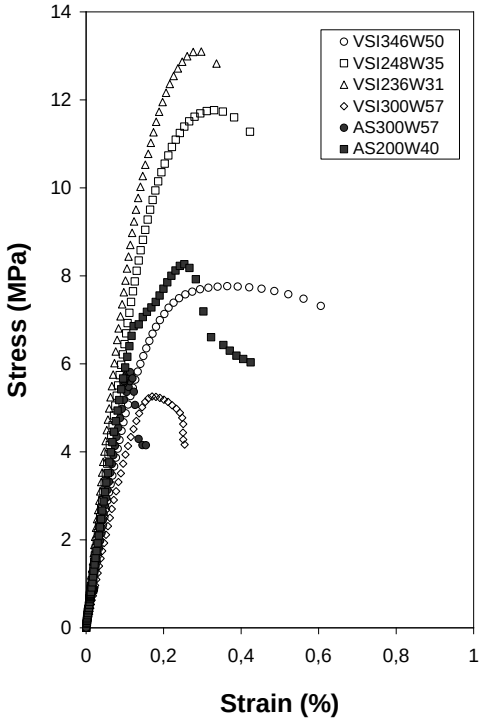

Figure 3-14 Typical stress-strain curves for specimens of stabilised silt after 180 days.

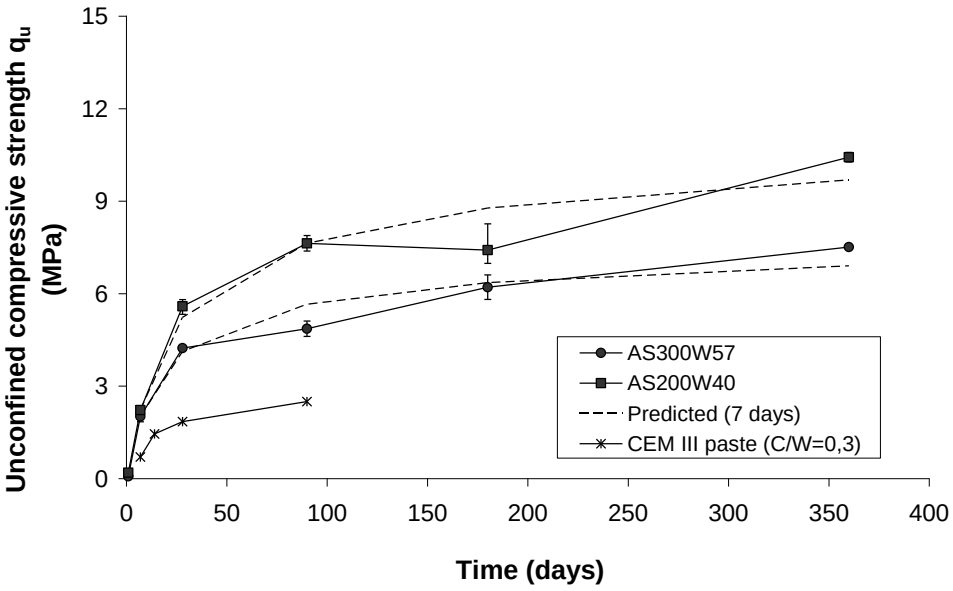

Figure 3-15 Unconfined compressive strength of artificial silt-cement mixes versus time - comparison with predicted strengths based on data obtained after 7 days.

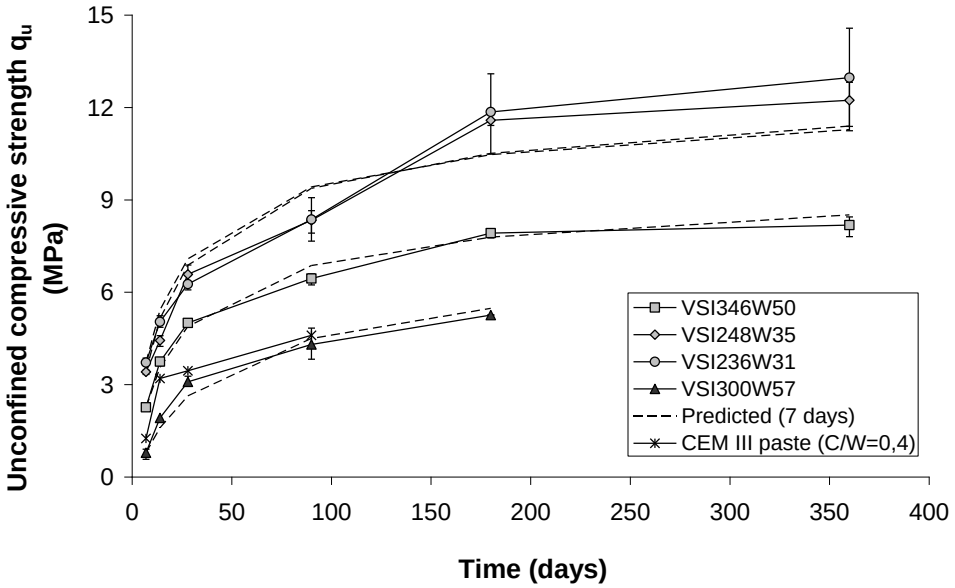

Figure 3-16 Unconfined compressive strength of Vernouillet silt-cement mixes versus time - comparison with predicted strengths based on data obtained after 7 days.

Mix	q_{u7} (MPa)	q_{u28} (MPa)	q_{u90} (MPa)	q_{u180} (MPa)	q_{u360} (MPa)	q_{u28}/q_{u7}	q_{u90}/q_{u28}	q_{u180}/q_{u90}	q_{u360}/q_{u180}
AS300W57	2.02	4.23	4.86	6.21	7.51	2.10	1.15	1.28	1.21
AS200W40	2.22	5.59	7.63	7.41	10.43	2.51	1.36	0.97	1.41
VSI300W57	0.79	3.09	4.30	5.26	-	3.93	1.39	1.22	-
VSI346W50	2.26	5.00	6.45	7.92	8.18	2.21	1.29	1.23	1.03
VSI248W35	3.41	6.58	8.34	11.58	12.23	1.93	1.27	1.39	1.06
VSI236W31	3.72	6.26	8.36	11.85	12.97	1.69	1.34	1.42	1.09

Table 3-5 Measured strengths and strength gains between different curing times for silt-cement mixes.

The other mixes of Vernouillet silt (VSI346W50; VSI248W35; VSI236W31) have cement-water ratios close to 0.40 (Table A-2, Appendix A). The strengths measured for these mixes are also higher than the matching cement paste with a C/W ratio of 0.40 (Figure 3-16). Strengths measured on specimens of mixes VSI248W35 and VSI236W31 are close for curing times up to 360 days. Lower strengths are measured on the specimens of mix VSI346W50 (despite the cement content is higher).

The differences in strength between the silt-cement mixes can be explained by the simultaneous and competing effects of cement content and water content. For the dosages tested in this study on both silts, high moisture contents appear to be the controlling and dominant factor for strength. The deleterious effect of moisture content is not compensated in this case by the addition of cement. All the silt-cement mixes have higher strengths than the cement pastes of equivalent C/W ratio. The addition of cement and water in proportions equal to the C/W ratio causes a decrease in strength for the dosages tested in this study.

The effect of moisture content on strength can partly be explained by the increase in total porosity induced by higher moulding water contents (Figure 3-12). Specimens of mix AS300W57 have lower strengths and higher porosities than specimens of mix AS200W40 (Table 3-4). Specimens of mixes VSI248W35 and VSI236W31 have similar strengths and porosities. The specimens of mix VSI346W50 have lower strengths and higher porosities than the other VSI-cement mixes with C/W close to 0.40.

The porosities of specimens of mixes AS300W57 and VSI300W57 are comparable. The difference in strength between the two soils can be attributed to grain size distribution and mineralogy.

Strength gain between 7 and 28 days of curing is significant for all mixes. The 28 to 7-day strength ratios q_{u28}/q_{u7} vary between 1.69 and 3.93 (Table 3-5). The rate of strength gain generally decreases with curing time. However, strength continues to increase between 90 and 360 days.

3.3.2.1.2 Strength growth in treated sands

The shapes of the stress-strain curves are similar for Fontainebleau sand (FS) treated with CEM I and CEM III cement (Figure 3-17). The development of unconfined compressive strength q_u with time for Fontainebleau sand mixed with CEM III and CEM I cement is presented in Figure 3-18 and Figure 3-19. The measured strengths and strength gains between different curing times for all sand-cement mixes are given in Table 3-6.

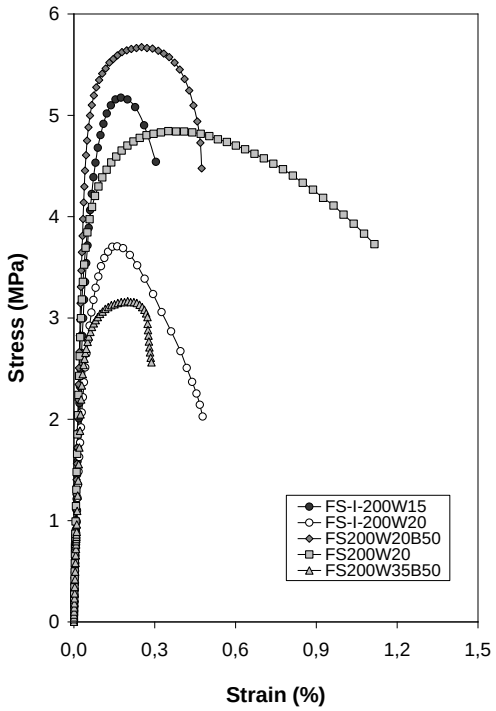

Figure 3-17 Typical stress-strain curves for specimens of stabilised Fontainebleau sand after 180 days.

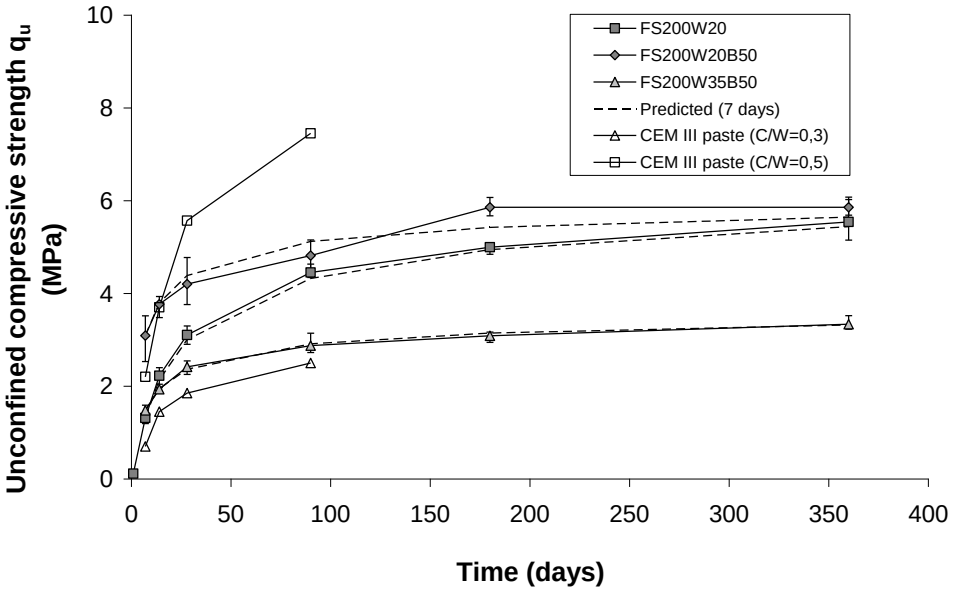

Figure 3-18 Unconfined compressive strength of Fontainebleau sand-CEM III cement mixes versus time - comparison with predicted strengths based on data obtained after 7 days.

Strength also increases with curing time for all the sand-cement mixes. Strength gains between 7 and 28 days of curing vary between 1.36 and 2.36 for the FS mixes containing CEM III (Table 3-6). The strengths of mixes FS200W20B50 and FS200W20 (C/W = 0.50) are lower than the strength of the CEM III cement paste with C/W = 0.50 (Figure 3-18). The strength of specimens of mix FS200W35B50 (C/W = 0.30) is slightly higher than the strength of the corresponding cement paste.

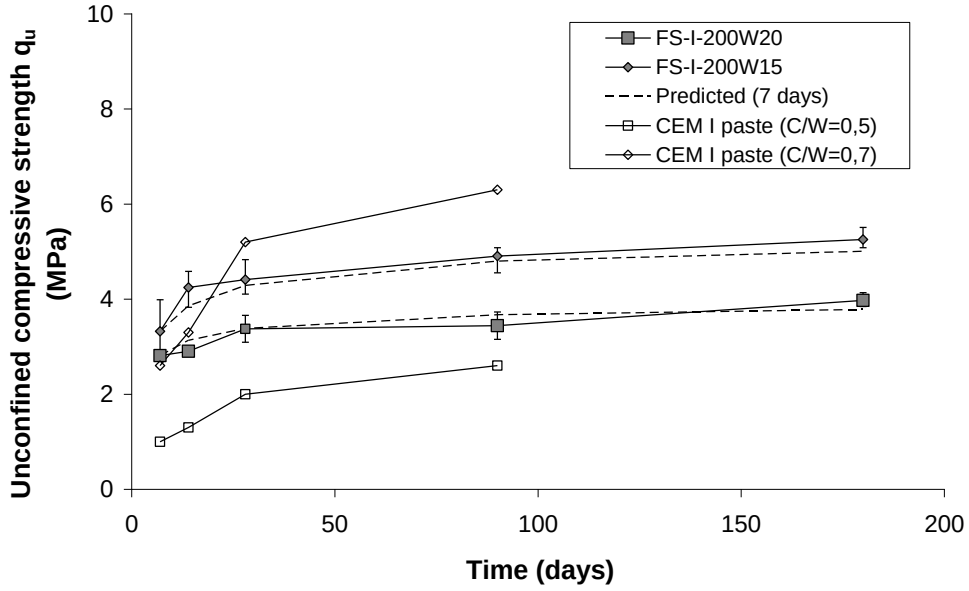

Figure 3-19 Unconfined compressive strength of Fontainebleau sand-CEM I cement mixes versus time - comparison with predicted strengths based on data obtained after 7 days.

Mix	q_{u7} (MPa)	q_{u28} (MPa)	q_{u90} (MPa)	q_{u180} (MPa)	q_{u360} (MPa)	q_{u28}/q_{u7}	q_{u90}/q_{u28}	q_{u180}/q_{u90}	q_{u360}/q_{u180}
FS200W20	1.32	3.10	4.45	5.00	5.54	2.36	1.43	1.12	1.11
FS200W20B50	3.09	4.20	4.82	5.86	5.86	1.36	1.15	1.22	1.00
FS200W35B50	1.48	2.41	2.87	3.09	3.34	1.63	1.19	1.07	1.08
FS-I-200W20	2.81	3.37	3.44	3.97	/	1.20	1.02	1.15	/
FS-I-200W15	3.32	4.41	4.90	5.25	/	1.33	1.11	1.07	/
VSA346W29	2.46	3.75	/	/	/	1.52	/	/	/
VSA249W17	4.02	6.88	/	/	/	1.71	/	/	/
VSA230W14	5.76	8.18	/	/	/	1.42	/	/	/

Table 3-6 Measured strengths and strength gains between different curing times for sand-cement mixes.

After 7 days of curing, the average strength measured on specimens of Fontainebleau sand mixed with CEM III containing 50 kg/m^3 of bentonite (3 MPa for FS200W20B50; Figure 3-18) is significantly higher than the strength of the specimens prepared with the same binder and moisture content but without bentonite (1.5 MPa for FS200W20). The difference in strength progressively reduces up 90 days. The strengths of mixes FS200W20B50 and FS200W20 are very close after 360 days.

These results are in agreement with the findings of Fardis et al. (1994). They performed compressive strength measurements on ordinary Portland cement mortars which indicate that the addition of clay increases strength during the early stages of hydration (10 to 100 hours). Results from a study on concrete showed that the presence of bentonite at replacement levels of 5 – 10 % can also lead to an increase in compressive strength at early ages (Targan et al., 2002). However, when used in combination with other materials, the addition of bentonite decreases the compressive strength of concrete.

The dry bentonite was not hydrated before it was added to the soil-cement mixtures (section 2.4.1.1). The high short-term strength of mix FS200W20B50 can be explained by the fact that the bentonite rapidly adsorbes large amounts of water during mixing which reduces the impact of the moisture content on strength. In the long-term, the strength of the mix without bentonite progressively increases as water is consumed by cement hydration. Since both mixes have the same cement content, long-term strengths are close.

The differences in strengths measured between the specimens of mixes FS200W20B50 (C/W = 0.50) and FS200W35B50 (C/W = 0.30) clearly illustrate the adverse effect of increasing moisture content on the mechanical properties of soil-cement mixtures.

The comparison of mixes FS200W20 and FS-I-200W20 shows that higher strengths are obtained by treating Fontainebleau sand with CEM III cement (Table 3-6). The 7-to-28 day strength ratios are lower for the FS-CEM I mixes (1.20 and 1.33, Table 3-6). This confirms the slower strength development of sand treated with CEM III (section 2.2.3).

The strengths of the specimens of mix FS-I-200W15 (C/W = 0.70) are slightly lower than the strengths of the corresponding CEM I paste whereas the strengths of specimens of mix FS-I-200W20 (C/W = 0.50) are higher than the paste with C/W = 0.50 (Figure 3-19). The higher

strengths measured for mix FS-I-200W15 can also be attributed to the lower moulding moisture content.

Summarising the comparisons between the strengths of sand-cement mixtures and the strengths of cement pastes with the same cement-water ratios:

- for low values of C/W (0.50 for CEM I and 0.30 for CEMIII), the strengths of the soil-cement mixtures are higher than the cement paste,
- for high values of C/W (0.70 for CEM I and 0.50 for CEMIII), the strengths of the soil-cement mixtures are lower than the cement paste.

These observations suggest that mixing Fontainebleau sand with diluted cement slurries (of low C/W ratios) forms a continuous solid skeleton which reinforces the microstructure. Conversely, in concentrated cement slurries, the addition of sand creates weaker bonds which fragilise the cement matrix.

For the mixes of Vernouillet sand, strengths after 28 days of curing are 1.42 to 1.71 times higher than after 7 days (Table 3-6). The strengths of the Vernouillet sand-cement mixes rise with increasing cement-water ratio (Table A-2, Appendix A).
The rate of strength development for all mixes decreases with curing time (Table 3-6). However, strength continues to increase between 90 and 360 days.

3.3.2.2 Prediction of strength development based on parameters obtained after short curing times

Many authors have proposed correlations predicting strength and stiffness increase with time for stabilised soils (Table 1-9). The data from the different soil-cement mixes produced in this study were fitted with the correlation for concretes proposed in Eurocode 2 (2005) based on measurements performed after 28 days:

$$q_{u,t} = q_{u,28} \times \exp\left[s_{28} \times \left(1 - \sqrt{\frac{28}{t}} \right) \right]$$

$q_{u,t}$ is the unconfined compressive strength after t days (MPa); $q_{u,28}$ is the unconfined compressive strength after 28 days (MPa); s_{28} is the empirical parameter used to predict strength increase based on 28-day data.

Table C-1 and Table C-2 in Appendix C give the predicted values of strength q_u calculated for different curing times. The relative errors $\%q_{u,28}$ $((q_{u,predicted} - q_{u,measured}) / q_{u,measured})$ are also presented for each mix. The values of the empirical parameter s_{28} are given in Table 3-7 and Table 3-8.

Mix	s_{28}	R^2	s_7	R^2	s_7 / s_{28}
AS300W57	0.66	0.92	1.43	0.93	2.17
AS200W40	0.73	0.91	1.71	0.93	2.34
VSI300W57	0.80	0.96	2.42	0.97	3.03
VSI346W50	0.70	0.99	1.54	0.99	2.20
VSI248W35	0.77	0.96	1.40	0.95	1.82
VSI236W31	0.87	0.95	1.29	0.91	1.48

Table 3-7 Values of the empirical parameters s_{28} and s_7 used to predict strength for silt-cement mixes.

Mix	s_{28}	R^2	s_7	R^2	s_7 / s_{28}
FS200W20	0.80	1.00	1.65	1.00	2.06
FS200W20B50	0.40	0.95	0.70	0.94	1.75
FS200W35B50	0.45	1.00	0.94	1.00	2.09
FS-I-200W20	0.20	0.86	0.37	0.85	1.85
FS-I-200W15	0.22	0.94	0.51	0.96	2.32
VSA346W29	/	/	0.84	1.00	/
VSA249W17	/	/	1.07	1.00	/
VSA230W14	/	/	0.70	1.00	/

Table 3-8 Values of the empirical parameters s_{28} and s_7 used to predict strength for sand-cement mixes.

For all mixes of treated sand and silt, the long-term strengths (after 90 or more days) are estimated reasonably well with maximum relative errors $\%q_{u28}$ of 17.34 % for the silts (Table C-1) and 8.62 % for the sands (Table C-2). It is interesting to note that the correlation between measured and predicted strengths for short curing times (before 28 days) is less accurate. The values of s_{28} for the silt-cement mixes are higher than the values for concrete and vary between 0.66 and 0.87 (Table 3-7). Values of s28 are lower for the sand-cement mixes (Table 3-8). They are closer to those given in Eurocode 2 (2005); especially for the FS-CEM I mixes. Ganne et al. (2010) found higher values of s_{28} between 0.96 and 1.71 on field samples.

The ability to predict long-term strength based on measurements carried out after short curing periods is of great interest as it could reduce the duration and minimise the number of trials needed in feasibility studies for soil mixing projects to evaluate the strength of soils stabilised with different dosages. To this end, the relation from Eurocode 2 (2005) was modified to estimate long-term strength growth using only 7-day strength data:

$$q_{u,t} = q_{u,7} \times \exp\left[s_7 \times \left(1 - \sqrt{\frac{7}{t}} \right) \right]$$

$q_{u,7}$ is the unconfined compressive strength after 7 days (MPa); s_7 is the empirical parameter used to predict strength increase based on 7-day data.

The predicted values calculated from 7-day data are plotted as dashed lines in Figure 3-15, Figure 3-16, Figure 3-18 and Figure 3-19. A good agreement is also found between measured and predicted long-term values of q_u using 7-day data (Table C-1 and Table C-2) with no loss in prediction accuracy (maximum relative errors of 18.34 % and 7.42 % were determined for

the silt and sand mixes respectively). The values of s_7 are 1.5 to 3 times higher than s_{28} (Table 3-7 and Table 3-8).

Data from the literature was used to investigate the use of the exponential relation with 7-day data to evaluate the increase in strength of clayey soils with high moisture contents treated with cement (Table C-3, Appendix C). The results show a good fit between measured and predicted strengths (Figure 3-20, Figure 3-21 and Figure 3-22). The values of s_7 for clay-cement mixes are slightly lower than those determined for silt-cement mixes (Table C-3). An average s_7 of 1.24 is obtained for the clay-cement data from the literature.

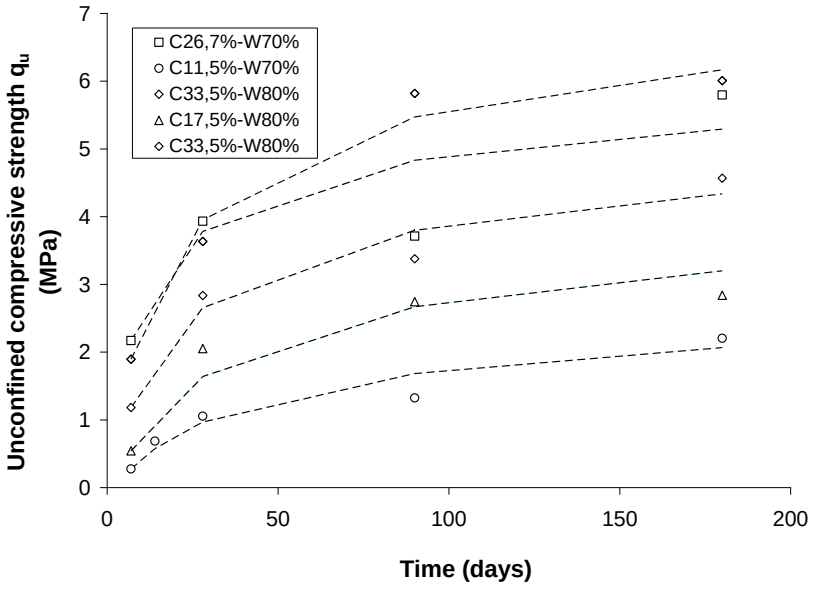

Figure 3-20 Compressive strength of argile du Puy-CEM III cement mixes versus time - comparison with predicted strengths based on data obtained after 7 days (data from Szymkiewicz (2011)).

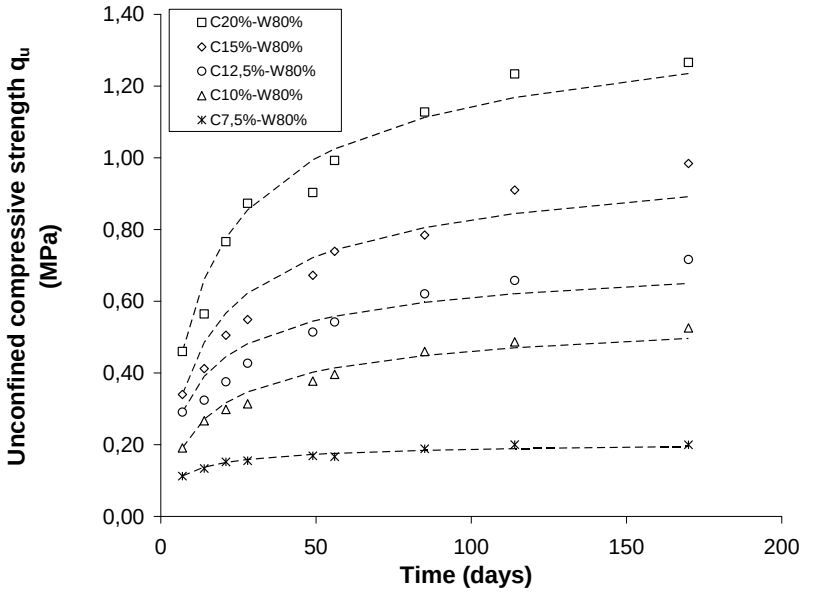

Figure 3-21 Compressive strength of Bangkok clay-Portland cement mixes versus time - comparison with predicted strengths based on data obtained after 7 days (data from Horpibulsuk et al. (2003)).

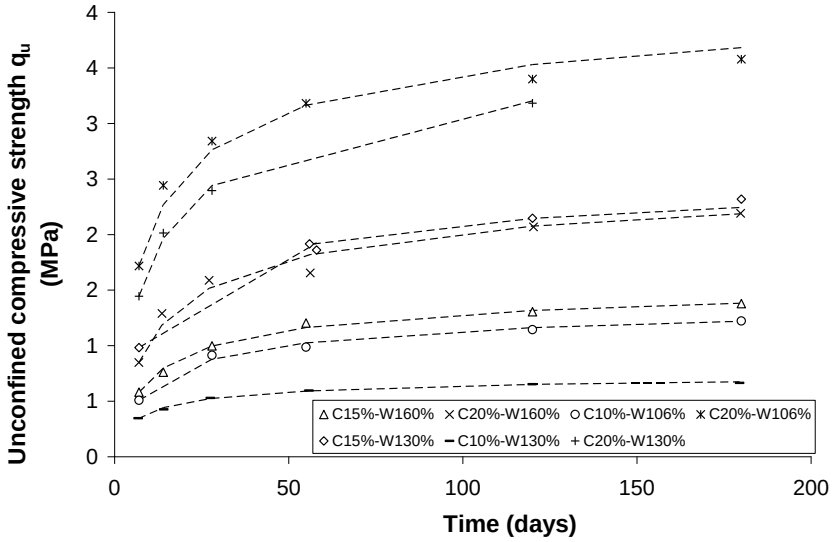

Figure 3-22 Compressive strength of Ariake clay-Portland cement mixes versus time - comparison with predicted strengths based on data obtained after 7 days (data from Horpibulsuk et al. (2003)).

The values of the empirical parameter s_7 appear to depend on many factors such as dosage and soil type. Large scatter can be seen in Figure 3-23 and no clear trend is found between s_7 and cement content, moisture content or strength after 7 days. However, the average value for all soil types is 1.25 with most results between 1 and 1.5.

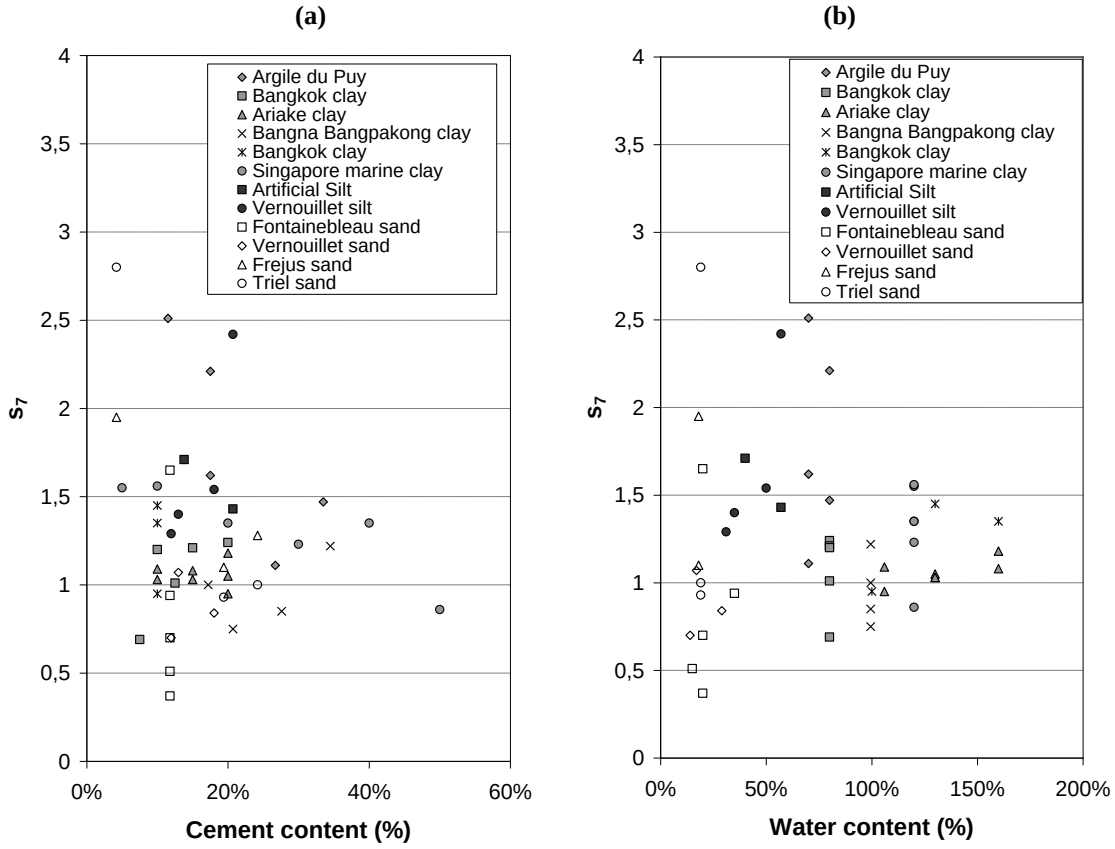

Figure 3-23 s_7 versus (a) cement and (b) water content for soils treated with cement.

3.3.3 Static deformation modulus

3.3.3.1 Loading procedures

As discussed in the literature review, different methods can be used to calculate the static deformation modulus based on stress-strain curves from compression tests on stabilised soils. Three loading procedures were tested on specimens of treated silt (mix AS300W57) cured for 14 days to compare the values of different deformation moduli. The loading procedures and calculated moduli from the stress-strain curves (Figure 3-24) are given in the Table 3-9.

Procedure	Loading	Deformation modulus
1	Simple loading at constant displacement rate of 1.5 %/min	- Secant $E_{0.001\%}$: secant modulus at a strain of 0.001 % - Secant E_{30}: secant modulus at a stress equal to 30 % of the maximum strength - Secant E_{50}: secant modulus at a stress equal to half the maximum strength
2	10 loading/unloading cycles between 10 % and 30 % of maximum strength	- Tangent E_{30}: for each loading/unloading cycle, tangent modulus calculated from the unloading part of the stress-strain curve
3	10 loading/unloading cycles between 30 % and 50 % of maximum strength	- Tangent E_{50}: for each loading/unloading cycle, tangent modulus calculated from the unloading part of the stress-strain curve

Table 3-9 Definition of deformation moduli calculated from different loading procedures tested on specimens of treated silt (mix AS300W57) cured for 14 days.

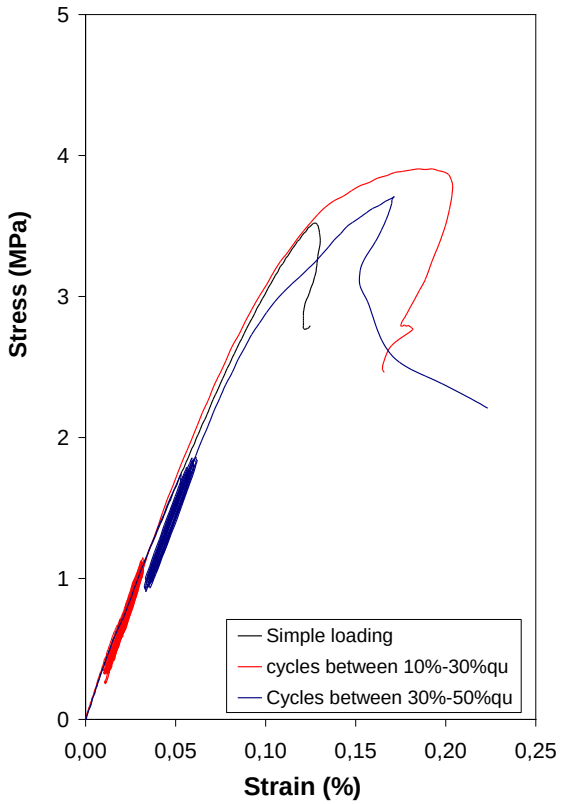

Figure 3-24 Stress-strain curves obtained from different loading procedures tested on specimens of treated silt (mix AS300W57) cured for 14 days.

For the tested silt specimens, calculated values for both secant and tangent E_{50} are slightly lower but very close to the values of secant and tangent E_{30} (Figure 3-25). Although structures

are merely loaded to only approximately one third of their maximum strength capacity, these results suggest that the use of E_{50} does not lead to significant overestimations of settlements in the case of silts treated with cement. No significant variations in tangent E_{30} and E_{50} were observed during successive loading/unloading cycles (Figure 3-25). This implies that, even at a stress equal the half the maximum strength, the behaviour of the tested silt material remains practically elastic. The small strain modulus $E_{0.001\%}$ is slightly higher than E_{30} and E_{50}. Details on the method used to calculate the dynamic modulus of elasticity (E_0) are given in section 3.3.4. The static to dynamic modulus ratio appears to be close to 2 for the treated artificial silt after 14 days of curing.

An additional test on a specimen of treated Fontainebleau sand (mixed FS200W20) also produced almost equal values of secant E_{50} and E_{30} (Figure 3-26).

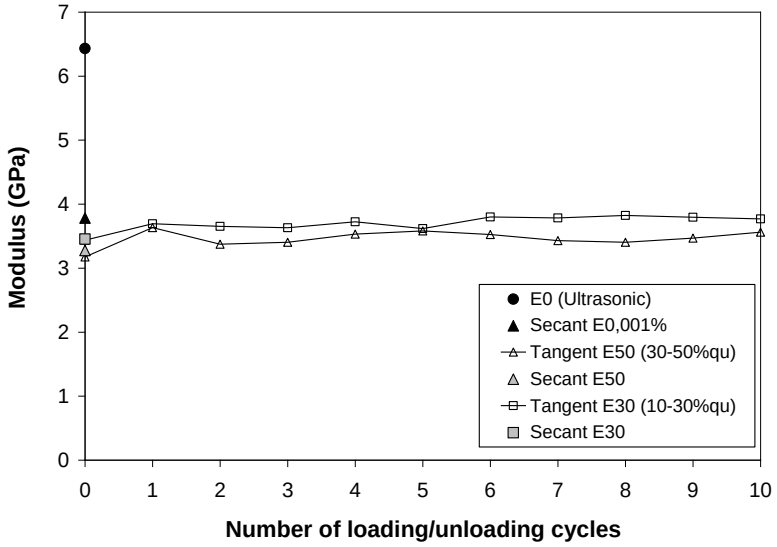

Figure 3-25 Deformation moduli calculated from different loading procedures tested on specimens of treated silt (mix AS300W57) cured for 14 days.

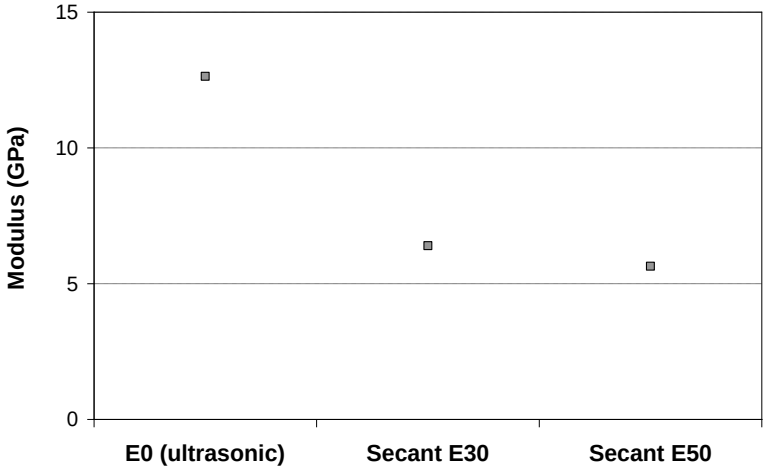

Figure 3-26 Deformation moduli calculated from stress-strain curve for treated sand (mix FS200W20) cured for 28 days.

Based on these results, E_{50} calculated from stress-strain curves as the secant modulus at a stress equal to half the maximum strength will be used throughout this study to evaluate the static stiffness of treated soil specimens.

3.3.3.2 Stiffness-strain curves for soils stabilised in the laboratory with cement

Figure 3-27 presents the secant stiffness-strain curves after different curing times for treated Fontainebleau sand and artificial silt specimens derived from the stress-strain curves in Figure 3-13.

At a given level of strain, the secant stiffness of the soil-cement mixes increases with curing time. As strain increases, stiffness decreases non-linearly for both soils. This decrease appears to be more pronounced for treated sand specimens (Figure 3-28). The stress-strain behaviour of uncemented soils is highly non-linear and soil stiffness significantly decreases with strain (Atkinson, 2000). The trends observed in Figure 3-27 are similar to characteristic stiffness-strain curves of natural soils described by Atkinson and Sallfors (1991) and Mair (1993).

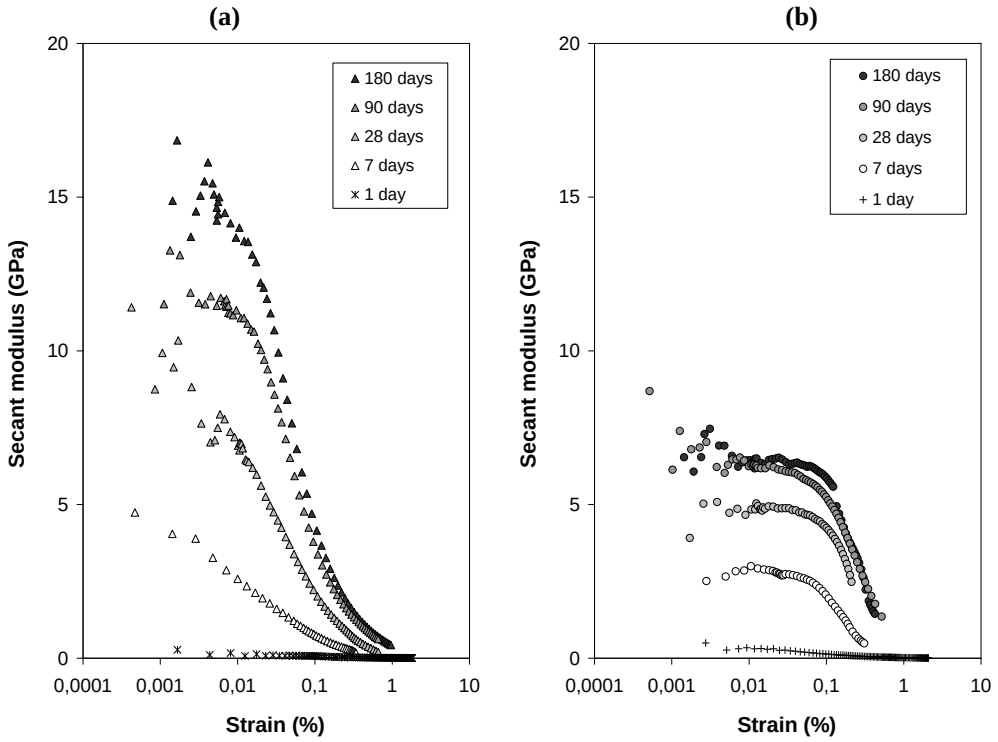

Figure 3-27 Typical secant stiffness-strain curves for (a) specimens of stabilised Fontainebleau sand (FS200W20) and (b) specimens of stabilised artificial silt (AS200W40).

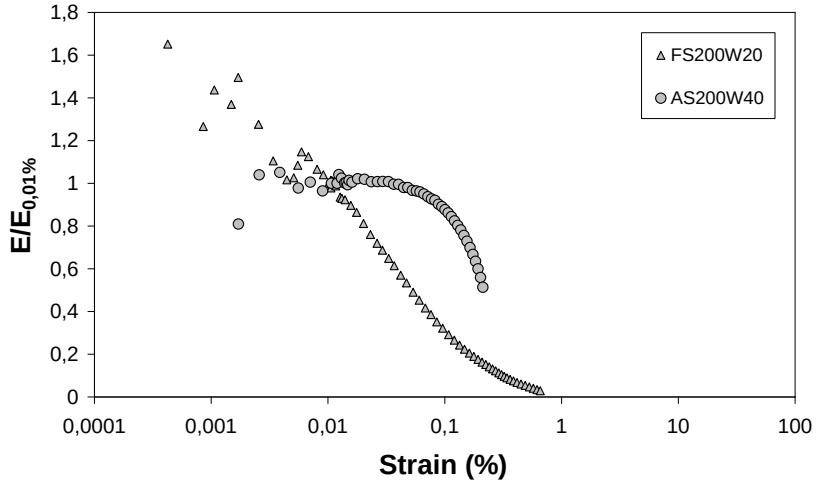

Figure 3-28 Normalised secant stiffness $E/E_{0.01\%}$ after 28 days for specimens of stabilised Fontainebleau sand (FS200W20) and specimens of stabilised artificial silt (AS200W40).

3.3.3.3 Strength – static stiffness relations for soils stabilised in the laboratory

The static stiffness E_{50} measured at various curing times for the four soils stabilised in the laboratory with different dosages are plotted versus unconfined compressive strength q_u in Figure 3-29.

The unconfined compressive strengths of the stabilised sand specimens (Fontainebleau FS and Vernouillet VSA) are between 0.1 and 9 MPa. The static modulus E_{50} varies between 0 and 15 GPa and appears to increase more or less linearly over the range of unconfined compressive strengths tested (a best fitting operation using a power law gives an exponent very close to 1).

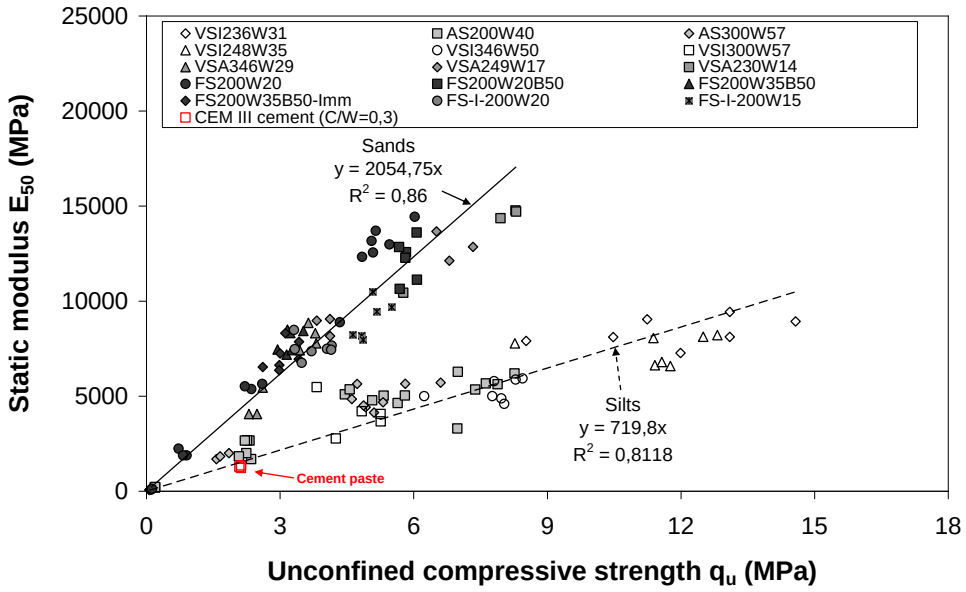

Figure 3-29 Static secant modulus E_{50} versus unconfined compressive strength q_u for laboratory specimens.

The unconfined compressive strengths of the tested stabilised silt specimens (artificial AS and Vernouillet VSI) vary between 0.1 and 15 MPa. At the same strength level, the static modulus E_{50} of the silt specimens is lower than that of the sand specimens. Although a slight non-linear tendency can be seen in the results, a linear relation provides a reasonable fit to the data (Figure 3-29):

For stabilised silts: $E_{50} \approx 720 \times q_u$

For stabilised sands: $E_{50} \approx 2055 \times q_u$

with E_{50} and q_u in MPa.

After 28 days of curing, specimens of CEM III paste (C/W = 0.3) have strengths close to 2 MPa and static stiffness E_{50} slightly higher than 1 GPa. The E_{50}/q_u ratio for these specimens is close to the trend found for silts in Figure 3-29.

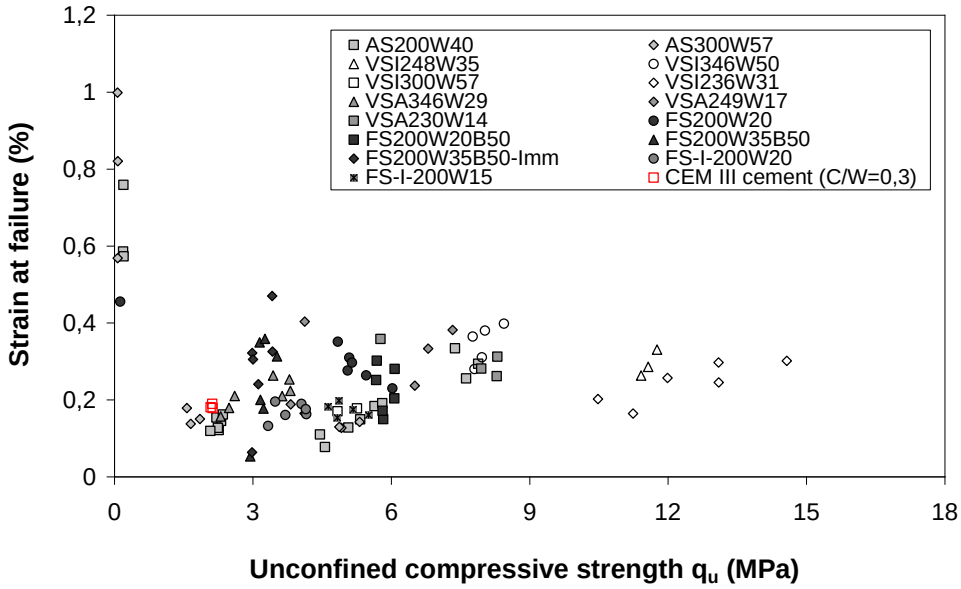

Figure 3-30 Strain at failure ε_f versus unconfined compressive strength q_u for laboratory specimens.

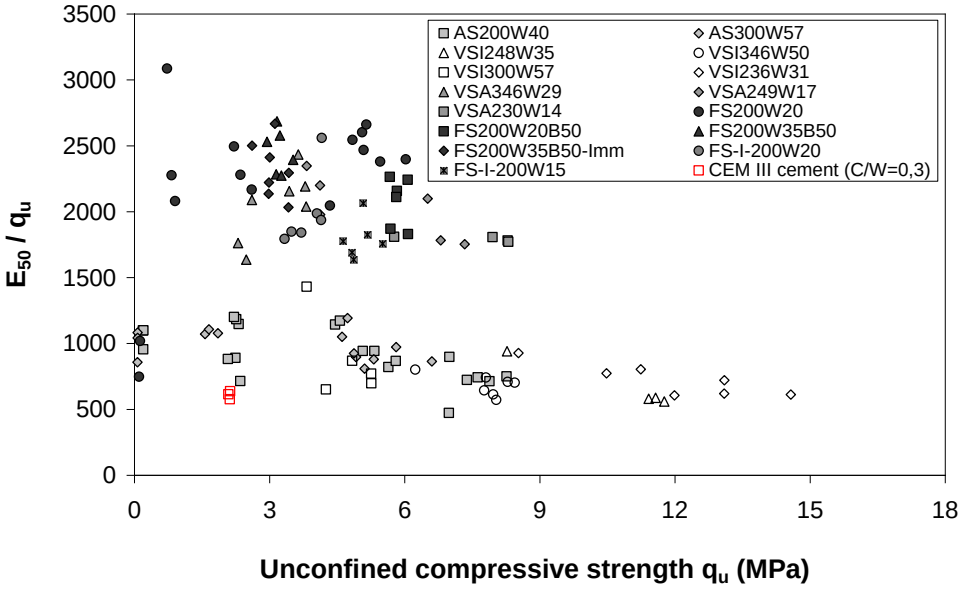

Figure 3-31 E_{50}/q_u versus unconfined compressive strength q_u for laboratory specimens.

The values of E_{50} determined in this study are higher than the majority of the results published in the literature (for example in Eurosoilstab, 2002). As discussed in Chapter 1, this can be explained by the different methods used to measure the longitudinal strains of specimens during loading. Studies have analysed the influence of strain measurements (external and local) on the stiffness of stabilised soils (Tan et al., 2002; Goto et al., 1991; Shibuya et al., 1992). The strains at failure of specimens of stabilised soils in unconfined compression tests and triaxial tests are generally between 1 and 5 % when the axial strain is measured externally between end-platens (CDIT, 2002; Åhnberg et al., 2003; Åhnberg, 2006). The strains at failure measured here using local displacement transducers on specimens stabilised in the laboratory are much lower (five to ten times lower) with values between 0.1 and 1.0 %

(Figure 3-30). The determination of stiffness at lower values of strain explains the high E_{50}/q_u ratios (2055 for the treated sands and 720 for the treated silts) presented in Figure 3-31.
Although linear relations fit well to the data, it is interesting to note that the E_{50}/q_u ratios appear to decrease with strength suggesting slightly non-linear strength-stiffness relations.

3.3.4 Dynamic modulus of elasticity

3.3.4.1 Choice of Poisson's ratio

The dynamic elastic modulus based on ultrasonic wave velocity measurements is calculated using the following equation:

$$E_0 = \rho \times \frac{(1+\nu)\times(1-2\nu)}{(1-\nu)} \times V_p{}^2$$

where E_0 is the dynamic elastic modulus (Pa), ρ is the density (kg/m^3), ν is the dynamic Poisson's ratio and V_p is the ultrasonic wave velocity (m/s).

Åhnberg and Holmen (2011) reported a dynamic Poisson's ratio of 0.30 for soft soils stabilised in the laboratory. The results from other researchers (CDIT, 2002) show that the Poisson's ratio of in situ cement-treated soils varies between 0.25 and 0.45. Eurocode 2 (2005) recommends the use of 0.20 for concrete.

In this study, the dynamic Poisson's ratio ν is assumed constant and equal to 0.25 for calculating the dynamic elastic modulus.
The sensitivity of the calculated modulus to the choice of Poisson's ratio is illustrated in Figure 3-32. Using ν = 0.25, the dynamic modulus is underestimated by 8 % for an actual Poisson's ratio of 0.20 and overestimated by 25 % for an actual Poisson's ratio of 0.35.

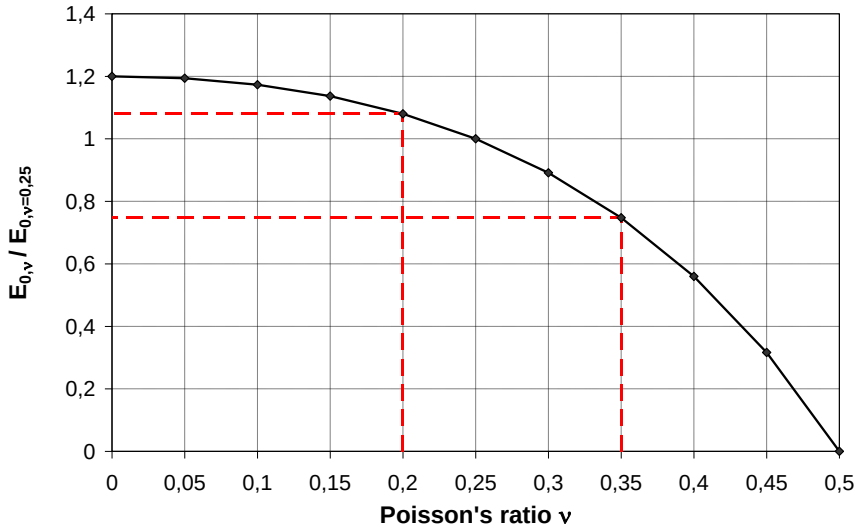

Figure 3-32 Effect of Poisson's ratio on calculated dynamic modulus of elasticity E_0.

3.3.4.2 Increase in dynamic modulus with time

3.3.4.2.1 In treated silts

Measured ultrasonic wave velocities V_p and dynamic moduli of elasticity E_0 for the silt-cement mixes are plotted versus time in Figure 3-33 and Figure 3-34. The graphs clearly show that V_p and E_0 increase with curing time.

After 1 day of curing, wave velocities of 1240 m/s and 1500 m/s are measured on specimens of mixes AS300W57 and AS200W40 respectively. The average velocities are of 2410 m/s for AS300W57 and 2520 m/s for AS200W40 after 360 days. The wave velocities measured through specimens of mix VSI300W57 are lower than for specimens of AS300W57. The velocities measured for mix VSI346W50 are lower than for mixes VSI248W35 and VSI236W31.

The measured values of E_0 and growths between different curing times are given in Table 3-10. High moulding moisture contents appear to have a similar effect on wave velocity, dynamic modulus and strength (as discussed in section 3.3.2.1.1). The rate of increase in seismic modulus decreases with curing time (Table 3-10). The ratios of E_0 between different curing times are lower than the ratios found for strength. Between 7 and 28 days of curing, the modulus ratio $E_{0,28}/E_{0,7}$ is between 1.10 and 1.27 (Table 3-10) whereas the strength ratio q_{u28} / q_{u7} varies between 1.69 and 3.93 (Table 3-5). However, E_0 continues to increase up to 360 days after moulding.

Mix	$E_{0,7}$ (MPa)	$E_{0,28}$ (MPa)	$E_{0,90}$ (MPa)	$E_{0,180}$ (MPa)	$E_{0,360}$ (MPa)	$E_{0,28}/E_{0,7}$	$E_{0,90}/E_{0,28}$	$E_{0,180}/E_{0,90}$	$E_{0,360}/E_{0,180}$
AS300W57	5507	6986	7496	8135	8073	1.27	1.07	1.09	0.99
AS200W40	6565	8040	8244	8990	9280	1.22	1.03	1.09	1.03
VSI300W57	4560	5484	6128	6867	7245	1.20	1.12	1.12	-
VSI346W50	5700	6531	7041	8221	8490	1.15	1.08	1.17	1.03
VSI248W35	6837	7488	8637	10056	10518	1.10	1.15	1.16	1.05
VSI236W31	7558	8458	9219	10623	11842	1.12	1.09	1.15	1.11

Table 3-10 Measured moduli and modulus gains between different curing times for silt-cement mixes.

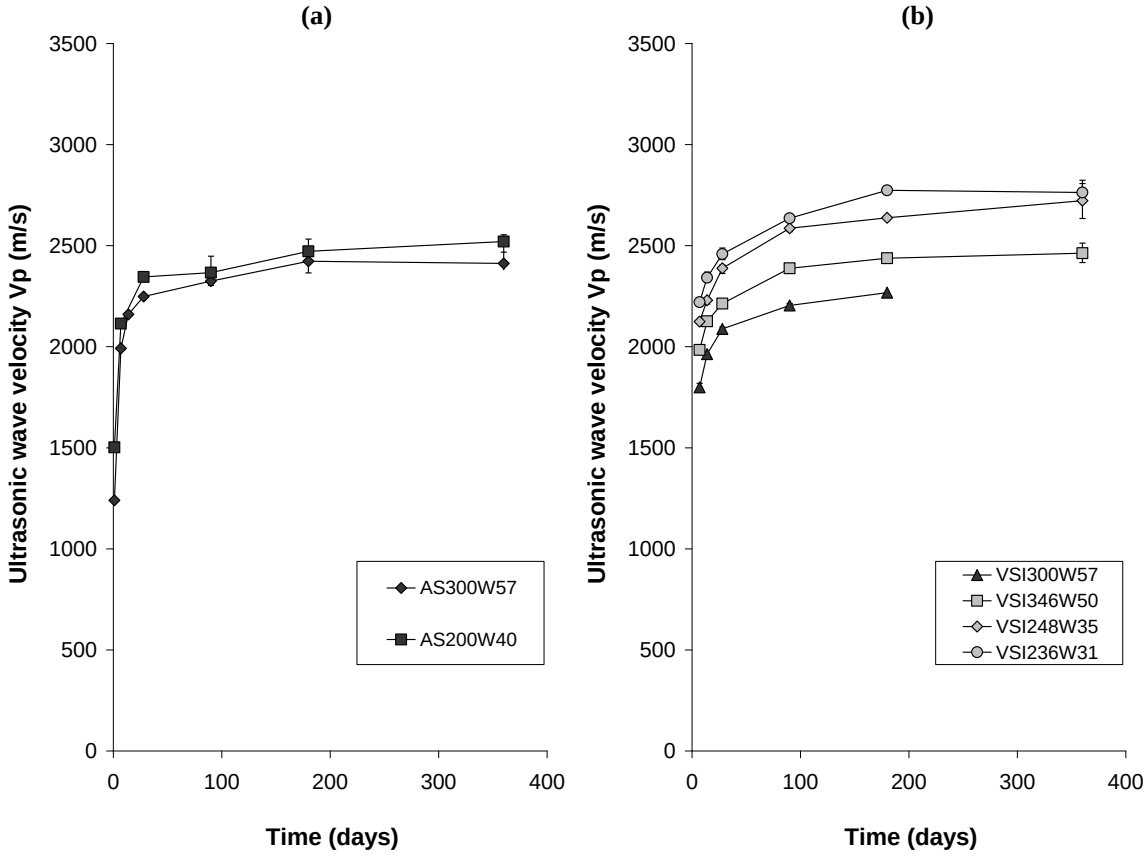

Figure 3-33 Ultrasonic wave velocity versus time for silt-cement mixes (a) AS; (b) VSI.

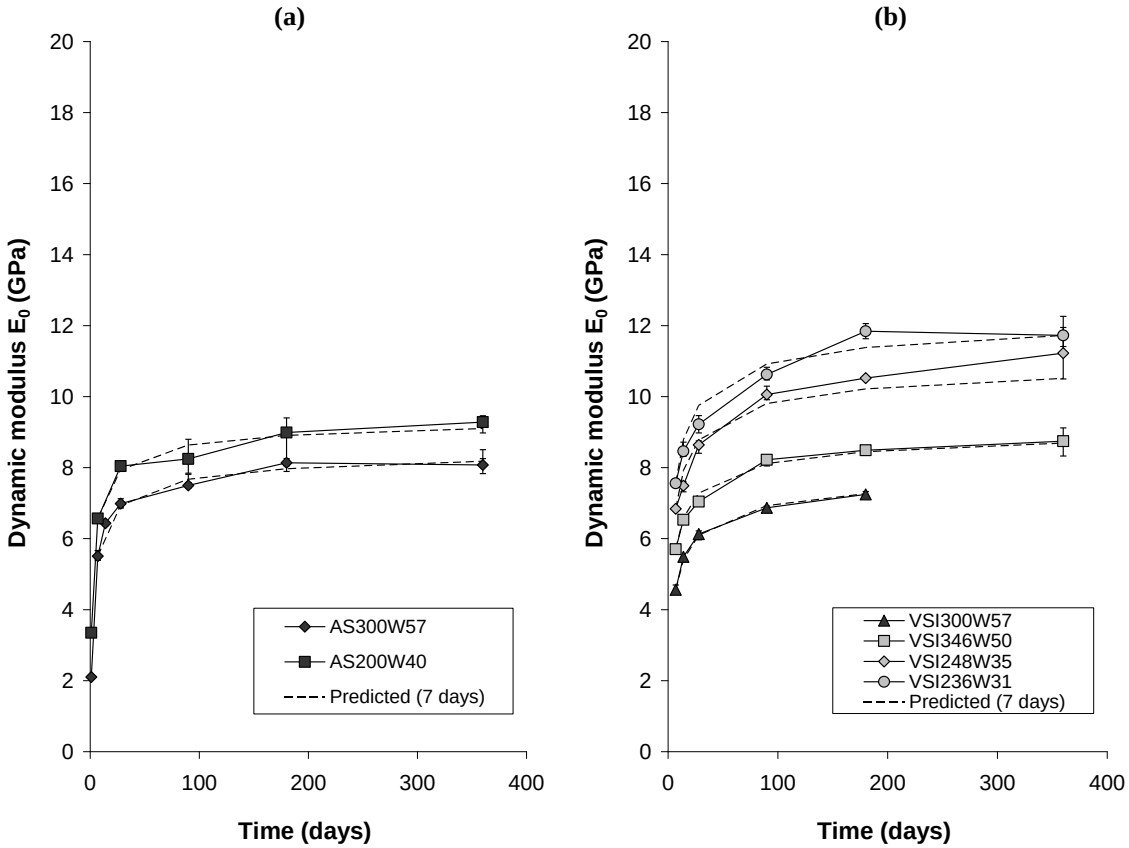

Figure 3-34 Dynamic modulus of elasticity versus time for silt-cement mixes a) AS; (b) VSI - comparison with predicted modulus based on data obtained after 7 days.

3.3.4.2.2 In treated sands

The measured ultrasonic wave velocities V_p and dynamic moduli of elasticity E_0 of all the Fontainebleau sand-cement mixes increase with time (Figure 3-35 and Figure 3-36).

The average velocity measured for specimens of mix FS200W20 grows from less than 1000 m/s after 1 day to close to 3300 m/s after 360 days.

The effects of bentonite on the ultrasonic wave velocity of stabilised Fontainebleau sand are comparable to the effects on unconfined compressive strength (Figure 3-35). After 7 days of curing, the average ultrasonic wave velocity measured in specimens with bentonite (2640 m/s for mix FS200W20B50) is considerably higher than the velocity measured in specimens of mix FS200W20 without bentonite (≈ 2080 m/s). For longer curing periods, the wave velocities measured for mix FS200W20 progressively increase and ultimately exceed the velocities measured for mix FS200W20B50 after 90 days.

The rate of increase in seismic modulus reduces with curing time (Table 3-11). In the case of sands, the ratios of E_0 between different curing times are also lower than the ratios found for strength (Table 3-6).

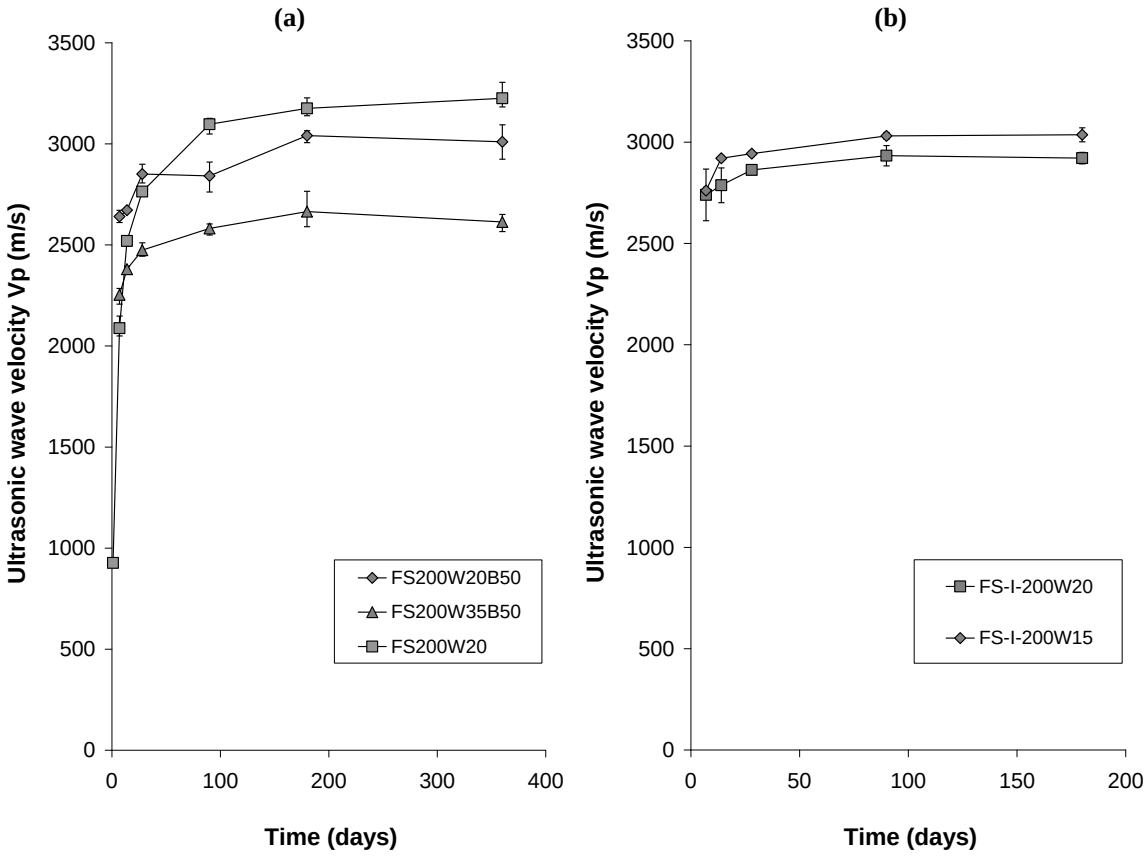

Figure 3-35 Ultrasonic wave velocity versus time for FS-cement mixes (a) CEM III; (b) CEM I.

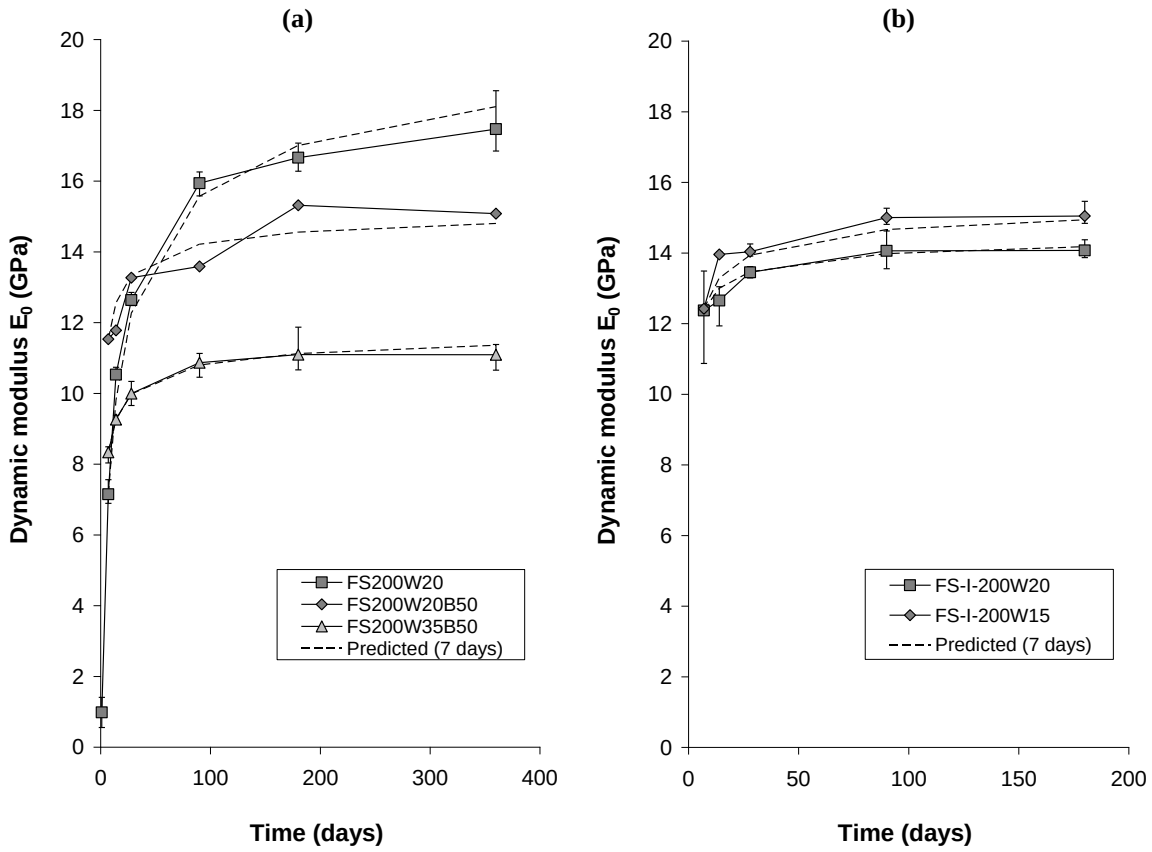

Figure 3-36 Dynamic modulus E_0 versus time for FS-cement mixes (a) CEM III; (b) CEM I.

Mix	$E_{0,7}$ (MPa)	$E_{0,28}$ (MPa)	$E_{0,90}$ (MPa)	$E_{0,180}$ (MPa)	$E_{0,360}$ (MPa)	$E_{0,28}/E_{0,7}$	$E_{0,90}/E_{0,28}$	$E_{0,180}/E_{0,90}$	$E_{0,360}/E_{0,180}$
FS200W20	7147	12638	15941	16659	17466	1.77	1.26	1.05	1.05
FS200W20B50	11533	13269	13584	15317	15078	1.15	1.02	1.13	0.98
FS200W35B50	8333	9994	10866	11095	11091	1.20	1.09	1.02	1.00
FS-I-200W20	12369	13453	14060	14073	/	1.09	1.05	1.00	/
FS-I-200W15	12422	14034	14999	15047	/	1.13	1.07	1.00	/
VSA346W29	11548	12861	/	/	/	1.11	/	/	/
VSA249W17	14605	18048	/	/	/	1.24	/	/	/
VSA230W14	16940	19927	/	/	/	1.18	/	/	/

Table 3-11 Measured moduli and modulus gains between different curing times for sand-cement mixes.

3.3.4.3 Prediction of stiffness development based on parameters obtained after short curing times

The increases in dynamic modulus of elasticity with time for the different soil-cement mixes considered in this study were fitted using a similar relationship to that used for the prediction of strength:

$$E_{0,t} = E_{0,28} \times \exp\left[q_{28} \times \left(1 - \sqrt{\frac{28}{t}} \right) \right]$$

$E_{0,t}$ is the modulus at curing time t (MPa); $E_{0,28}$ is the modulus after 28 days (MPa); q_{28} is the empirical parameter used to predict the modulus based on 28-day data.

A good agreement is found for all mixes between the measured and calculated values of E_0 with maximum relative errors $\%E_{28}$ of 11.42 % for the silts and 12.75 % for the sands (Table D-1 and Table D-2, Appendix D). The values used for q_{28} are given in Table 3-12 and Table 3-13.

As for strength, the capacity to calculate long-term stiffness based on measurements carried out after short curing times is of great importance. The correlation was modified to estimate long-term stiffness growth using only 7-day data:

$$E_{0,t} = E_{0,7} \times \exp\left[q_{7} \times \left(1 - \sqrt{\frac{7}{t}} \right) \right]$$

$E_{0,t}$ is the modulus at curing time t; $E_{0,7}$ is the modulus after 7 days; q_7 is the empirical parameter used to predict E_0 based on 7-day data.

A good correlation is also found between measured and predicted long-term values of E_0 using 7-day data with even a gain in prediction accuracy (Table D-1 and Table D-2, Appendix D). Maximum relative errors of 6.32 % and 4.97 % were determined for the silt and sand mixes.

The values of the empirical parameters q_7 and q_{28} vary with both soil type and dosage (Table 3-12 and Table 3-13). No clear relations between these parameters and the strength and stiffness data were identified. However, a relatively constant ratio is found between q_7 and s_7 and between q_{28} and s_{28}. This ratio is on average close to 0.31 for the silt-cement mixes and near 0.50 for the sand-cement mixes. These values, inferior to 1, show that strength develops more rapidly than stiffness in stabilised soils.

Mix	q_{28}	R^2	q_7	R^2	q_7 / q_{28}	q_7 / s_7	q_{28} / s_{28}
AS300W57	0.20	0.97	0.46	0.98	2.30	0.32	0.30
AS200W40	0.18	0.94	0.38	0.95	2.11	0.22	0.25
VSI300W57	0.24	0.98	0.58	1.00	2.42	0.24	0.30
VSI346W50	0.25	0.97	0.49	0.99	1.96	0.32	0.36
VSI248W35	0.28	0.98	0.50	0.96	1.79	0.36	0.36
VSI236W31	0.28	0.94	0.51	0.95	1.82	0.40	0.32

Table 3-12 Values of the empirical parameter q_{28} and q_7 used to predict stiffness for silt-cement mixes.

Mix	q_{28}	R^2	q_7	R^2	q_7 / q_{28}	q_7 / s_7	q_{28} / s_{28}
FS200W20	0.45	0.99	1.08	0.99	2.40	0.65	0.56
FS200W20B50	0.20	0.88	0.29	0.87	1.45	0.41	0.50
FS200W35B50	0.19	0.98	0.36	0.99	1.89	0.38	0.42
FS-I-200W20	0.12	0.85	0.17	0.96	1.42	0.46	0.60
FS-I-200W15	0.16	0.78	0.23	0.94	1.44	0.45	0.73
VSA346W29	/	/	0.22	1.00	/	0.26	/
VSA249W17	/	/	0.42	1.00	/	0.39	/
VSA230W14	/	/	0.33	1.00	/	0.47	/

Table 3-13 Values of the empirical parameter q_{28} and q_7 used to predict stiffness for sand-cement mixes.

3.3.4.4 Summary for the prediction of strength and stiffness growth

Summarising the results on the prediction of strength and dynamic modulus increase with curing time for soils treated with cement in the laboratory, the following correlation can be used to obtain a reasonable estimate of the growth in unconfined compressive strength from data obtained after 7 days:

$$q_{u,t} = q_{u,7} \times \beta \qquad \text{with} \qquad \beta = \exp\left[s_7 \times \left(1 - \sqrt{\frac{7}{t}} \right) \right]$$

$q_{u,t}$ is the strength at curing time t; $q_{u,7}$ is the strength after 7 days; s_7 is the empirical parameter used to predict the strength based on 7-day data.

For clays: $0.69 \leq s_7 \leq 2.51$ (average $s_7 = 1.24$)

For silts: $1.29 \leq s_7 \leq 2.42$ (average $s_7 = 1.63$)

For sands: $0.37 \leq s_7 \leq 1.65$ (average $s_7 = 0.84$)

Since $q_7 \approx 0.30 \times s_7$ for silts and $q_7 \approx 0.50 \times s_7$ for sands, the following relations can provide a reasonable estimate of the increase in dynamic modulus with curing time based on data measured after 7 days:

For silts: $E_{0,t} = E_{0,7} \times \beta^{0.30}$

For sands $E_{0,t} = E_{0,7} \times \beta^{0.50}$

$E_{0,t}$ is the modulus at curing time t; $E_{0,7}$ is the modulus after 7 days.

3.3.4.5 Strength – dynamic stiffness relations for soils stabilised in the laboratory

Figure 3-37 presents the compression wave velocities V_p obtained from ultrasonic pulse wave velocity measurements versus unconfined compressive strength. For both types of soil, the wave velocities increase with strength. The P-wave velocities of the specimens of stabilised silt vary between 1200 and 2850 m/s. The P-wave velocities of the specimens of stabilised sand lie between 750 and 3400 m/s. The relations between q_u and V_p are clearly non-linear. Power laws were chosen to fit the data (Figure 3-37). A best fiting operation gives an exponent of 6.5 for silts and close to 3.5 for sands.

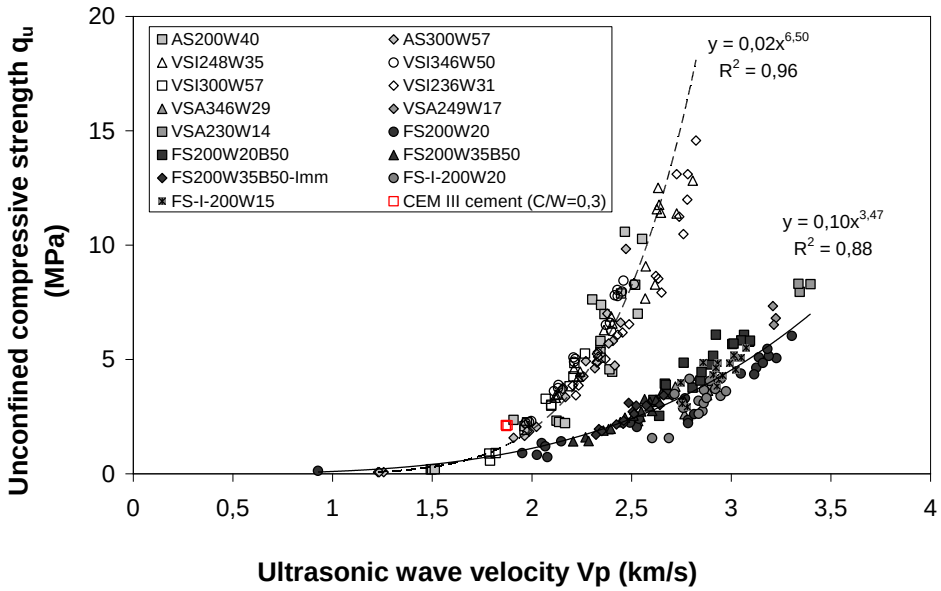

Figure 3-37 Unconfined compressive strength q_u versus ultrasonic wave velocity V_p for laboratory specimens.

Khan et al. (2006) also found a power law relation between V_p and q_u with an exponent close to 4 for specimens of silica sand mixed in the laboratory with gypsum cement.
Differences in wave velocity-strength relations between different soil types have been reported by Asaka and Abe (2011). They found larger wave velocities for treated sands than for clays with the same strength, which is compatible with the data in Figure 3-37.

For both silt and sand specimens, E_0 increases non-linearly with strength q_u (Figure 3-38). Values of E_0 range between 1.4 and 20 GPa for the sands and between 2 and 12 GPa for the silts. E_0 is close to 3.5 GPa for the CEM III paste after 28 days. As the strength q_u of the sand specimens is nearly proportional to V_p^4 (Figure 3-37), and the dynamic modulus E_0 is calculated using V_p^2, E_0 is found to be approximately proportional to the square root of q_u (exponent of 0.52, Figure 3-38). For the silt specimens, E_0 is found to correlate to more or less the cube root of q_u (exponent of 0.31, Figure 3-38). The dynamic moduli E_0 of the silt specimens are lower than those of the treated sand specimens of equivalent strengths, confirming the difference found for E_{50} (Figure 3-29).

It is worth noting that the exponents of the power relations between E_0 and q_u are identical to the q_7/s_7 ratios for the increase in strength and dynamic stiffness with curing time.

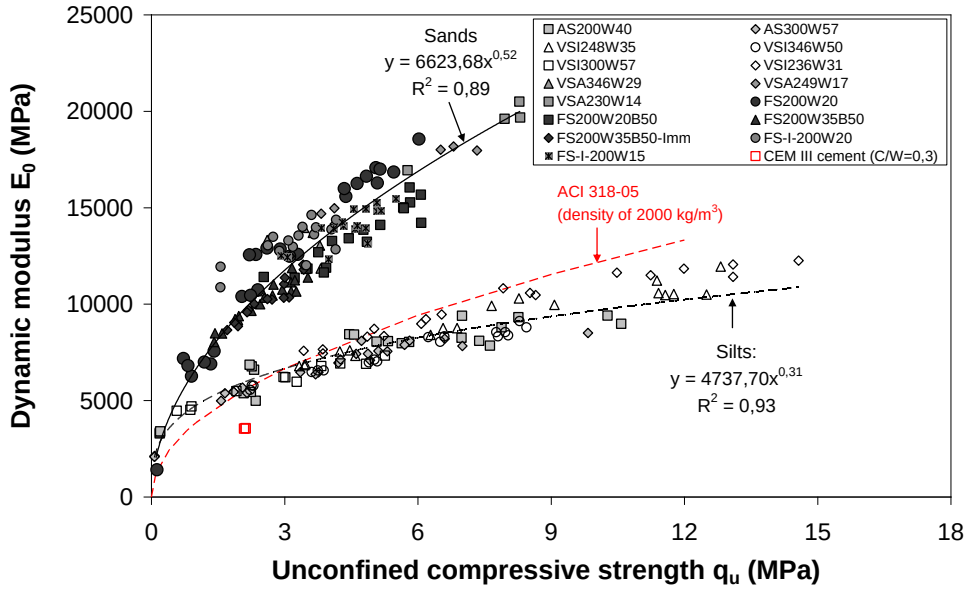

Figure 3-38 Dynamic elastic modulus E_0 versus unconfined compressive strength q_u for laboratory specimens.

According to Clayton (2011), the stiffness at very small strain of a granular material depends on three factors:

- the void ratio of the specimen,
- the interparticle contact stiffness, which depends on mineralogy, angularity and effective stress,
- and the deformation within individual particles, which depends on particle mineralogy and shape.

In the case of cemented soils, stiffness depends on the stiffness of the bonds created by the binder between particles.

Assuming the binder contents were sufficient to eliminate the interparticle contacts and that the stiffness of the bonds created by the binder is the same for all soils, the differences in global stiffness (both static E_{50} and dynamic E_0) between the treated silt and sand specimens result from the combined effects of void ratio and particle deformation. Clayton (2011) found that, above a certain dosage, the stiffness of sand treated with two different types of cement measured in the resonant column apparatus decreased with void ratio and was independent of the effective stress applied during testing. The porosities of the silt mixes are higher than the porosities of the sand-cement mixes due to higher initial water contents (Table 3-4). These different porosities partly explain the differences in stiffness observed between the treated silt and treated sand specimens (the silt specimens of higher porosities have lower stiffness). The detrimental effect of porosity on stiffness is revealed in Figure 3-39.

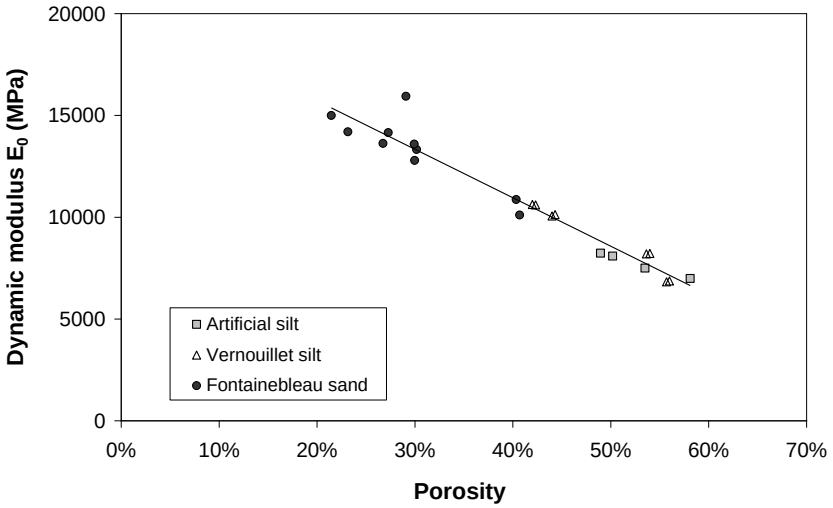

Figure 3-39 Dynamic elastic modulus E_0 versus porosity after 28 and 90 days for laboratory specimens.

It is well known that the stiffness and volumetric proportion of aggregates significantly affect the modulus of elasticity of concrete (Page and Page, 2007). In general, stiffer aggregates increase the modulus of concrete. In the present case, it is reasonable to assume that the stiffness of sand (quartz) particles is greater than the stiffness of the clay particles contained in the silts (Speswhite kaolin for the artificial silt). This also certainly contributes to the differences in stiffness observed between specimens of silt and sand with similar unconfined compressive strengths.

Many researchers have published various empirical relationships between unconfined compressive strength and ultrasonic wave velocity or dynamic modulus of concrete (Panesar and Shindman, 2011).
The equation linking compressive strength to modulus given in ACI 318-05 (2005) is:

$$E = 0.043 \times \rho^{1.5} \times \sqrt{q_u}$$

with q_u in MPa; ρ in kg/m^3 and E in MPa.

This relation is interesting as the measured values of E_0 for the specimens of stabilised sand are proportional to the square root of q_u (Figure 3-38). In addition, the equation includes the unit weight which is an important difference between treated sands and silts (Figure 3-7 and Figure 3-8). However, assuming a density of 2000 kg/m^3, the ACI 318-05 relationship underestimates the stiffness of the stabilised sand mixes (Figure 3-38). The calculated values of E_0 are much closer to those measured for the specimens of stabilised silt.

The following empricial relations were found to relate the unconfined compressive strength and dynamic elastic modulus in the conditions of this study (Figure 3-40 and Figure 3-41):

For stabilised silts: $E_0 \approx 2.63 \times \rho \times \sqrt[3]{q_u}$

For stabilised sands: $E_0 \approx 3.42 \times \rho \times \sqrt{q_u}$

with q_u in MPa; ρ in kg/m^3 and E_0 in MPa.

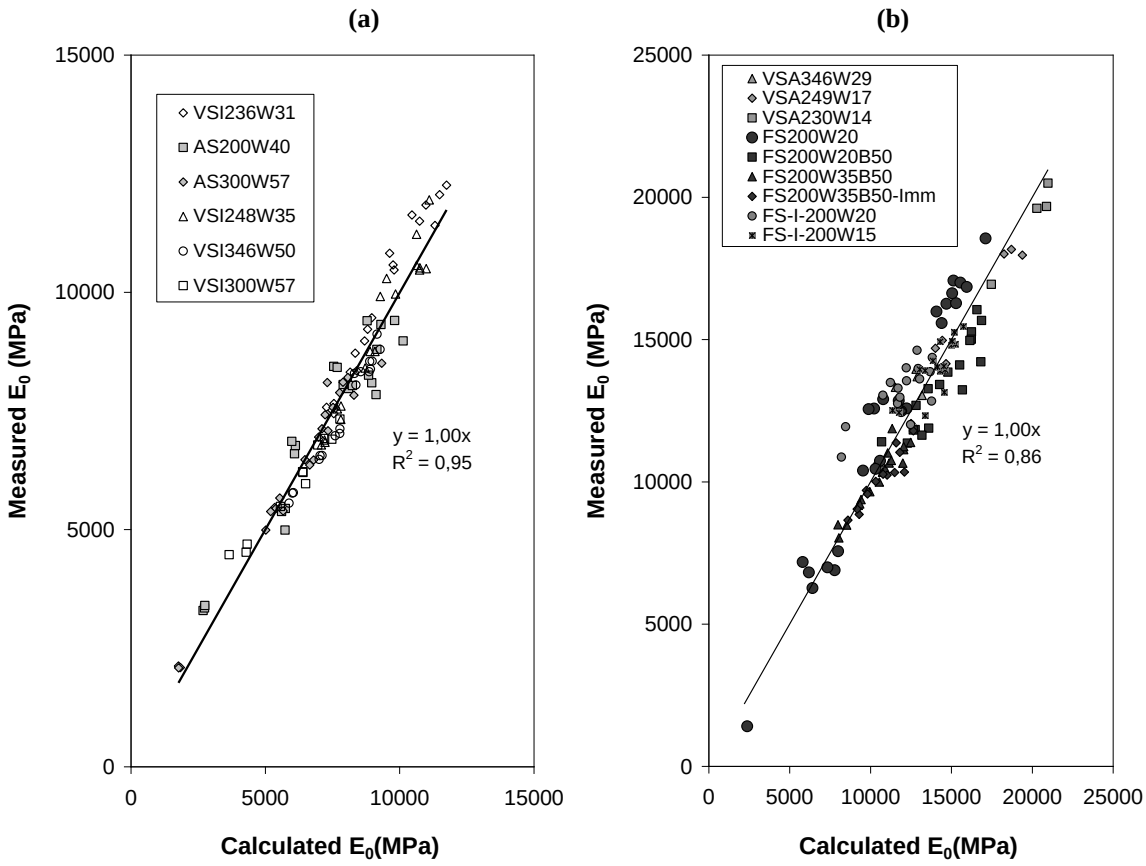

Figure 3-40 Comparison between measured and calculated values of E_0 using modified ACI 318-05 relations taking into account measured densities (a) silts; (b) sands.

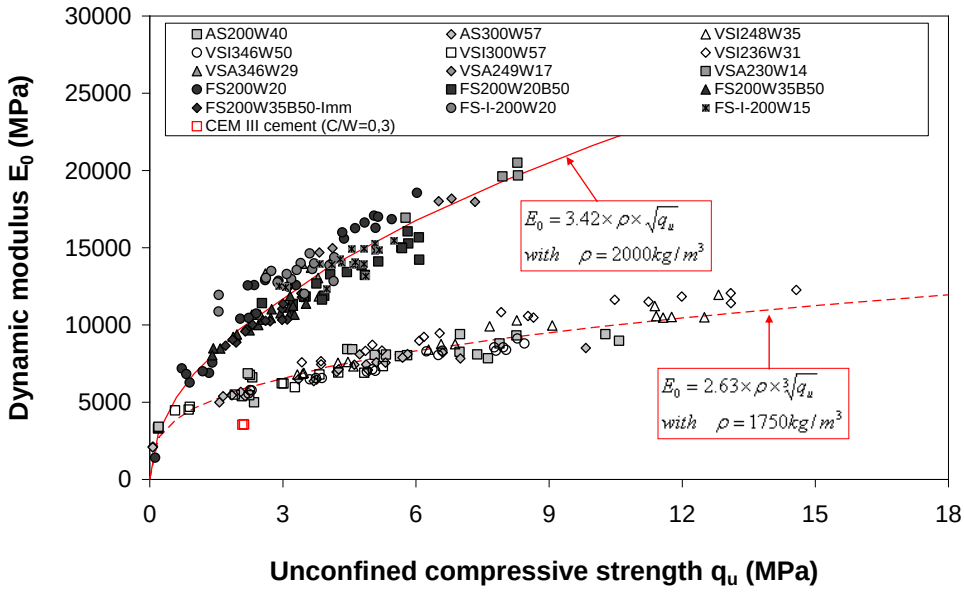

Figure 3-41 Dynamic modulus versus strength - Comparison between measured and calculated values of E_0 using modified ACI 318-05 relations.

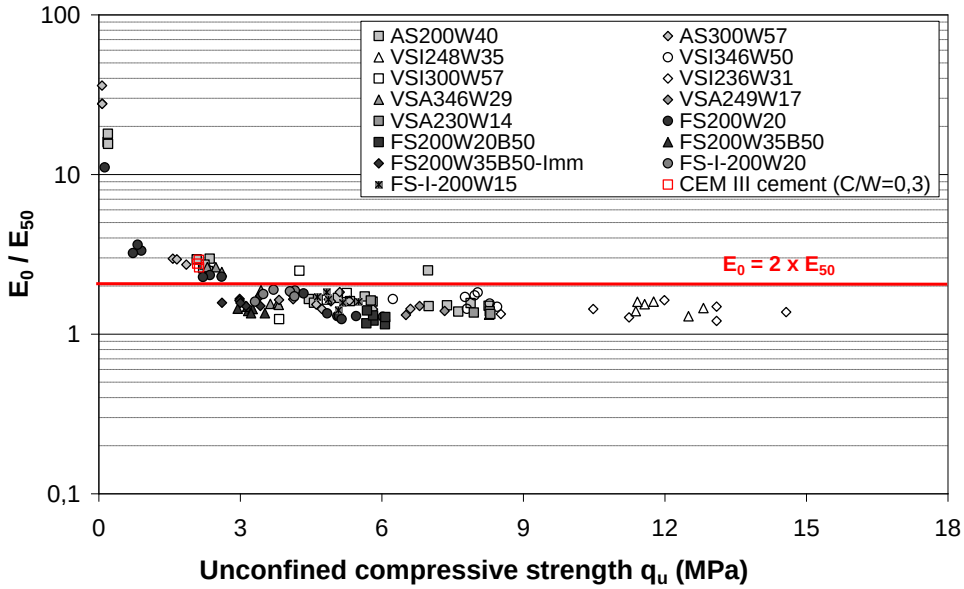

Figure 3-42 E_0/E_{50} versus unconfined compressive strength q_u.

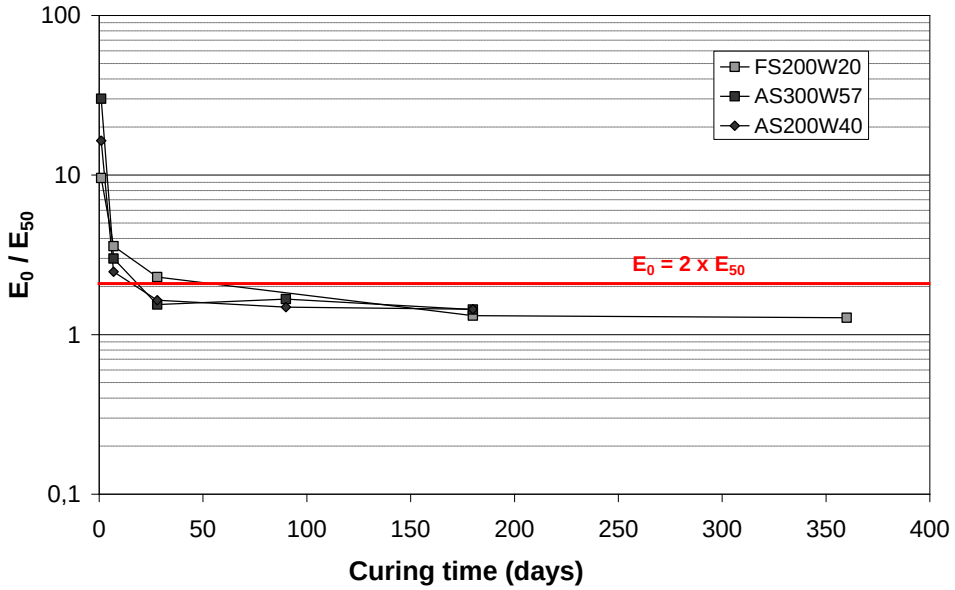

Figure 3-43 E_0/E_{50} versus curing time.

There are few published studies on correlations between static deformation properties and S-wave and P-wave velocities. The propagation of shear and compression waves occurs along the fastest pathway in stabilised soil specimens and can therefore be assumed to strongly correlate to static stiffness as these parameters are influenced by similar factors, such as porosity, microstructure, and particle bonding (Larsson, 2005). The static modulus E_{50} is lower than the seismic modulus E_0 (Figure 3-42). This can be explained by the non-linear reduction of stiffness with strain (Figure 3-27). The strains produced by the passage of compression waves are smaller than the strains generated during compression tests. The ratio of dynamic stiffness to static stiffness E_0/E_{50} decreases from over 10 for strengths close to 100 kPa to a minimum of 1.2 for strengths higher than 3 MPa (Figure 3-42). The values of E_0/E_{50}

are similar for sands and silts. Most of the decrease in E_0/E_{50} with time occurs before 7 days of curing (Figure 3-43).

Based on the relations found between E_0 and q_u and assuming that static stiffness increases linearly with strength, E_{50} can be estimated from the dynamic elastic modulus using the following empirical relations:

For stabilised silts: $$E_{50} \approx 720 \times \left(\frac{E_0}{2.63 \times \rho} \right)^3$$

For stabilised sands: $$E_{50} \approx 2055 \times \left(\frac{E_0}{3.42 \times \rho} \right)^2$$

with ρ in kg/m^3; E_{50} and E_0 in MPa.

These relations are plotted in Figure 3-44 and fit well to the data obtained on silts and sands in this study.
Furthermore, the static modulus E_{50} can be calculated directly from the ultrasonic wave velocity values, independently of the unit weight as:

For silts: $$E_{50} \approx 720 \times \left(\frac{\rho \times \frac{(1+\nu)\times(1-2\nu)}{(1-\nu)} \times {V_p}^2}{2.63 \times \rho} \right)^3 \approx 720 \times \left(\frac{\frac{(1+\nu)\times(1-2\nu)}{(1-\nu)} \times {V_p}^2}{2.63} \right)^3$$

For sands: $$E_{50} \approx 2055 \times \left(\frac{\rho \times \frac{(1+\nu)\times(1-2\nu)}{(1-\nu)} \times {V_p}^2}{3.42 \times \rho} \right)^2 \approx 2055 \times \left(\frac{\frac{(1+\nu)\times(1-2\nu)}{(1-\nu)} \times {V_p}^2}{3.42} \right)^2$$

Taking a Poisson's ratio of 0.25, the empirical relations become:

For silts: $$E_{50} \approx 22.6 \times {V_p}^6$$

For sands: $$E_{50} \approx 121 \times {V_p}^4$$

with E_{50} in MPa and V_p in km/s.

These relations are compared to the data in Figure 3-45.

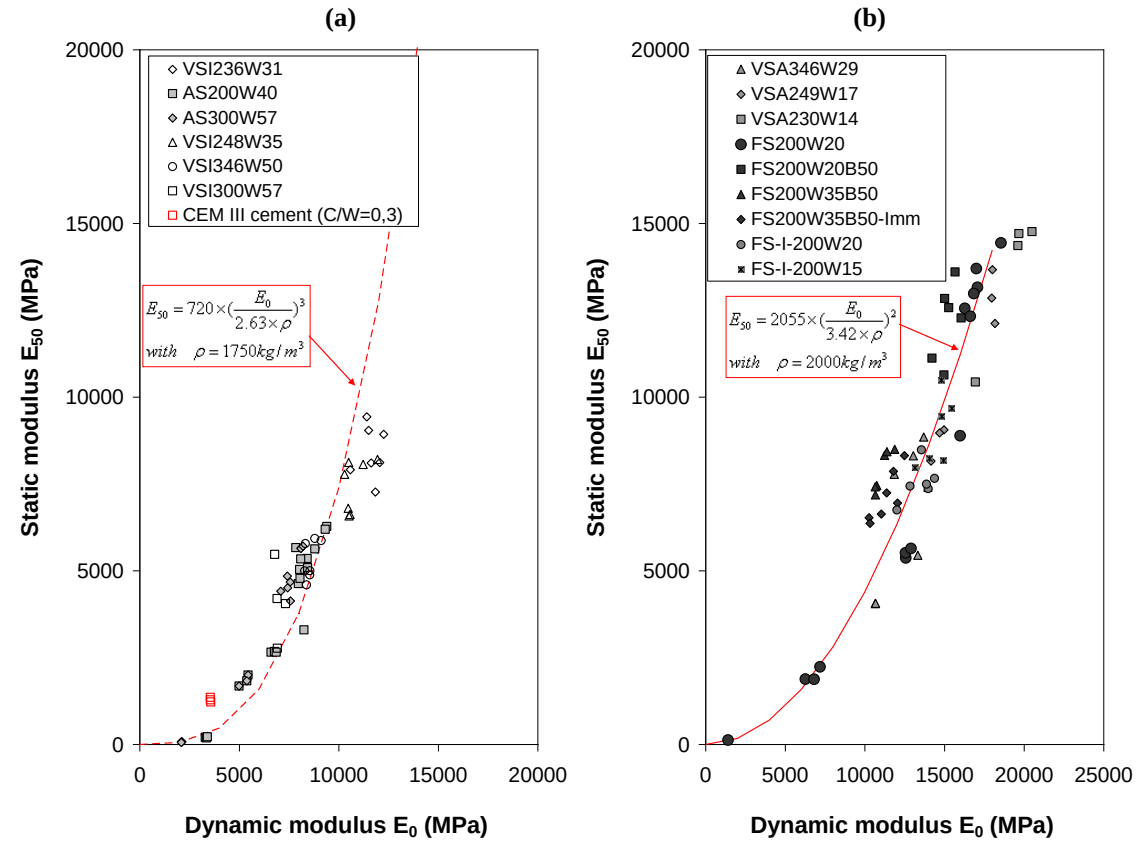

Figure 3-44 Comparison between measured and calculated values of E_{50} based on dynamic modulus measurements (a) silts; (b) sands.

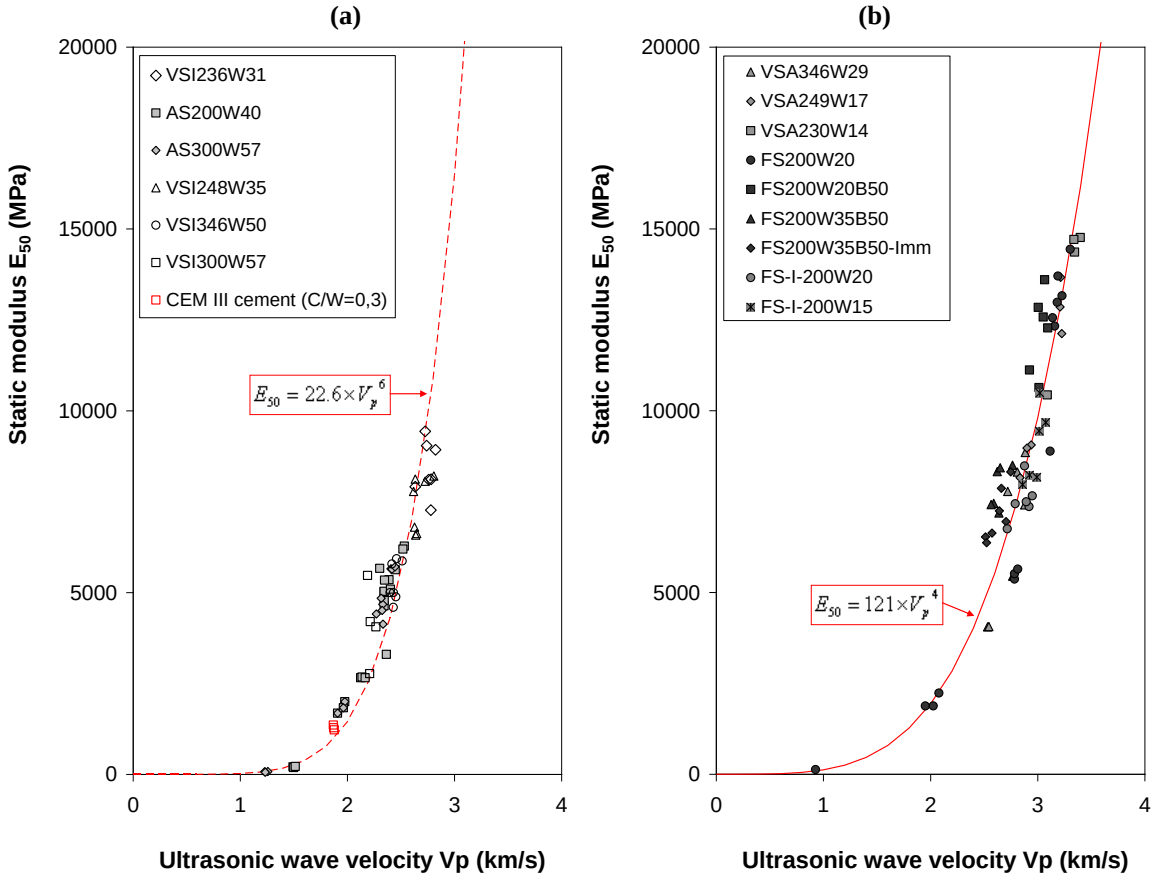

Figure 3-45 Static modulus E_{50} versus ultrasonic wave velocity V_p (a) silts; (b) sands.

Yesiller et al. (2000a) found linear relations between wave velocity and secant modulus for stabilised soils after curing times of 7 and 28 days. The data collected in this study after short curing times reveals that in fact a non-linear relationship exists between V_p and E_{50} (Figure 3-45). The non-linear relation is connected to the rapid decrease of the E_0/E_{50} ratio before 7 days of curing.

3.3.4.6 Rigidity and degree of non-linearity for soils stabilised in the laboratory

According to Atkinson (2000), non-linear stress-strain behaviour can be characterised from measurements of very small strain stiffness E_0, strength q_u and strain at failure ε_f. These parameters are used to determine the rigidity and degree of nonlinearity of the tested material.

The rigidity of linear elastic materials is defined as the ratio of stiffness to strength:

$E/q_u = 1/\varepsilon_f$

The rigidity of materials which exhibit non-linear stress-strain behaviour is:

$E_0/q_u = 1/\varepsilon_r$

where ε_r is a theoretical strain representing the strain at failure if the material was linear elastic (Figure 3-46).

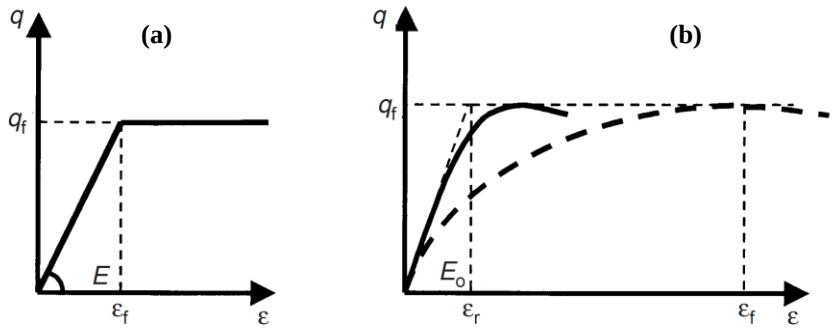

Figure 3-46 Stress-strain behaviour of simple materials: (a) linear material; (b) non-linear material (Atkinson, 2000).

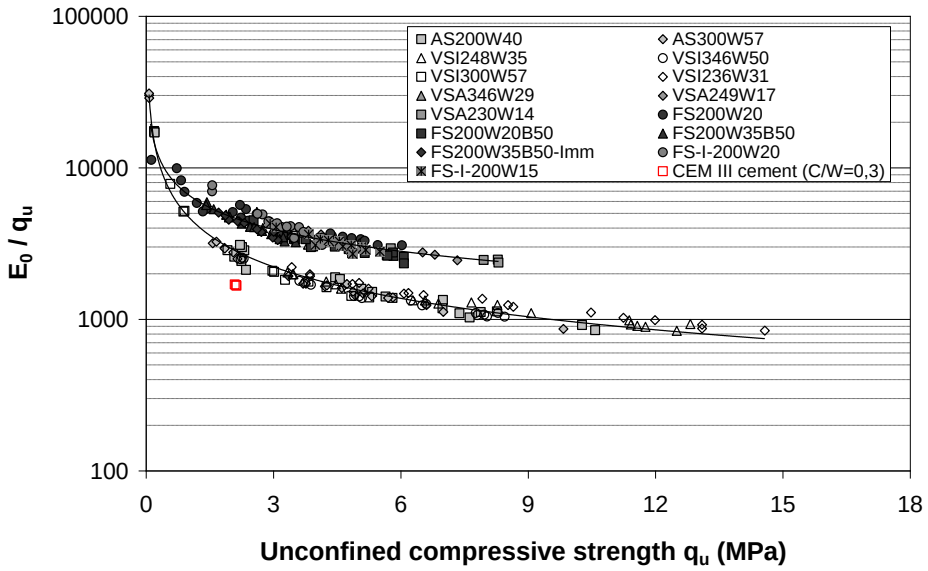

Figure 3-47 Rigidity E_0/q_u versus unconfined compressive strength q_u for laboratory specimens.

The rigidity (E_0/q_u) of the treated silt and sand specimens are plotted versus unconfined compressive strength on a semi-logarithmic scale in Figure 3-47. The E_0/q_u ratios of the sand specimens are higher than those of the silt specimens. Rigidity decreases as the strength of the specimens increases for both soils.

The strains at failure of non-linear materials ε_f are greater than ε_r. The ratio $\varepsilon_f / \varepsilon_r = n_L$ is a measure of the degree of non-linearity, also plotted on a semi-logarithmic scale in Figure 3-48. For specimens of very low strengths (approximately 100 kPa obtained after 1 day of curing), the degree of non-linearity is close to typical values given for soft soils by Atkinson (2000). For strengths greater than 1 MPa, the non-linearity of soils stabilised with cement at dosages representative of those used in soil mixing projects are between typical values for concrete and stiff soils.

After mixing, the rigidity (E_0/q_u) of the soil-mix material decreases with time (Figure 3-47) and the stress-strain behaviour (represented by the degree of non linearity) of stabilised soils evolves from "soft soil-like" to "stiff soil/concrete-like" behaviour (Figure 3-50).
The values of the degree of non-linearity calculated for the specimens of treated sand are higher than those of the specimens of treated silt (Figure 3-48). These results confirm observations made on the stiffness-strain curves (Figure 3-27), i.e. non-linearity is more pronounced for the treated sand specimens.

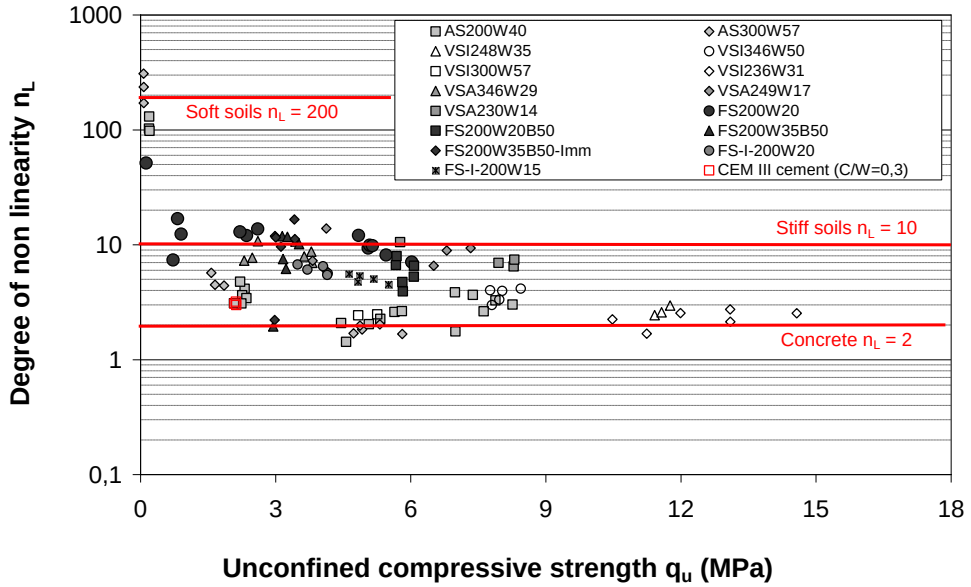

Figure 3-48 Degree of non-linearity n_L versus unconfined compressive strength q_u for laboratory specimens.

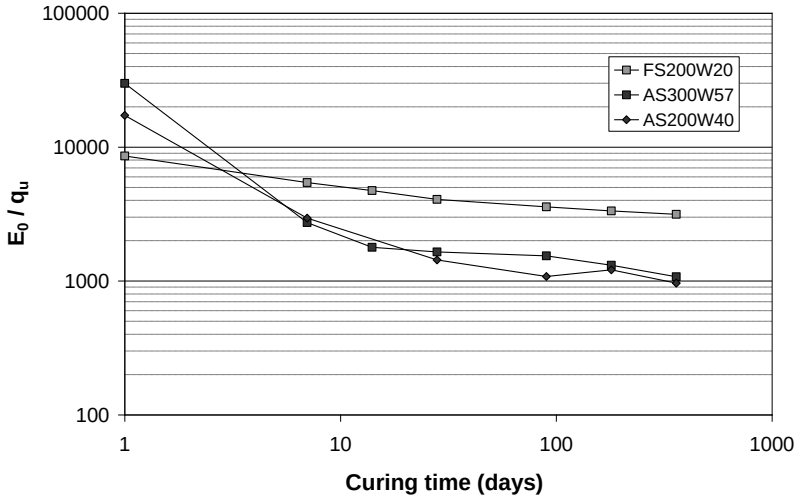

Figure 3-49 Rigidity E_0/q_u versus curing time for laboratory specimens.

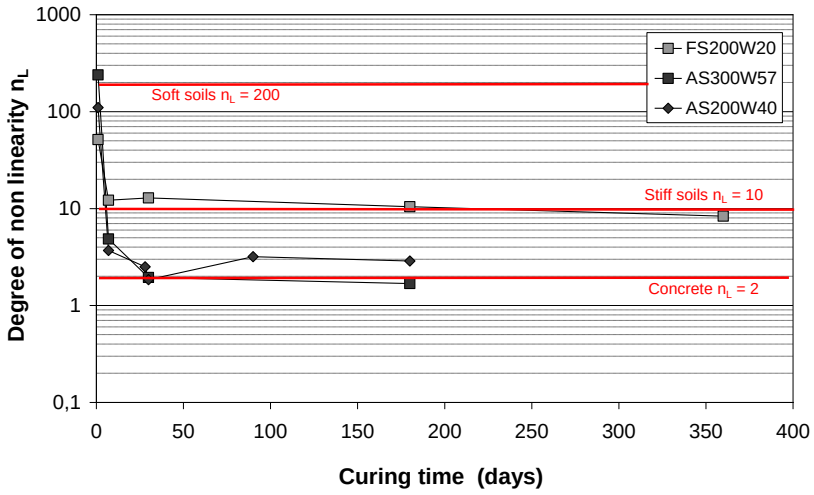

Figure 3-50 Degree of non-linearity n_L versus curing time for laboratory specimens.

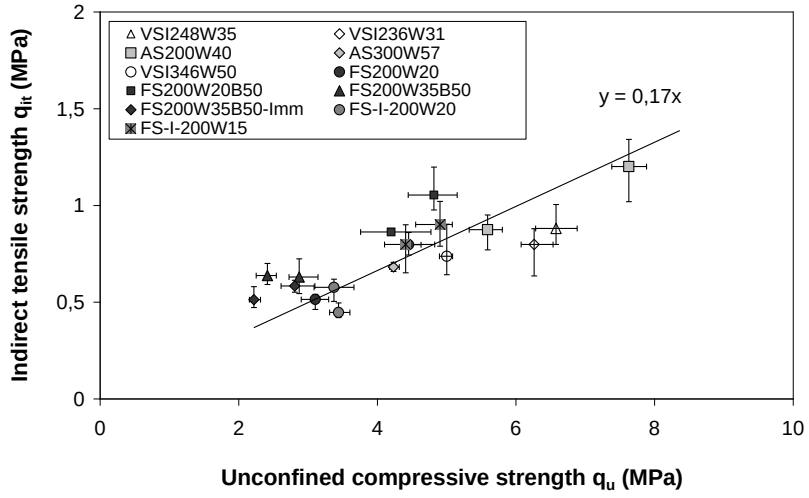

Figure 3-51 Indirect tensile strength versus unconfined compressive strength for soil-cement mixes prepared in the laboratory.

3.3.5 Indirect tensile strength

Figure 3-51 shows the relationship between indirect tensile (Brazilian) strength q_{it} and unconfined compressive strength q_u measured on laboratory specimens after 28 and 90 days. The figure shows that the indirect tensile strength increases with increasing q_u. The average q_{it}/q_u ratio is 0.17. This result indicates that the effect of cementation is equivalent for both tensile and compressive strength.

3.3.6 Summary of results on hardened materials

Laboratory tests were performed on two silts and two sands mixed with varying quantities of cement and water to examine the mechanical properties of soils stabilised in the laboratory. The testing program mainly consisted of unconfined compression strength tests, indirect tensile strength tests and ultrasonic wave velocity measurements. The following conclusions can be drawn from the results of these tests:

- During the first 7 to 14 days after treatment, a noticeable decrease in water content occurs due to cement hydration for specimens kept in endogenous curing conditions. For longer curing times, wet density and moisture content remain constant.
- The density and total porosity of soil-cement mixtures depend on the initial moulding moisture content. The increase in porosity is approximately linear with increasing moisture content. Wet density generally decreases as the moulding moisture content increases.
- The strength and stiffness of soils mixed with cement develop with curing time. Strength increases more rapidly than stiffness. Empirical correlations (exponential functions of time) based on data measured after short curing times (7 or 28 days) provide reasonable estimates of long-term strength and stiffness growth (Table 3-14).
- For a given cement content, higher moulding moisture contents have an adverse effect on strength and stiffness.
- In some cases, an increase in moisture content produces a loss in strength and stiffness which is not compensated by the addition of cement to maintain a constant cement-water ratio C/W.
- The stress-strain behaviour of soils stabilised with cement is non-linear and stiffness significantly decreases with strain. This non-linearity is more pronounced for treated sands than for treated silts. The stress-strain behaviour of soils mixed with cement evolves with curing time from “soft soil-like” to “stiff soil/concrete-like” behaviour. In the conditions of this study, concrete-like behaviour was reached rapidly after 7 days.
- Soil type has an effect on the relations between strength (q_u) and stiffness (static E_{50} and dynamic E_0). Different relations were observed for the silt and sand specimens tested in this study. For a given strength, the static and dynamic stiffness of specimens of treated silt are lower than those of specimens of stabilised

sand. This is attributed to the combined effects of porosity and particle deformation.

- The relationships between strength and static stiffness are linear whereas power law relations exist between strength and dynamic stiffness. Empirical relations based on strength q_u and ultrasonic wave velocity V_p are proposed to estimate the static modulus E_{50} and dynamic modulus E_0 (Table 3-14).
- The dynamic modulus E_0 is higher than the static modulus E_{50}. The E_0/E_{50} ratio decreases with strength (and curing time) from values higher than 10 to a minimum of approximately 1.2.
- The indirect tensile strength of treated soils increases with increasing compressive strength.

Observed relationships	Silts	Sands
Increase in strength q_u with curing time	$q_{u,t} = q_{u,7} \times \beta$ with $\beta = \exp\left[s_7 \times \left(1 - \sqrt{\frac{7}{t}} \right) \right]$	
	$1.29 \leq s_7 \leq 2.42$	$0.37 \leq s_7 \leq 1.65$
Increase in dynamic modulus E_0 with curing time	$E_{0,t} = E_{0,7} \times \beta^{0.30}$	$E_{0,t} = E_{0,7} \times \beta^{0.50}$
Relation between static modulus E_{50} and q_u	$E_{50} = 720 \times q_u$	$E_{50} = 2055 \times q_u$
Relation between E_0 and q_u	$E_0 = 2.63 \times \rho \times \sqrt[3]{q_u}$	$E_0 = 3.42 \times \rho \times \sqrt{q_u}$
Relation between E_{50} and ultrasonic wave velocity V_p	$E_{50} = 22.6 \times V_p^{\ 6}$	$E_{50} = 121 \times V_p^{\ 4}$

Table 3-14 Summary of relationships between mechanical parameters derived from testing.

3.4 Conclusions

Observations made in the field on the relation between installation parameters and strength and homogeneity of treated soils could be explained by the shear-thinning behaviour of clays. Yield stress is influenced by moisture content and could be a relevant tool to study the workability of fresh soil-cement mixtures.

Hardened specimens of silts and sands mixed with cement were prepared and tested in the laboratory. The results point out characteristic trends in long-term strength and stiffness growth and different relations between strength, static modulus and dynamic modulus.
These relationships are compared to the results obtained on soils treated in situ by soil mixing in Chapter 4.

Chapter 4. Characteristics of soils stabilised in situ by deep mixing

4.1 Introduction

Specimens from four different test sites on which soil-cement columns were installed by Soletanche Bachy were tested. Most of the data in this chapter was obtained on cored and wet-grab samples taken from the RUFEX project test site in Vernouillet. In addition, wet-grab samples were also taken from three other sites.

The objective is to examine the mechanical properties of soils stabilised in situ and to compare the results with soils mixed in the laboratory. The purpose is:

- to evaluate the strength and stiffness of in situ deep mixed soils,
- to determine the effects of sampling and mixing conditions on the properties of treated soils.

The test sites and column installation processes are described in sections 4.2 and 4.3. The results of laboratory tests performed on the treated soils from the different sites are presented in section 4.4. In section 4.5, measured mechanical properties were used in finite element analyses carried out to model a real-scale static load test performed on a column in Vernouillet. Finally, the effects of the mixing conditions and sampling methods on the strength and stiffness of treated soils are discussed in section 4.6.

4.2 Vernouillet test site

4.2.1 Site location

The RUFEX test site is located in Vernouillet (Yvelines), France, approximately 35 km North-West of Paris (Figure 4-1). The test site is occupied by a marshalling yard (Figure 4-2) and is located near the river Seine (roughly 500 m).

Figure 4-1 Site location maps (www.geoportail.fr).

Figure 4-2 Ariel photography of the test site (www.geoportail.fr).

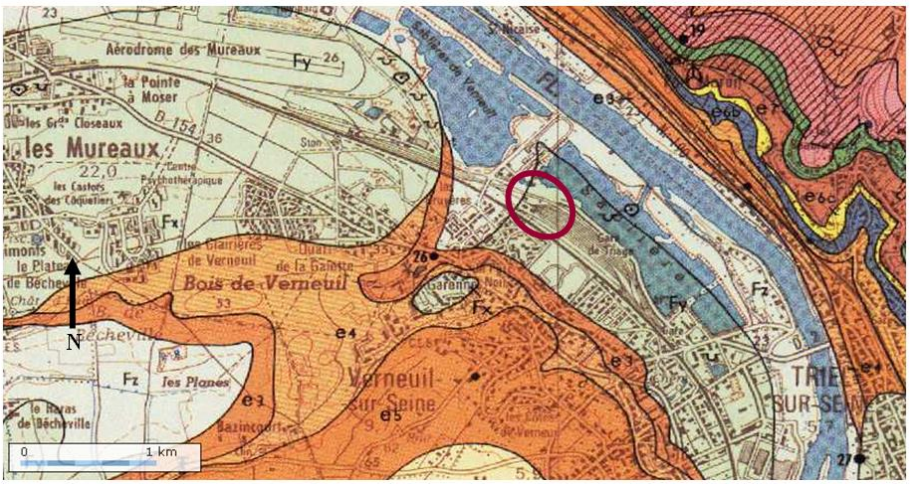

Figure 4-3 Extract from the geological map of Pontoise (BRGM n°152).

According to the geological map (BRGM n ° 152, scale 1/50000), the ground at the test site in Vernouillet consists of old alluvium deposits (Fy) from the river Seine (Figure 4-3). The alluvium is composed of sandy and gravely deposits with large blocks of sandstone. The thickness of the old alluvium varies between 3 and 10 meters.

4.2.2 Site investigation

A preliminary site investigation was carried out to determine the ground conditions at the test site. The ground investigation consisted of 2 trial pits (dug down to approximately 2 m), 15 dynamic penetration tests and 3 boreholes drilled down to depths of 6 and 9 m. Three pressuremeter tests were performed at different depths in each borehole. Soils sampled from the trial pits were characterised in the laboratory by moisture content measurements (CEN, 2005a), grain size distribution analyses (CEN, 2005b) , methylene blue value tests (AFNOR, 1998) and Atterberg limits (CEN, 2005d). The drained shear strength parameters were determined by shear box tests (CEN, 2005c).

4.2.3 Ground conditions

The ground investigation revealed that the site is covered by a 0.50 m thick layer of fill consisting of dark greyish brown sandy gravel, overlaying a 3 m thick layer of brownish beige silt. An average penetration resistance of 4 MPa and pressuremeter limit pressures between 0.70 and 1.70 MPa were measured in this silt layer. Underlaying the silt are old alluvium deposits of the river Seine which may be described as dense brownish orange gravely sand. This sand is present down to a depth of at least 9 m below ground level. The average penetration resistance in this layer is much higher with 16 MPa. Pressuremeter limit pressures greater than 2.40 MPa were measured. No groundwater was encountered during the site investigation. The geotechnical properties of the soils from the Vernouillet test site are summarised in Table 4-1.

Strata		**Silt VSI**	**Sand VSA**
Thickness (m)		3	>5.5
In situ moisture content w (%)		11.9 to 19.7	5 to 7.6
% passing 80 µm		72.5	17.9
Methylene Bleu Value MBV		1.38	0.71
Atterberg Limits	**W_L (%)**	30	/
	PI (%)	10	/
Dynamic penetration resistance q_d (MPa) (AFNOR, 2000a)		4	16
Presuremter limit pressure pl* (MPa) (AFNOR, 2000b)		0.70 to 1.70	>2.40
Cohesion (kPa)		2	0
Friction angle (°)		27	37

Table 4-1 Summary of soil characteristics from Vernouillet.

4.2.4 Field trial – Outline of column installation works

4.2.4.1 Soil mixing equipment and column installation procedure

Soil-cement columns were installed in Vernouillet in May 2011 using a Casagrande C4 drilling rig (Figure 4-4).

Figure 4-4 Casagrande C4 drilling rig used to install the soil-cement columns in Vernouillet

Soil mixing was performed with the Springsol mixing tool developed by Soletanche Bachy (Figure 4-5). This tool is equipped with two mixing blades that spread out under the action of springs. In its folded configuration, the tool diameter is 160 mm enabling its insertion into a temporary casing. Two different diameters were tested for the open configuration: 400 and 600 mm. The binder is delivered through outlet holes in the drag bit located at the bottom end of the tool.

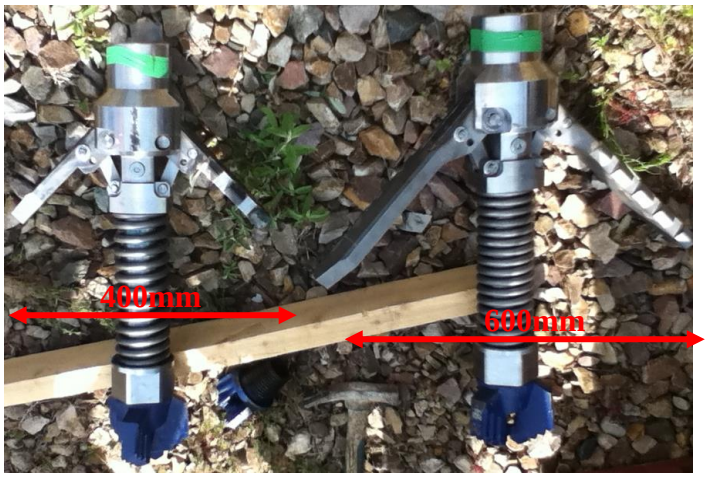

Figure 4-5 Springsol mixing tools (400 mm (left) and 600 mm (right) diameters).

Soil mixing was carried out by the wet method: the binder was mixed with water forming a slurry before it was added into the soil. The slurry was injected during the penetration (downward) phase. The binder used was the same CEM III blastfurnace cement used in the laboratory trials. The grout was prepared on site using a mobile production unit. Three dosages of grout were tested: C/W = 0.6, C/W = 0.8 and C/W = 1. Approximately 1.5 kg of bentonite was added per 100 L to stabilise the cement grout.

Depending on the column, the penetration rates used in Vernouillet varied between 10 and 25 metres per hour (m/hr) and the tool rotation speed was between 70 and 160 revolutions per minute (rpm). The blade rotation number for the columns in Vernouillet was between 600 and 1500 rotations/m. The cement factors (mass of dry binder per cubic meter of soil) tested varied between 200 and 400 kg/m^3. It is important to note that these cement contents represent the amount of binder injected into the columns. The actual binder contents are probably slightly lower as spoil returns to the surface during mixing operations. This spoil was immediately pumped and evacuated as the column installation process continued.

In total, 26 soil-mix columns of 400 and 600 mm diameters were executed under and beside an existing track. All columns were drilled down to the gravely sand layer approximately 5 m below ground level. From the columns installed beside the existing platform, eight were installed to be excavated. The aim was to verify the geometry of the columns, to examine the homogeneity of the soil-mix material and to perform laboratory tests to determine the characteristics of the stabilised soils. The installation parameters (drilling parameters, binder contents) of the excavated columns are given in Table 4-2. Two columns (named X3 and X6) were built using the 600 mm tool. The other six columns were of 400 mm in diameter. The

excavated columns were designed to study the influence of mixing parameters. Three columns were excavated 28 days after construction (X4 – X5 – X6). The remaining five columns (X1 – X2 – X3 – C1 – C2) were extracted after 180 days. Column C2 was subjected to a static loading test following the procedure described in standard NF 94-150-1 (1999b) approximately 90 days after installation.

	Column	Diameter (mm)	Grout injection rate (L/min)	C/W (grout)	Grout injection rate (L/m)	Binder content C (kg/m^3)	Penetration rate (m/h)	Rotation speed (rpm)	Blade rotation number T
Excavated after 180 days	C1	400.0	8.8	1.0	39.8	229.62	13.3	119.5	1076.5
	C2	400.0	9.3	1.0	48.6	280.39	11.5	122.9	1279.5
	X1	400.0	21.8	0.8	59.7	297.8	21.9	149.5	818.7
	X2	400.0	11.1	0.8	50.1	249.8	13.2	148.0	1340.6
	X3	600.0	21.5	0.8	99.0	219.6	13.0	82.5	761.3
Excavated after 28 days	X4	400.0	21.3	0.8	51.1	254.8	25.1	146.2	700.2
	X5	400.0	18.3	0.6	95.8	369.2	11.4	146.8	1540.0
	X6	600.0	21.4	0.8	94.1	208.8	13.6	86.4	761.0
Spoil	N2	400.0	18.0	0.6	101.0	389.25	10.7	75.3	843.3
Penetration tests	N4	400.0	17.3	0.6	84.9	327.20	12.2	72.9	715.3
FVT	N8	400.0	7.2	1.0	43.1	248.66	10.0	82.9	994.8
	N9	400.0	9.7	0.8	47.0	234.3	12.4	84.7	818.3

Table 4-2 Characteristics of the columns tested in Vernouillet.

4.2.4.2 Quality control during construction

Quality control on site during construction of the columns in Vernouillet included:

- monitoring and recording the execution parameters,
- grout density measurements,
- fresh spoil density measurements,
- dynamic penetration tests in the fresh columns,
- vane tests in the fresh columns.

Execution parameters

The mixing process was monitored with the Enpamix system (developed by Soletanche Bachy). The parameters recorded during the installation of the columns were the volume of grout injected, the mixing torque, the vertical thrust on the mixing tool, the

penetration/withdrawal rates and the tool rotation speed. The recordings for three columns are shown in Figure 4-6. The average execution parameters given in Table 4-2 were derived from these recordings.

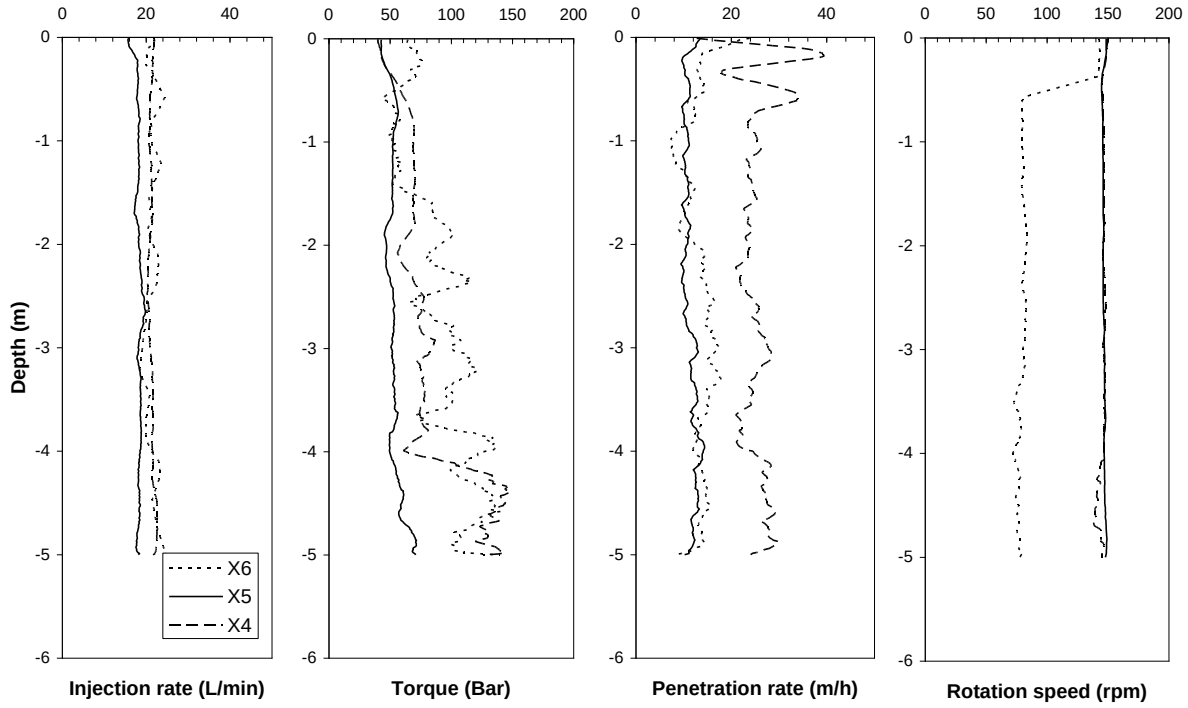

Figure 4-6 Execution parameters recorded during installation of columns X4, X5 and X6.

Grout density measurements

Grout density was controlled on site using a Baroid mud balance. The measured densities confirmed that the slurries were prepared with the appropriate cement-water ratios (Table 4-3).

Dosage C/W	Target density	Measured density
0.6	**1.34**	1.30
		1.33
0.8	**1.42**	1.41
		1.40
		1.42
		1.40
1	**1.48**	1.49
		1.46
		1.47

Table 4-3 Grout densities measured during installation of soil-cement columns in Vernouillet.

Tests performed on fresh soil-mix material

The spoil produced during mixing of the columns was light yellowish brown to beige, visually homogeneous, liquid to pasty and composed of a mixture of silt and grout. Density

measurements on the spoil were also carried out using a mud balance. The spoil density varied between 1.73 and 1.99 (Table 4-4).

Column	Dosage grout C/W	Target density grout	Spoil density
N2	0.6	1.34	1.73
X5	0.6	1.34	1.89
X3	1	1.48	1.99
C1	1	1.48	1.86

Table 4-4 Spoil densities measured during installation of soil-cement columns in Vernouillet.

These values, higher than those of the grouts, confirm the presence of significant amounts of soil in the spoil and hence the blending of the slurry with the soil produced by the mixing process.

Wet-grab samples of spoil were taken from the surface during column installation for laboratory testing to determine the mechanical properties of the soil-mix material.

The homogeneity and strength of the fresh soil-mix material in column N4 (Table 4-2) were evaluated by two dynamic penetration tests performed approximately one hour after the installation of the column. The penetration tests were performed vertically in the centre of the column (PDN4) and at a distance of 10 cm along the radius (PDN4/10). These tests were carried out to depths of 3.95 and 4.57 m below ground level. The penetration resistance profiles are compared with the results obtained in the untreated soil (PD650) in Figure 4-7. The penetration resistances measured in fresh column N4 are significantly lower than in the surrounding soil because of the destructuration performed by the mixing tool during drilling. The slight difference between PDN4 and PDN4/10 could be explained by the presence in the central/axial part of the column section of a more homogeneous slurry-rich zone filling the void left by the drilling tool during withdrawal.

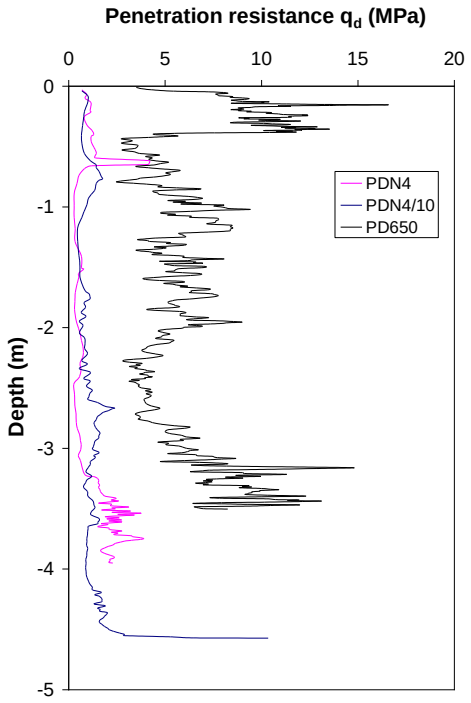

Figure 4-7 Penetration resistance profiles.

Field vane tests (FVT N8 and FVT N9) were performed every 0.50 m down to a depth of 2.50 m in columns N8 and N9 (Table 4-2) approximately one hour after installation. The measured undrained shear strengths Cu increase with depth between 2.5 and 62 kPa (Figure 4-8). It is worth noting that the friction along the vane rod was not taken into account for the calculation of Cu. In the untreated silt layer 1 m below ground level, Cu was greater than 260 kPa (limit of the vane equipment).

The following correlation is used to estimate the unconfined compressive strength q_u of soil mixing columns from the penetration resistance q_d (Porbaha, 2002):

$q_d = q_u \times \delta$
with δ between 5 and 7.

Assuming $\delta = 5$ and $Cu = q_u / 2$, an acceptable agreement is obtained between the measured values of Cu (FVT N8 and N9) and the shear strength values estimated from the penetration tests performed in column N4 (PDN4 PDN4/10).
Destructuration of soil by a mixing tool can be quantified by the disturbance ratio DR (Larsson, 2003):

$DR = Cu_{initial\ soil} / Cu_{destructured\ soil}$

Taking $Cu_{initial\ soil} = 400$ kPa (estimate from dynamic penetration test) and $Cu_{destructured\ soil} = 50$ kPa, a disturbance ratio of 8 is obtained for the Springsol tool in the silt of Vernouillet.

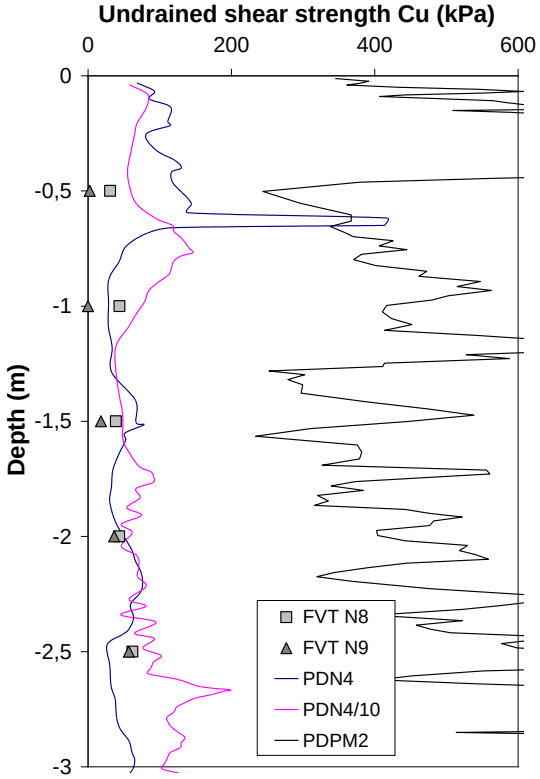

Figure 4-8 Undrained shear strength Cu measured by vane tests and estimated from penetrometer tests.

Larsson (2003) found disturbance ratios between 2 and 5 in sensitive grey clay using vane tests. The relatively high value of DR obtained in Vernouillet can be explained by the high (probably over-estimated) strength of the undisturbed silt and by the significant amount of mixing performed. The blade rotation numbers (Table 4-2) are higher than typical values used in the Scandinavian method (Table 1-3).

4.2.4.3 Column excavation

Eight columns were excavated with a 20-ton mechanical excavator (Figure 4-9 (a) and (b)). Three columns were excavated after 28 days (X4, X5 and X6) and five after 180 days (C1, C2, X1, X2 and X3).

All extracted columns had a length of 5 m. Two columns were installed through a short steel casing. The head of these columns was cone-shaped marking the spreading of the mixing blades as the Springsol tool entered the soil (Figure 4-9 (a) and (c)). All columns were found to be well mixed with few inhomogeneities visible.

The first 2 meters of the columns generally consisted of treated silt. Centimetric inclusions of beige/brown soil were visible in a matrix of mixed soil-cement (Figure 4-9 (e)). The central/axial part of the column section appeared to be more homogeneous and concentrated in slurry. The diameter of the columns in the silt layer was close to the diameter of the tool used. Centimetric striations were visible on the outer surface of the columns (Figure 4-9 (d)). These striations were drawn by the rotation of the tool during the installation of the column. They probably have a significant effect on the skin friction mobilised in cohesive soils. No deterioration near the external surface of the columns resembling the degradations described in section 1.4.1.2 was observed.

Between depths of 2.5 and 3.5 m, a transition zone between the treated silt and the stabilised sand was observed in the columns.

The lower part of the columns consisted of stabilised sand down to 5 m. The mixture produced was visually homogeneous with no soil inclusions (Figure 4-9 (f)) pointing to the fact that it is easier to obtain well mixed soil-cement columns in coarse grained soils than in fine grained soils. The diameter of the lower part of the columns was slightly larger than that of the tool (about 70 cm for column X6) due to the migration of slurry in the permeable sand strata.

Block samples were taken from the excavated columns for laboratory testing to determine the mechanical properties of the soil-mix material. Specimens of soil-cement were cored from these blocks (Figure 2-4).

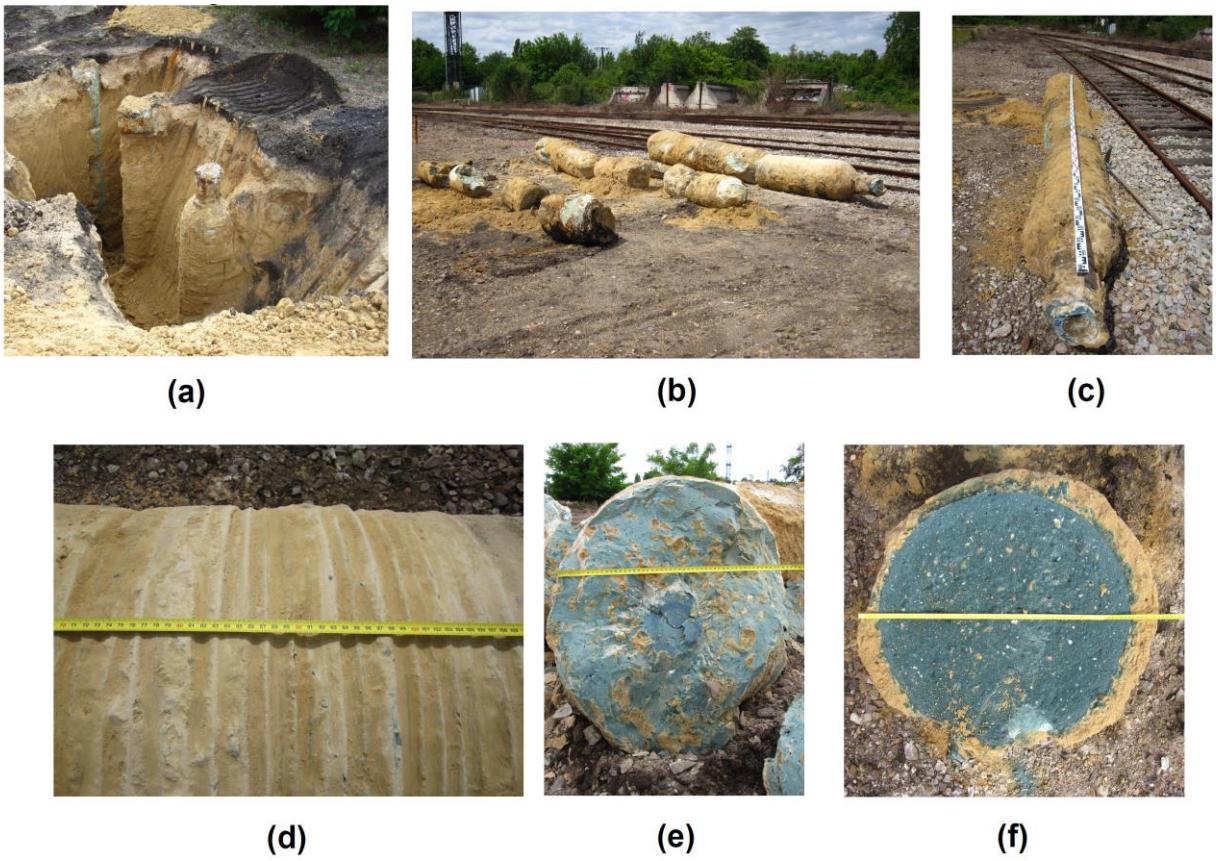

Figure 4-9 Excavation of three columns after 28 days.

4.3 Other sites

Wet-grab samples were taken from three other sites in the Paris region on which soil-cement columns were installed by Soletanche Bachy. Details on the ground conditions and the column installation process are given in Table 4-5.

Site	Soil type	Mixing method	Number of mixing blades	Column Diameter (mm)	Cement	C/W (grout)	Binder content C (kg/m^3)	Blade rotation number T
Site P	Silty sandy clay	wet	2 (Springsol)	600	CEM III	0.5 - 0.6	≈320	≈1200
Site G	Sandy gravely silt (fill)	wet	6	600	CEM III	0.65	≈320	≈2250
Site B	Sandy silt (fill)	wet	6	400	CEM III	0.5	≈200	≈2150

Table 4-5 Ground conditions and column installation process for sites on which wet-grab samples were taken.

4.4 Results of laboratory tests performed on specimens of in situ deep mixed soils

In this section, the results from laboratory tests performed on cored and wet-grab samples are compared to the results obtained on soil-cement mixes prepared in the laboratory. The testing program involved compression tests, splitting tensile tests, resonance tests, porosity and ultrasonic wave velocity measurements.

For graphs of data from Vernouillet plotted versus depth, the results between 0 and 3 m are compared to the average values obtained on Vernouillet silt-cement mixes prepared in the laboratory (Table A-2) to reproduce the dosages used in the field in 3 columns. Between 4 and 5 m, the results are compared to the laboratory Vernouillet sand-cement mixes (Table A-2).

Although missing 180-day strength and stiffness data for the laboratory mixes of Vernouillet sand could be estimated using the empirical relations described in Chapter 3, the results on field specimens are only compared to actual measured data.

4.4.1 Moisture content

Samples were taken for the specific purpose of measuring the water content at different depths during excavation of the columns in Vernouillet.

Water contents in the columns are generally higher than the moisture contents measured in the untreated soil (Figure 4-10). The moisture contents decrease with depth (lower in the sand than silt). They are mostly in the same range as the moisture contents measured on the specimens prepared in the laboratory and cured in endogenous conditions (moisture contents of lab mixes are assumed constant between 28 and 180 days).

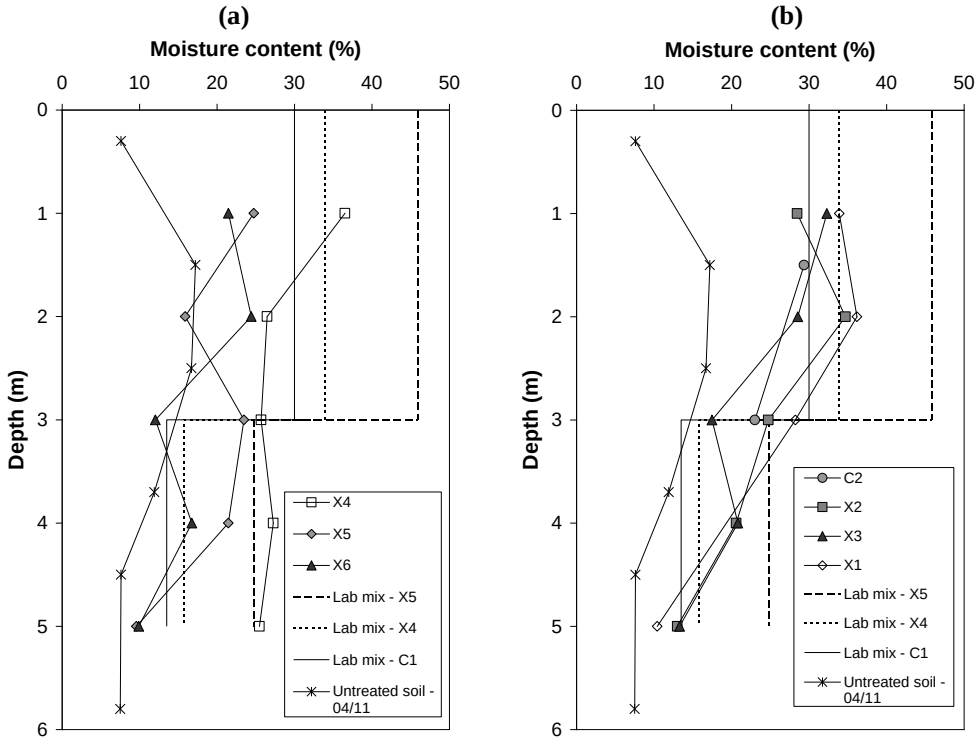

Figure 4-10 Moisture contents in columns excavated (a) after 28 days; (b) after 180 days.

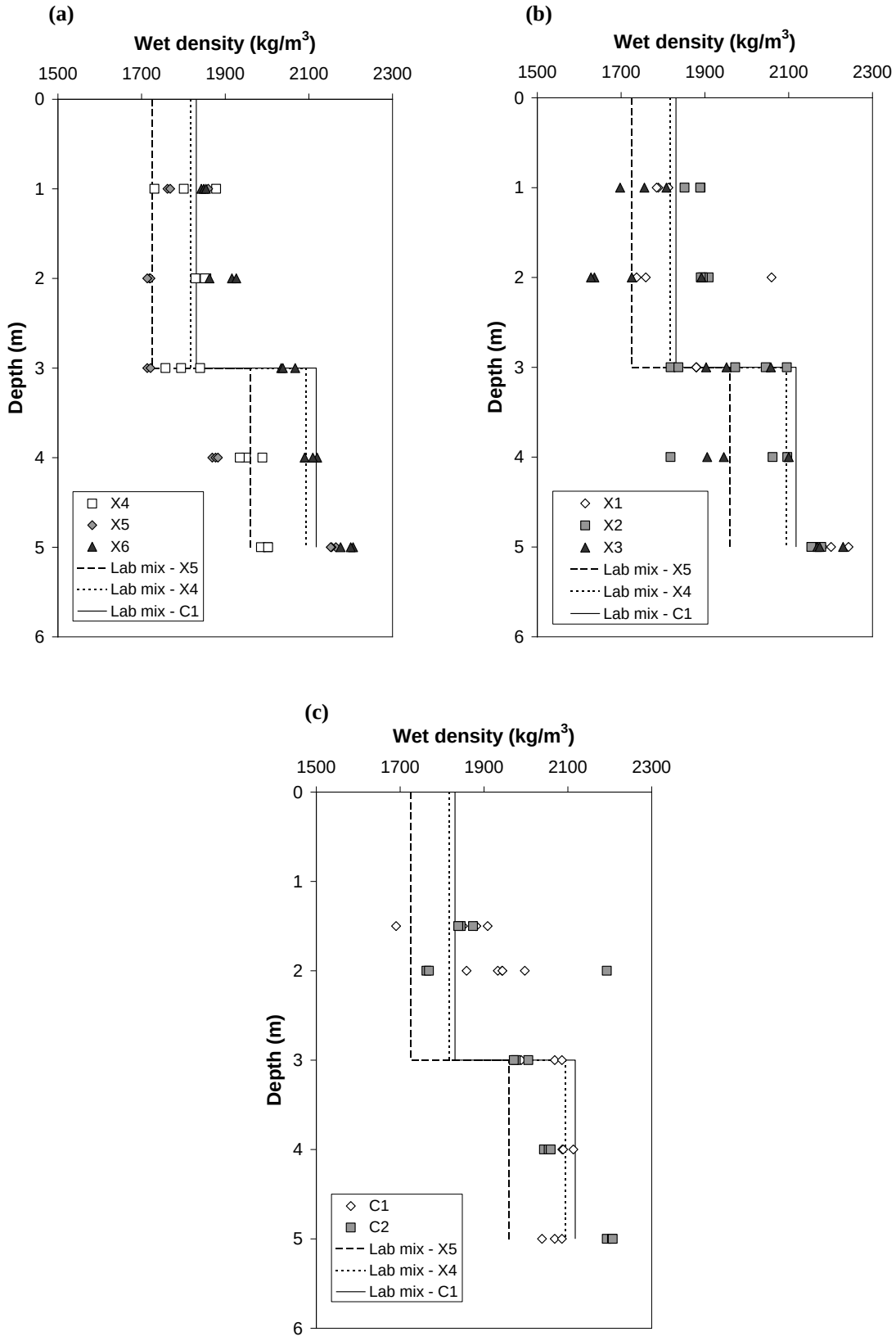

Figure 4-11 Wet density of specimens cored in blocks from columns excavated (a) after 28 days; (b) and (c) after 180 days.

The water contents of wet-grab specimens from Vernouillet after 7 days of curing in the laboratory are given in Table 4-6:

Column (diam. 400mm)	C/W Grout	Vol. of grout (L/m)	Average W (%)	Max. (%)	Min. (%)	Standard deviation (%)	Coefficient of variation (%)
N4	**0.6**	**84.9**	31.77	35.36	29.78	3.12	9.82
X2	**0.8**	**50.1**	34.11	35.22	32.79	0.85	2.50
N8	**1**	**43.1**	34. 90	36.81	28.82	3.02	8.67

Table 4-6 Moisture contents in wet-grab specimens from Vernouillet after 7 days.

After 60 days of curing, water contents of 38.4 % were measured on samples of spoil from column N4, 35.8 % and 28.2 % for specimens from column N8. The moisture contents of the spoil samples are similar to those obtained in the upper silty part of the columns.

4.4.2 Wet density

Wet densities of the specimens cored from the excavated columns in Vernouillet generally increase with depth following the change in soil type around 3 m below ground level (Figure 4-11). The densities are relatively close to the densities obtained for the specimens of silt and sand mixed in the laboratory. The densities of specimens cored in the upper silty part of the columns (depths of 1 to 3 m) generally lie between 1600 and 2000 kg/m^3 whereas the densities of the specimens cored from blocks extracted in the sandy base of the columns (4 and 5 m) are higher between 1800 and 2300 kg/m^3 (Figure 4-12).

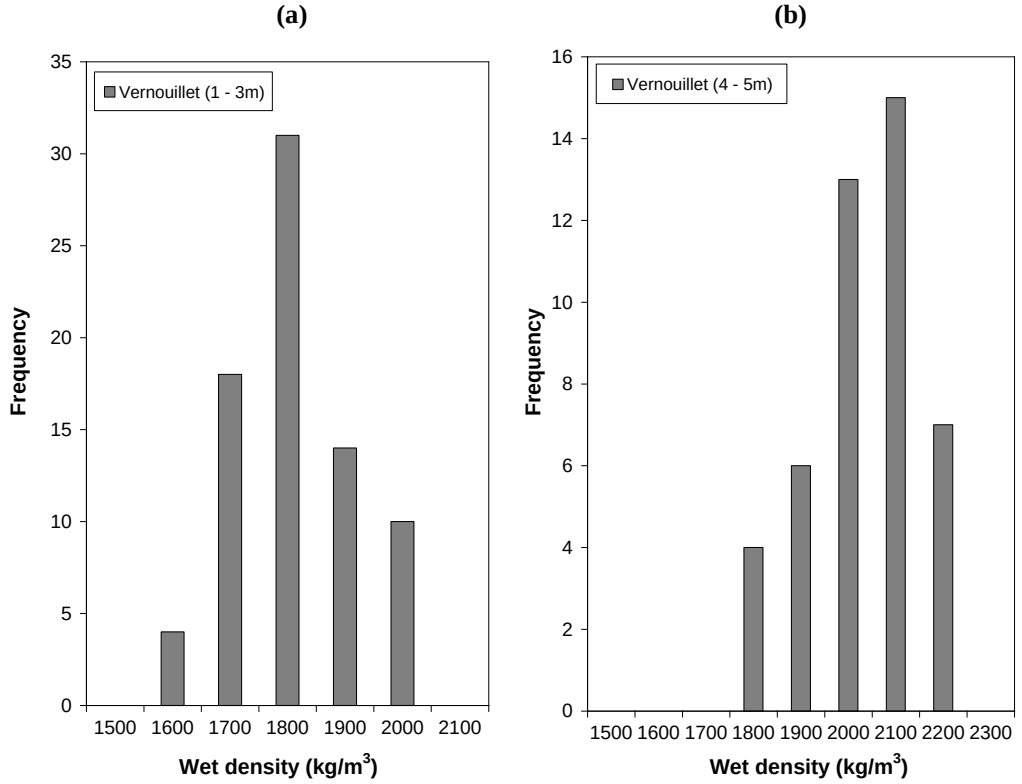

Figure 4-12 Distribution of wet densities for specimens cored in blocks from excavated columns (a) in the silt between 1 and 3 m; (b) in the sand between 4 and 5 m.

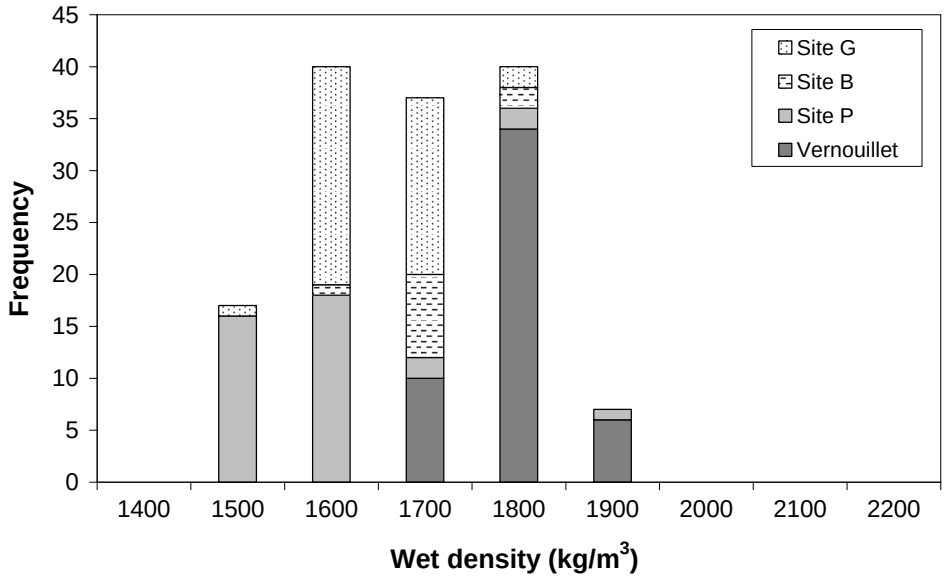

Figure 4-13 Distribution of wet densities of wet-grab specimens taken from different sites.

The density of the wet-grab specimens taken from Vernouillet (Figure 4-13) are comparable to the densities of the specimens cored between 1 and 3 m (in the section of the columns composed predominantly of silt). They are also in the same range as the densities of the fresh spoil (Table 4-4). The wet-grab specimens from the other test sites have lower densities between 1500 and 1800 kg/m^3 (Figure 4-13).

4.4.3 Porosity accessible to water

The porosities of the specimens of soils treated in situ vary between 20 and 70 % (Figure 4-14). The specimens cored from blocks taken from the silt part of the columns in Vernouillet had porosities between 40 and 55 %. The specimens taken from the lower sandy parts of the columns had porosities between 20 and 40 %. The porosities of the wet-grab specimens taken from site P and site G were higher between 50 and 70 %.

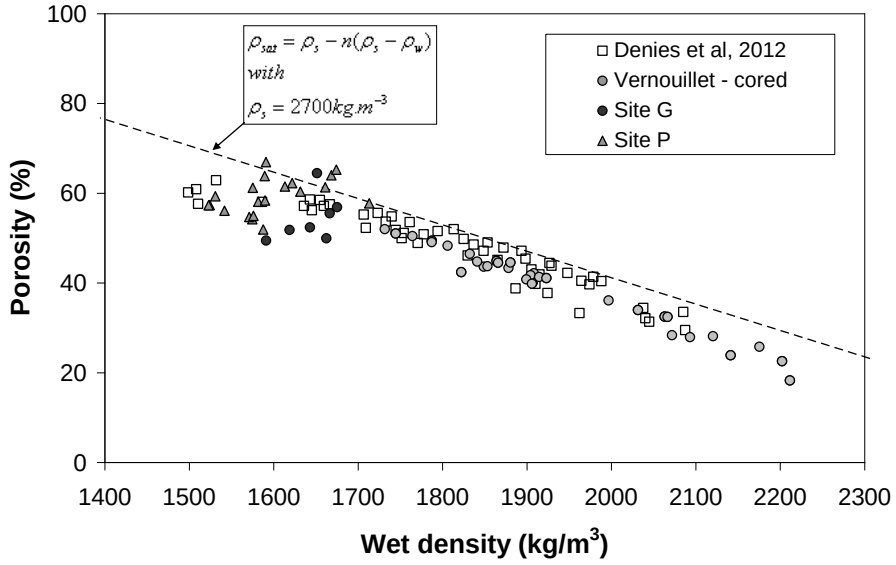

Figure 4-14 Relationship between wet density and porosity for field samples.

The higher porosities of the wet-grab samples may be due to the type of soil but can also be related to the sampling method (the spoil return is fairly liquid with a high moisture content and most likely mainly contains the fine fraction of the mixed soils). The porosities of soil-mix materials from this study and from Denies et al. (2012) are slightly lower than the porosities of saturated untreated natural soils due to cementation (Figure 4-14).

4.4.4 Unconfined compressive strength

Typical stress-strain curves for specimens cored from blocks of the columns excavated in Vernouillet are shown in Figure 4-15.

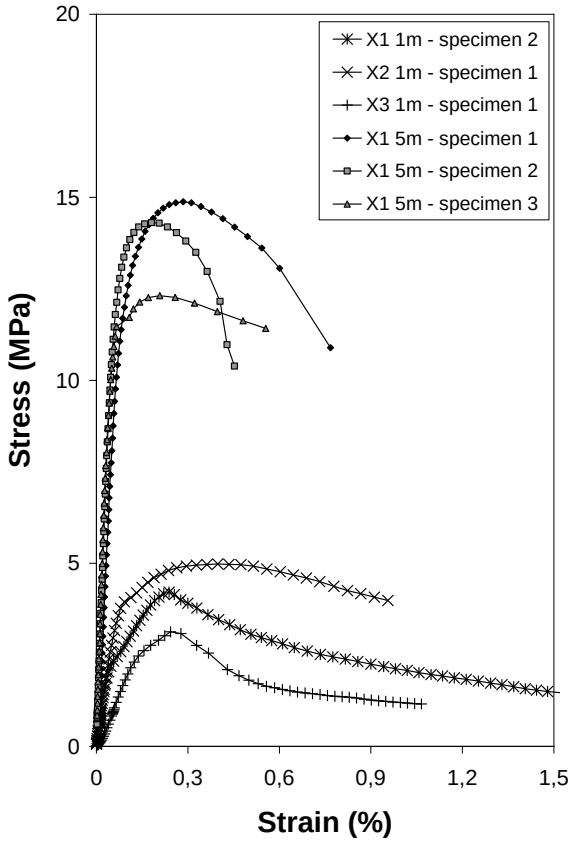

Figure 4-15 Typical stress-strain curves for specimens cored from blocks of columns excavated in Vernouillet after 180 days.

The unconfined compressive strength profiles with depth from Vernouillet are presented in Figure 4-16.

A general increase in the strength of the soil-mix material with depth is observed and related to the change in soil type. The average unconfined compressive strength measured on the cored specimens of stabilised silt is close to 3 MPa after 28 days. After 180 days, the average strength is of 5.25 MPa (Table 4-7).

Combining the data from all columns, the coefficients of variation of strength in the silt (ratio of the standard deviation to the mean) are of 47 % after 28 days (26 samples tested) and 61 %

after 180 days (52 samples tested). These values can be related to the heterogeneity of the initial soil, variations in binder distribution and dosage, variations in the execution parameters (different sets of parameters were tested) and to the presence of some soil inclusions in the tested specimens.

Strengths measured in the sand layer are much higher than in the silt and as variable between the different columns with coefficients of variation of 65 % for the specimens tested after 28 days and 33 % after 180 days (Table 4-7). The variations in the sand can largely be attributed to the heterogeneity of the initial alluvial sand layer which contains lenses of gravel. These heterogeneities in the soil were observed during the coring of the block samples (Figure 2-5) and are responsible for the very high strengths obtained at the base of most columns. The coefficients of variation evaluated from compression tests on specimens from Vernouillet are in the range of those compiled by Larsson (2005) from a number of reported studies (Figure 1-14).

Strengths measured on the specimens cored in the first 3 m of the columns are generally lower than the strengths of the specimens of silt-cement prepared in the laboratory (Figure 4-16). This is in agreement with most comparisons between laboratory and field samples published in the literature (Figure 1-37). After 28 days, the strengths of cored sand specimens from column X4 are lower than the corresponding laboratory mix (Figure 4-16). For column X5, laboratory and field strengths are very close at 4 m. The strengths of the field specimens taken at 5 m are higher than the laboratory strength.

Site	Sampling	Soil	Time	Average q_u (MPa)	Standard deviation (MPa)	$q_{u5\%}$ (MPa) (test population)	$q_{u5\%}$ (MPa) (Gaussian distribution)	$q_{u5\%}$ (MPa) (Lognormal distribution)	number of specimens
Vernouillet	Cored	silt (1 to 3m)	28 days	2.82	1.32	1.18	0.64	1.21	26
		silt (1 to 3m)	180 days	5.25	3.20	1.59	-0.02	1.54	52
		sand (4 - 5m)	28 days	7.06	4.57	2.90	-0.47	2.27	18
		sand (4 - 5m)	180 days	14.08	4.60	6.88	6.51	7.13	27
Other sites	Wet-grab	various	28 days	2.56	1.11	1.11	0.74	1.13	65
		various	90 days	3.34	1.16	1.89	1.44	1.75	30

Table 4-7 Results of unconfined compression tests: characteristic strength values.

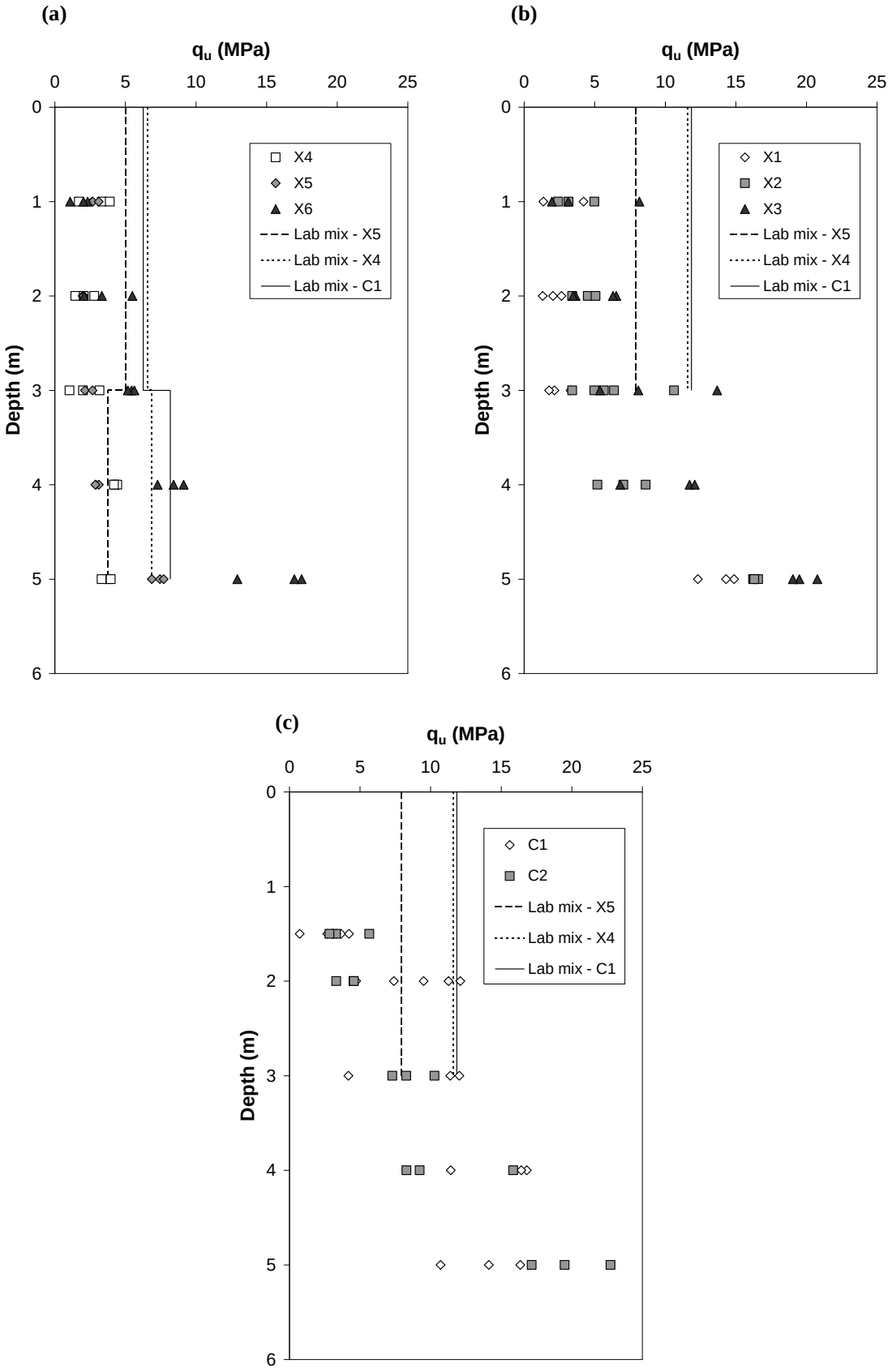

Figure 4-16 Unconfined compressive strength of specimens cored in blocks from columns excavated (a) after 28 days; (b) and (c) after 180 days.

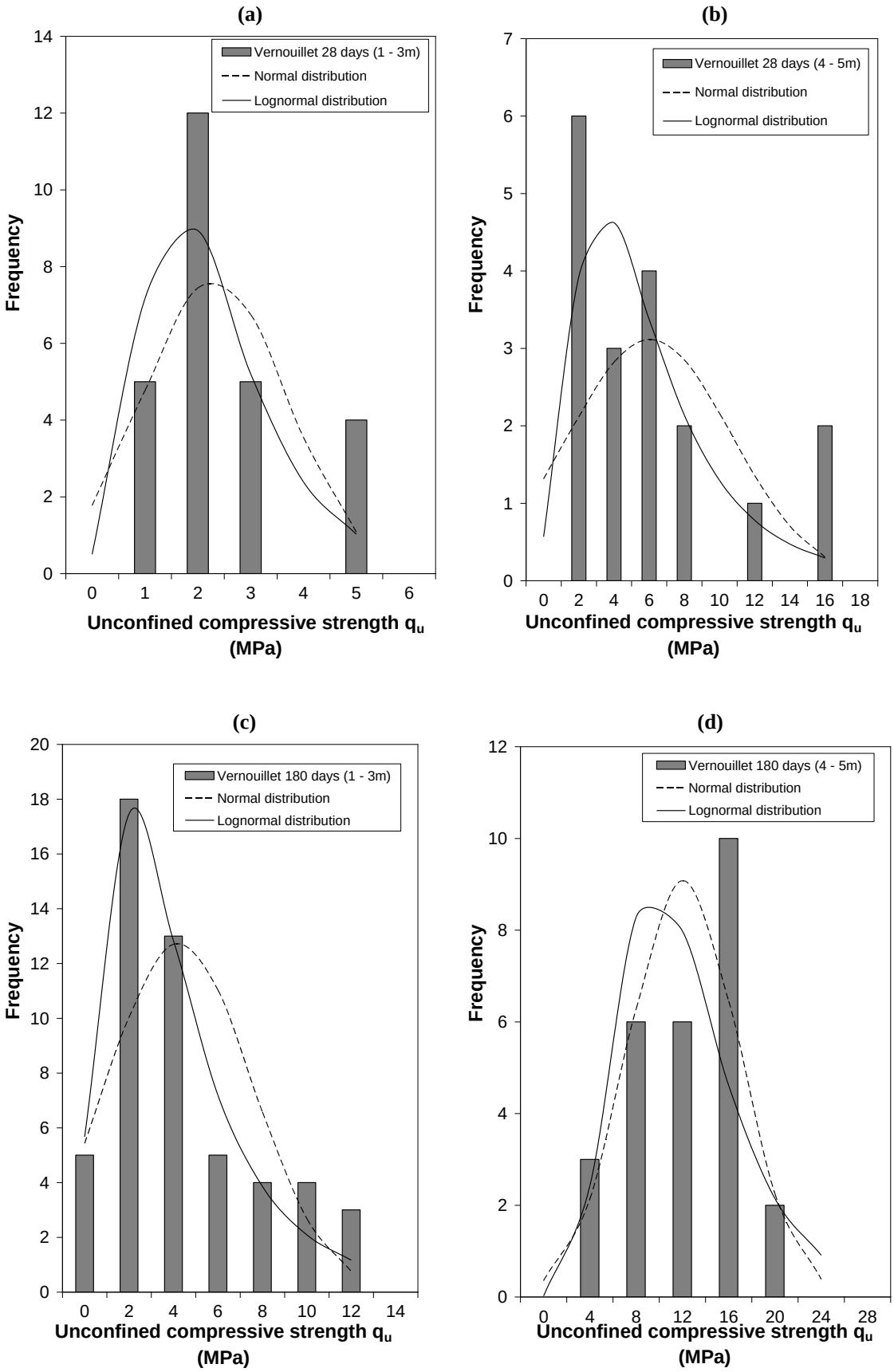

Figure 4-17 Distributions of unconfined compressive strength for specimens cored in blocks from columns excavated after 28 days (a) between 1 and 3 m and (b) between 4 and 5 m; after 180 days (c) between 1 and 3 m and (d) between 4 and 5 m.

Although the number of samples is limited, the distributions of unconfined compressive strengths measured in the treated silt and sand are shown in Figure 4-17 and compared with normal (Gaussian) and log normal distributions.

The characteristic strength value often considered in design is defined as the 5 % fractile value of the unconfined compressive strength $q_{u5\%}$ (Eurocode, 2006).
Characteristic strengths were determined by calculating the 5 % fractile (Table 4-7):

- lowest strength value from the measured test results,
- assuming a Gaussian distribution of q_u,
- assuming a lognormal distribution of q_u.

Characteristic strength values calculated assuming a normal distribution are quite pessimistic, generally much lower than the 5 % fractile lowest strength obtained from the actual compressive strength test results (Table 4-7). Because of the asymmetry of the strength distributions, particularly visible here in Figure 4-17, the use of lognormal distributions seems more appropriate for the determination of $q_{u5\%}$. The values calculated with this distribution are in line with the 5 % fractile lowest values obtained from the strength test results (Table 4-7). Similar results are obtained for the strength of the wet-grab specimens from different sites (Figure 4-18). Ganne et al. (2010) reported these observations on soil-mix materials in Belgium.

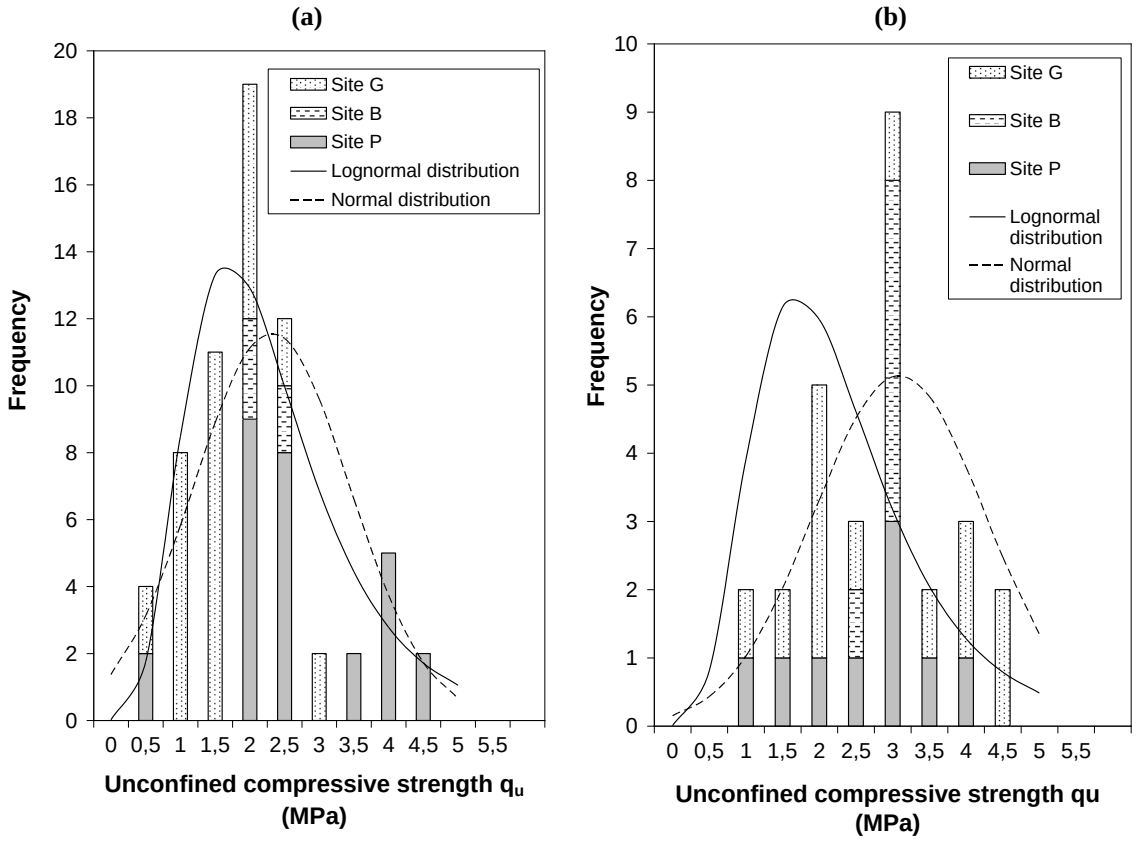

Figure 4-18 Distributions of unconfined compressive strengths for wet-grab specimens from different sites (a) after 28 days; (b) after 90 days.

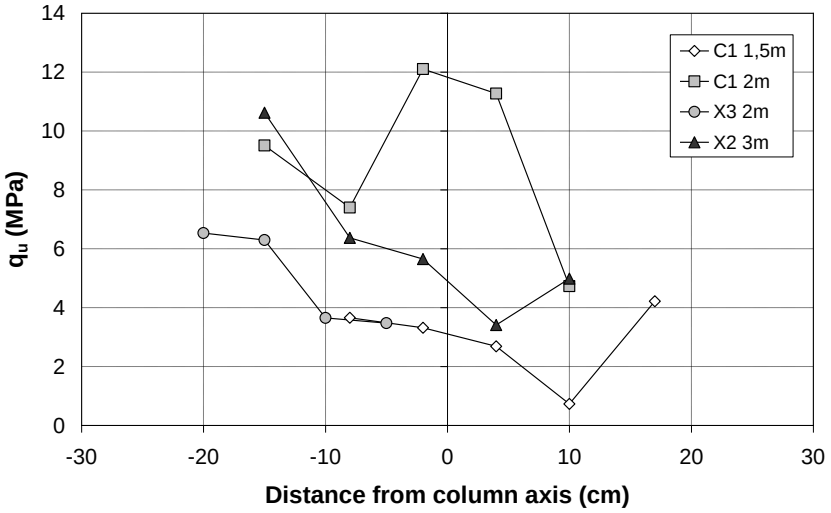

Figure 4-19 Variations in unconfined compressive strength with the position of the cored specimens from the axis of the columns.

Scatter in unconfined compressive strength is attributed to the heterogeneity and type of initial soil, variations in binder distribution, dosage, variations in execution parameters and to the presence of some soil inclusions. Figure 4-19 shows that at a given depth, strength varies depending of the horizontal position of the cored specimens within the column although no clear relation between strength and position can be identified.

The coefficients of variation of strength q_u (ratio of the standard deviation to the mean) measured on cored specimens from Vernouillet are plotted versus blade rotation number T in Figure 4-20. Each point in the graph represents the variation in strength observed within a block taken at a certain depth. The blade rotation numbers were computed for each depth from the execution parameter recordings. The number of specimens used to calculate the coefficient of variation for each point is given on the figure.

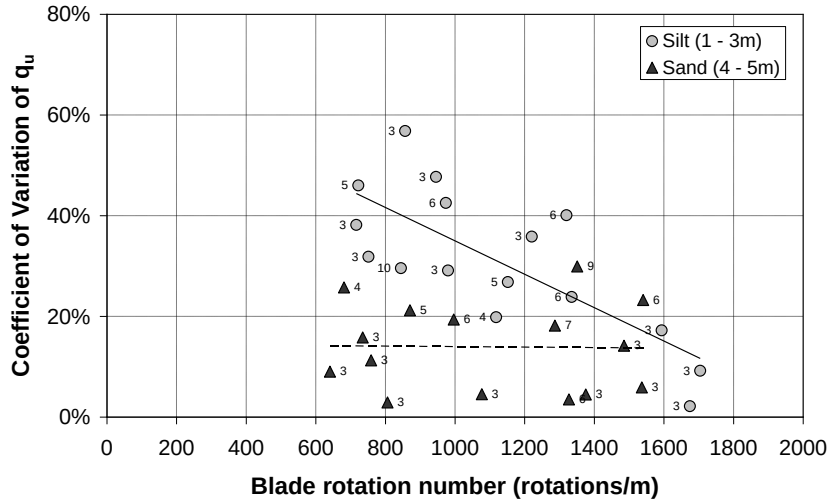

Figure 4-20 Coefficient of variation of strength from cored specimens from Vernouillet versus blade rotation number T.

Figure 4-20 clearly shows the influence of the mixing process on the homogeneity of treated soils produced by soil mixing. For the cored silt specimens, the coefficient of variation of q_u noticeably decreases as the blade rotation number increases.

Extensive mixing (with a high blade rotation number) improves the destructuration of the initial soil and facilitates the blending of the soil with the binder. This results in a more homogeneous material of less variable strength. Less soil inclusions are probably present in the specimens cored from columns installed with high blade rotation numbers.

All coefficients of variation of strength at a given depth in the sand are lower than 30 % (Figure 4-20). These results confirm that it is easier to obtain well mixed soil-cement columns in coarse grained soils than in fine grained soils. The drilling parameters used on site in Vernouillet (blade rotation numbers > 600) were sufficient to obtain a relatively homogeneous mixture in this type of soil.

More data is required to confirm these trends. Depending on the soil type and the targeted degree of homogeneity, a graph similar to Figure 4-20 can be used to select the minimum blade rotation number required for execution and provides an aid to define the mixing parameters.
It is important to note that the size of the samples has an effect on measured strength (Vervoort et al., 2012). Tests performed on larger specimens may give different results. Unfortunately, coring of larger diameter specimens was not possible in this study. Nevertheless, the results obtained here clearly illustrate the influence of the mixing process on the strength and homogeneity of the soil-mix material.

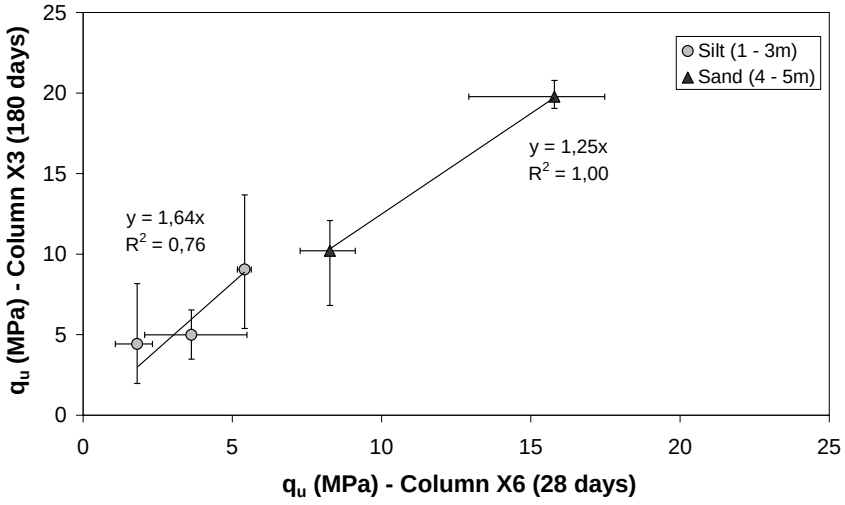

Figure 4-21 Increase in strength with time: comparison of average strengths measured from columns X6 (after 28 days) and X3 (after 180 days).

Columns X3 and X6 were installed with approximately identical execution parameters and binder contents (Table 4-2). Each point in Figure 4-21 represents the average strengths measured at the same depth in both columns. Despite the scatter in strength (Figure 4-17),

Figure 4-21 reveals that the average unconfined compressive strength increased between 28 and 180 days by a factor of 1.64 for the silt and by a factor of 1.25 for the sand. Considering the exponential relation used to estimate the increase in strength with time for laboratory specimens, these factors correspond to values of s_{28} of 0.82 for the silt and 0.37 for the sand:

$$\beta_{sand} = \exp\left[s_{28} \times \left(1 - \sqrt{\frac{28}{t}} \right) \right] = \exp\left[0.37 \times \left(1 - \sqrt{\frac{28}{180}} \right) \right] = 1.25$$

$$\beta_{silt} = \exp\left[0.82 \times \left(1 - \sqrt{\frac{28}{180}} \right) \right] = 1.64$$

These values are consistent with those obtained for silts and sands treated in the laboratory (Table 3-7 and Table 3-8).

4.4.5 Static deformation modulus

4.4.5.1 Static stiffness in columns from Vernouillet

The longitudinal strains during compression tests were measured locally in the central part of the specimens cored from the columns excavated after 180 days.

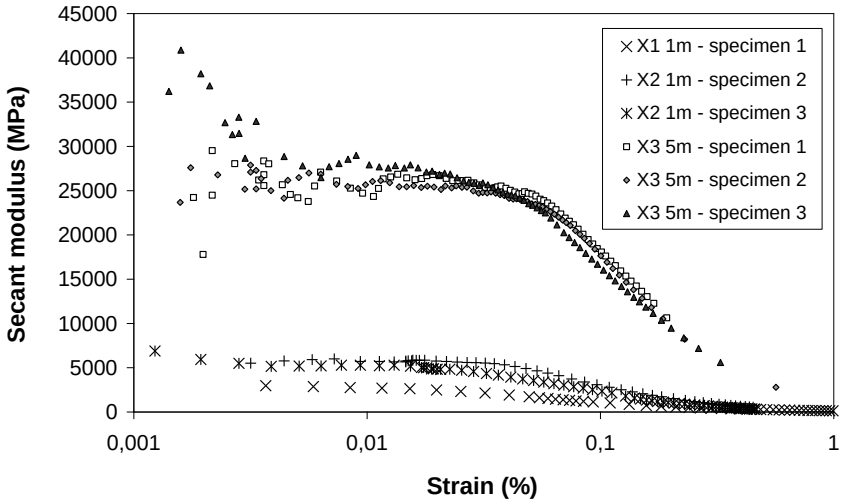

Figure 4-22 Typical secant stiffness-strain curves for cored specimens from Vernouillet.

Figure 4-22 presents typical secant stiffness-strain curves. As strain increases, the secant stiffness decreases non-linearly.

The static modulus increases with depth (Figure 4-23) following the change in soil type around 3 m. After 180 days, the maximum modulus of the specimens of silt is generally close to 10 GPa. For the sand, E_{50} is higher between 10 and 25 GPa.

Although there is some scatter in the results, the data shows that static moduli of cored specimens in the silt are relatively close to the moduli determined on laboratory samples (Figure 4-23). This trend for static modulus differs from the clear overestimation of the in situ strength of the treated silt based on laboratory mixes (Figure 4-16).

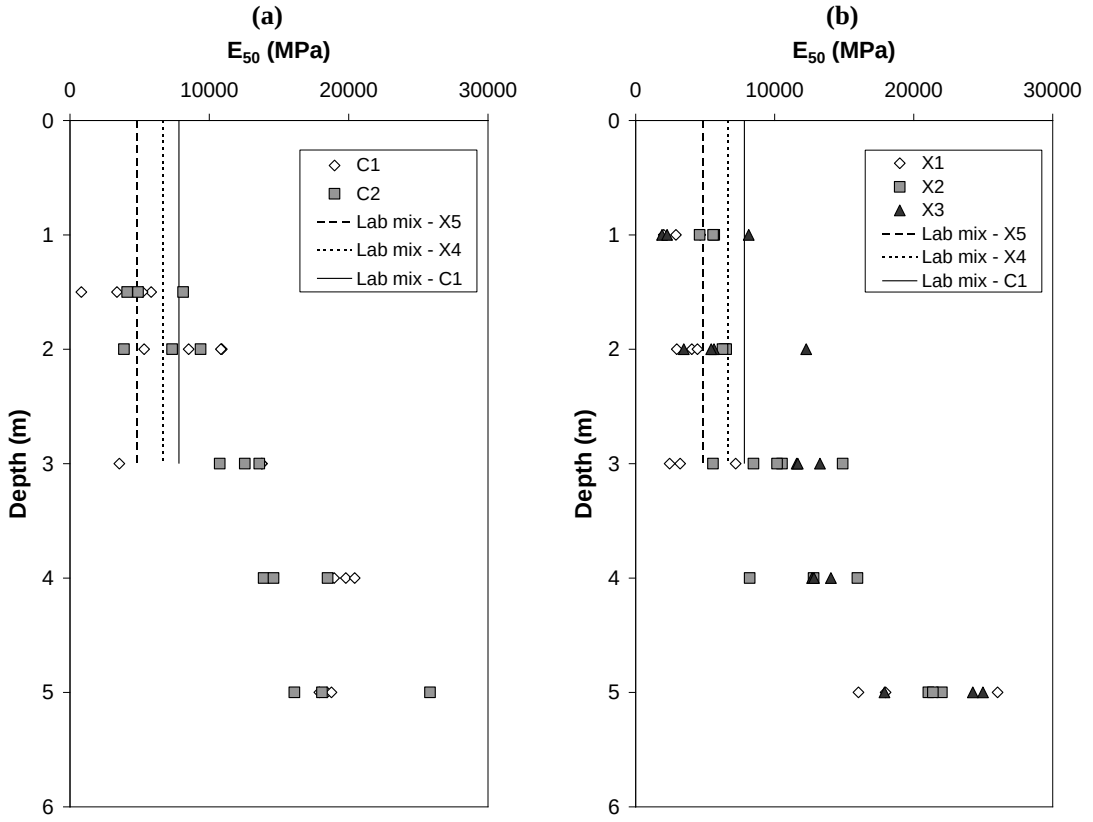

Figure 4-23 Static modulus of specimens cored in blocks from excavated columns after 180 days (a) columns C1-C2; (b) columns X1-X2-X3.

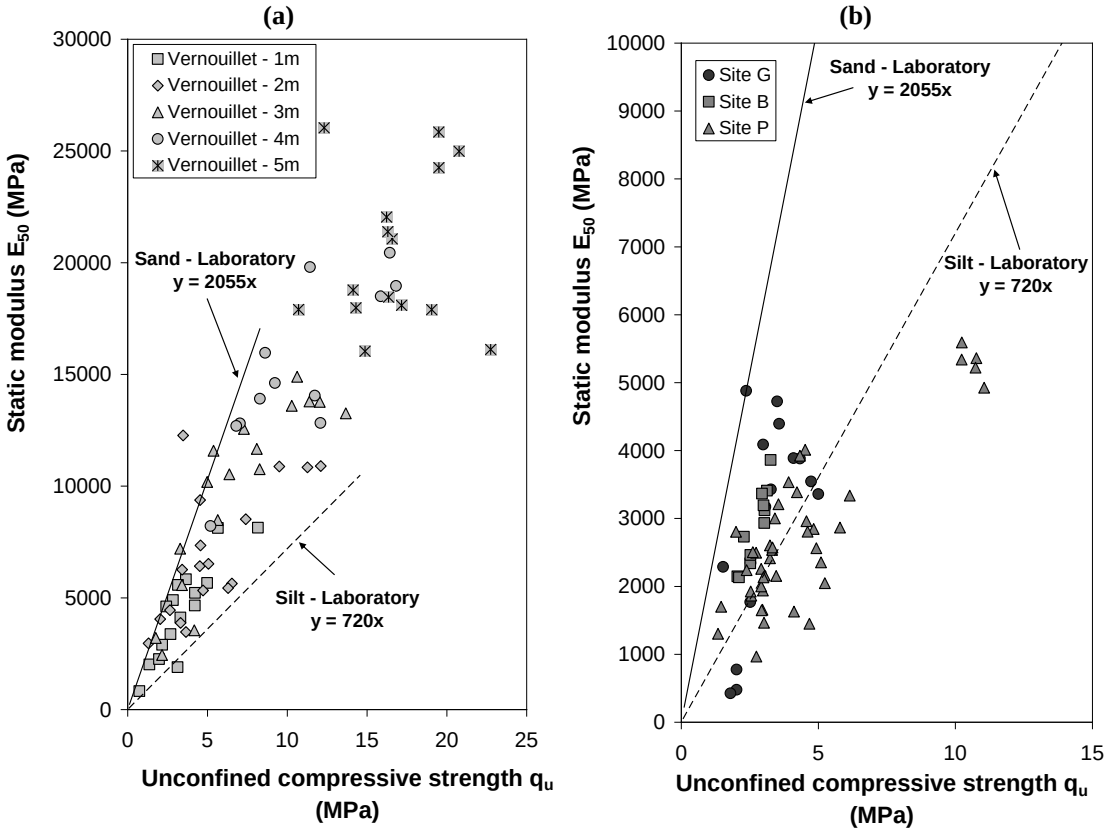

Figure 4-24 Static secant modulus E_{50} versus unconfined compressive strength q_u (a) cored specimens; (b) wet-grab samples.

4.4.5.2 Strength – static stiffness relations for soils stabilised in situ by deep mixing

The measured static deformation moduli E_{50} of cored and wet-grab samples are plotted versus unconfined compressive strength q_u in Figure 4-24.

With the exception of the specimens from site P, the static moduli of both cored and wet-grab specimens generally lie between the relations found for silts and sands mixed in the laboratory (720 and 2055 times the unconfined compressive strength). The results on the cored specimens from Vernouillet are somewhat closer to the relation found for sands whereas E_{50} values measured on wet-grab specimens are closer to the trend observed for silts. This can be explained in part by the high sand content in the cored specimens from Vernouillet. The higher porosity in the wet-grab samples (Figure 4-14) is also responsible for the lower stiffness (Figure 4-25). The high porosity and low stiffness measured on the specimens from site P may also be related to the clay content of the soil, as it is reasonable to assume that the stiffness-strength ratio for clays is lower than the ratio for silts.

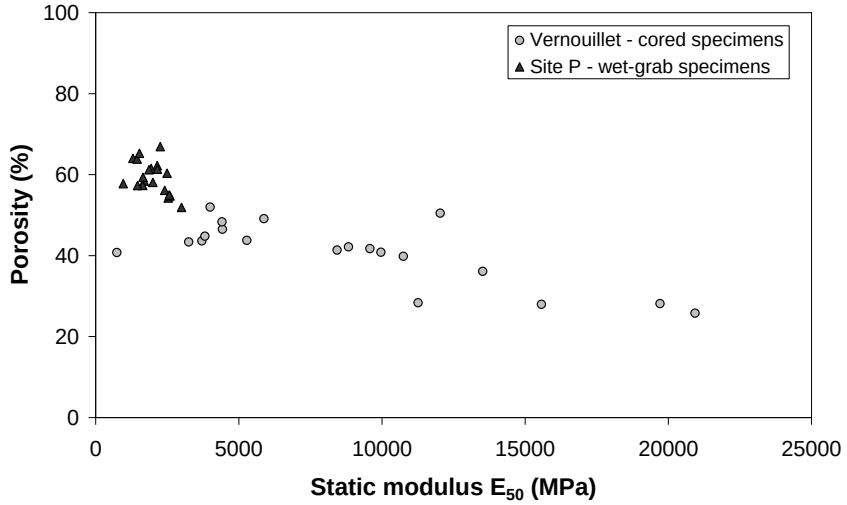

Figure 4-25 Porosity versus static modulus E_{50}.

The strains at failure measured using local displacement transducers are between 0.05 and 0.8 % (Figure 4-26).

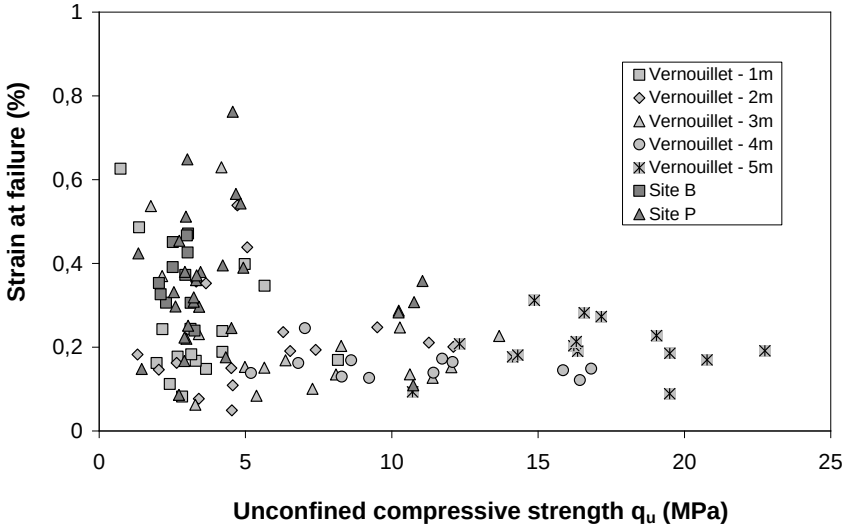

Figure 4-26 Strain at failure versus unconfined compressive strength q_u.

4.4.6 Ultrasonic wave velocity

4.4.6.1 Wave velocities in columns from Vernouillet

In general, the ultrasonic wave velocity V_p increases with depth in the columns of Vernouillet (Figure 4-29). In the silt (first 3 meters), most of the results are between 2300 and 3000 m/s. In the sand, they vary between 2600 and 4100 m/s. Unlike for compressive strength, the wave velocities of the cored specimens are generally higher than the velocities measured in the specimens prepared in the laboratory. The ultrasonic wave velocities of the specimens cored after 180 days from the columns in Vernouillet correlate linearly with wet density. Correlations with density are obviously dependant on time as V_p increases during curing. All specimens were tested after the same curing period of 6 months. No noticeable increase in average wave velocity is observed when comparing the results from columns X3 and X6 (Figure 4-28).

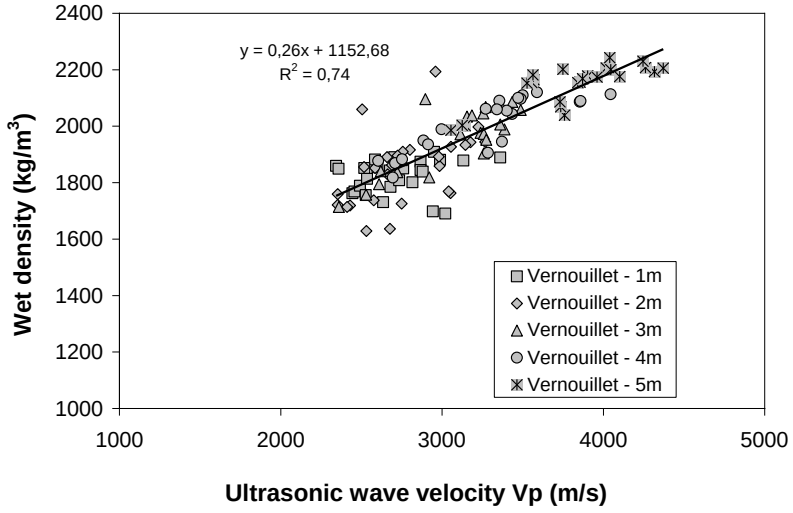

Figure 4-27 Relation between wet density and ultrasonic wave velocity for cored specimens from Vernouillet.

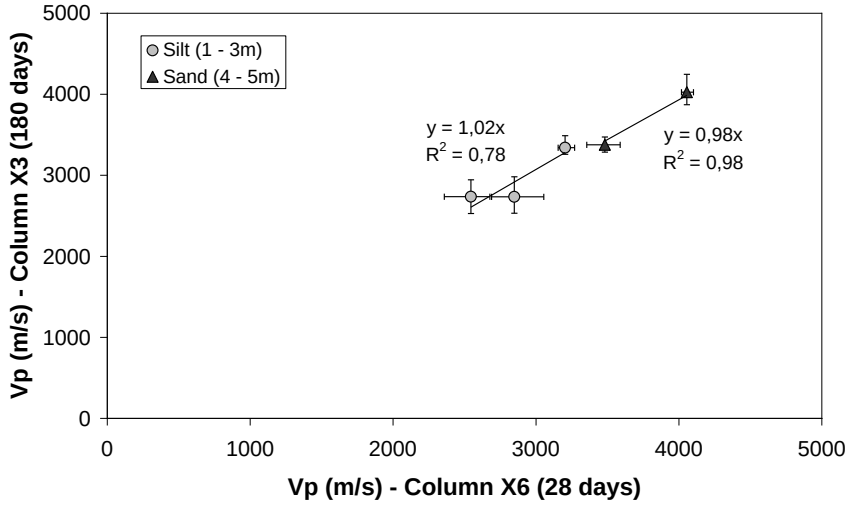

Figure 4-28 Comparison of average ultrasonic wave velocities measured on cored specimens from columns X3 and X6.

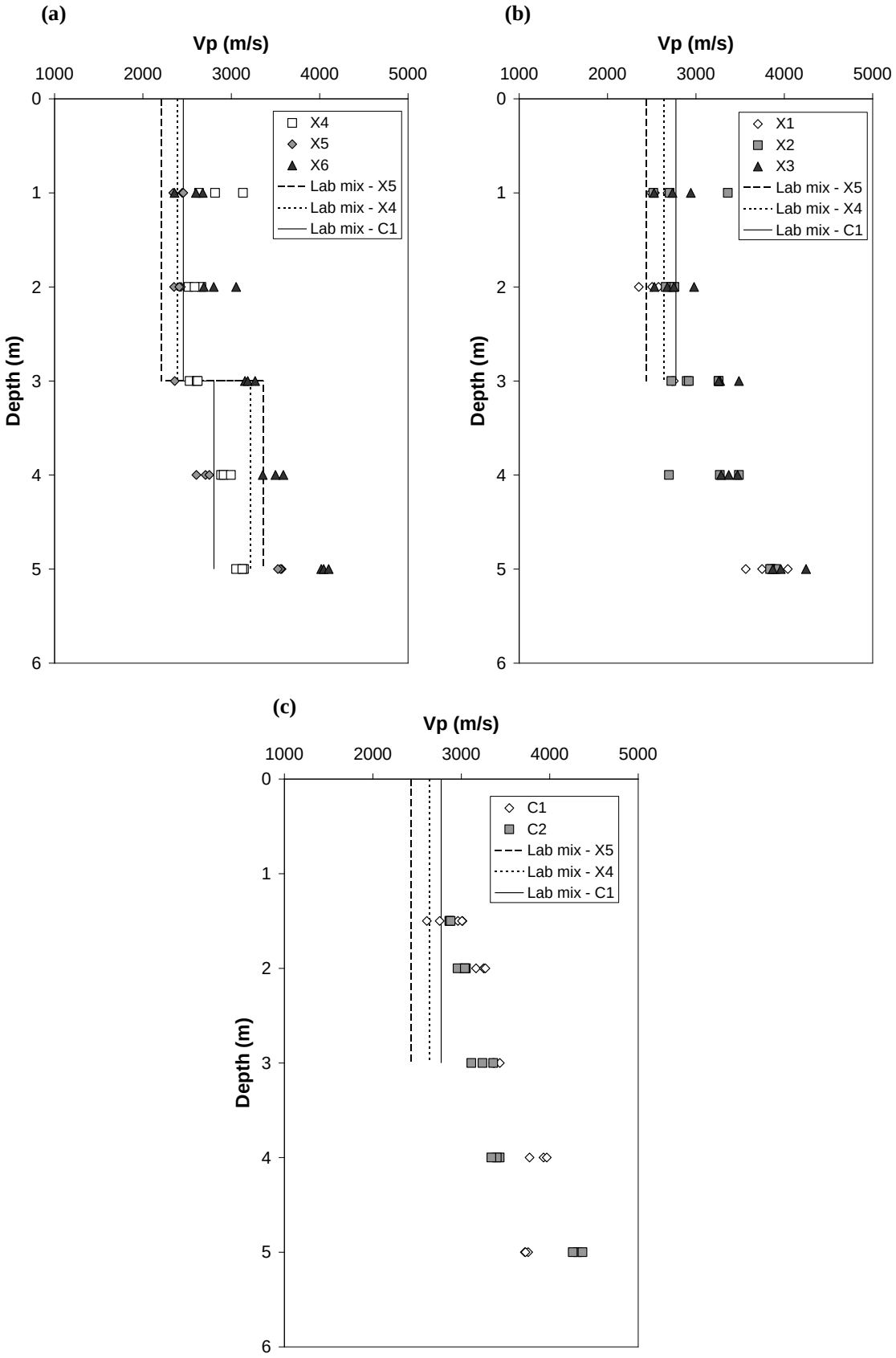

Figure 4-29 Ultrasonic wave velocities of specimens cored in blocks from columns excavated (a) after 28 days; (b) and (c) after 180 days.

4.4.6.2 Relation between wave velocity and strength

Figure 4-30 shows that the relation between ultrasonic wave velocity V_p and unconfined compressive strength q_u for specimens treated in situ by deep mixing is non-linear. The values of V_p generally lie between or close to the boundaries determined from the laboratory mixed specimens of silt and sand. The behaviour of the cored specimens appears to be closer to the trend found for sands mixed in the laboratory. Although large scatter is evident in the results on wet-grab samples for strengths lower than 5MPa, the results appear to follow the trend established for silts. The scatter in the results can be related to previously mentioned factors such as the heterogeneity of the initial soil, variations in binder content, variations in column execution parameters and to the presence of soil inclusions in the specimens.

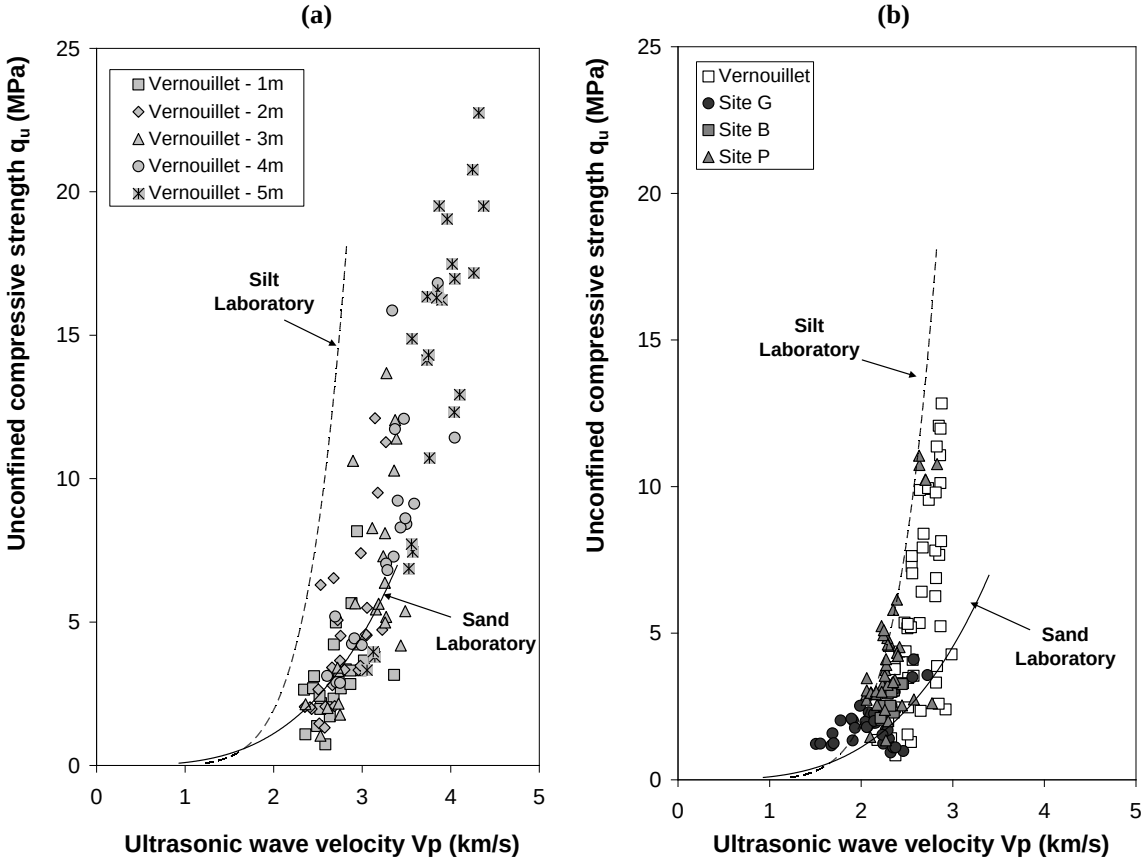

Figure 4-30 Unconfined compressive strength q_u versus ultrasonic wave velocity V_p for (a) cored and (b) wet-grab specimens.

4.4.6.3 Relation between wave velocity and static modulus

The relation between V_p and E_{50} for cored and wet-grab samples is also non-linear (Figure 4-31). The correlations determined for soils mixed in the laboratory are close but slightly overestimate the modulus of cored and wet-grab samples.

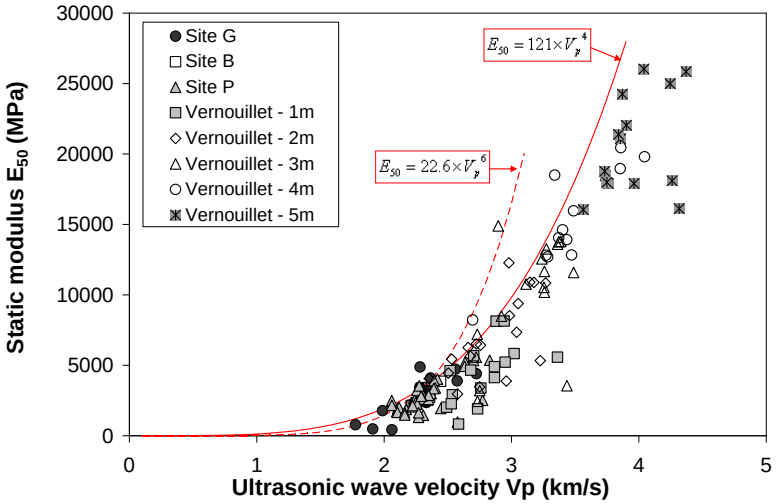

Figure 4-31 Relation between static modulus E_{50} and ultrasonic wave velocity V_p for cored and wet-grab specimens.

4.4.7 Dynamic modulus of soils stabilised in situ by deep mixing

4.4.7.1 Dynamic modulus in columns from Vernouillet

In general, E_0 increases with depth in the columns from Vernouillet (Figure 4-33). In the silt (first 3 meters), most of the results are between 10 and 20 GPa. In the sand, E_0 varies between 10 and 35 GPa. The dynamic modulus of the cored specimens is in general equal to or higher than the modulus measured on specimens prepared in the laboratory. Bhadriraju et al. (2008) subjected in situ wet-grab samples to strength and small strain stiffness tests (using bender elements) in the laboratory. They also found a good agreement between test results from field cores and laboratory fabricated specimens. These results differ from those reported by Madhyannapu et al. (2010). They found that the small strain shear modulus of field specimens was lower than the modulus of laboratory prepared specimens.

No perceptible increase in dynamic modulus between 28 and 180 days is observed when comparing the average results from columns X3 and X6 (Figure 4-32).

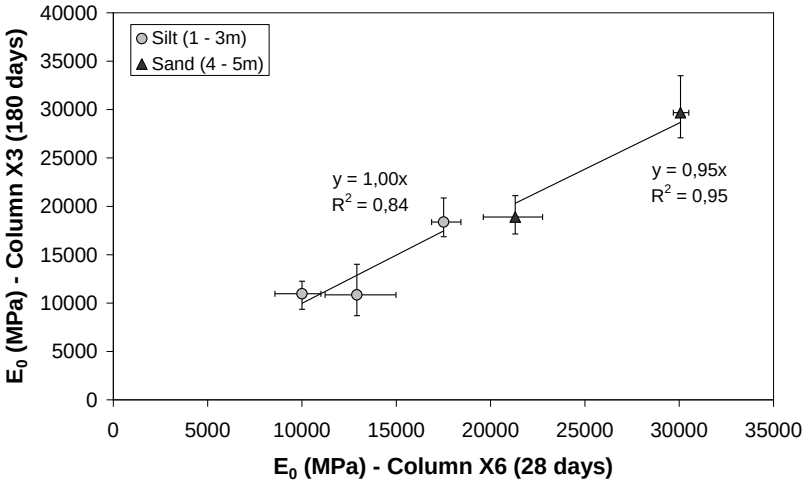

Figure 4-32 Comparison of average dynamic modulus E_0 measured on cored specimens from columns X3 and X6.

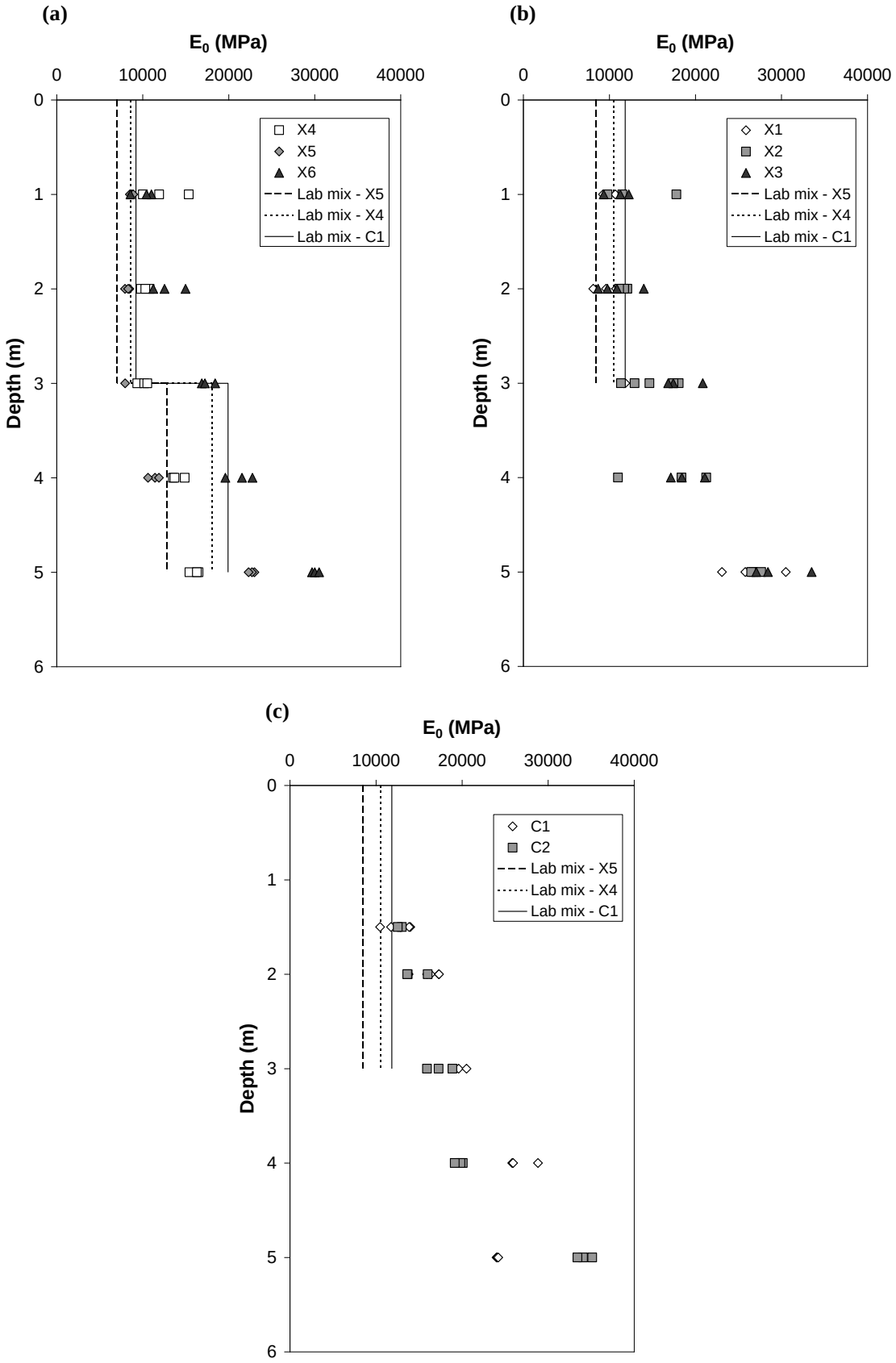

Figure 4-33 Dynamic modulus E_0 of specimens cored in blocks from columns excavated (a) after 28 days; (b) and (c) after 180 days.

4.4.7.2 Relation between dynamic modulus and strength

The relations between dynamic modulus E_0 and strength for cored and wet-grab specimens are presented in Figure 4-34 and Figure 4-35. The values of E_0 generally lie between the correlations determined from the laboratory mixed specimens of silt and sand. The cored specimens follow the relation for sands using the square root of q_u whereas the general trend for the wet-grab samples appears to be parallel to the relation obtained for silts. However, some scatter is visible for strengths lower than 5 MPa. The stiffness of the wet-grab samples from Vernouillet are in general lower than the stiffness of the cored specimens of equivalent strength.

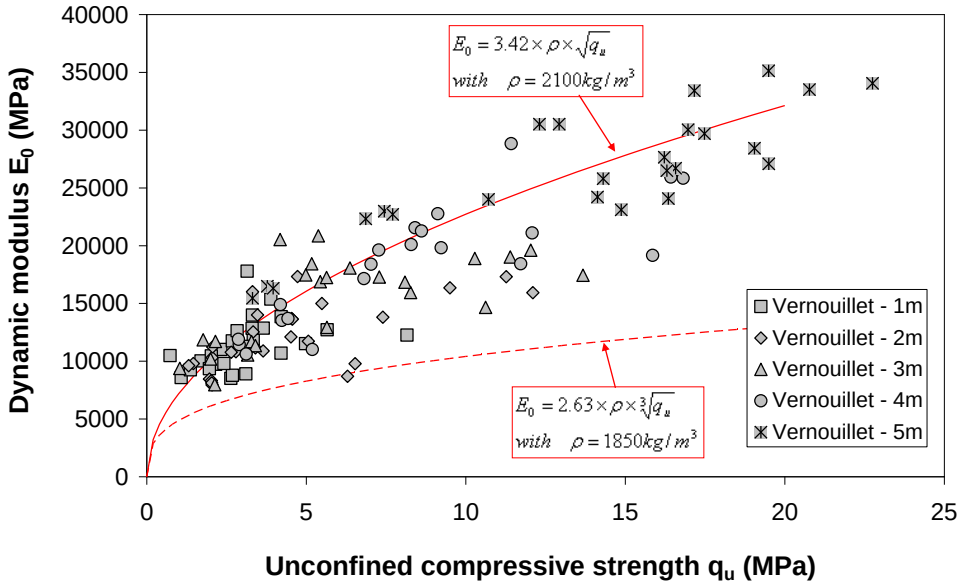

Figure 4-34 Relation between dynamic modulus E_0 and strength for specimens cored in blocks from excavated columns.

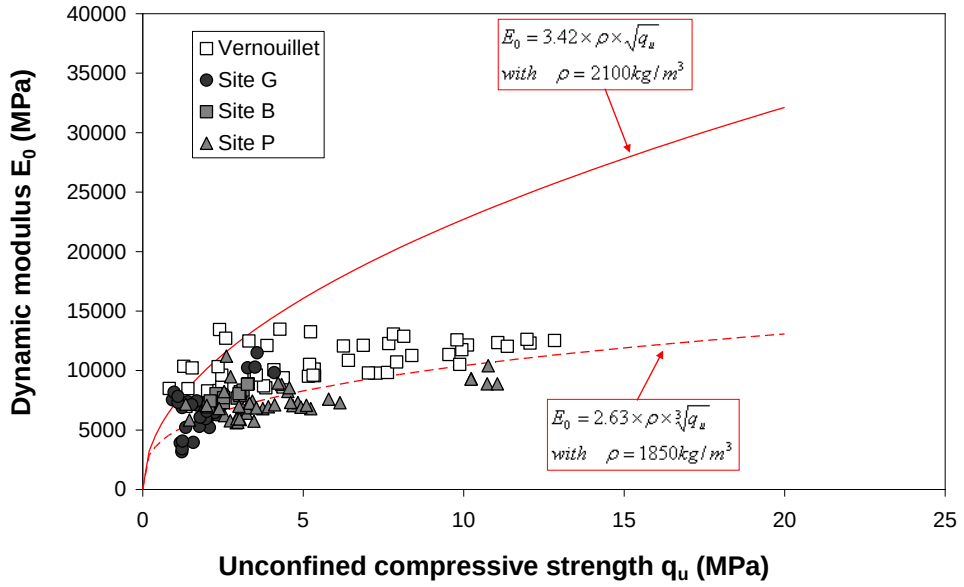

Figure 4-35 Relation between dynamic modulus E_0 and strength for wet-grab specimens.

Using the actual measured wet densities, an excellent agreement is found between the measured and calculated values of E_0 based on the square root of q_u for the cored specimens (Figure 4-36 (a)). The relation using the cube root of q_u underestimates the modulus of wet-grab specimens (Figure 4-36 (b)).

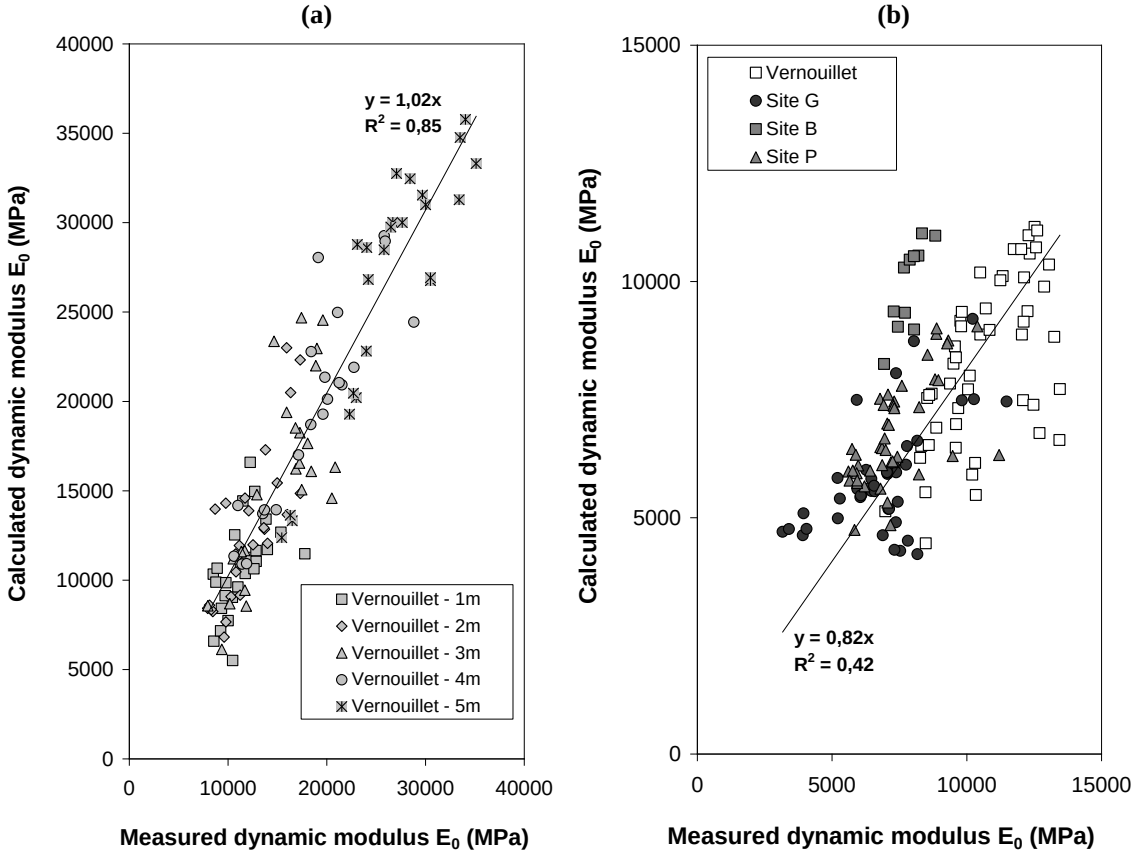

Figure 4-36 Comparison between measured and calculated values of E_0 for (a) cored and (b) wet-grab specimens.

The lower moduli of the wet-grab specimens are related to the higher porosities (Figure 4-37).

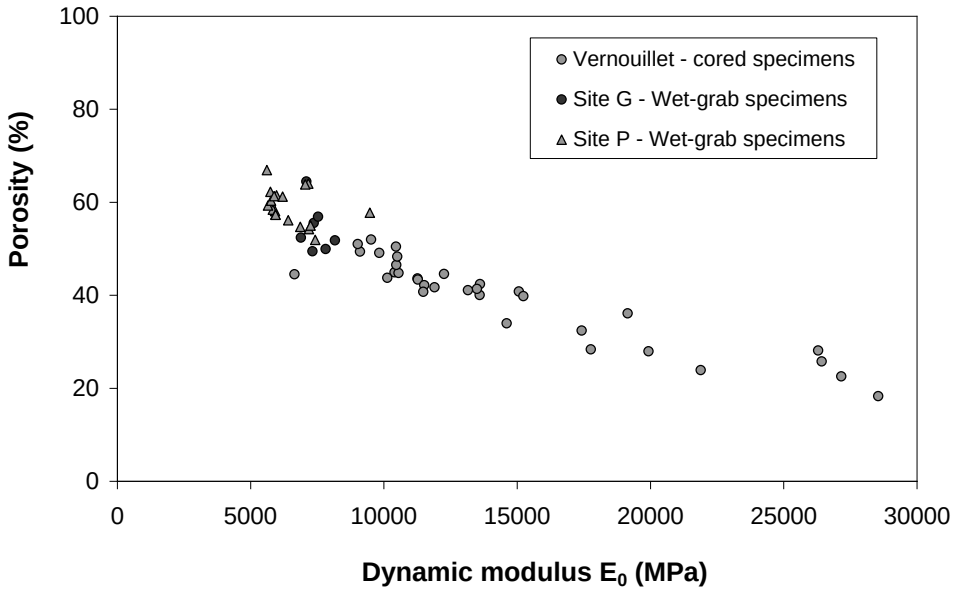

Figure 4-37 Porosity versus dynamic modulus E_0 for field specimens.

The rigidity of field specimens decreases with unconfined compressive strength (Figure 4-38).

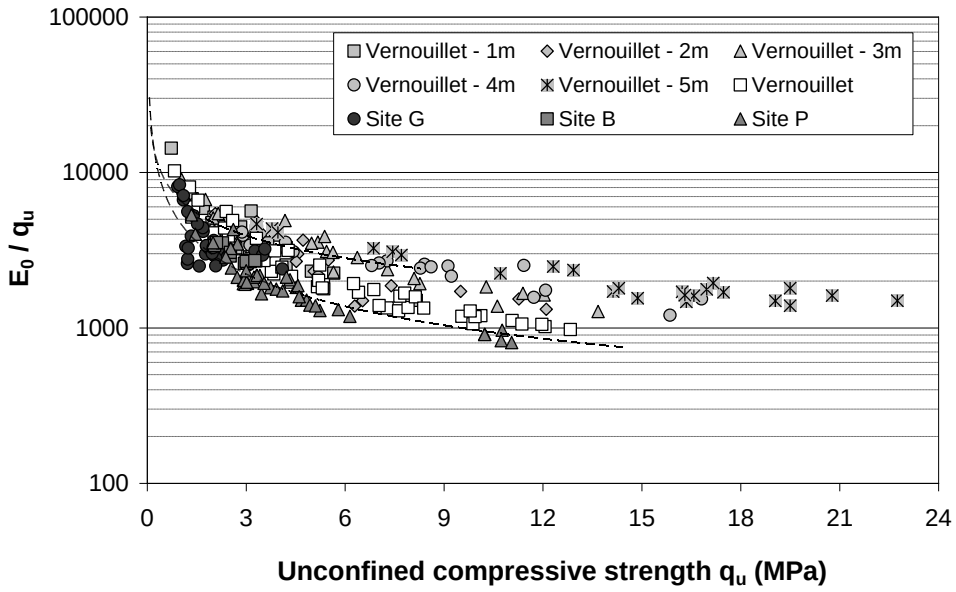

Figure 4-38 Rigidity of cored and wet-grab specimens versus unconfined compressive strength.

The dynamic to static modulus ratio E_0/E_{50} decreases non-linearly from over 10 for strengths lower than 3 MPa to a minimum close to 1 at higher strengths (Figure 4-39). The values of E_0/E_{50} are similar for both wet-grab and cored specimens. This shows that the effect of sampling is identical on static and dynamic stiffness. Studies on concrete showed that the dynamic to static elastic modulus ratio is between 1.7 and 1.3 (Panesar and Shindman, 2011) and decreases with age (Mesbah et al., 2002).

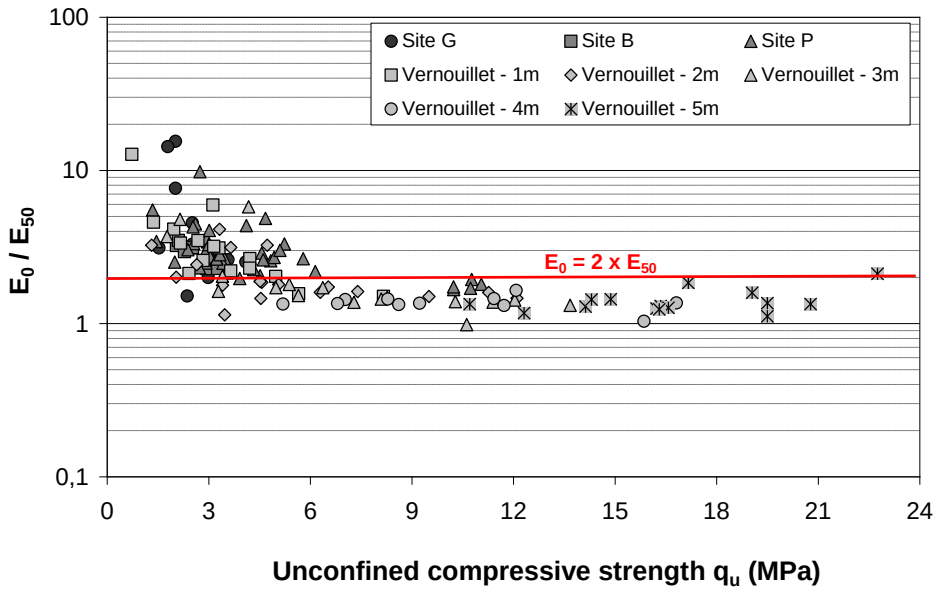

Figure 4-39 E_0/E_{50} versus unconfined compressive strength q_u for field specimens.

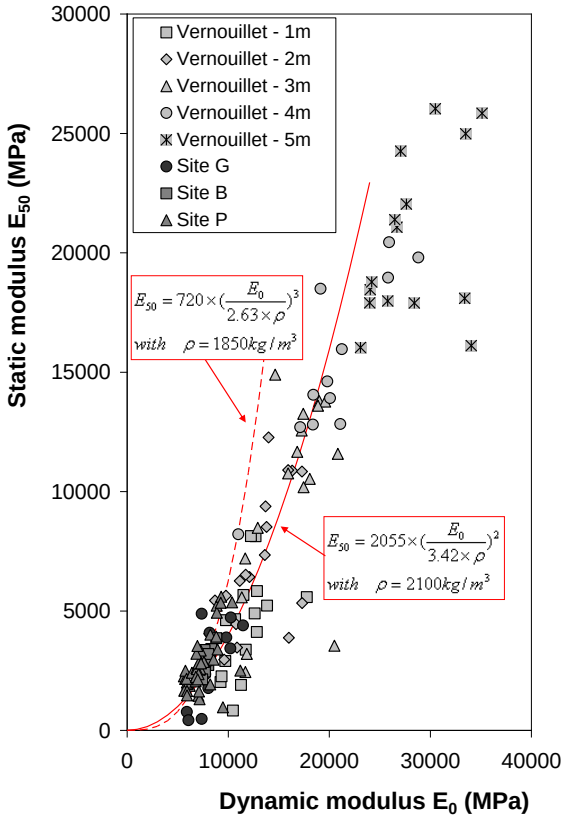

Figure 4-40 Relation between static and dynamic modulus for field specimens.

Despite some scatter, the relation between dynamic and static modulus for field samples is similar to the relations found for soils mixed in the laboratory for values of E_0 lower than 10 GPa (Figure 4-40). For higher values up to 15 GPa, the relation for sands provides a reasonable fit to the data from cored specimens.

4.4.8 Shear wave velocity and small strain shear modulus

4.4.8.1 Wave velocities from resonance testing

Resonance testing (described in section 2.5.2.2) was used to determine the shear and compressive wave velocities of some specimens cored from the columns excavated in Vernouillet after 180 days.

The compressive wave velocities measured by the resonance method are approximately 20 % lower than the wave velocities obtained using the ultrasonic device (Figure 4-41). This can be related to the decrease of stiffness with strain in soil-mix materials. It is reasonable to assume that the strains involved in the measurements of the velocity of ultrasonic waves through the tested specimens are smaller than the strains induced by the resonance method in which a mechanical stress is applied by tapping the specimen.

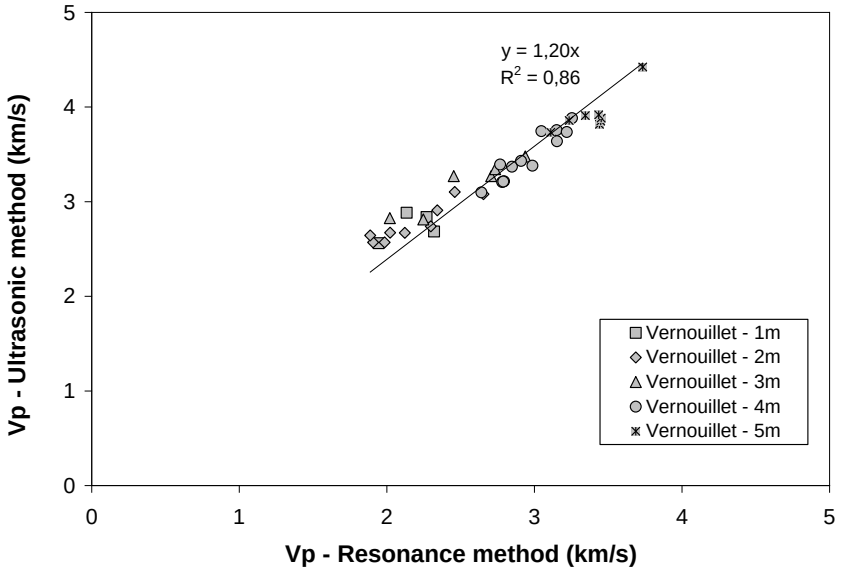

Figure 4-41 Comparison between compressive wave velocities obtained by the ultrasonic method and the resonance method.

Figure 4-42 presents the shear wave velocities evaluated from free-free resonance tests versus unconfined compressive strength. For the cored specimens from Vernouillet, the wave velocities increase with strength. The unconfined compressive strengths of the tested specimens vary between 2 and 20 MPa. The S-wave velocities are between 800 and 2200 m/s.

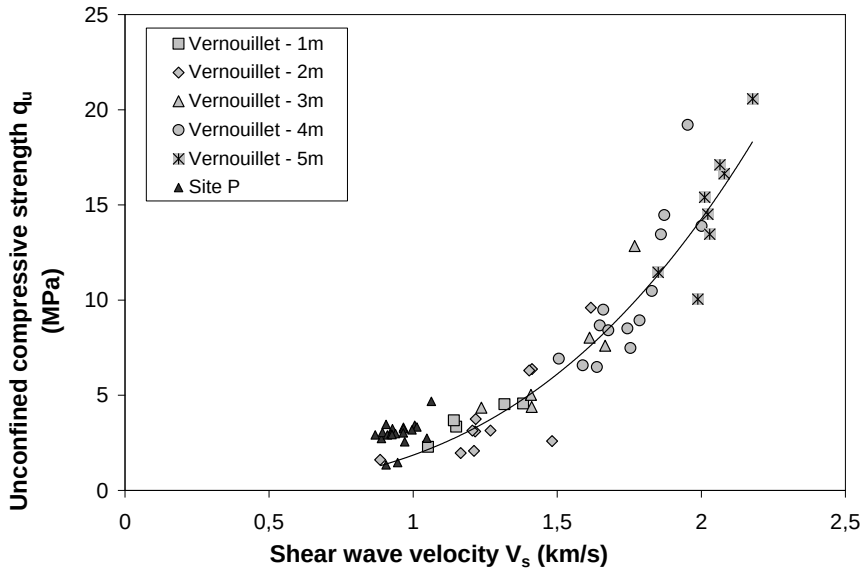

Figure 4-42 Shear wave velocities obtained by the resonance testing.

Shear wave velocity data for stabilised soils of high strengths are scarce in the literature. Some published results of measurements performed in the laboratory and in situ by different methods on different types of soils, stabilised with different binders, with strengths generally up to 5 MPa were added to the data from this study in Figure 4-43 (Åhnberg and Holmen, 2011; Porbaha et al., 2005; Hird and Chan, 2005; Nishikawa et al., 1996). The graph confirms

that a non-linear relation also exists between shear wave velocity and unconfined compressive strength, for strengths in the range of 0 to 20 MPa.

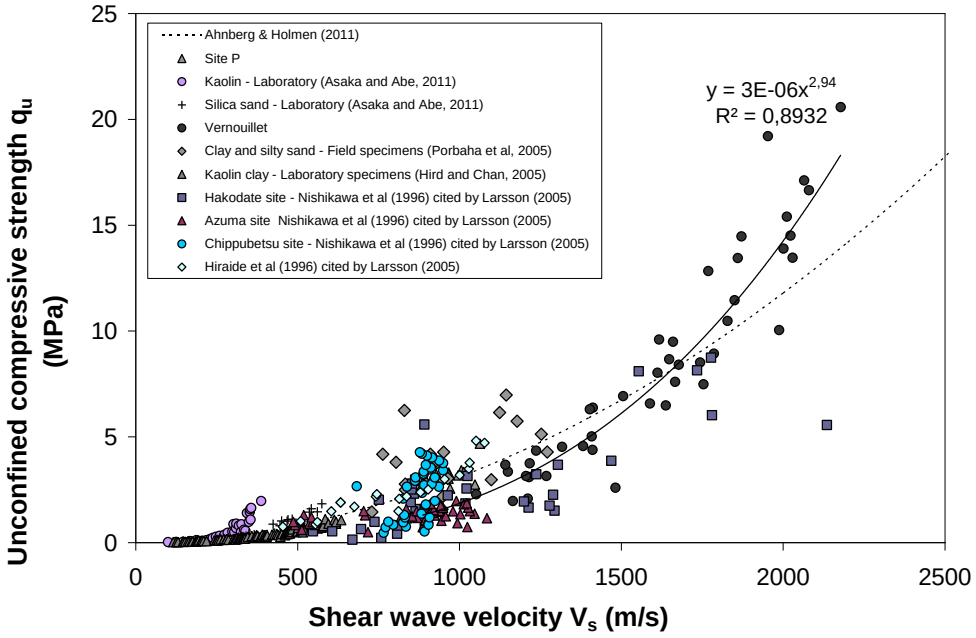

Figure 4-43 Shear wave velocity V_s (data compiled from the literature).

Based on tests performed on specimens of maximum strength approximately 1 MPa, Åhnberg and Holmen (2011) proposed an empirical relation (polynomial equation) to estimate q_u from V_s. Although this correlation was established based on results obtained on soft stabilised soils, when extrapolated to higher strengths, it provides a reasonably good agreement with the data collected in the present study. However, it appears that a simpler power law relationship provides an acceptable fit for the specimens of this study having strengths greater than 2 MPa. Nevertheless, the power law relation seems to underestimate the strength in the lower wave velocity range.

4.4.8.2 Dynamic shear modulus and Poisson's ratio

The small strain shear moduli G_0 are plotted versus unconfined compressive strength in Figure 4-44.

In the range of strengths tested, G_0 increases with strength. The relation appears to be slightly non-linear. The calculated Poisson's ratio is variable in the Vernouillet silt (depths of 1 to 3 m, Figure 4-45). It appears to be relatively constant for the sand at approximately 0.22. These results show that the use of a Poisson's ratio of 0.25 is reasonable to calculate the dynamic modulus E_0 from ultrasonic wave velocity measurements.

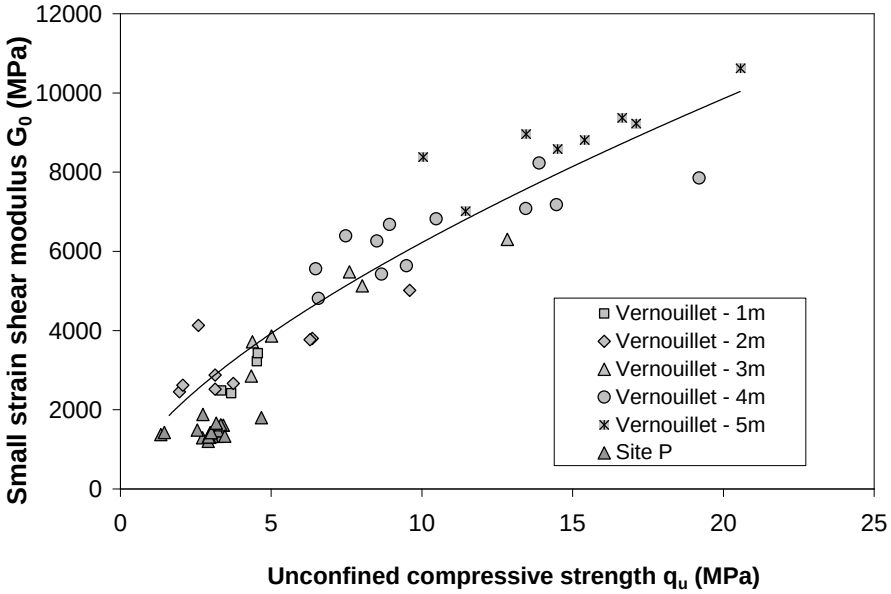

Figure 4-44 Small strain shear modulus of in situ specimens.

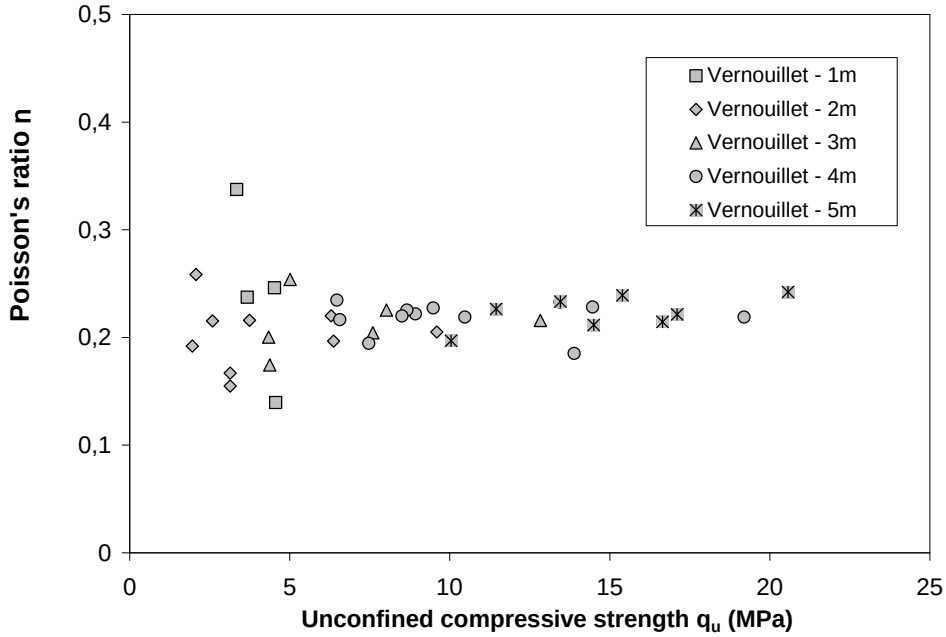

Figure 4-45 Poisson's ratio of cored specimens from Vernouillet.

4.4.8.3 Correlation with density

The tested specimens of stabilised silt cored from block samples of soil-mix columns between 1 and 3 m have densities of 1800 to 2000 kg/m^3. The density of the sand specimens (4 and 5m) subjected to FFR-testing varies between 2000 and 2300 kg/m^3. The S-wave velocities increase linearly with density (Figure 4-46).

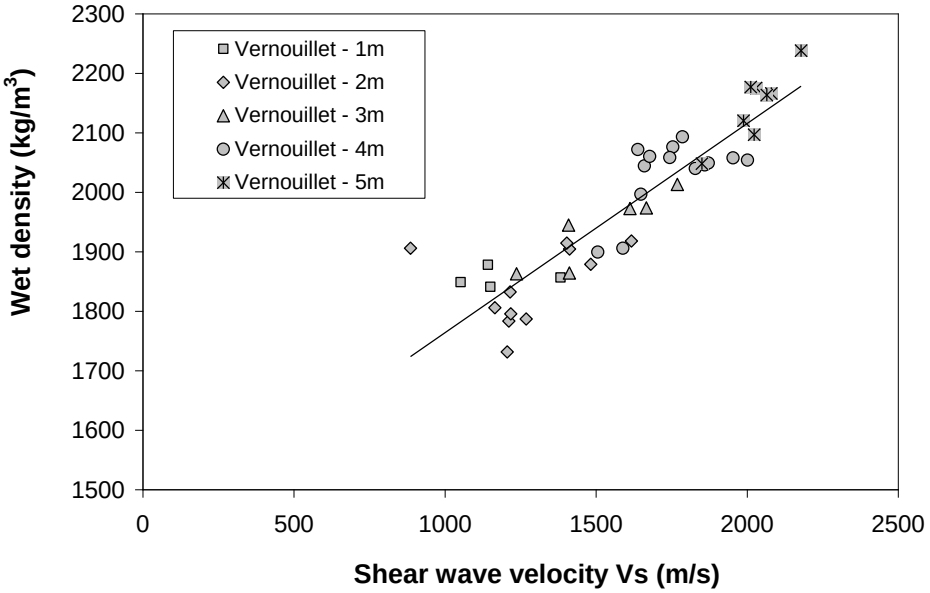

Figure 4-46 Correlation between density and shear wave velocity.

4.4.8.4 Relation with static deformation modulus

Figure 4-47 shows that the correlation between shear wave velocity V_s and static modulus E_{50} is non-linear. A power law with an exponent close to 3 fits to the data.

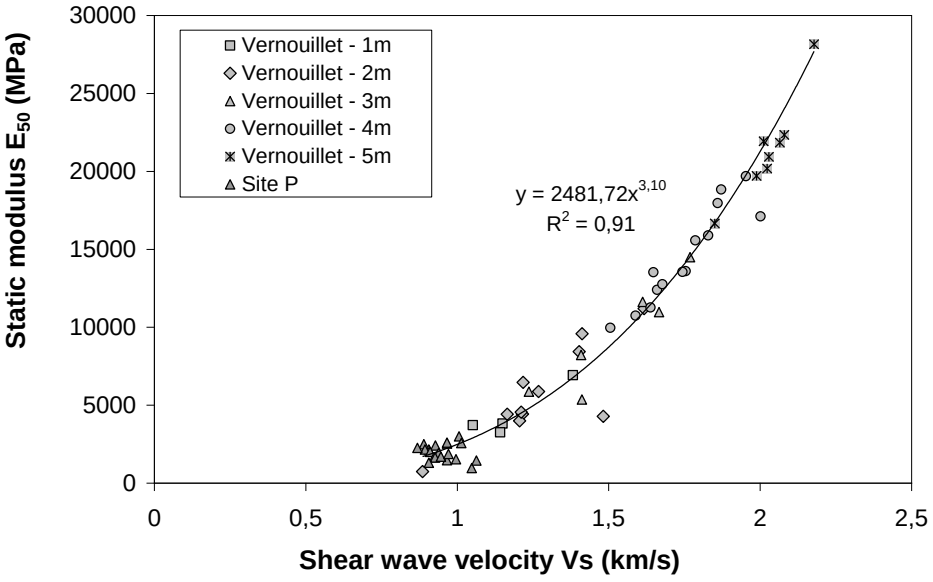

Figure 4-47 Correlation between static modulus E_{50} and shear wave velocity Vs.

4.4.8.5 Relation with porosity

The porosities of the tested specimens of soils treated in situ vary between 20 and 70 %. These values are much higher than typical porosities for concretes. Both shear and compression wave velocities decrease as porosity increases (Figure 4-48).

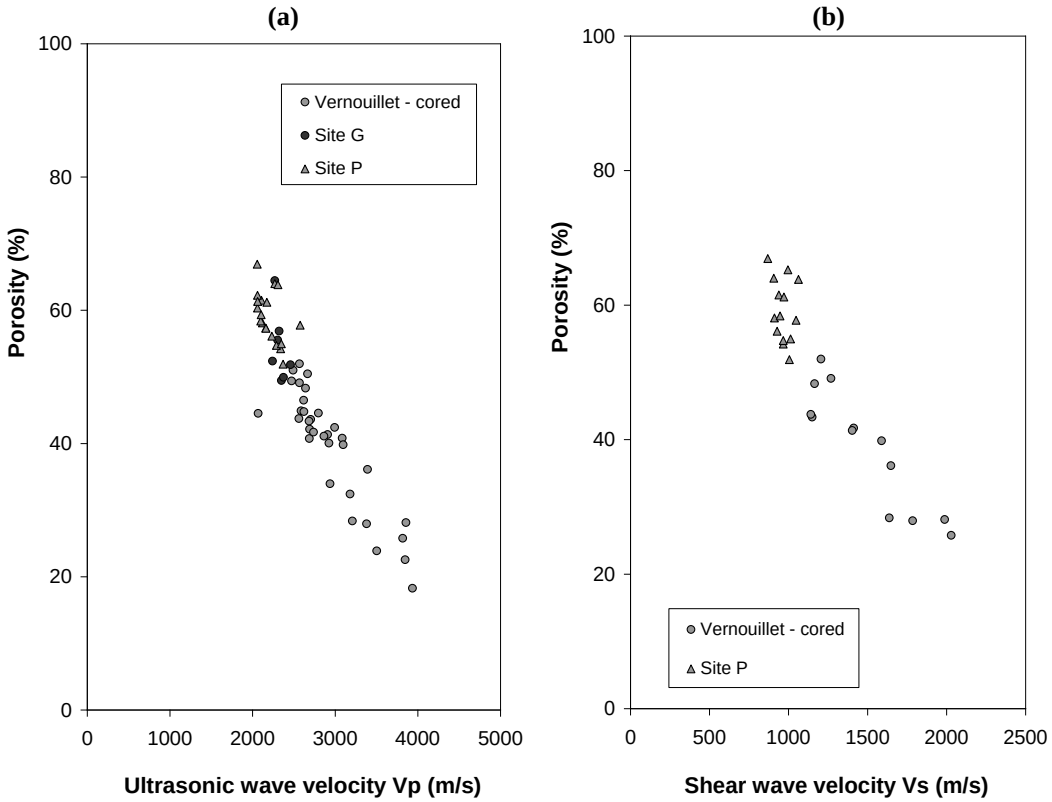

Figure 4-48 Relationship between porosity and (a) compression wave velocity; (b) shear wave velocity.

4.4.9 Indirect tensile strength

Figure 4-49 shows the relationship between indirect tensile (Brazilian) strength q_{it} and unconfined compressive strength q_u measured on specimens cored from Vernouillet after 28 and 180 days. Each point in Figure 4-49 represents the average strengths measured at the same depth in different columns. The figure shows that the indirect tensile strength increases almost linearly with increasing q_u. The average q_{it}/q_u ratio is 0.18, close to the relation found for laboratory mixed specimens (Figure 3-51).

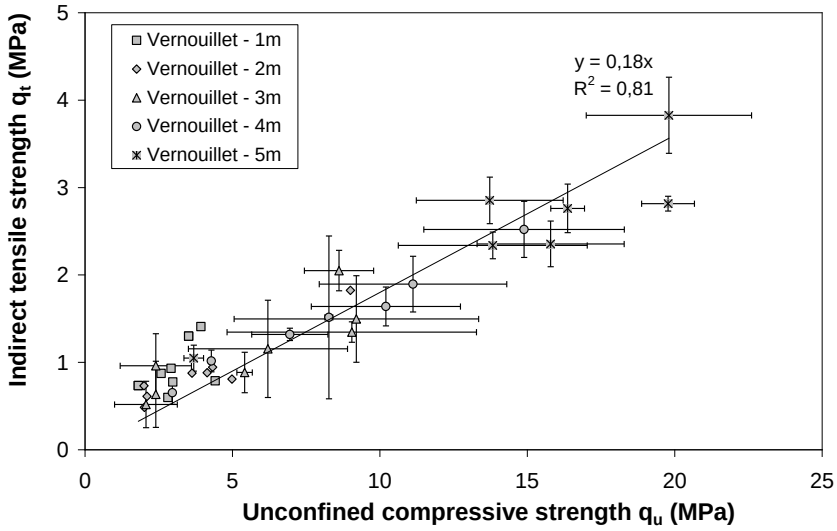

Figure 4-49 Indirect tensile strength q_{it} versus unconfined compressive strength q_u.

4.5 In situ load test – Input parameters for numerical analyses

4.5.1 Load test procedure

Column C2 was subjected to a static loading test following NF 94-150-1 (AFNOR, 1999b) approximately 90 days after installation.

The objective of the static load test was to evaluate the bearing capacity of the column. The reaction frame (Figure 4-50) consisted of a steel beam installed on two scaffolds and connected at each end to a micropile. The force on the head of the column was applied by a hydraulic jack equipped with a ball joint. The head of C2 was confined in a metal collar to ensure that the load was correctly transmitted to the column. During the static load test, the vertical displacement of the column head was measured by four displacement transducers. The load was applied monotonously by increments of 50 kN.

Figure 4-50 Set-up for static load test on column C2.

4.5.2 Load test results

Eight load increments of 50 kN were applied during the test. Each load was maintained for 30 minutes. The measured load-settlement curve is shown in Figure 4-51. Loading was stopped for a maximum load of 400 kN, when the settlement of the head of the column exceeded 40 mm ($1/10^{th}$ of the diameter). This maximum load corresponds to a pressure of approximately 3.2 MPa, close to the average strength measured on cored specimens after 28 days in the silt (Table 4-7).

After 180 days, column C2 was excavated to identify the failure mode produced by the loading test. Cracks and fractures were visible in a zone of the column located around a depth of 1 m (Figure 4-52). The presence of this destructured zone suggests that failure occurred within the material of the column. This hypothesis concerning the mode of failure is reinforced by the fact that the theoretical bearing capacity of the column (calculated from the results of pressuremeter tests, Table 4-1) was higher than the internal strength (estimated from the results of tests on cored specimens).

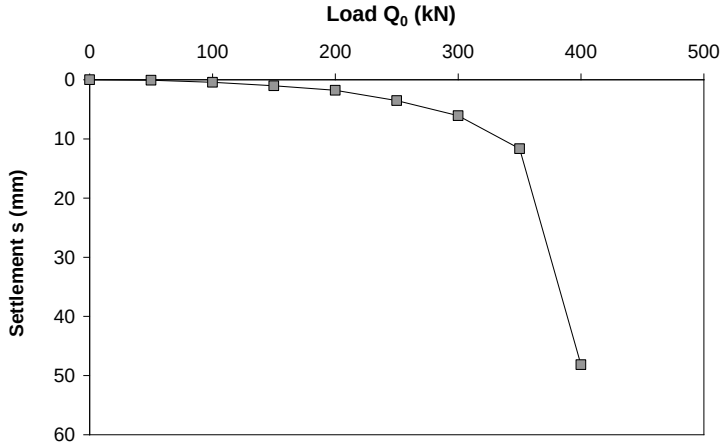

Figure 4-51 Load-settlement curve obtained from load test on column C2.

Figure 4-52 Cracks and fissures observed on column C2 approximately 1 m below ground level.

4.5.3 Numerical models

Finite element analyses were used to model the load test performed on column C2 (Cuira et al., 2013). Three models were constructed with different software based on average mechanical parameters measured on the specimens cored from block samples. The input parameters are given in Table 4-8. The soil-mix material was modelled as linear elastic perfectly plastic (Mohr-Coulomb failure criteria).

The shear strength parameters were estimated using the following relation:

$$q_u = 2 \times c \times \tan\left(\frac{\pi}{4} + \frac{\phi}{2}\right)$$

where c is the cohesion (kPa) and ϕ is the angle of friction.

The values of E_{50} were calculated using the average measured stiffness to strength ratio (=1280).

	Treated silt	Transition zone	Treated sand
Depth (m)	0,5 - 2,5	2,5 – 3,5	3,5 - 5,0
Strength q_u (MPa)	3,7	7,6	11,9
Stiffness E_{50} (MPa)	1280 x q_u	1280 x q_u	1280 x q_u
Angle of friction (°)	42	42	42
Cohesion (kPa)	700	1700	2800

Table 4-8 Input parameters for numerical analyses.

Figure 4-53 shows the loading curves derived from the numerical simulations. A very good agreement is observed between calculated settlements and measurements up to a load of 300 kN (75 % of the measured failure load). The models found a load at failure between 350 and 400 kN, close to the final load measured on site.

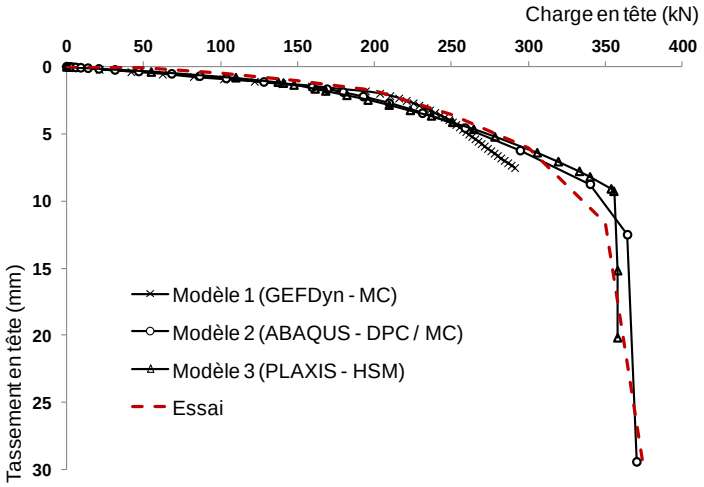

Figure 4-53 Results of numerical models to simulate the load test performed on column C2 (Cuira et al., 2013).

Furthermore, the models predict that failure of the column occurs in a cone shaped zone in the upper part of the column around a depth of 1 m (Figure 4-54). This corroborates the observations made on site during excavation of the column.

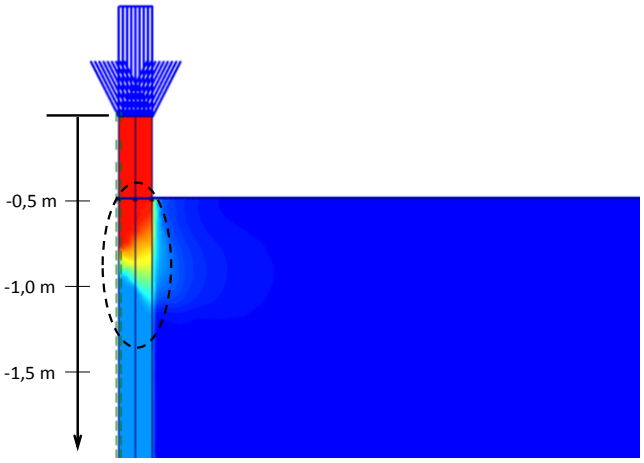

Figure 4-54 Modelled development of failure mechanism in column C2 (Cuira et al., 2013).

The results of numerical analyses show that the mechanical parameters derived from testing of the cored specimens from Vernouillet can be used to correctly model the behaviour of the soil-cement columns. Furthermore, the models found that the stiffness parameters were adapted to accurately calculate the deformation of the columns in the first stages of loading, emphasizing the use of local strain measurements for the determination of static stiffness.

4.6 Discussion – Effects of mixing conditions and sampling method

4.6.1 Comparison between field and laboratory specimens

Although the general trends for strength and stiffness are similar, the discrepancies between the results obtained on field and laboratory specimens can be explained by many factors. As previously mentioned, scatter in field data can essentially be related to the heterogeneity of the initial soil, variations in dosage and to the presence of some intact soil inclusions.

Soil inclusions were visible in the upper silty parts of the columns excavated from Vernouillet (Figure 4-55) and were present in the specimens cored from the silt blocks. The lower sandy parts of the columns were visually homogeneous with no soil inclusion in the cored specimens.

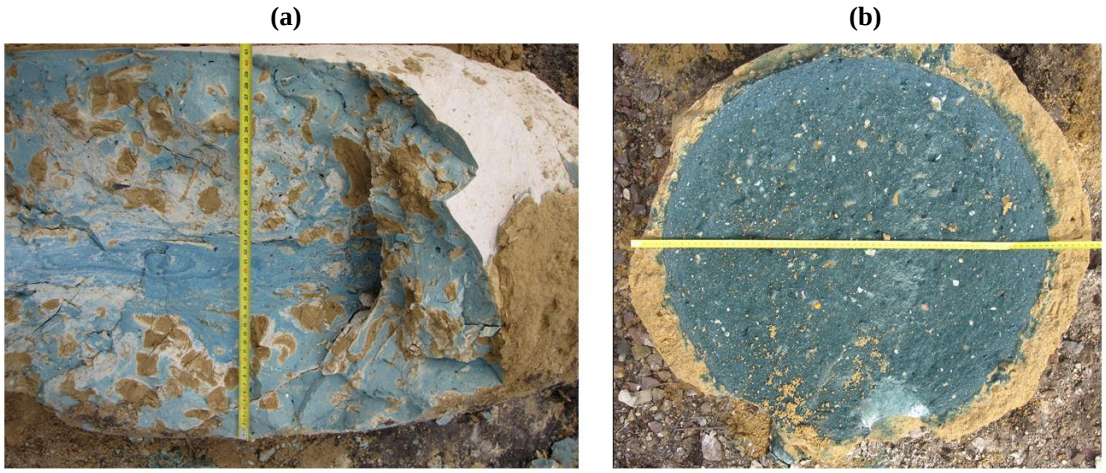

Figure 4-55 Fragments of columns from Vernouillet (a) silt; (b) sand.

Although no quantitative method was used in this study to assess the amount of inclusions present in field samples, comparisons with the results on homogeneous laboratory specimens provide information regarding the effects of inclusions on the mechanical properties of soil-mix materials.

The unconfined compressive strengths q_u of cored treated silt specimens are significantly lower than the values measured on laboratory specimens (Figure 4-16). However, the static modulus E_{50} (Figure 4-23) and dynamic modulus E_0 (Figure 4-33) values measured on field samples of treated silt are relatively close those obtained on laboratory specimens.

As the mixes of Vernouillet silt prepared in the laboratory cover a wide range of dosages (236 to 346 kg/m^3, Table A-2), it is reasonable to assume that these differences are not related to

different binder contents. Since the silt layer in Vernouillet is relatively homogeneous, the discrepancies between field and laboratory properties are most likely due to the presence of inclusions in the field samples. The results from Vernouillet provide experimental data that suggests that the adverse effect of inclusions in treated fine grained soils is more pronounced on strength than on stiffness. The effects of soil inclusions appear to be strain-dependent. From the small strain region (E_0) up to strains induced by stresses of at least half the maximum strength (E_{50}), the stress-strain response of treated soils in not significantly influenced by inclusions. For higher strains, the presence of inclusions results in a reduction of strength (q_u).

The amount of soil inclusions mainly depends on the type of soil. Denies et al. (2012b) found less than 3.5 % inclusions in treated sands, between 3 and 10 % in treated silts and up to 35 % in stabilised clays. The size and shape of inclusions is also important. In a study on the effects of soil aggregates on the stiffness of a compacted lime-treated clayey soil, Tang et al. (2011a) found that the aggregate size has an impact on stiffness. Stiffness decreases as the aggregate size increases. Aggregates in compacted treated soils are comparable to inclusions in deep-mixed soils.
Vervoort et al. (2012) conducted numerical simulations to study the effects of inclusions on the properties of treated soils. They showed that even a small percentage of intact soil inclusions can significantly alter the strength of soil-mix materials. Their results indicate that the presence of 1 % to 10 % of inclusions reduces strength by 20 % to 50 % respectively. The impact of inclusions on stiffness is less pronounced. Numerical models suggest that the presence of 1 % of inclusions decreases stiffness by only 3 %, and that 10 % of inclusions leads to an average modulus reduction of 30 %. The results of the present study are in line with the findings of Vervoort et al. (2012).

The effects of inclusions on the stress-strain response of treated fine grained soils measured in unconfined compression tests are illustrated in Figure 4-56.

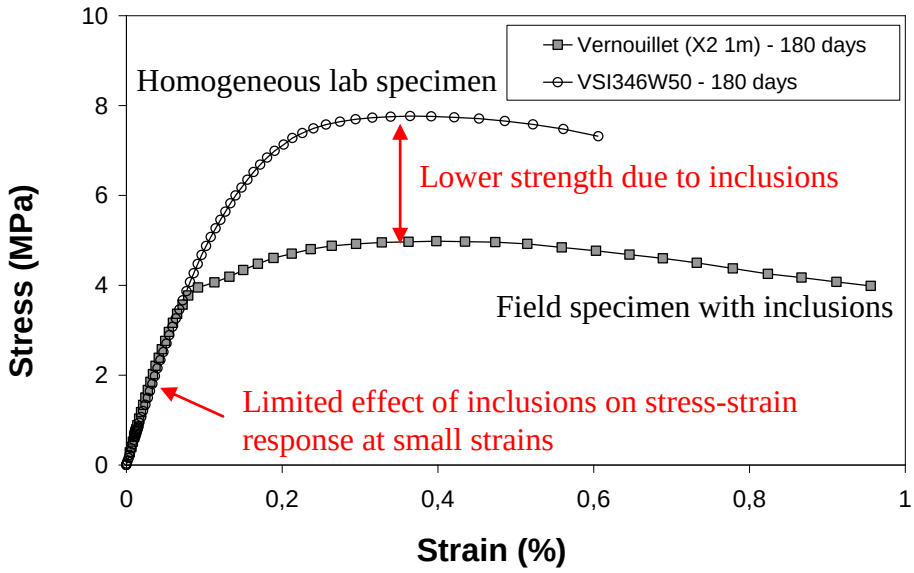

Figure 4-56 Effects of inclusions on the stress-strain relation for treated fine grained soils.

Based on these observations, it is reasonable to assume that, if the numerical analyses presented in section 4.5.3 were carried out using input data from laboratory-mixed specimens (i.e. higher strength, similar stiffness), the models would correctly follow the deformation of the column but overestimate the ultimate bearing capacity.

4.6.2 Influence of soil type and sampling method

Compiling all the data from this study (laboratory and field) and results from the literature, the static modulus, measured using local strain measurements, can be roughly estimated from unconfined compressive strength tests by multiplying strength q_u by a factor between 400 and 2000 (Figure 4-57).

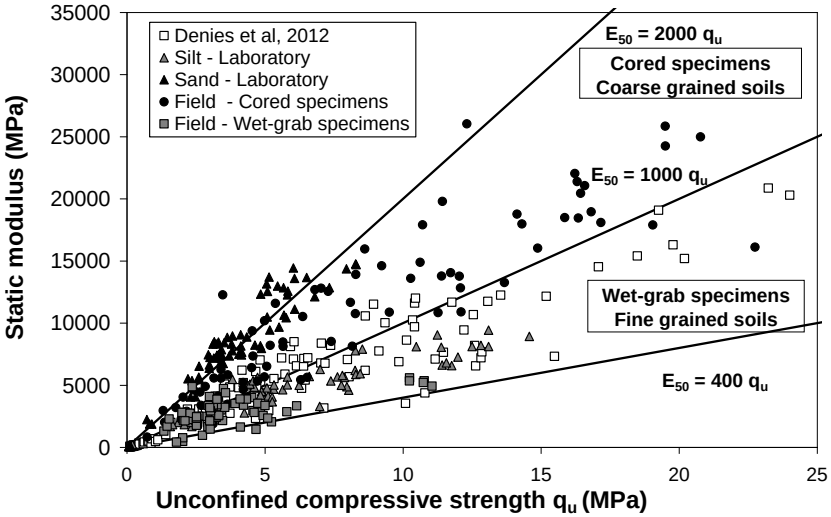

Figure 4-57 Relation between strength and static modulus (data from this study and from the literature).

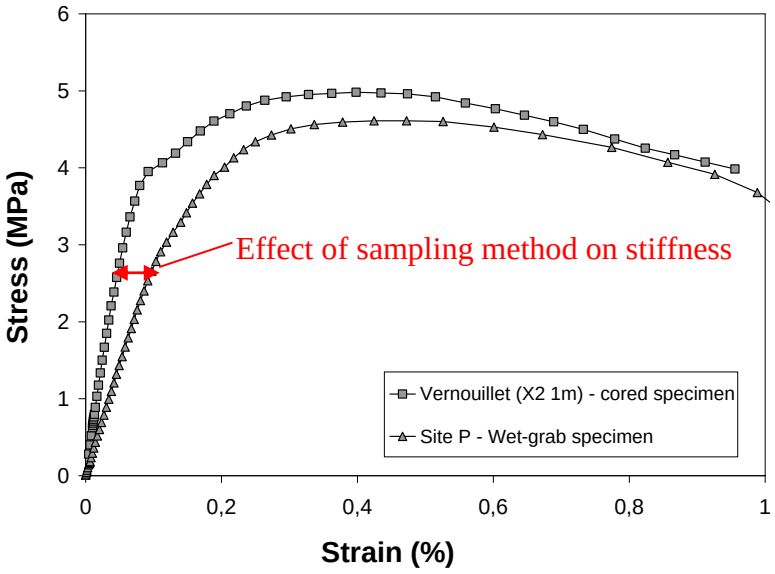

Figure 4-58 Effects of sampling on the stress-strain relation for treated fine grained soils.

Two separate zones are proposed to account for soil type and sampling method. For fine grained soils and wet-grab specimens, the factor appears to vary between 400 and 1000. The static modulus for coarse grained soils and cored specimens is higher between 1000 and 2000 times q_u. Static modulus values obtained on field specimens by Denies et al. (2012b) using local strain measurements lie within the boundaries defined by the data from this research (Figure 4-57). The difference in stiffness for a given strength between wet-grab and cored specimens is mainly attributed to porosity and fine content (spoil return to the surface is fairly liquid and mainly contains the finer fraction of soils). The effect of sampling is illustrated in Figure 4-58.

The compressive wave velocity points obtained in this study on laboratory and field specimens are gathered, with data from the literature, in Figure 4-59. The compressive wave velocities collected from the literature were measured on various types of soils treated both in the laboratory and in the field using different testing methods.
The scattered data clearly displays the non-linear relation between compression wave velocity and strength. Two separate zones are also proposed to account for soil type and sampling method. This graph shows than non-destructive compression wave velocity measurements can be used to obtain a gross estimate of the strength of soil-cement specimens. However, as the values of V_p reach a maximum for strengths around 5 - 10 MPa, compression wave velocities are not suitable to accurately estimate the strength of in situ deep mixed soils.
A graph similar to Figure 4-59 is obtained when compiling the dynamic stiffness – strength data from laboratory and field specimens.

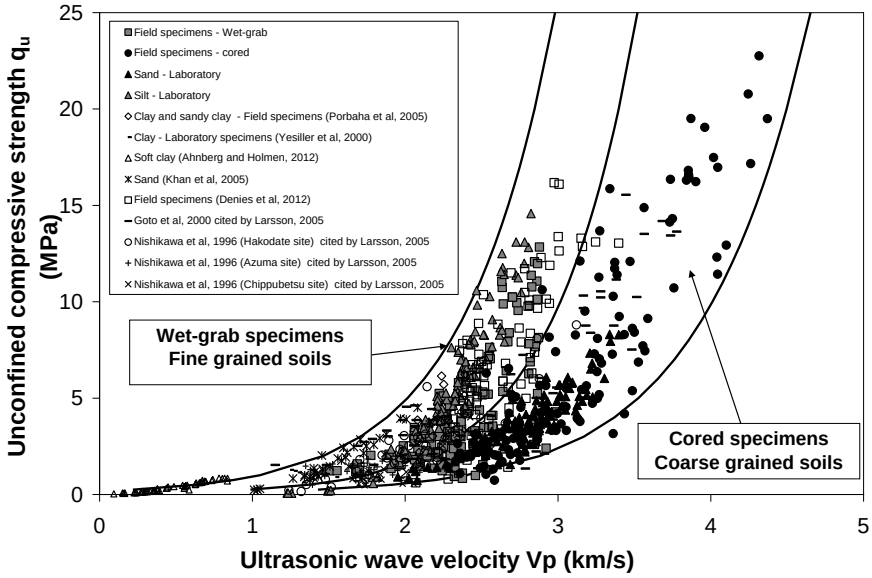

Figure 4-59 Relation between compression wave velocity V_p and strength q_u (data from this study and from the literature).

4.7 Conclusions

The results of laboratory tests carried out on specimens from four different test sites on which soil-cement columns were installed by the wet method were presented in this chapter. Wet-

grab samples were taken from all sites. Specimens were cored from block samples of eight columns excavated from one site after 28 and 180 days.

The objective was to determine the characteristics of soils stabilised in situ by wet deep mixing and to compare the results with those obtained on soils treated in the laboratory.

The following conclusions can be drawn:

For in situ soil-mix material in the fresh state:

- The density of fresh spoil is higher than the density of the injected grout. This confirms the presence of substantial amounts of soil in the spoil and hence the blending of the slurry with the soil produced by the mixing process. Density in the fresh state is close to the density of the hardened soil-cement material.
- The shear strength of fresh soil-mix material measured in situ almost immediately after mixing by vane and dynamic penetration tests is significantly lower than the strength of the untreated soil due to the destructuration performed by the mixing tool.

For hardened soil-mix material:

- Results of unconfined compressive strength tests showed an increase in strength with curing time. The exponential relation used for laboratory specimens applies to estimate the long-term increase in strength with time of soils mixed and cured in situ.
- Scatter in unconfined compressive strength data is attributed to the heterogeneity and type of initial soil, variations in binder distribution, dosage, variations in execution parameters and to the presence of some soil inclusions. It is found that the use of a lognormal distribution seems appropriate for the determination of characteristic strength values as reported in the literature.
- Mixing at high blade rotation numbers improves the destructuration of the initial soil and facilitates the blending of the soil with the binder. This results in a more homogeneous material of less variable strength. It is easier to obtain well mixed soil-cement columns in coarse grained soils than in fine grained soils.
- The relations between strength, wave velocity, static modulus and dynamic modulus for soils mixed in situ are similar to those obtained for soils mixed in the laboratory.
- The static modulus E_{50} determined using local strain measurements is in general between 400 and 2000 times the unconfined compressive strength q_u.
- Sampling method has an effect on stiffness. For the soils tested in this study, the static and dynamic stiffness of wet-grab samples taken from the surface are generally lower than the stiffness of cored specimens of equivalent strength. This is attributed to higher porosity and fine content in wet-grab specimens.
- Both compression and shear wave velocities increase non-linearly with strength. The relations between E_0, G_0 and unconfined compressive strength q_u are also non-linear.

The dynamic-to-static modulus ratio decreases with strength from 10 to a minimum close to 1.

- Measured total porosities vary between 20 and 70 %. P-wave and S-wave velocities decrease as porosity increases.
- The indirect tensile strength of field specimens increases linearly with unconfined compression strength. The q_{it}/q_u ratio (of 0.18) is similar to the ratio measured on soils mixed in the laboratory.
- Field specimens contain inclusions of intact soil due to the mixing process. Comparisons between the results on cored specimens of treated silt and the results on homogeneous laboratory specimens suggest that the adverse effect of soil inclusions is strain-dependant and more pronounced on strength than on stiffness.
- Despite the presence of soil inclusions, numerical analyses show that the mechanical parameters derived from testing of cored specimens are representative of the behaviour of the soil-mix columns.

The results from this study, combined with available data from the literature, highlight distinctive trends in terms of strength (compressive and tensile) and stiffness (static and dynamic), specific to soil-mix materials. The data could be used as an empirical database to estimate the characteristics of in situ deep mixed soils. However, relatively large scatter in the compiled data confirms that treated soils are complex materials, with variable mechanical properties that depend on multiple factors. Correlations established in certain conditions cannot be assumed to be systematically valid and must be verified.

The durability of soils stabilised with cement is an important concern for the design of permanent deep mixing structures. Similarities in the general properties suggest that results concerning the durability of soils mixed in the laboratory are transposable to soils stabilised in situ. In Chapter 5, the results of tests performed to study the effects of potential degradation mechanisms on the properties of soil-cement mixtures prepared in the laboratory are presented.

Chapter 5. Durability of stabilised soils

The presence of chemical compounds (section 5.1) and the effects of drying (section 5.2) are the two potential degradation mechanisms studied to assess the durability of cement-mixed soils.

5.1 Effects of the presence of potential deleterious chemical compounds on the long-term mechanical properties of stabilised soils

5.1.1 Introduction

In this section, the influence of 3 potential deleterious compounds (calcium sulfate, sodium chloride and diesel) on the long-term characteristics of soils stabilised with cement is studied. Specimens of silt and sand treated with different dosages of CEM I and CEM III cement were mixed with the tested compounds and placed in different curing conditions. The compositions of the mixes are given in Table A-4. The testing program is shown in Table A-5.

The effects of the tested compounds on the measured values of unconfined compressive strength q_u, ultrasonic wave velocity V_p and dynamic modulus of elasticity E_0 at different curing times are presented on a logarithmic scale to allow for a better visualisation and to facilitate comparison of results for short curing times. The results correspond to the average values measured on 3 specimens; the error bars represent the minimum and maximum values.

Microstructural investigations (scanning electron microscopy, x-ray diffraction analyses and mercury intrusion porosimetry) were carried out to interpret the influence of the tested compounds on the mechanical properties of treated soils.

5.1.2 Fontainebleau sand treated with CEM I

Calcium sulfate ($CaSO_4$) was added in two mixes of Fontainebleau sand treated with CEM I (FS-I-200W15-CaSO4-endo and FS-I-200W20-CaSO4-endo; Table A-4).

5.1.2.1 Effect on unconfined compressive strength and static modulus

For both dosages, the strengths of the specimens of Fontainebleau sand treated with CEM I containing sulfates increase between 7 and 180 days (Figure 5-1).

For all curing times, the strengths of the specimens with a moisture content of 15 % remain higher than the strengths of the specimens with a moisture content of 20 %. After 7 days, strengths of 1.3 MPa and 1.6 MPa are measured for mixes FS-I-200W20-$CaSO_4$ and FS-I-200W15-$CaSO_4$ respectively. Average strengths reach 3 MPa for FS-I-200W20-$CaSO_4$ and 3.6 MPa for FS-I-200W15-$CaSO_4$ after 180 days. However, the strengths of the mixes containing sulfates are approximately 20 to 30 % lower than the strengths of the mixes without sulfates.

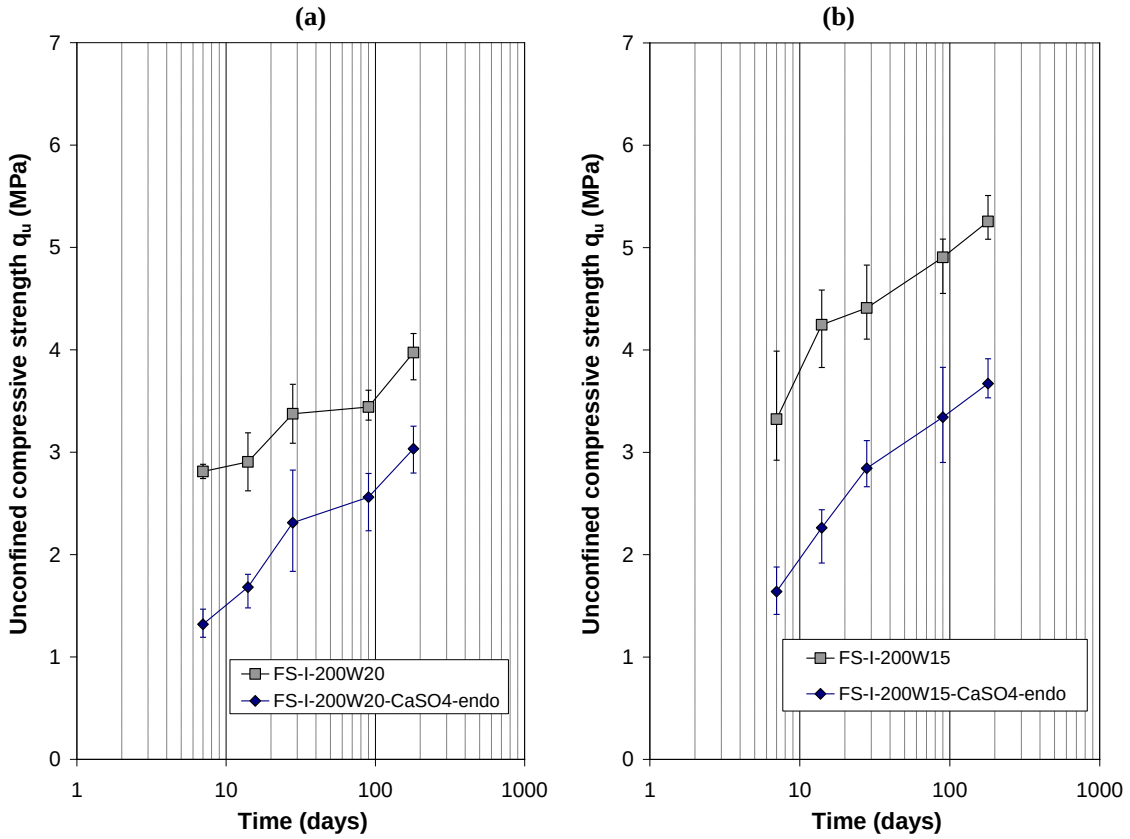

Figure 5-1 Effect of sulfates on the unconfined compressive strength of Fontainebleau sand-CEM I cement mixes (a) FS-I-200W20; (b) FS-I-200W15.

Figure 5-2 shows that lower values of strength and modulus E_{50} are measured for the specimens containing sulfates. Nevertheless, the addition of sulfates does no significantly alter the relation between E_{50} and q_u.

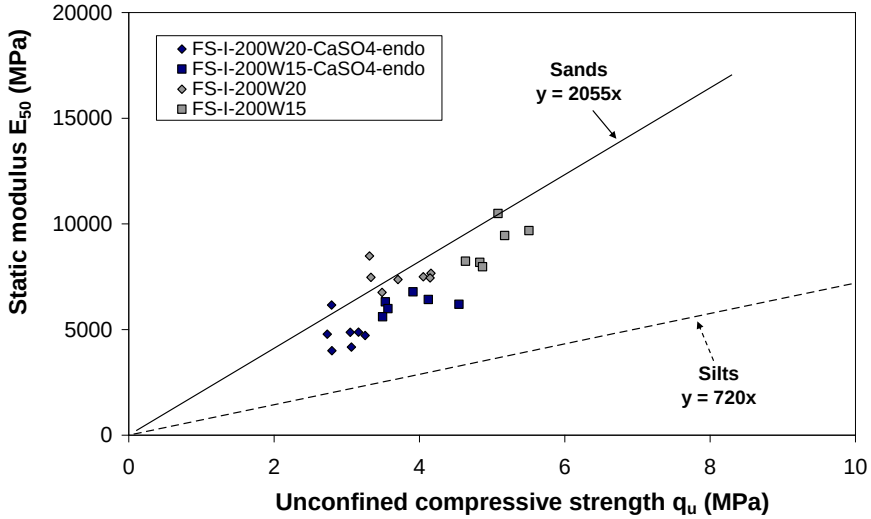

Figure 5-2 Effect of sulfates on the static modulus E_{50} of Fontainebleau sand-CEM I cement mixes.

5.1.2.2 Effect on ultrasonic wave velocity and dynamic modulus

The ultrasonic wave velocities measured for the specimens containing sulfates also increase with curing time but stay lower than the values for the specimens prepared without sulfates (Figure 5-3). Average wave velocities vary from 2230 m/s after 7 days to 2800 m/s after 180 days for specimens of FS-I-200W20-$CaSO_4$. For FS-I-200W15-$CaSO_4$, the velocities are of 2260 and 2760 m/s after 7 and 180 days.

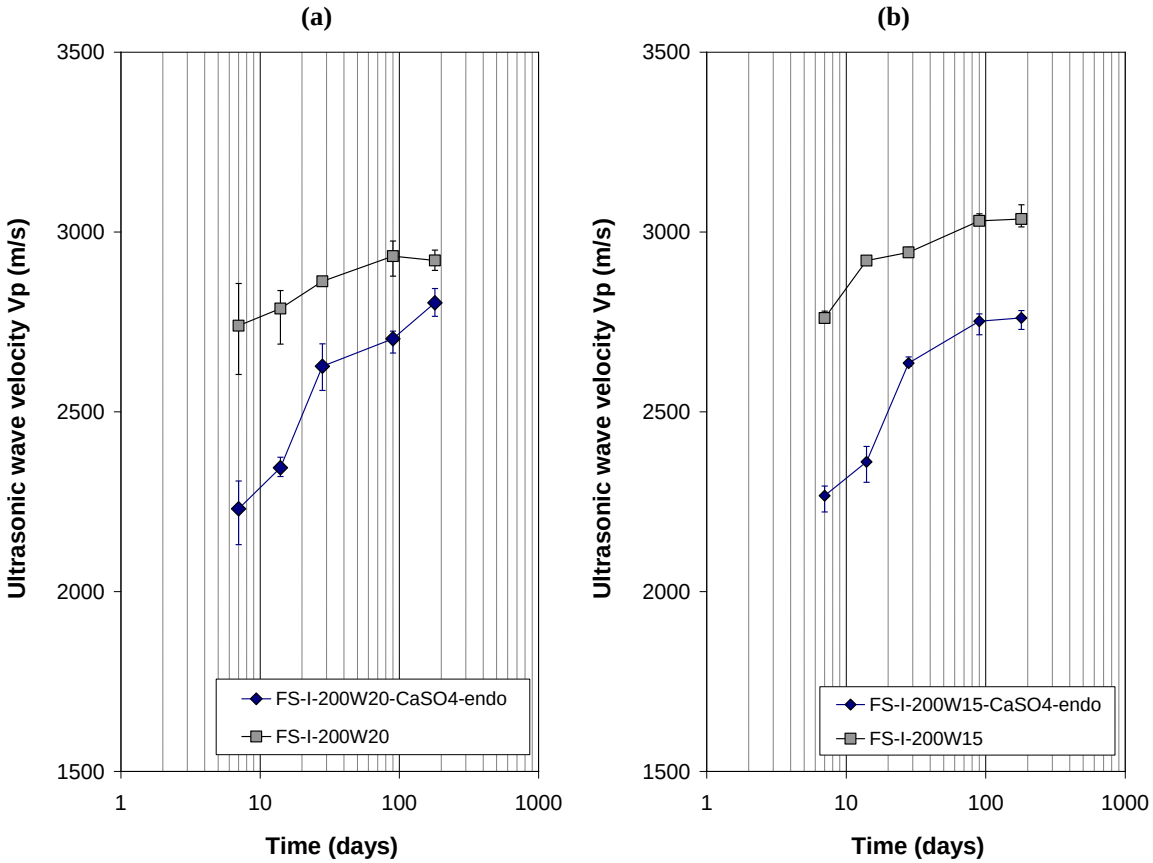

Figure 5-3 Effect of sulfates on the ultrasonic wave velocity of FS-CEM I mixes (a) FS-I-200W20; (b) FS-I-200W15.

The effect of sulfates on the dynamic modulus of specimens of Fontainebleau sand mixed with CEM I is identical to the effect on ultrasonic wave velocity as the addition of sulfates did not modify the wet density of the mixtures. E_0 increases with curing time but also remains lower than the values measured for the specimens prepared without sulfates (Figure 5-4). Average values vary from 8 GPa after 7 days to 13 GPa after 180 days for specimens of FS-I-200W20-$CaSO_4$-endo. For FS-I-200W15-$CaSO_4$-endo, the values are of 8.4 and 12.5 GPa after 7 and 180 days.

Strength and dynamic stiffness are equally affected by the presence of sulfates. Figure 5-5 shows that the relation between E_0 and q_u is unchanged by $CaSO_4$.

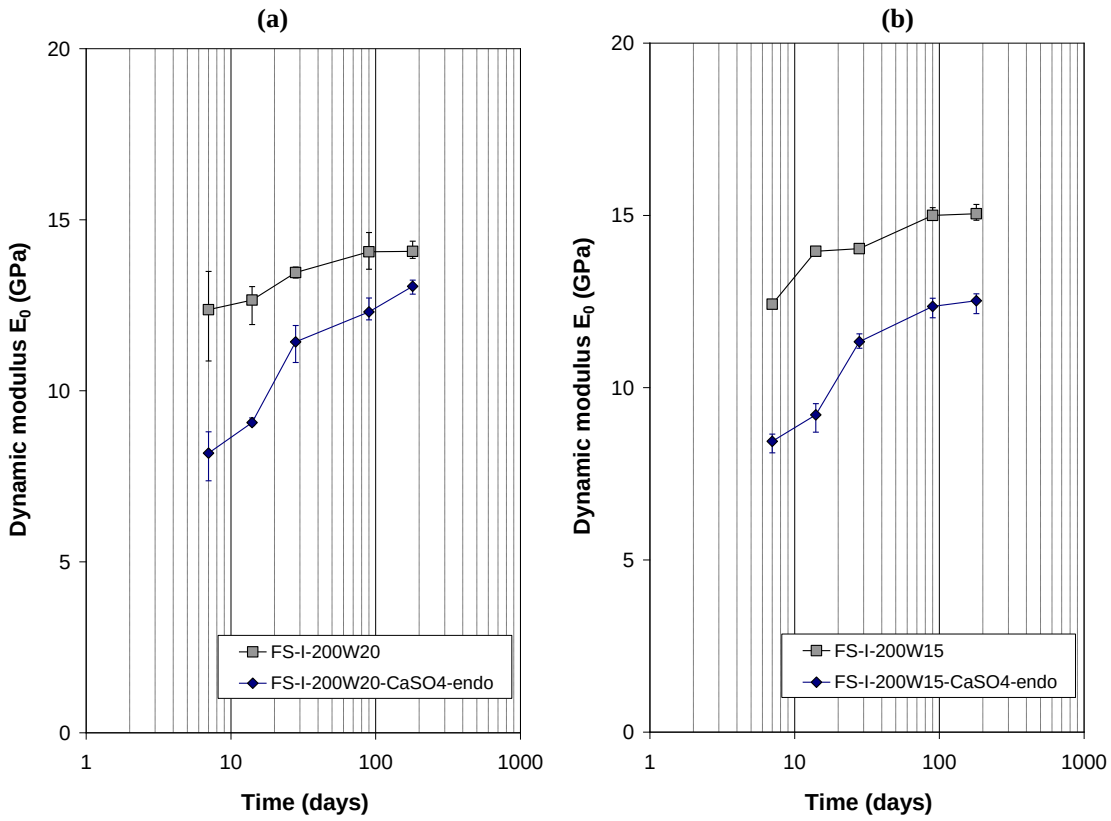

Figure 5-4 Effect of sulfates on the dynamic modulus of FS-CEM I mixes (a) FS-I-200W20; (b) FS-I-200W15.

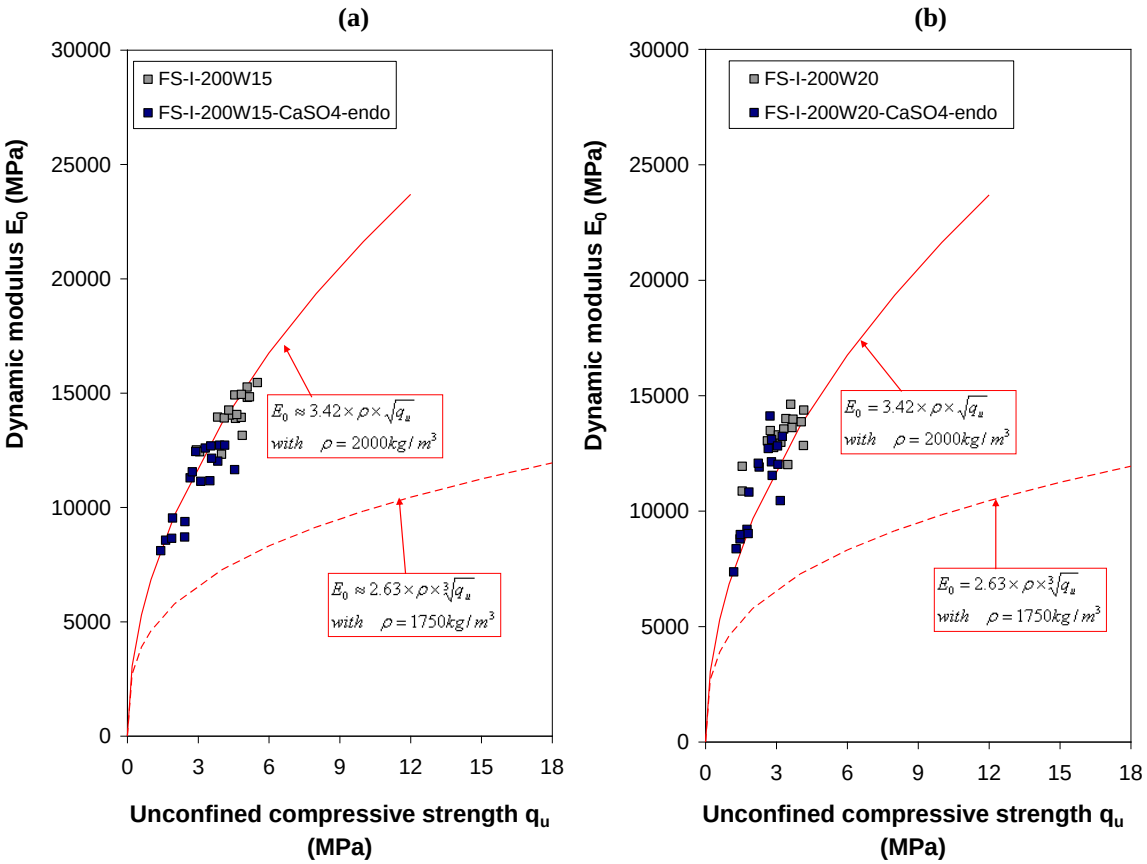

Figure 5-5 Effect of sulfates on the relation between dynamic modulus E_0 and strength q_u of Fontainebleau sand-CEM I cement mixes (a) FS-I-200W20; (b) FS-I-200W15.

5.1.2.3 Effect on indirect tensile strength

The indirect tensile strengths of the mixes containing sulfates measured after 28 and 90 days of curing are lower than strengths of the mixes without sulfates (Figure 5-6).

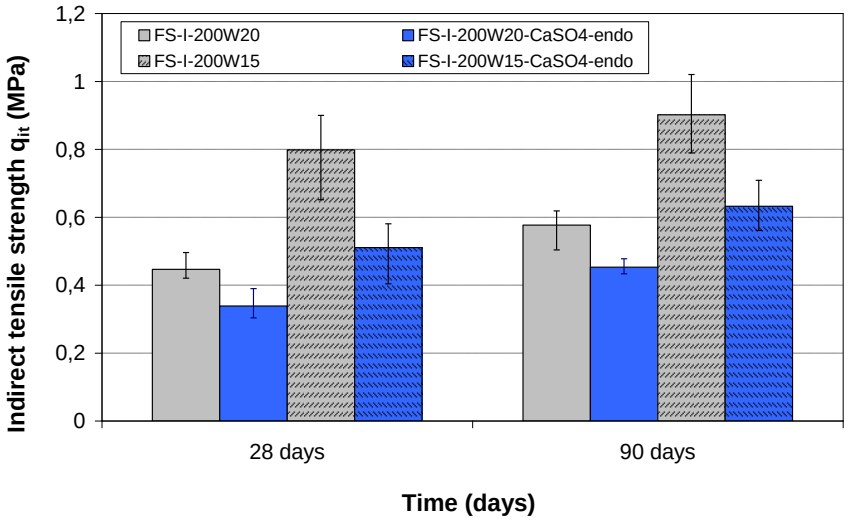

Figure 5-6 Effect of sulfates on the indirect tensile strength of Fontainebleau sand-CEM I cement mixes.

5.1.2.4 Effect on porosity

The total porosity of specimens of Fontainebleau sand treated with CEM I is not significantly changed by the presence of sulfates (Figure 5-7). In 3 out of 4 cases, the porosities of the specimens with sulfates are 1 to 2 % higher.

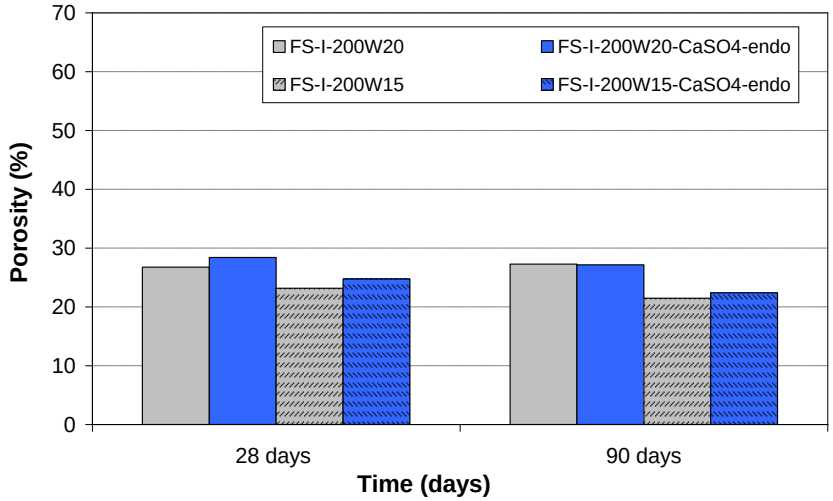

Figure 5-7 Effect of sulfates on the total porosity of Fontainebleau sand-CEM I cement mixes.

The results of MIP measurements for mixes FS-I-200W20 and FS-I-200W20-$CaSO_4$-endo are given as cumulative mercury intrusion curves in Figure 5-8 and as pore size density function curves (derivative of the cumulative mercury intrusion curves) in Figure 5-9.

It can be observed that the total volume of mercury intruded is almost identical for both tests (Figure 5-8). The derived total porosities (30.0% for FS-I-200W20 and 30.2% FS-I-200W20-

$CaSO_4$-endo) are slightly higher than the porosities determined by hydrostatic weighing (Figure 5-7).

The majority of pores have entrance diameters between 0.5 and 2 µm (Figure 5-9). The mix containing $CaSO_4$ has somewhat less small pores between 0.02 and 2 µm and a higher amount of large pores between 2 and 10 µm.

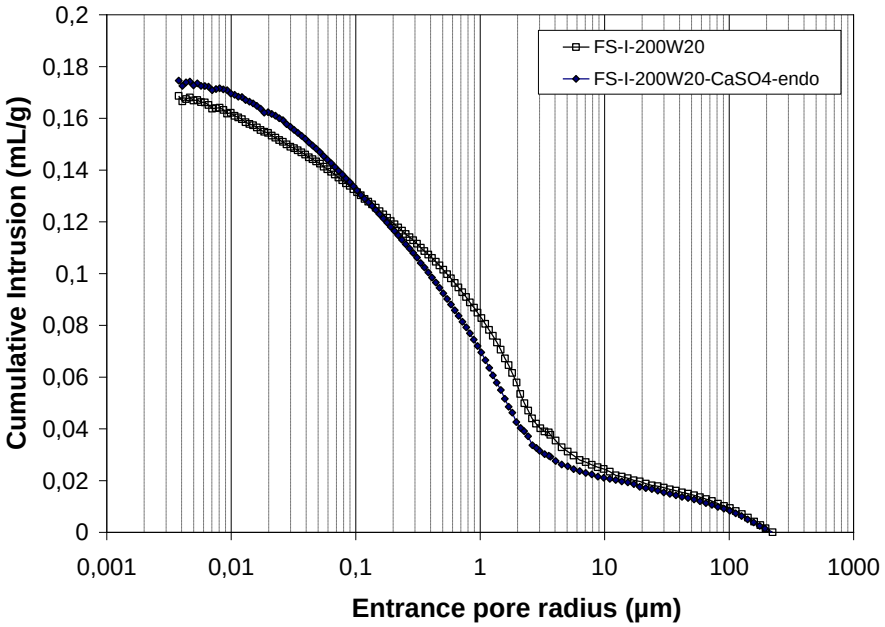

Figure 5-8 Effect of $CaSO_4$ on the microstructure of Fontainebleau sand treated with CEM I (Cumulative intrusion curves).

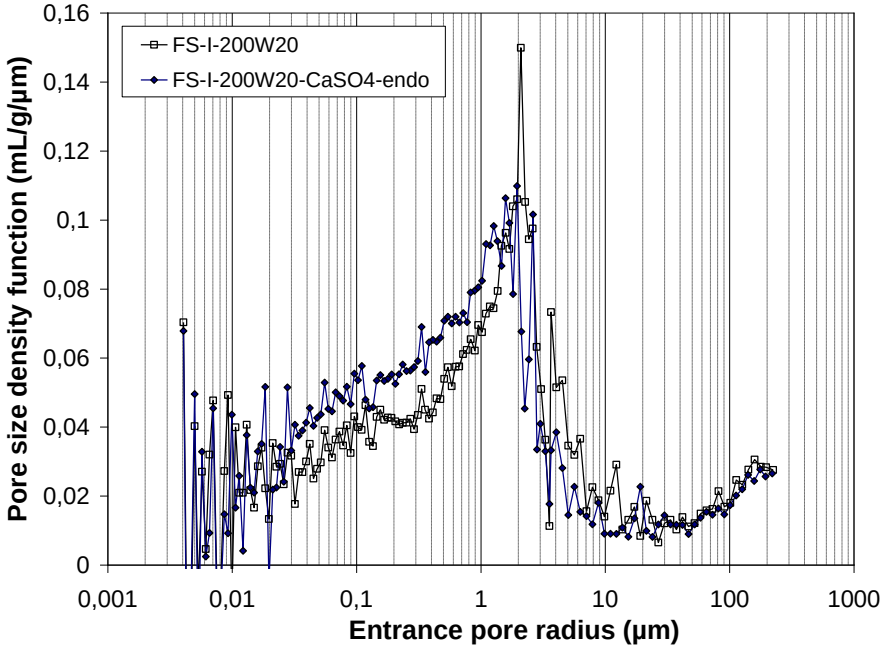

Figure 5-9 Effect of $CaSO_4$ on the microstructure of Fontainebleau sand treated with CEM I (pore size density function).

5.1.2.5 Scanning electron microscopy

Figure 5-10, Figure 5-11 and Figure 5-12 present scanning electron microscopy images of treated Fontainebleau sand using different magnifications between 100 and 10000. The cementation and coating of the quartz grains are visible in Figure 5-10 and Figure 5-11.

(a) **(b)**

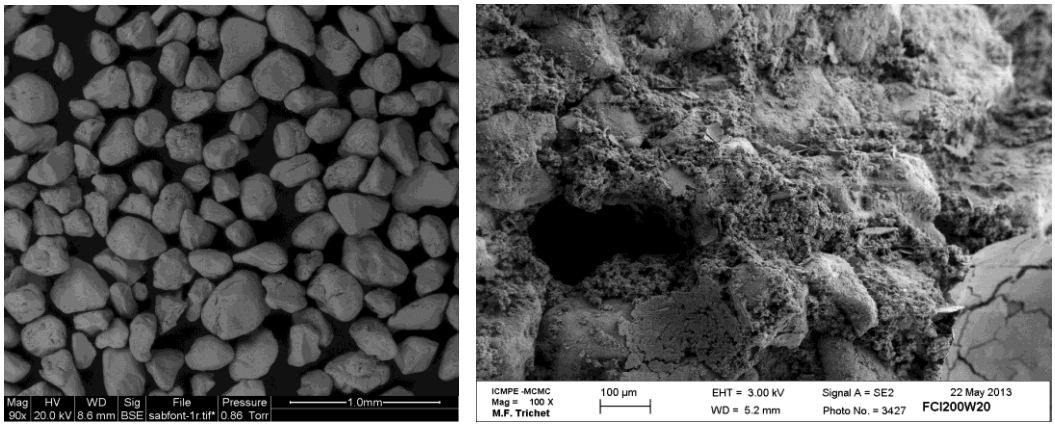

Figure 5-10 Scanning electron microscopy images. (a) Fontainebleau sand (90x) (b) Fontainebleau sand treated with CEM I after 360 days (100x).

(a) **(b)**

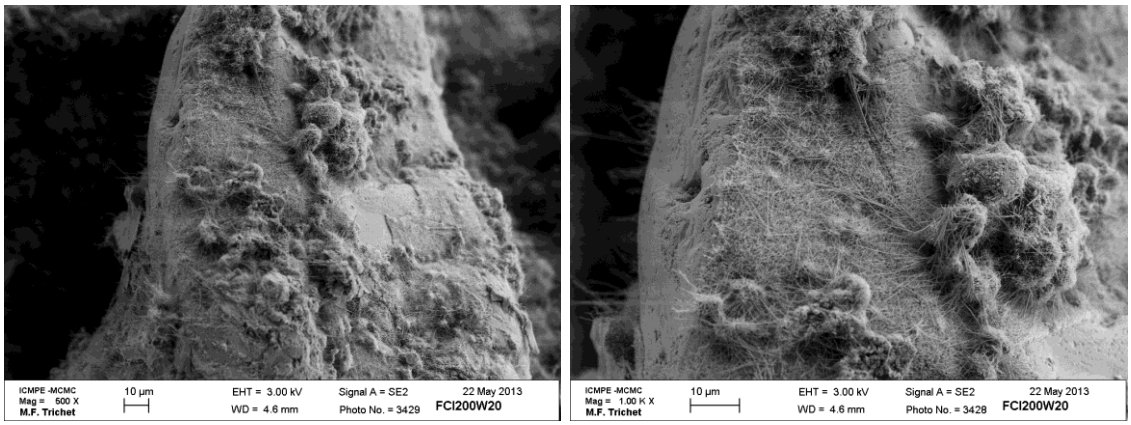

Figure 5-11 Scanning electron microscopy images. Coating of Fontainebleau sand grain with CEM I (a) 500x; (b) 1000x.

The images in Figure 5-12 show an abundance of flaky fibrous calcium silicate hydrates (C-S-H) in the cement paste. C-S-H crystals appear to be larger and far more developed in the specimen without sulfates which can explain the higher strength. This difference in microstructure can also explain the differences in pore size distributions observed in the results of MIP measurements. The specimens with sulfates have a larger amount of "smaller" pores between relatively small C-S-H crystals compared to the specimens without sulfates.
The specimens also contain some portlandite (calcium hydroxide C-H, Figure 5-12 (d)). In the specimen from mix FS-I-200W20-$CaSO_4$-endo, fibrous ettringite crystals were visible (Figure 5-13).

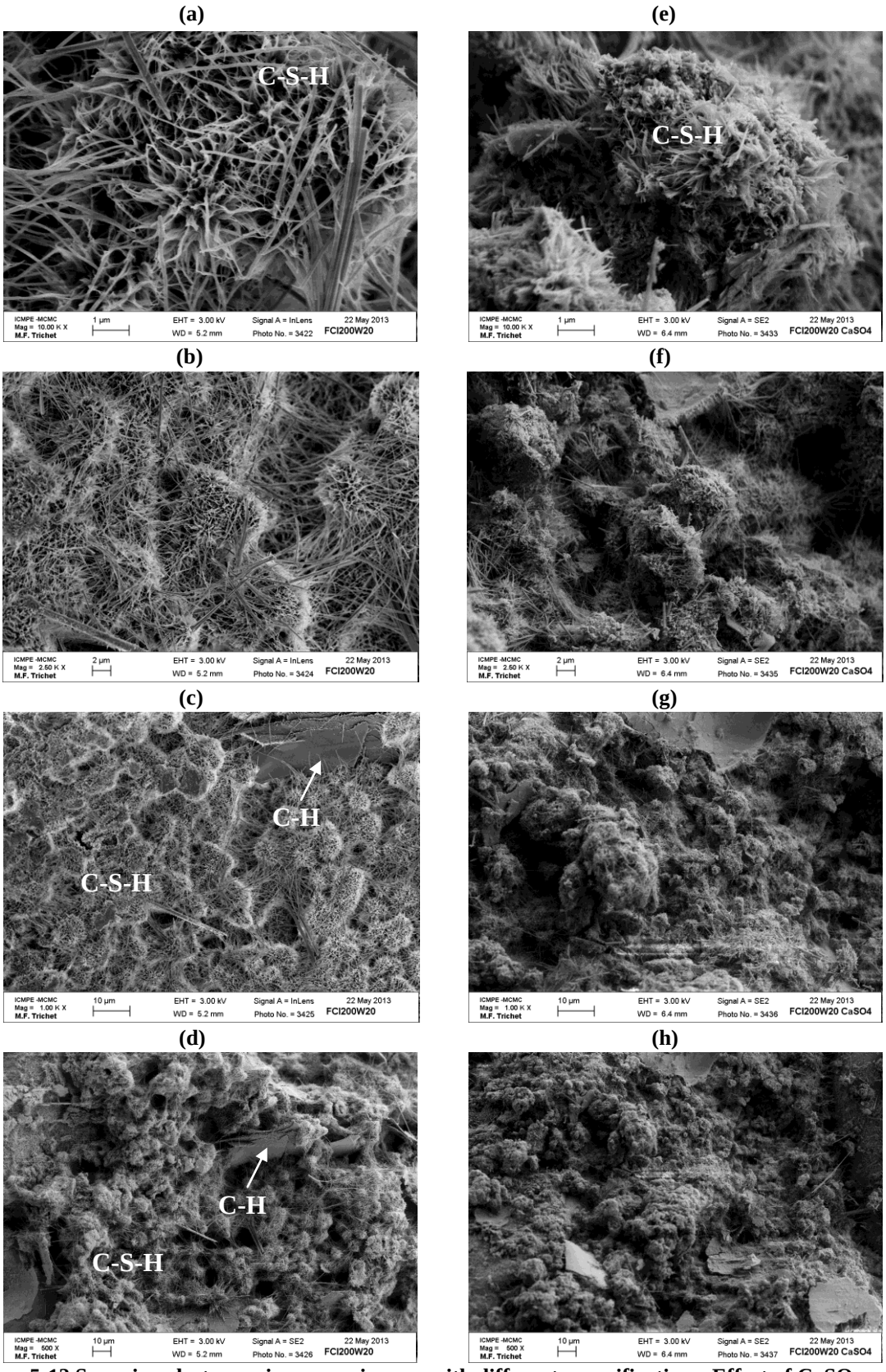

Figure 5-12 Scanning electron microscopy images with different magnifications. Effect of $CaSO_4$ on the microstructure of Fontainebleau sand treated with CEM I after 360 days. (a), (b), (c), (d): FS-I-200W20; (e), (f), (g), (h): FS-I-200W20-CaSO4 endo.

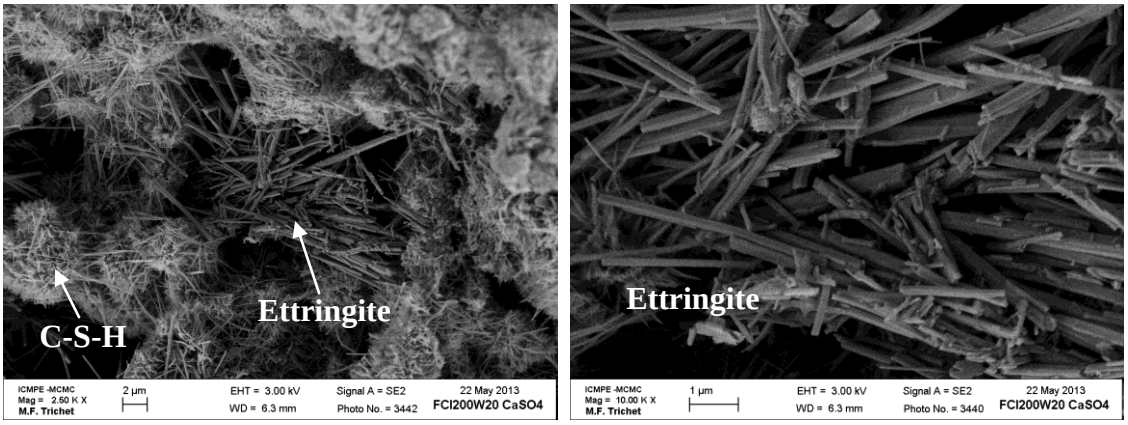

Figure 5-13 Scanning electron microscopy images. Presence of ettringite in specimens of mix FS-I-200W20-CaSO4 endo.

5.1.2.6 Conclusions

The well-known adverse effects of $CaSO_4$ on the properties of soils treated with Portland cement are confirmed. The results show that sulfates affect equally strength, static modulus and dynamic modulus as the relations between these parameters remain altogether unchanged. The indirect tensile strength also decreases but the total porosity is not significantly influenced by sulfates. These observations are correlated to microstructural differences identified by mercury porosity measurements and scanning electron microscopy.

5.1.3 Fontainebleau sand treated with CEM III

Calcium sulphate $CaSO_4$, sodium chloride NaCl and diesel oil were added in mixes of Fontainebleau sand treated with CEMIII (FS200W35B50, Table A-4).

5.1.3.1 Effects on unconfined compressive strength and static modulus

The average unconfined compression strengths of specimens of Fontainebleau sand mixed with CEM III cement and containing the equivalent of 50 kg/m^3 of bentonite (FS200W35B50) are compared to the strengths measured on specimens of the same mix containing calcium sulphate $CaSO_4$ (FS200W35B50-$CaSO_4$-endo), sodium chloride NaCl (FS200W35B50-NaCl-endo) and diesel oil (FS200W35B50-diesel-endo) in Figure 5-14. The specimens were cured in endogenous conditions.

The figure shows that the addition of NaCl and $CaSO_4$ has a detrimental effect on the strength of the tested Fontainebleau sand mix. Between 7 and 360 days, the average strengths of the specimens of the reference mix are between 1.20 and 1.60 times higher than the strength of specimens containing $CaSO_4$. For the specimens in which NaCl was added, the ratio is close to 1.40 for all curing times. It is interesting to note that the addition of NaCl and $CaSO_4$ have similar effects on strength.

The strength of the specimens containing diesel is slightly more variable but remains close to the averages strengths measured for the reference mix (Figure 5-14).

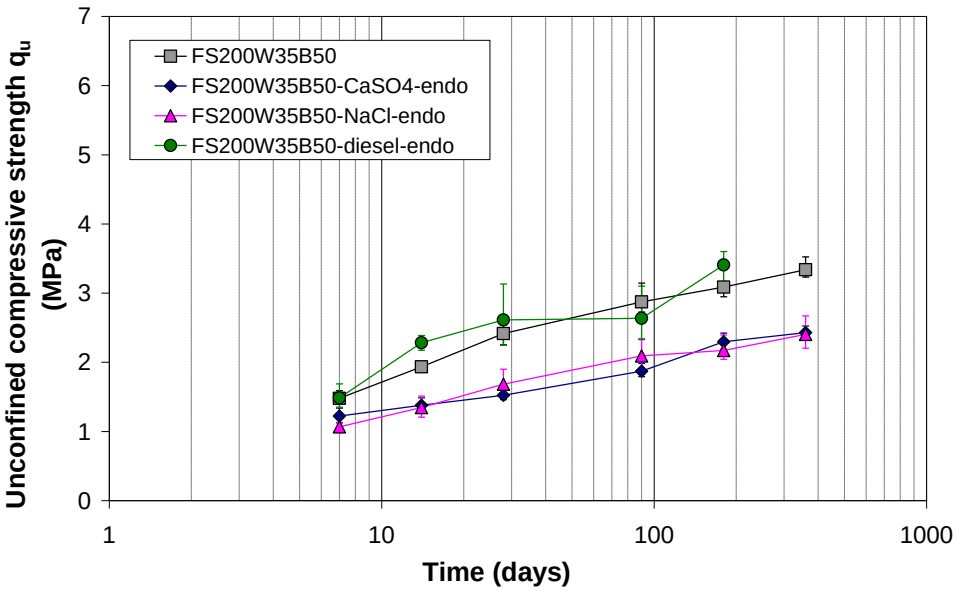

Figure 5-14 Effect of $CaSO_4$, NaCl and diesel on the strength of Fontainebleau sand-CEM III cement mixes.

Immersion in water has a relatively small influence on average strength (Figure 5-15) as the ratios of soaked to un-soaked strengths vary between 0.92 to 0.97 for the mixes without sulfates (FS200W35B50 and FS200W35B50-Imm) and between 0.89 and 0.91 for the mixes in which sulfates were added (FS200W35B50-$CaSO_4$-endo and FS200W35B50-$CaSO_4$-Imm). The decrease in strength due to immersion can be attributed to the well-known dissolution of cement hydration products in water. In this case, the impact on strength is limited as the water was not changed during curing and was rapidly saturated. Different results may have be obtained if the specimens were exposed to continuous "fresh" water circulation (Le Runigo et al., 2011).

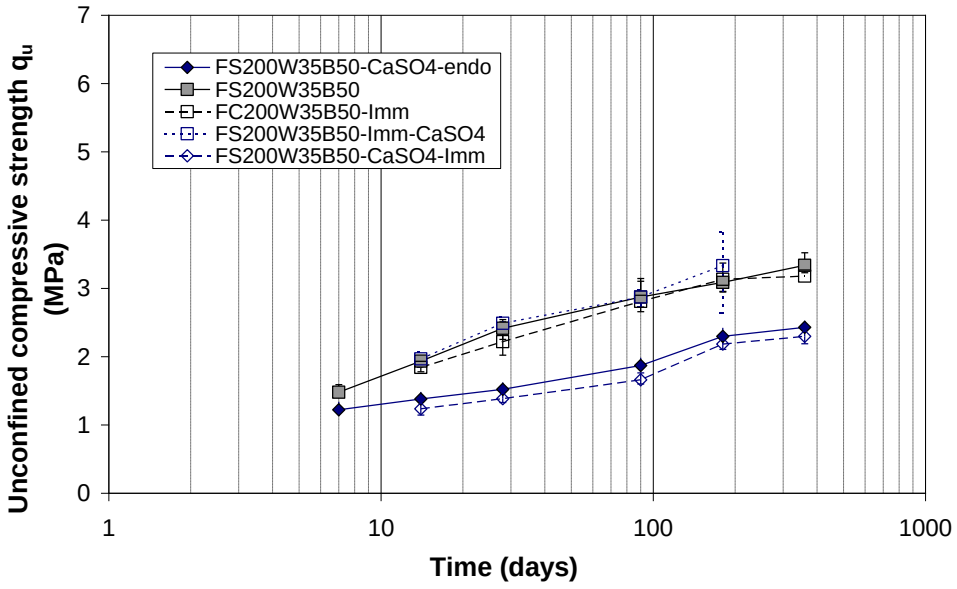

Figure 5-15 Effect of $CaSO_4$ on the strength of immersed specimens of Fontainebleau sand-CEM III mixes.

The predominant effect of the addition of sulfates before mixing is confirmed by the results obtained for the specimens prepared without $CaSO_4$ but stored in tap water in which 1g/L of $CaSO_4$ was dissolved (FS200W35B50-Imm-CaSO4). The strengths of the specimens of this mix are very close to the strengths of the specimens of the reference mix (Figure 5-15).

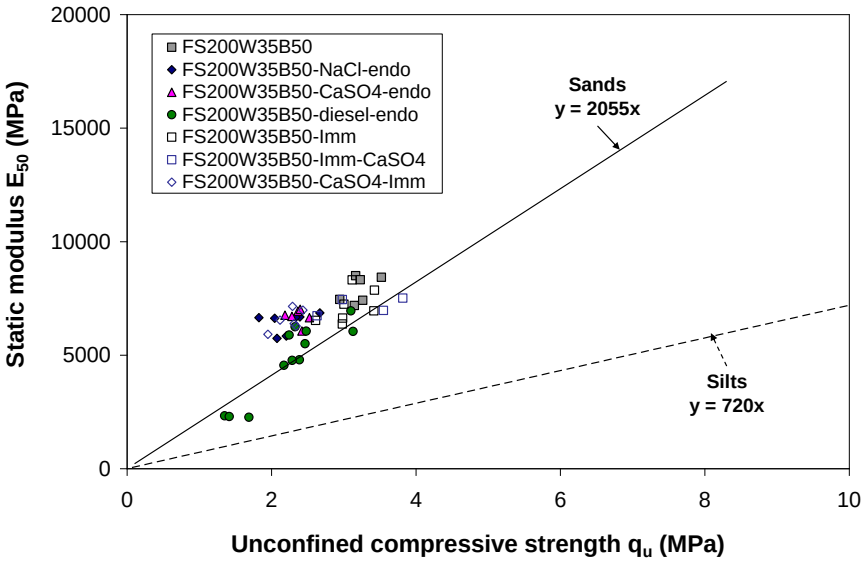

Figure 5-16 Effect of $CaSO_4$, NaCl and diesel on the relation between strength and static modulus of Fontainebleau sand-CEM III cement mixes.

The relation between strength and static modulus E_{50} is not drastically changed by $CaSO_4$, NaCl or diesel as all specimens from FS-CEM III mixes fall close to the trend line established for sands (Figure 5-16).

5.1.3.2 Effects on ultrasonic wave velocity and dynamic modulus

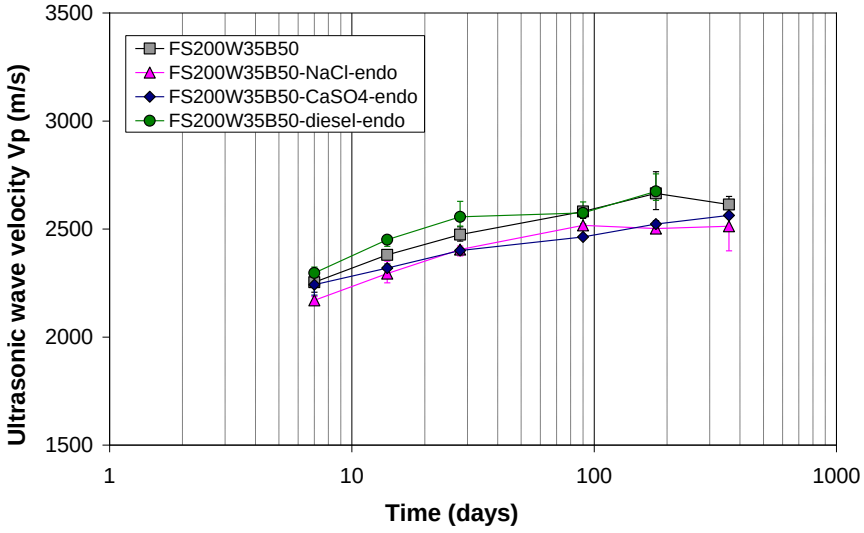

Figure 5-17 Effect of $CaSO_4$, NaCl and diesel on the ultrasonic wave velocity of Fontainebleau sand-CEM III cement mixes.

$CaSO_4$ and NaCl also tend to lower the ultrasonic wave velocities of treated sand specimens although the effects seem to be less pronounced than for unconfined compressive strength (Figure 5-17). Diesel does not significantly affect the ultrasonic wave velocity as the measured values are very close to the reference mix after 90 and 180 days.

The effects on the dynamic modulus are the same as for V_p (Figure 5-18). All tested compounds did not modify the relation between E_0 and q_u (Figure 5-19).

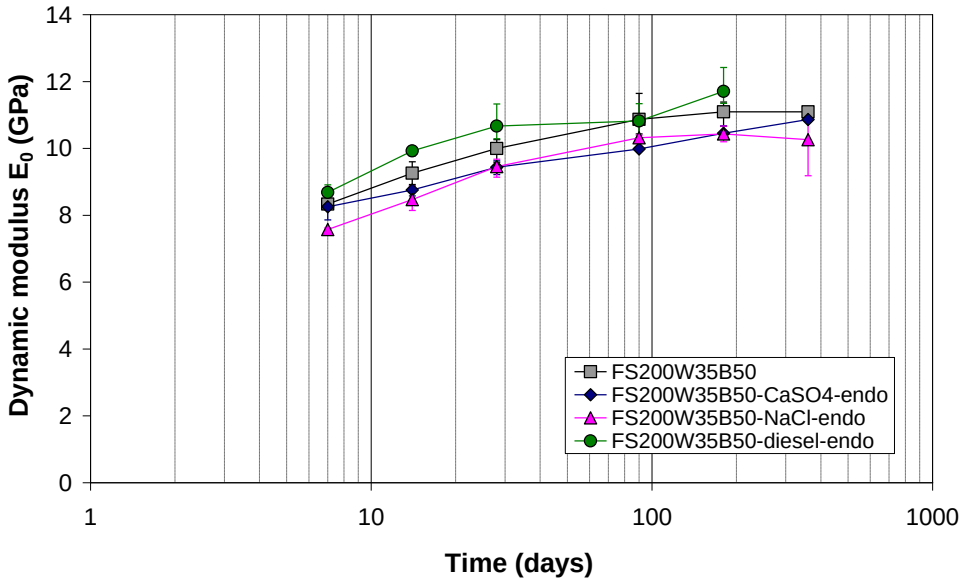

Figure 5-18 Effect of $CaSO_4$, NaCl and diesel on the dynamic modulus of elasticity of Fontainebleau sand-CEM III cement mixes.

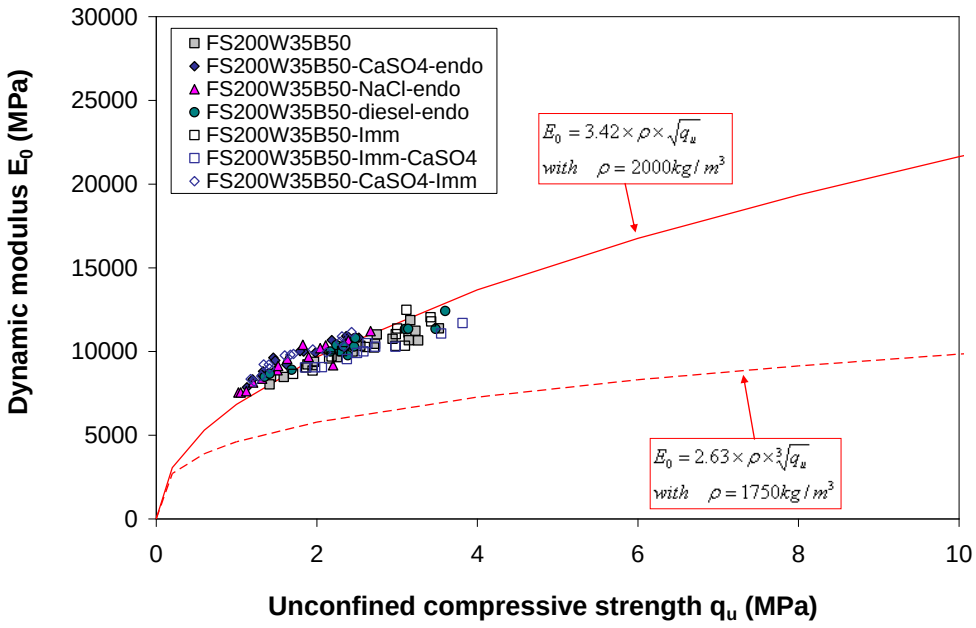

Figure 5-19 Effect of $CaSO_4$, NaCl and diesel on the relation between dynamic modulus and strength for Fontainebleau sand – CEM III cement mixes.

5.1.3.3 Effects on indirect tensile strength

Average indirect tensile strengths of 630 kPa and 510 kPa were measured after 28 days on specimens of the reference mixes FS200W35B50 and FS200W35B50-Imm respectively (Figure 5-20). Lower tensile strengths of approximately 420 kPa were measured on the specimens in which $CaSO_4$ (FS200W35B50-$CaSO_4$-endo and FS200W35B50-$CaSO_4$-Imm) and NaCl (FS200W35B50-NaCl-endo) was added before mixing.

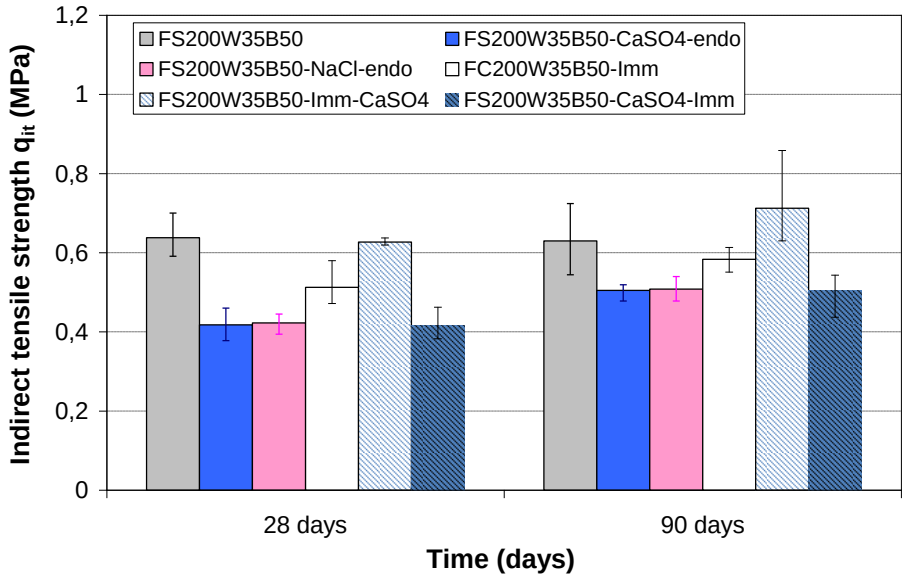

Figure 5-20 Effect of $CaSO_4$ and NaCl on the indirect tensile strength of Fontainebleau sand-CEM III cement mixes.

After 90 days, the tensile strengths of these mixes remained lower than the reference mixes with values close to 505 kPa. The specimens prepared without sulfates but immersed in water containing 1g/L of $CaSO_4$ gave the highest average strength after 90 days.

5.1.3.4 Volumetric swelling

Volumetric swelling measurements were performed following a procedure similar to standard NF P94-100 (AFNOR, 1999a). Volumetric swelling was measured on specimens of the three mixes cured in immersed conditions. The volumes of the specimens were evaluated by hydrostatic weighing. The initial volume of the specimens was determined after 6 days of curing as sufficient time was required for the sand-cement specimens to harden in order to be easily manipulated. The volumetric swelling was calculated as the ratio between the initial volume 6 days after mixing and the volume after a certain curing time up to 90 days.

The results show that in general no swelling of the specimens in contact with sulfates was measured (Figure 5-21). An increase in volume of 1 % was measured on one specimen of mix FS200W35B50-Imm-CaSO4 between 6 and 7 days but no further variation in volume was observed up to 90 days. As sulfate attack in stabilised soils is usually accompanied by significant swelling, these results suggest that the lower strengths measured for the specimens containing sulfates are not caused by the formation of ettringite.

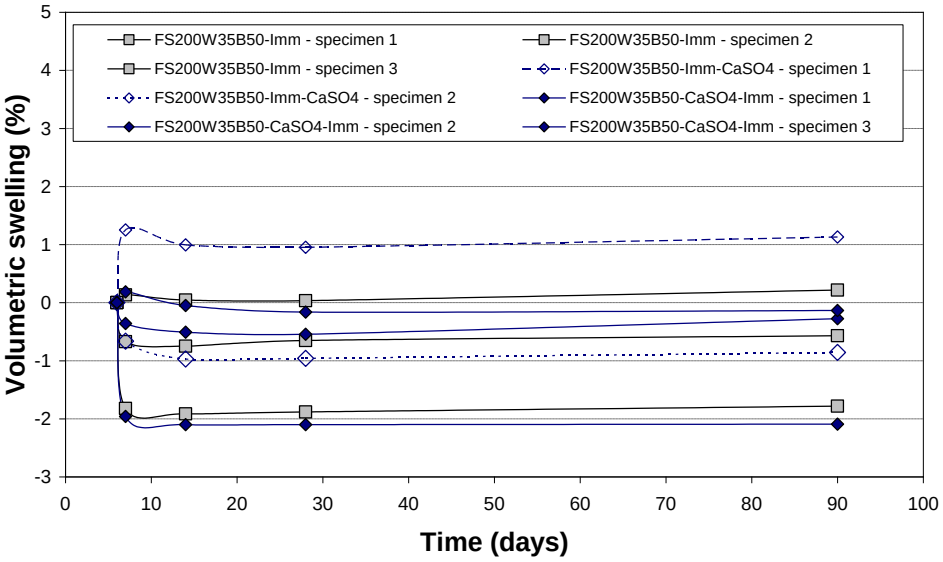

Figure 5-21 Volumetric swelling of Fontainebleau sand-CEM III cement mixes.

5.1.3.5 X-ray diffraction

Figure E-1 (Appendix E) shows the effect of $CaSO_4$ and NaCl on the X-ray diffraction pattern of the Fontainebleau sand-CEM III cement mix FS200W35B50. The three patterns are almost identical with no new peaks for the mixes containing sulfates and chlorides. This indicates that ettringite (for sulfates) or Friedel's salts (for chlorides) were not formed as expected due to the composition of the CEM III cement (resistant to sulfates and chlorides). The differences in strength between FS200W35B50, FS200W35B50-$CaSO_4$-endo and FS200W35B50-NaCl-endo are not due to the crystallisation of new minerals.

5.1.3.6 Effects on porosity and permeability

Results presented in Figure 5-22 show that the total porosity of Fontainebleau sand-CEM III cement mixes does not significantly vary with curing time between 28 and 90 days and is not influenced by the presence of NaCl and $CaSO_4$. Porosity mainly depends on the initial moisture content (Figure 3-12).

The results of MIP measurements are presented as cumulative mercury intrusion curves in Figure 5-23 and as pore size density function curves (derivative of the cumulative mercury intrusion curves) in Figure 5-24.

It can be observed that the total volume of mercury intruded is very close for the three tests (Figure 5-23). Total porosities of 38.7 %, 39.7 % and 38.4 % were derived from the intruded volumes of mercury for FS200W35B50, FS200W35B50-NaCl-endo and FS200W35B50-$CaSO_4$-endo respectively. These total porosities are slightly lower than the porosities determined by hydrostatic weighing after saturation (Figure 5-22). The differences suggest that the porosity was not totally measured by MIP tests. The range of pressure used only allowed the identification of pores with entrance radii varying between 0.004 μm and 220 μm.

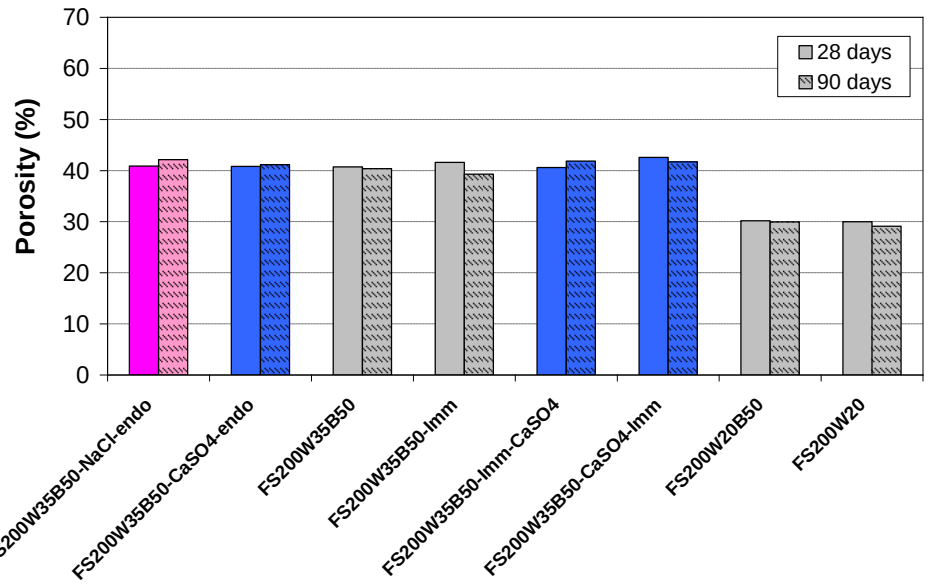

Figure 5-22 Effect of $CaSO_4$ and NaCl on the total porosity of Fontainebleau sand-CEM III cement mixes.

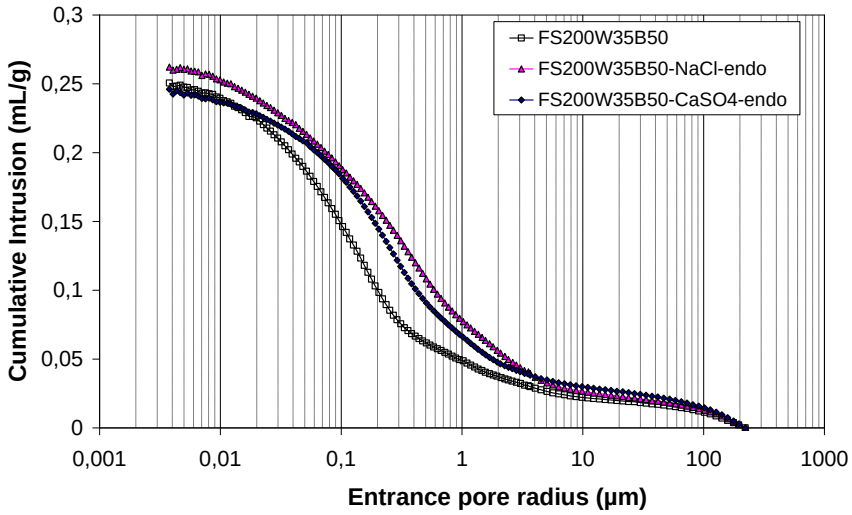

Figure 5-23 Effect of $CaSO_4$ and NaCl on the microstructure of Fontainebleau sand-cement mixes (cumulative intrusion curves).

The majority of pores for FS200W35B50 have an entrance radius around 0.1 - 0.2 µm (Figure 5-24). The main families of pores for the mixes with $CaSO_4$ and NaCl have larger entrance radii centred on 0.2 - 0.3 µm for FS200W35B50-$CaSO_4$-endo and on 0.3 - 0.6 µm for FS200W35B50-NaCl-endo (Figure 5-24). More generally, the mixes containing $CaSO_4$ and NaCl have less small pores between 0.02 and 0.2 µm and a higher amount of large pores between 0.2 and 5 µm.

The presence of these large pores between 0.2 and 5 µm could be responsible for the lower compressive and tensile strengths of the specimens with NaCl and $CaSO_4$ (Figure 5-14 and Figure 5-20).

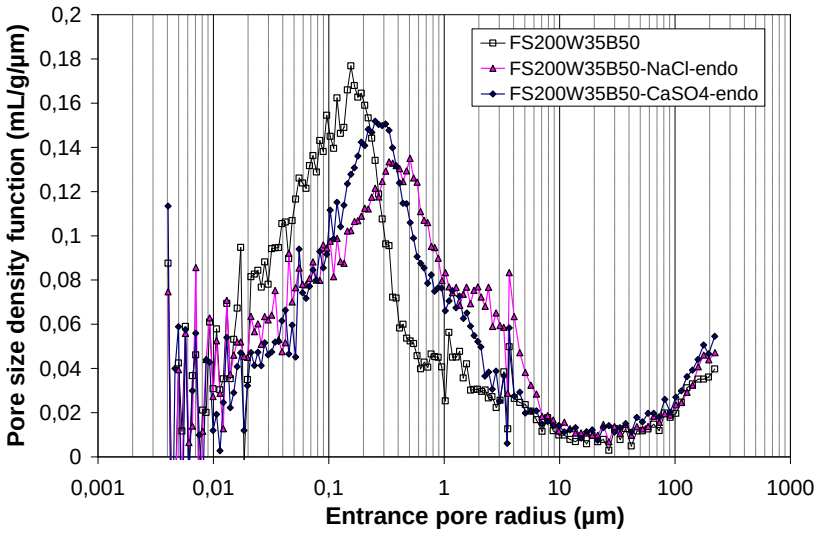

Figure 5-24 Effect of $CaSO_4$ and NaCl on the microstructure of Fontainebleau sand-cement mixes (pore size density function).

As swelling measurements and X-ray diffraction analyses suggest that NaCl and $CaSO_4$ did not react with the blastfurnace cement, the existence of these large pores could be caused by the interaction of NaCl and $CaSO_4$ with the bentonite present in the mixtures.

It is well known that electrolytic solutions cause flocculation of bentonite particles. Many studies have show that sodium chloride (Mishra et al., 2009) and gypsum (Yilmaz and Civelekoglu, 2009) tend to decrease the liquid limit and plasticity index of bentonite. Settling time of clay suspensions significantly increases as the electrolyte concentration increases (Hsi and Clifton, 1962). The aggregate size of clays flocculated in distilled water with various electrolyte concentrations was studied by Stawinski et al. (1990). For bentonite, they found that the mean radius of the aggregates decrease with an increase of Na^+ and Ca^{2+} concentration, reaching a minimum; and further increases in concentration led to an increase of the mean radius.

Given the high initial water content (w = 35 %; C/W = 0.30), the addition of bentonite is essential for the stability of the FS200W35B50 mixture. In addition, bentonite was found to have a positive effect on the compressive strength of Fontainebleau sand treated with CEM III (mix FS200W20B50, Figure 3-18).

It is hypothesised that the electrolyte solutions created aggregates or clusters of flocculated bentonite-cement which modified the microstructure, cancelling the positive effect on strength and creating larger pores.

Although the dissolved calcium ions Ca^{2+} from the cement in the pore water probably have a flocculating effect on the bentonite during mixing, the pouring of the electrolyte directly on the bentonite before mechanical mixing is started as described in the specimen preparation procedure (section 2.4.2.2) probably significantly increased the flocculating effect. The specimen preparation process may largely be responsible for the differences in strength.

Smaller pores may be formed within the flocculated bentonite aggregates however, as MIP measurements only quantify “connected porosity”, these pores may exist but not be detected by this method.

As for total porosity, the permeability of FS-CEM III mixes does not drastically change with curing time between 28 and 90 days. The permeabilities of the mixes with an initial moisture content of 35 % are slightly higher but in the same range as the permeabilities of the specimens with an initial moisture content of 20 %. Although the number of tests is insufficient to draw definitive conclusions, the results presented in Table 5-1 suggest that the permeability of FS-CEM III mixes is not drastically modified by the presence of $CaSO_4$.

Mix	Permeability (m/s)	
	28 days	90 days
FS200W20	4.5×10^{-10}	0.52×10^{-10}
FS200W35B50-Imm	/	4.7×10^{-9}
FS200W35B50-Imm-CaSO4	/	1.4×10^{-8}
FS200W35B50-CaSO4-Imm	/	4.7×10^{-9}

Table 5-1 Permeability of Fontainebleau sand-cement mixes.

5.1.3.7 Scanning electron microscopy

The scanning electron microscopy images in Figure 5-25 show the cementation of the Fontainebleau sand grains. For the most part, the sand grains are surrounded by cement paste although some direct contacts between grains can be seen.

In Figure 5-26, a clear difference in the microstructure of the cement paste between the different mixes can be seen. The paste in FS200W35B50 (Figure 5-26 (a) and (b)) shows a relatively dense structure with little obvious porosity, whereas the other samples show more porous structures with large aggregates/clusters (Figure 5-26 (c) to (f)).

These observations are consistent with the results from MIP measurements given above and support the hypothesis of flocculation caused by the addition of electrolyte solutions. Indeed, the size of the pores (of the order of 1 to 2 µm), particularly noticeable here in the images of the sample of mix FS200W35B50-$CaSO_4$-endo (Figure 5-26 (c) and (d)) is in agreement with the results given in Figure 5-24.

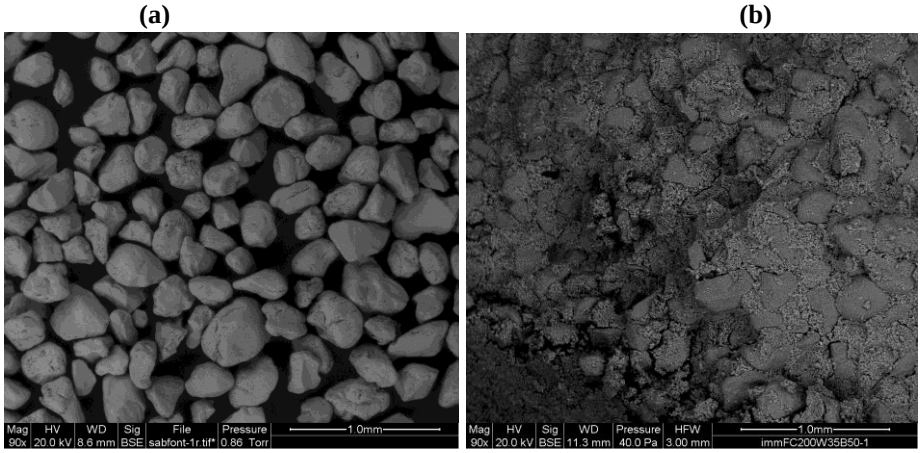

Figure 5-25 Scanning electron microscopy images. (a) Fontainebleau sand (90x) (b) Fontainebleau sand treated with CEM III after 90 days FS200W35B50 (90x).

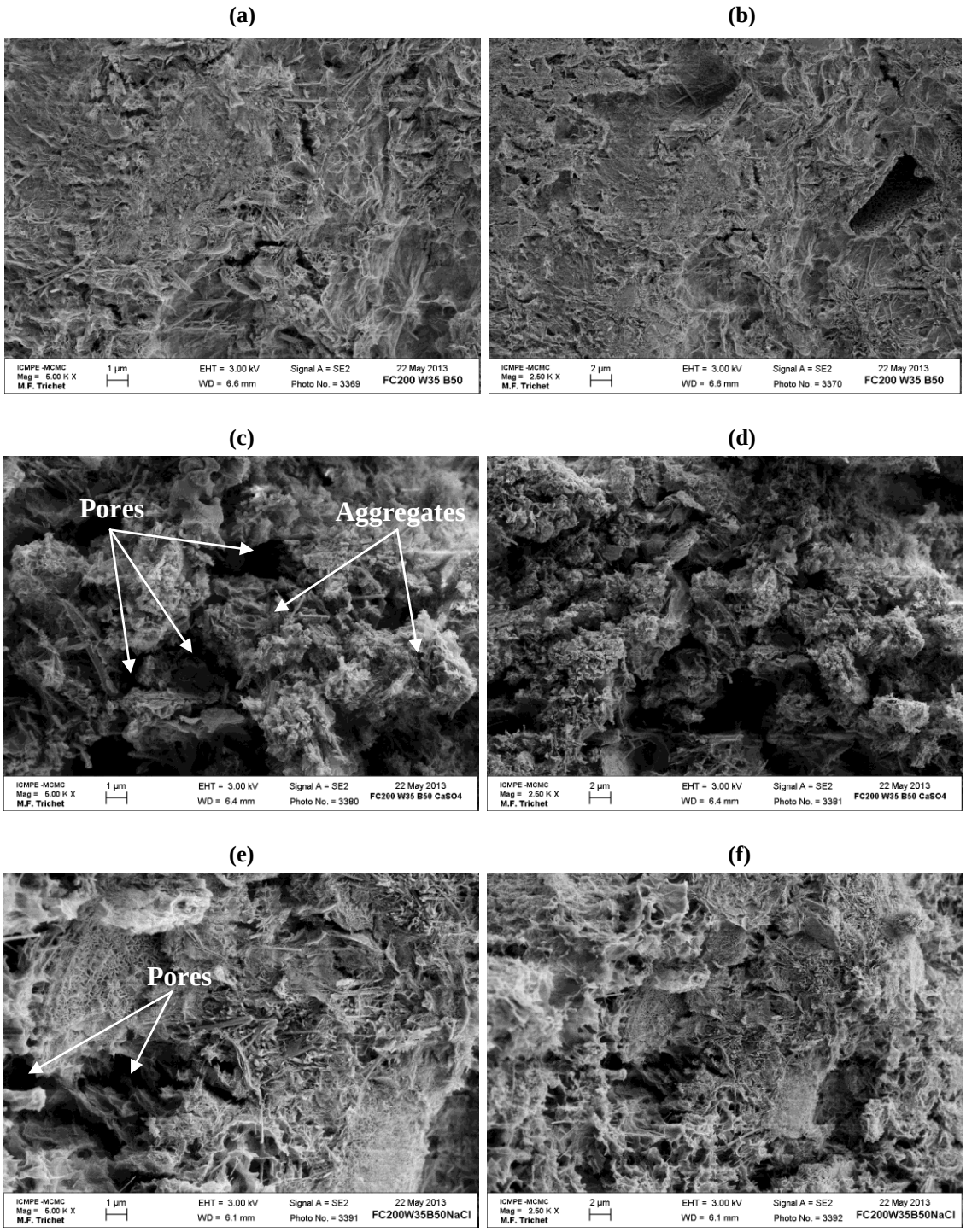

Figure 5-26 Scanning electron microscopy images (5000x and 2500x). Effect of $CaSO_4$ and NaCl on the microstructure of the cement paste in Fontainebleau sand treated with CEM III after 360 days. (a), (b): FS200W35B50; (c), (d): FS200W35B50-CaSO4 endo; (e), (f): FS200W35B50-NaCl endo.

5.1.4 Artificial silt treated with CEM III

Calcium sulfate $CaSO_4$, sodium chloride NaCl and diesel oil were added in two mixes of artificial silt treated with CEMIII (Table A-4).

5.1.4.1 Effects on unconfined compressive strength and static modulus

The unconfined compressive strength of specimens of treated artificial silt containing $CaSO_4$, NaCl and diesel appear to be more variable than for Fontainebleau sand (Figure 5-27).

The strengths of the specimens of all mixes cured in endogenous conditions increase with curing time. The strengths of the mixes with $CaSO_4$, NaCl and diesel oscillate around the values obtained for the reference mixes (AS200W40 and AS300W57) and no clear improving or deteriorating effect of the tested compounds can be clearly identified (Figure 5-27).

The lowest strengths were measured on the specimens placed in a climatic chamber at a temperature of 20 °C and a relative humidity of 65 % after 28 days (AS200W40-ac and AS300W57-ac). After 90 days, the strengths of the air-cured specimens are lower than the initial 28-day strength. Strength further decreases between 90 and 180 days.

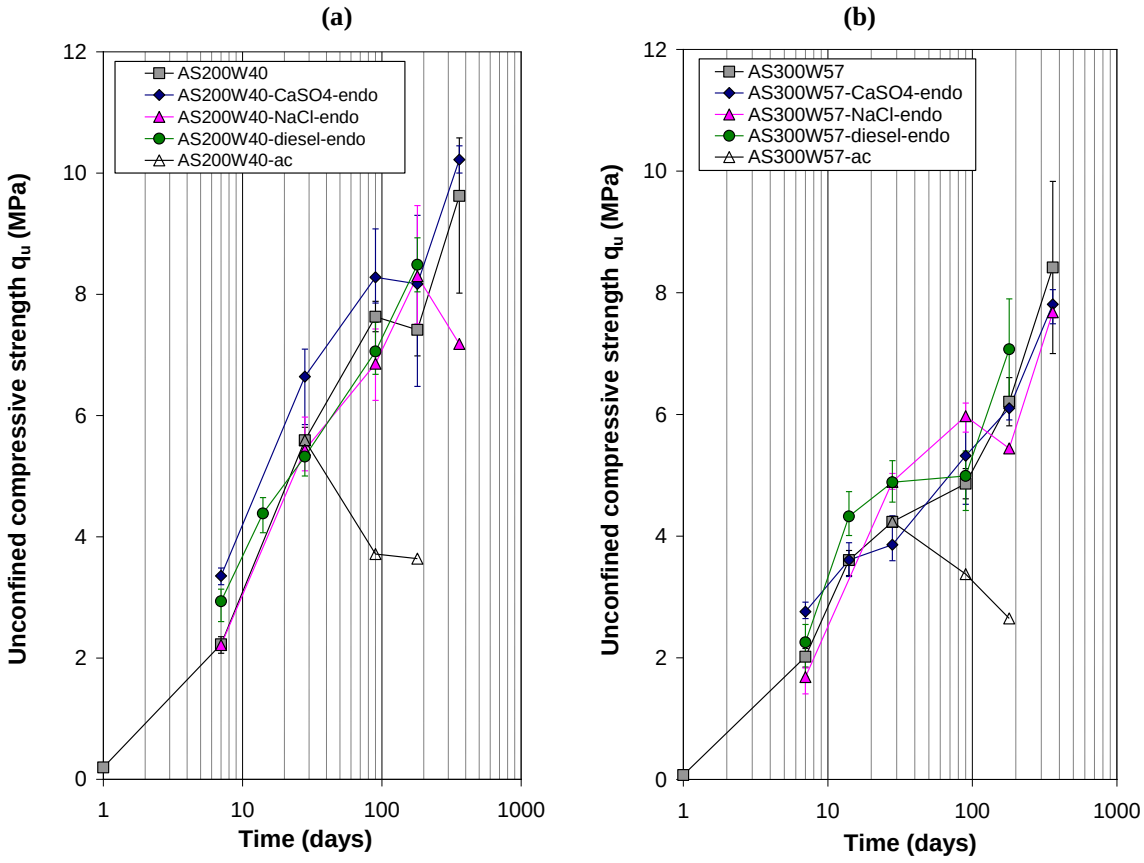

Figure 5-27 Effect of $CaSO_4$, NaCl, diesel and air-curing on the unconfined compressive strength of specimens of artificial silt stabilised with CEM III (a) AS200W40; (b) AS300W57.

$CaSO_4$, NaCl or diesel did not modify the relation between strength and static modulus E_{50}. The E_{50}/q_u ratios of all specimens are close to ratios of the reference mixes. The data for the treated artificial silt all plot slightly above the trend line determined for silts (Figure 5-28).

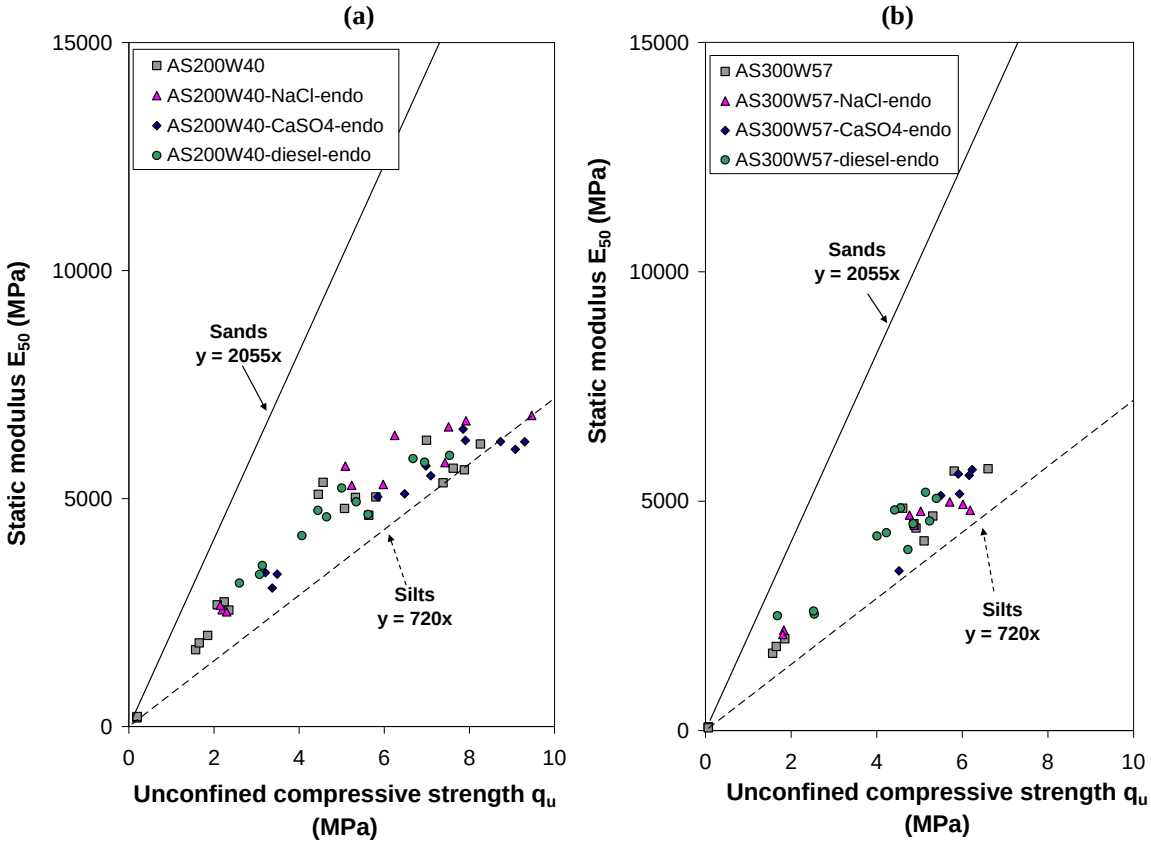

Figure 5-28 Effect of $CaSO_4$, NaCl and diesel on the static modulus E_{50} of specimens of artificial silt stabilised with CEM III (a) AS200W40; (b) AS300W57.

5.1.4.2 Effects on ultrasonic wave velocity and dynamic modulus

Between 7 and 360 days, the ultrasonic wave velocities of the specimens of treated artificial silt increase despite the presence $CaSO_4$, NaCl or diesel (Figure 5-29).

Although the position of measured wave velocities relative to the velocities of the reference mixes varies with curing time, the general trends for the mixes containing $CaSO_4$, NaCl and diesel are close. Velocities after 360 days are in the same range around 2500-2600 m/s for mixes of AS200W40 and 2400-2500 m/s for mixes of AS300W57.

The effects $CaSO_4$, NaCl and diesel on the dynamic modulus are similar to the effects on V_p (Figure 5-30) as no variation in wet density was measured. The dynamic modulus E_0 of the mixes with $CaSO_4$, NaCl and diesel increases between 7 and 360 days. Figure 5-31 shows that the correlation between E_0 and q_u for silts remains valid for all mixes (Figure 5-31).

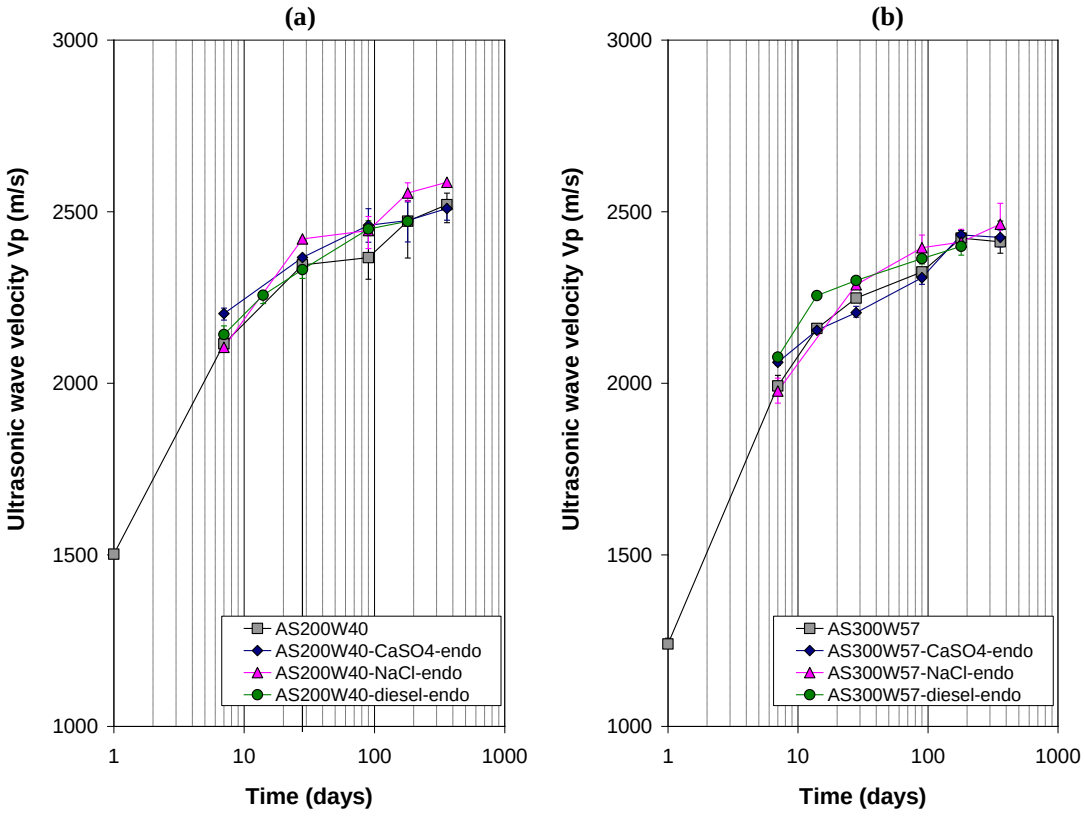

Figure 5-29 Effects of $CaSO_4$, NaCl and diesel on the ultrasonic wave velocity V_p of specimens of artificial silt stabilised with CEM III (a) AS200W40; (b) AS300W57.

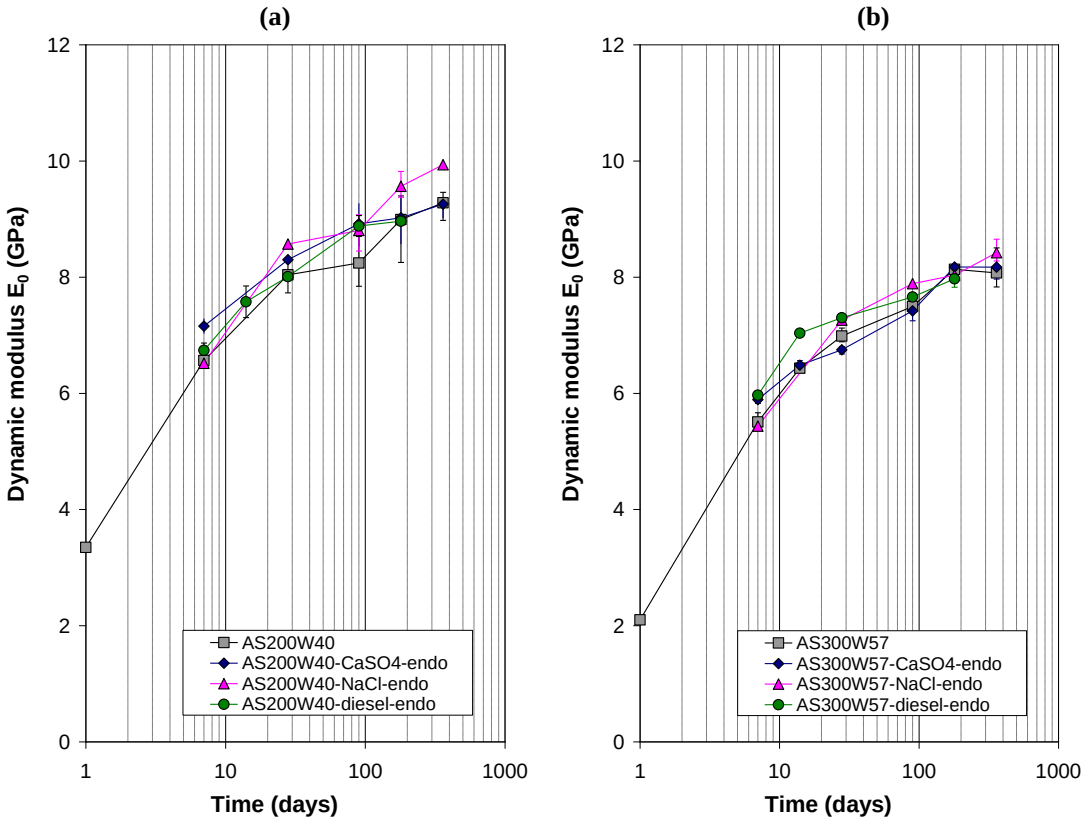

Figure 5-30 Effect of $CaSO_4$, NaCl and diesel on the dynamic modulus E_0 of specimens of artificial silt stabilised with CEM III (a) AS200W40; (b) AS300W57.

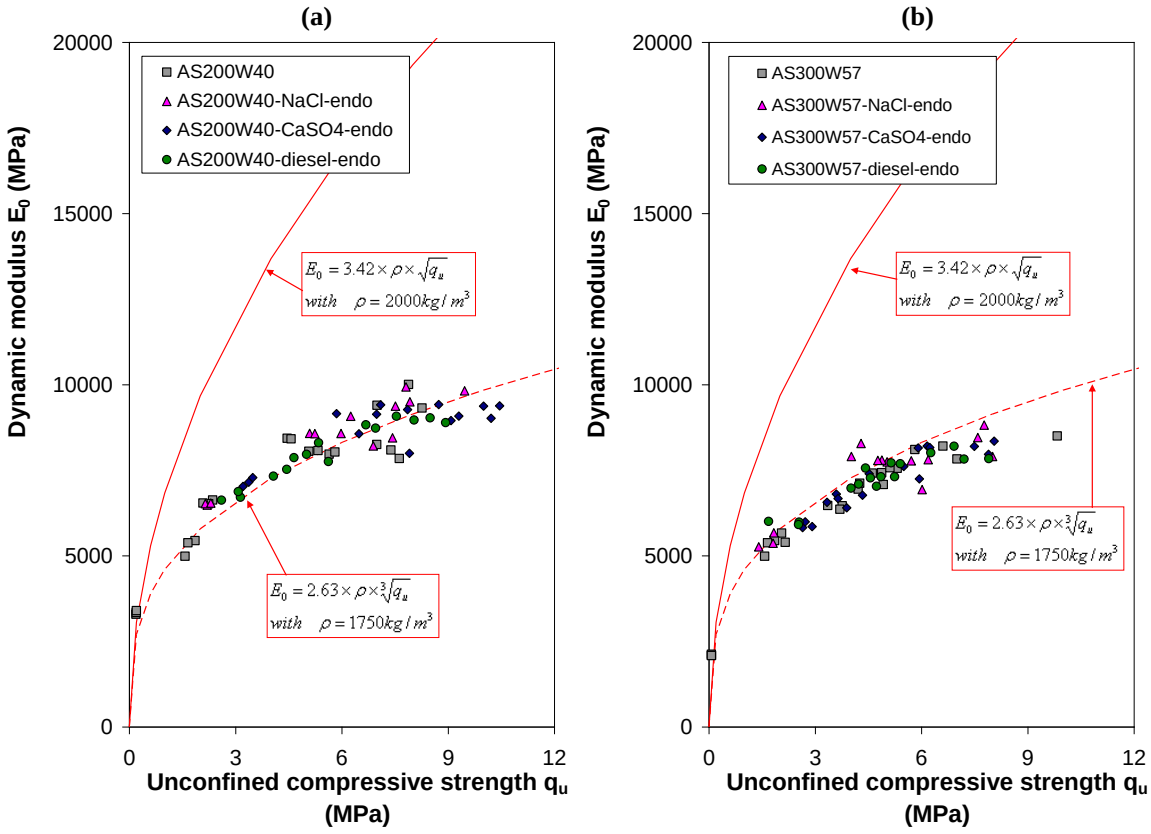

Figure 5-31 Effect of $CaSO_4$, NaCl and diesel on the relation between dynamic modulus and strength for artificial silt-CEM III cement mixes (a) AS200W40; (b) AS300W57.

5.1.4.3 Effects on indirect tensile strength

Average indirect tensile strengths of 680 kPa and 875 kPa were measured after 28 days on specimens of the reference mixes AS300W57 and AS200W40 respectively (Figure 5-32).

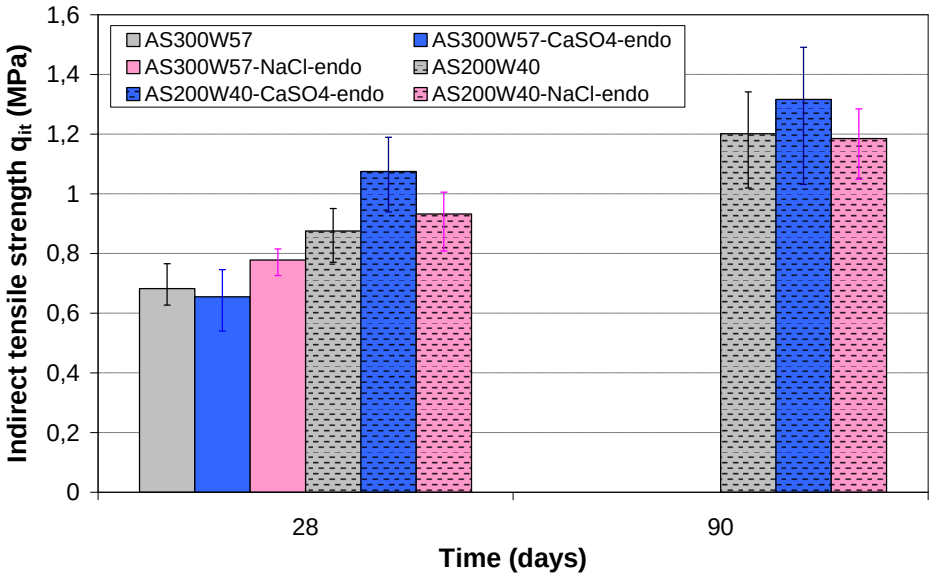

Figure 5-32 Effect of $CaSO_4$ and NaCl on the indirect tensile strength of artificial silt-CEM III cement mixes.

After 90 days, the indirect tensile strength for AS200W40 increased and was close to 1.2 MPa. The data in Figure 5-32 shows that NaCl and $CaSO_4$ do not alter the tensile strength. On the contrary, the average tensile strengths of the mixes containing NaCl and $CaSO_4$ are higher than the average strengths of the reference mixes (except AS300W57-CaSO4-endo).

5.1.4.4 X-ray diffraction

Comparison of the three X-ray diffraction patterns in Figure E-2 shows that no new peaks are present for the mixes of artificial silt containing sulfates and chlorides.

5.1.4.5 Effects on porosity and permeability

Figure 5-33 shows that the total porosity of artificial silt-CEM III mixes does not change with curing time between 28 and 90 days. The data also shows that total porosity is not influenced by the presence of NaCl and $CaSO_4$. The porosity mainly depends on the initial moisture content as discussed in section 3.3.1.

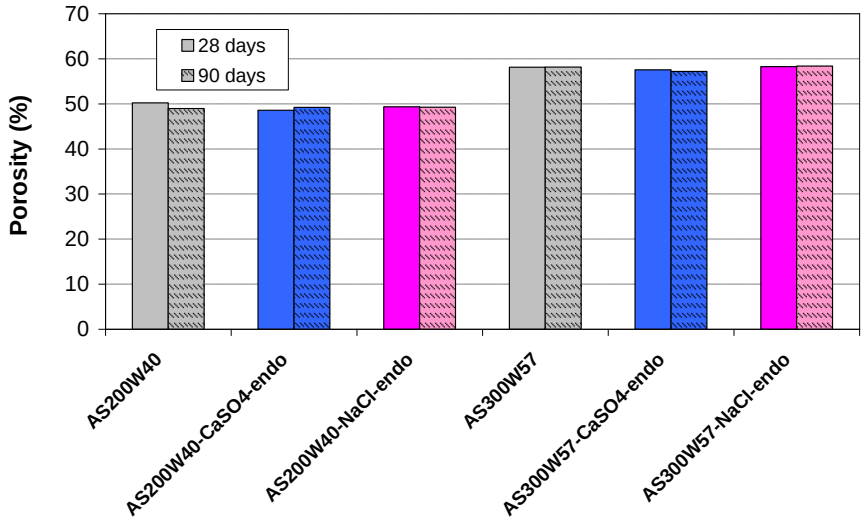

Figure 5-33 Effect of $CaSO_4$ and NaCl on the total porosity of artificial silt-CEM III cement mixes.

The results of MIP measurements performed on cryodessicated fragments of specimens of AS300W57, AS300W57-CaSO4-endo and AS300W57-NaCl-endo are presented in Figure 5-34 (cumulative mercury intrusion curves) and in Figure 5-35 (pore size density function curves).

The total volume of mercury intruded is very close for the three tests around 0.5 mL of mercury per gram (Figure 5-34). Total porosities of 54.5 %, 55.9 % and 55.0 % were derived from the intruded volumes of mercury for AS300W57, AS300W57-CaSO4-endo and AS300W57-NaCl-endo respectively. These total porosities are 2 to 3 % lower than the porosities determined by hydrostatic weighing after saturation (Figure 5-33).
NaCl and $CaSO_4$ did not affect the microstructure of the treated silt as the pore size density functions are almost identical (Figure 5-35). The majority of pores have entrance radii between 0.03 and 0.1 µm.

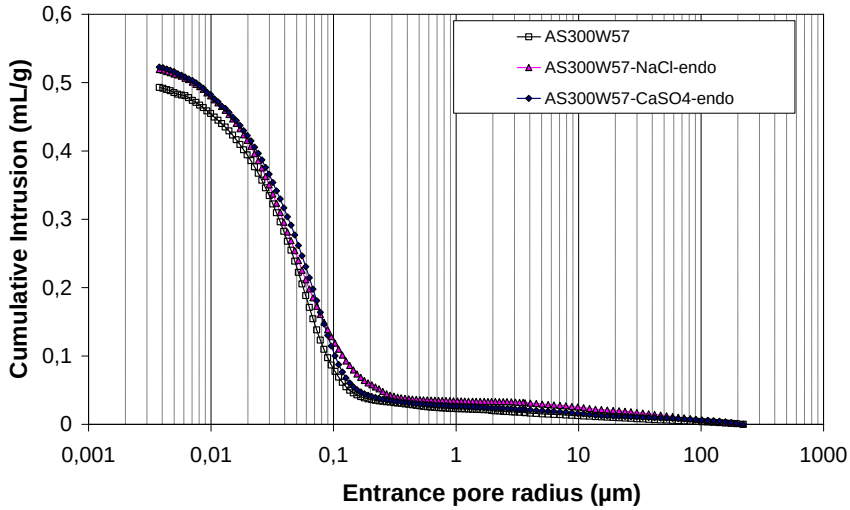

Figure 5-34 Effect of $CaSO_4$ and NaCl on the microstructure of artificial silt-cement mixes (cumulative intrusion curves).

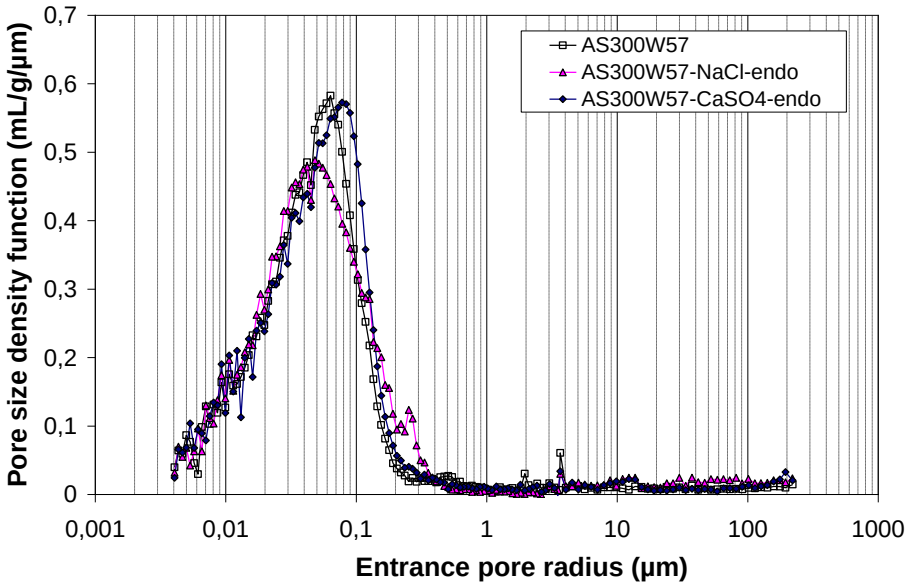

Figure 5-35 Effect of CaSO4 and NaCl on the microstructure of artificial silt-cement mixes (pore size density function).

Mix	Permeability (m/s)	
	28 days	90 days
AS200W40	$4{,}6 \times 10^{-10}$	$0{,}47 \times 10^{-10}$
AS200W40-CaSO4-endo	$2{,}1 \times 10^{-10}$	$0{,}64 \times 10^{-10}$
AS200W40-NaCl-endo	$6{,}5 \times 10^{-10}$	$1{,}5 \times 10^{-10}$
AS300W57	$3{,}3 \times 10^{-10}$	$0{,}34 \times 10^{-10}$
AS300W57-CaSO4-endo	$1{,}5 \times 10^{-10}$	$0{,}62 \times 10^{-10}$
AS300W57-NaCl-endo	$3{,}5 \times 10^{-10}$	$0{,}53 \times 10^{-10}$

Table 5-2 – Permeability of artificial silt – CEM III cement mixes.

As with porosity, the permeability of AS-CEM III mixes does not considerably change with curing time between 28 and 90 days. All measured permeabilities are close to 10^{-10} m/s. The

results presented in Table 5-2 suggest that the permeability of AS-CEM III mixes is not modified by the presence of $CaSO_4$ or NaCl.

5.1.4.6 Scanning electron microscopy

The scanning electron microscopy images in Figure 5-36 show the effects of cementation on the microstructure of the artificial silt. The structure is relatively dense with no obvious large porosity for a magnification of 600 times.

Examination of the images with higher magnifications (25000 and 10000 times) shows that the treated silt exhibits a fairly open type of microstructure (Figure 5-37). The images show no significant effect of the addition of NaCl and $CaSO_4$ on the microstructure of artificial silt treated with CEM III. These observations are in agreement with the results from MIP measurements.

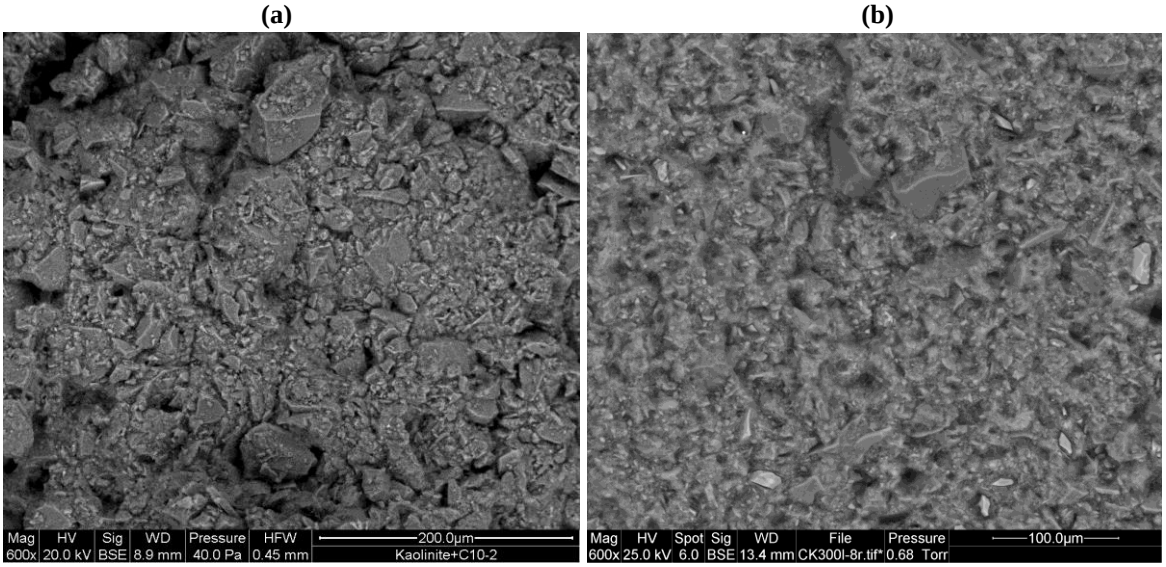

Figure 5-36 Scanning electron microscopy images. (a) Artificial silt (90x) (b) Artificial silt treated with CEM III after 90 days AS300W57 (90x).

5.1.1 Summary of results

It is difficult to give a general quantitative assessment of the effects of the compounds tested in this study on the properties of treated soils. The repeatability of the results was not verified by a large number of samples. However, for each test, the coefficient of variation for 3 specimens of every soil-cement mix was determined for each curing time up to 360 days. Based on the analysis of these coefficients of variation, the thresholds given in Table 5-3, equal to the maximum coefficient of variation measured on 3 specimens, were used to evaluate the effects of the chemical compounds on the treated soils.

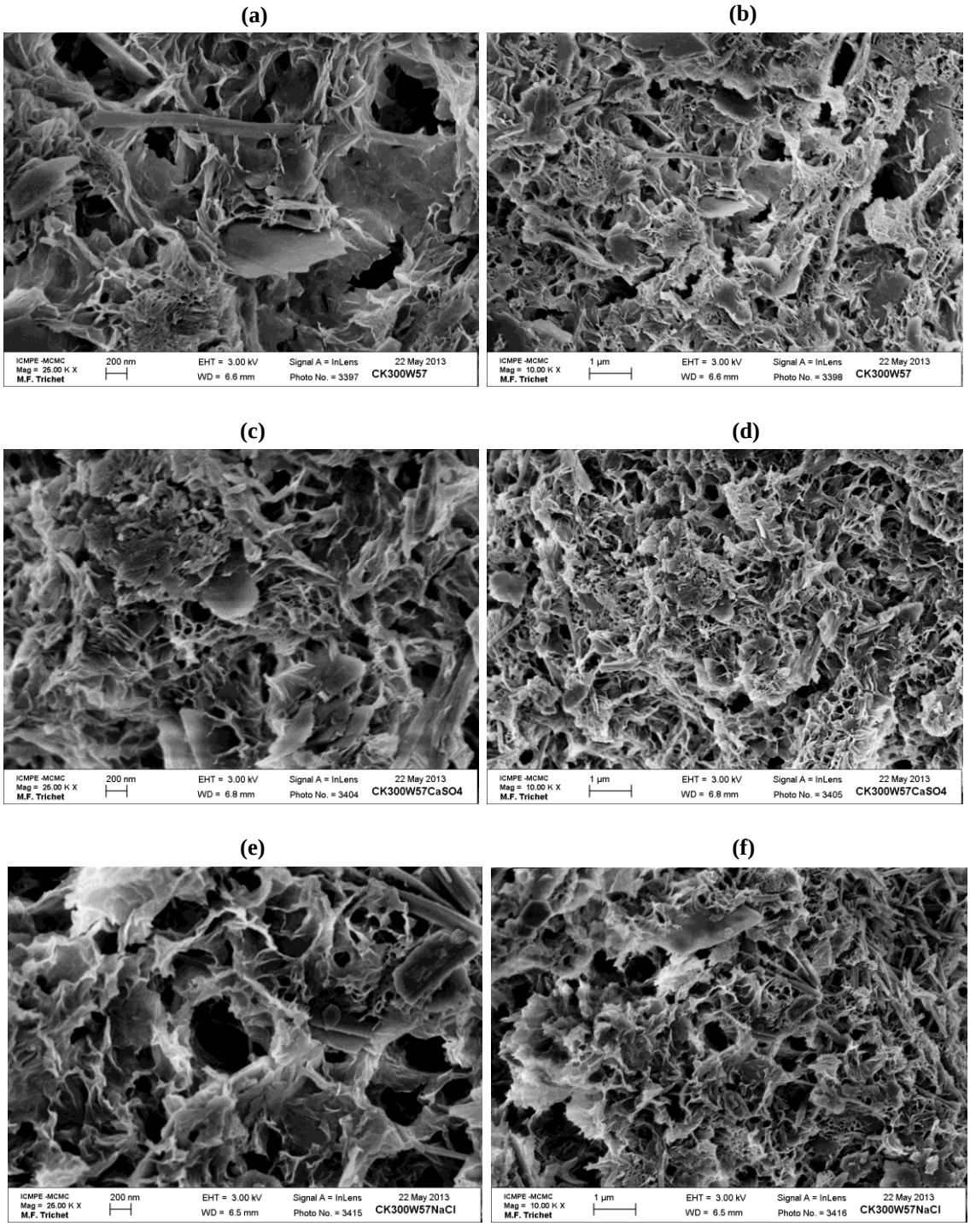

Figure 5-37 Scanning electron microscopy images (25000x and 10000x). Effect of $CaSO_4$ and NaCl on the microstructure of the cement paste in artificial silt treated with CEM III after 360 days. (a), (b): AS300W57; (c), (d): AS300W57-CaSO4 endo; (e), (f): AS300W57-NaCl endo.

Parameter	Threshold
Unconfined compressive strength q_u	15 %
Indirect tensile strength q_{it}	15 %
Dynamic modulus E_0	7 %

Table 5-3 Thresholds chosen to evaluate the effects of chemical compounds on the properties of treated soils.

Note that the threshold for the dynamic modulus E_0 is lower as the data is less subjected to scatter due to the testing procedure. Synthetic qualitative overviews of the results for the different mixes in this study using the determined thresholds are presented in Table 5-4 and Table 5-5.

The following symbols are used to indicate qualitatively the relative difference between the values of a parameter measured on specimens with and without the potential deleterious compound:

For q_u and q_{it}: -- < -30% < - < -15% < = < 15% < + < 30% <++

For E_0: -- < -14% < - < -7% < = < 7% < + < 14% <++

Reference mix	Chemical compound	Parameter	Curing time (days)					
			7	14	28	90	180	360
FS-I-200W20	**+ 10g/kg $CaSO_4$**	**q_u**	--	--	--	-	-	/
		E_0	--	--	--	--	-	/
		q_{it}	/	/	--	=	/	/
FS-I-200W15	**+ 10g/kg $CaSO_4$**	**q_u**	--	--	--	--	--	/
		E_0	--	--	--	--	--	/
		q_{it}	/	/	--	-	/	/
FS200W35B50	**+ 10g/kg $CaSO_4$**	**q_u**	-	-	--	--	-	-
		E_0	=	=	=	-	=	=
		q_{it}	/	/	--	-	/	/
	+ 2g/kg NaCl	**q_u**	-	--	--	-	-	-
		E_0	-	-	=	=	=	-
		q_{it}	/	/	--	-	/	/
	+ 30g/kg Diesel	**q_u**	=	+	=	=	=	/
		E_0	=	+	=	=	=	/

" / ": indicates an absence of data

Table 5-4 Qualitative assessment of the effects of chemical compounds on the properties of treated Fontainebleau sand.

Table 5-4 clearly puts forward the well-known altering effect of sulfates on soils treated with Portland cement. Microstructural investigations suggest that the negative effects of NaCl and $CaSO_4$ on the properties of FS200W35B50 specimens are probably due to the interaction between the salts and the bentonite present in the mix as no effect of the compounds on the cement was detected. Diesel oil does not modify the properties of FS200W35B50. For the artificial silt treated with CEM III, the properties remained generally unchanged in presence of the three compounds (Table 5-5).

Reference mix	Chemical compound	Parameter	Curing time (days)				
			7	28	90	180	360
AS200W40	+ 10g/kg $CaSO_4$	q_u	++	+	=	=	=
		E_0	+	=	+	=	=
		q_{it}	/	+	=	/	/
	+ 2g/kg NaCl	q_u	=	=	=	=	-
		E_0	=	=	=	=	+
		q_{it}	/	=	=	/	/
	+ 2g/kg Diesel	q_u	+	=	=	=	/
		E_0	=	=	=	=	/
AS300W57	+ 10g/kg $CaSO_4$	q_u	++	=	=	=	=
		E_0	=	=	=	=	=
		q_{it}	/	=	/	/	/
	+ 2g/kg NaCl	q_u	-	+	+	=	=
		E_0	=	=	=	=	=
		q_{it}	/	=	/	/	/
	+ 2g/kg Diesel	q_u	=	+	=	=	/
		E_0	+	=	=	=	/

" / ": indicates an absence of data

Table 5-5 Qualitative assessment of the effects of chemical compounds on the properties of treated artificial silt.

5.1.2 Conclusions on the effects of potential deleterious compounds

In this section, the influence of three potential deleterious compounds on the long-term characteristics of soils stabilised with cement was studied. Specimens of silt and sand treated with different dosages of CEM I and CEM III cement were mixed with the tested compounds and placed in different curing conditions. The following conclusions, valid in the conditions of this study, can be drawn from the results:

- The wet density, total porosity and permeability of treated silt and sand do not significantly vary with curing time and are not affected by the addition of NaCl, $CaSO_4$ or diesel.
- In endogenous curing conditions, all the soil-cement specimens containing $CaSO_4$, NaCl or diesel hardened and the strength and dynamic modulus of all soil-cement mixes increased with time.
- However, $CaSO_4$ has an adverse effect on the compressive and tensile strength of Fontainebleau sand treated with CEM I. The dynamic modulus E_0 is also diminished by $CaSO_4$.
- The use of blastfurnace slag cement is found to be effective in preventing the potential deleterious effects of the tested compounds. For the two dosages tested, the strength and dynamic modulus of silt treated with CEM III is not significantly affected by the addition of NaCl or $CaSO_4$. NaCl and $CaSO_4$ lowered the tensile and compressive strength of specimens of Fontainebleau sand treated with CEM III in which bentonite was added to stabilise the mixture. Microstructural investigations suggest that this effect could be linked

to the specimen preparation procedure. The presence of diesel did not modify the strength or dynamic modulus of the silt and sand treated with CEM III.

- The relation between q_u and E_{50} and between q_u and E_0 remained valid for all soil-cement mixes.

Curing conditions have a major effect on the strength of treated soils.
The strengths of specimens of sand treated with CEM III immersed in water were slightly lower than the strengths of the specimens cured in endogenous conditions.

A drastic decrease in strength was measured on specimens of treated silt subjected to air drying in a climatic chamber after 28 days of endogenous curing. A specific testing program was implemented to address the issue of the effects of air drying on the strength and stiffness of cement-treated soils. The results are given in the following section.

5.2 Influence of drying on the stiffness and strength of stabilised soils

5.2.1 Introduction

The aim of this program is to investigate the effects of different curing conditions (immersion in water, cycles of wetting and drying, air curing) on the mechanical properties of specimens of soil treated with blast furnace cement in the laboratory.
The effects of drying and wetting-drying cycles are examined on three artificial soil-cement mixes: FS200W20, AS300W57 and AS200W40 (Table A-1). The testing program is described in section 2.4.2.3.

5.2.2 Small strain shear modulus of specimens immersed in water

Figure 5-38 presents the evolution of shear modulus G_0 and moisture content w with time for specimens cured in water (condition (1), Figure 2-7).

The results correspond to the average values measured on 3 specimens; the error bars represent the minimum and maximum values.

For all three tested mixes, the moisture contents stayed approximately constant between 7 and 30 days at values of 18 % for the sand FS200W20 (slightly lower than the moulding water content), 40.6 % for the silt of mix AS200W40 (close to moulding content) and 55 % for the silt of mix AS300W57 (again slightly inferior to the moulding water content). The shear modulus G_0 increases with time. After 7 days, G_0 is close to 1.5 GPa for the sand and silt specimens treated with the equivalent of 200 kg/m^3 of cement (mixes FS200W20 and AS200W40). The specimens of silt mixed with 20.7 % cement (AS300W57) have a lower shear modulus after 7 days (0.83 GPa). The average shear moduli G_0 measured after 30 days of curing in water are given in Table 5-6.

Soil-cement mix	Curing conditions (time of testing)	Testing age	q_u (MPa)	E_{50} (GPa)	E_{50} / q_u	ε_f (%)	G_0 (GPa)	G_0 / q_u
FS200W20 Sand (C=11.8%)	**Immersed (0-7 days)**	7	0.82	2.00	2443	0.15	1.51	1849
	Immersed (0-30 days)	30	2.39	5.51	2305	0.24	3.80	1592
	Cyclic wetting-drying (7-30 days)	30	2.57	4.33	1685	0.34	2.96	1154
	Air cured (7-30 days)	30	1.37	2.37	1728	0.11	1.27	929
AS200W40 Silt (C=13.8%)	**Immersed (0-7 days)**	7	2.26	2.66	1177	0.14	1.43	631
	Immersed (0-30 days)	30	5.59	5.08	908	0.11	2.44	436
	Cyclic wetting-drying (7-30 days)	30	4.49	2.81	627	0.34	1.50	334
	Air cured (7-30 days)	30	2.27	0.08	37	2.02	0.22*	/
AS300W57 Silt (C=20.7%)	**Immersed (0-7 days)**	7	1.69	1.84	1085	0.16	0.83	491
	Immersed (0-30 days)	30	5.04	4.53	900	0.13	2.08	414
	Cyclic wetting-drying (7-30 days)	30	4.17	3.34	801	0.16	1.62	388
	Air cured (7-30 days)	30	1.92	0.05	24	2.81	0.08*	/

*: values measured 18 days after moulding.

Table 5-6 Average values derived from testing.

Variations in the dimensions of the specimens during curing in water measured using a digital calliper were found to be relatively small (average volume increases of 1.35 % (mix FS200W20), 0.79 % (mix AS200W40) and 0.45 % (mix AS300W57) were observed after 30 days).

Small strain shear modulus development with time of cement-treated soils, as measured here between 7 and 30 days, can be characterised by an exponential relation similar to the formula used to estimate the long-term strength q_u and dynamic modulus E_0 in Chapter 3. The following relation was applied to calculate G_0 after 30 days using data measured after 7 days:

$$G_t = G_7 \times \exp(k_7 \times (1 - \sqrt{\frac{7}{t}}))$$

$G_{0,t}$ is the shear modulus measured after t days of curing in water; $G_{0,7}$ is the initial shear modulus measured after 7 days of curing in water; k_7 is an empirical parameter.

Mix	k_7	R^2	Prediction error $\%G_{0,30} = (G_{0,30} - G_{calculated}) / G_{0,30}$
FS200W20	2.10	0.99	-1.91 %
AS200W40	1.03	0.93	-3.02 %
AS300W57	1.98	0.90	-12.40 %

Table 5-7 Experimental parameters, coefficients of correlation and prediction errors for exponential relations.

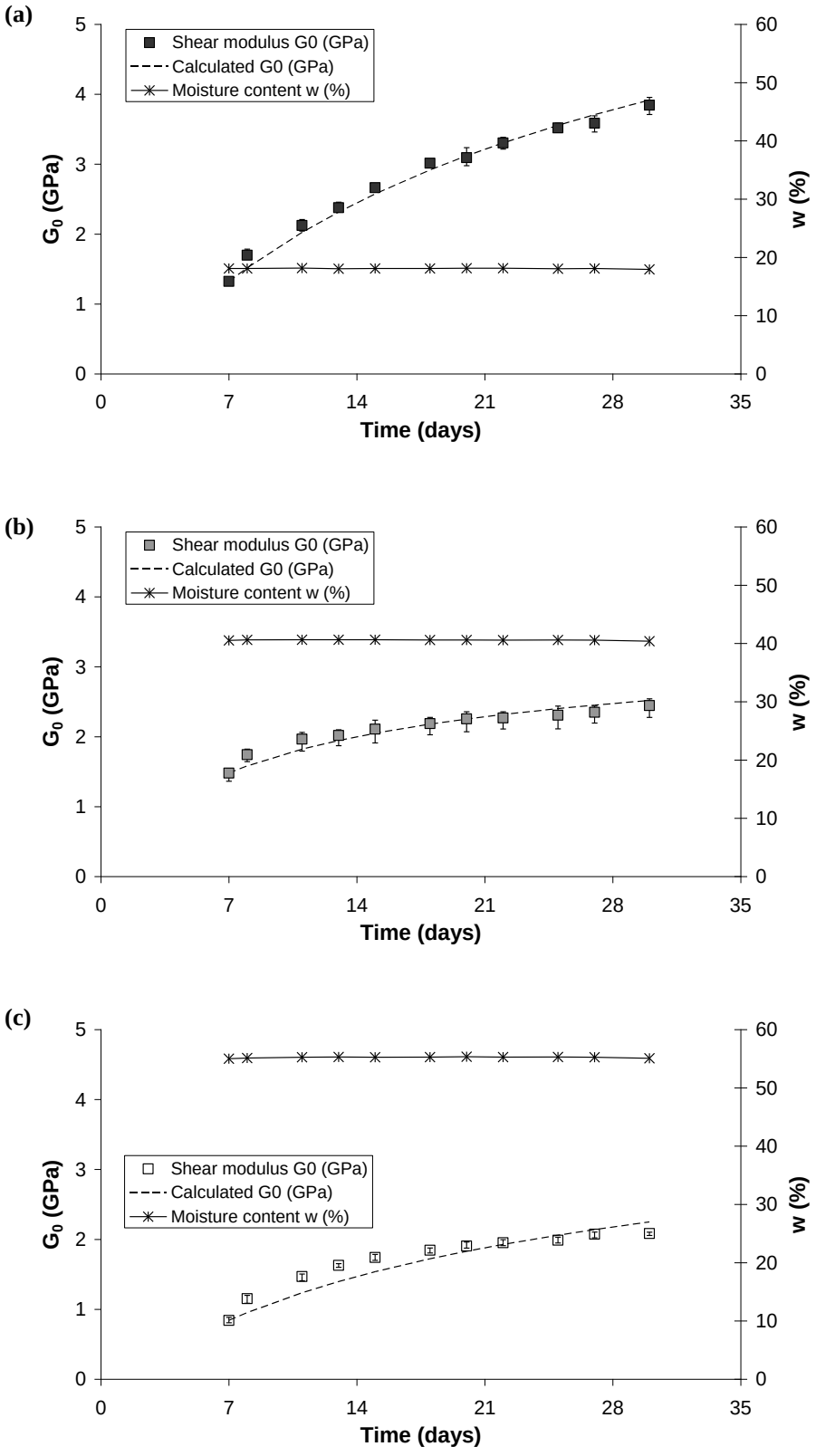

Figure 5-38 Small strain shear modulus G_0 and moisture content w versus time for specimens cured in water (a) FS200W20; (b) AS200W40; (c) AS300W57.

The calculated values of G_0 are shown as dashed lines in Figure 5-38. The experimental parameters appear to be dependent on both soil type and dosage (Table 5-6).
The shear moduli of the specimens of mix AS300W57 (C = 20.7 %) are lower than the moduli of the specimens of mix AS200W40. This observation can be explained by the opposite and competitive effects of cement and moisture content. The higher stiffness of mix AS200W40 can be attributed to the lower porosity induced by the lower moulding moisture content which is not compensated by the higher cement content.

5.2.3 Effects of cyclic wetting and drying on small strain shear modulus

The small strain shear moduli G_0 of specimens subjected to successive periods of wetting and drying (curing condition (2), Figure 2-7) after the initial 7-days curing in water are shown in Figure 5-39.

The corresponding moisture contents determined at the end of each curing period are also presented and give an indication on the curing conditions at a specific time: an increase in moisture content indicates soaking whereas a decrease points to periods of drying. The phases of curing in water lasted between 1 and 4 days. The specimens were submitted to drying for 24 hours (except between 20 and 22 days where two successive 24h drying periods were applied).

After 30 days, the dimensions of the specimens under cyclic wetting and drying were found to have slightly increased for the silt mixes (average volumes increased by 0.38 % (AS200W40) and 0.21 % (AS300W57)) whereas shrinkage was measured for the treated sand specimens (-0.70 %).

A general increase in stiffness G_0 can be seen for mixes FS200W20 and AS300W57 between 7 and 30 days. The values of G_0 measured at 30 days are lower than for the specimens cured in water (Table 5-6) indicating a disruptive effect of the imposed wetting-drying cycles on stiffness increase. A significant decrease in shear modulus G_0 was measured for the silt mixed with 13.7 % cement (AS200W40) after the first drying period (Figure 5-39 (b)). This reduction in stiffness was associated with the development of microcracks on the surface of the specimens (Figure 5-40) which were not observed for mixes FS200W20 and AS300W57. Further cyclic wetting and drying did not increase the cracking. The modulus G_0 of the specimens of mix AS200W40 followed closely the variations in moisture content (thus in mass density) imposed by the periods of wetting and drying. The average stiffness of these specimens after 30 days was almost identical to the stiffness measured after 7 days of curing (Table 5-6).

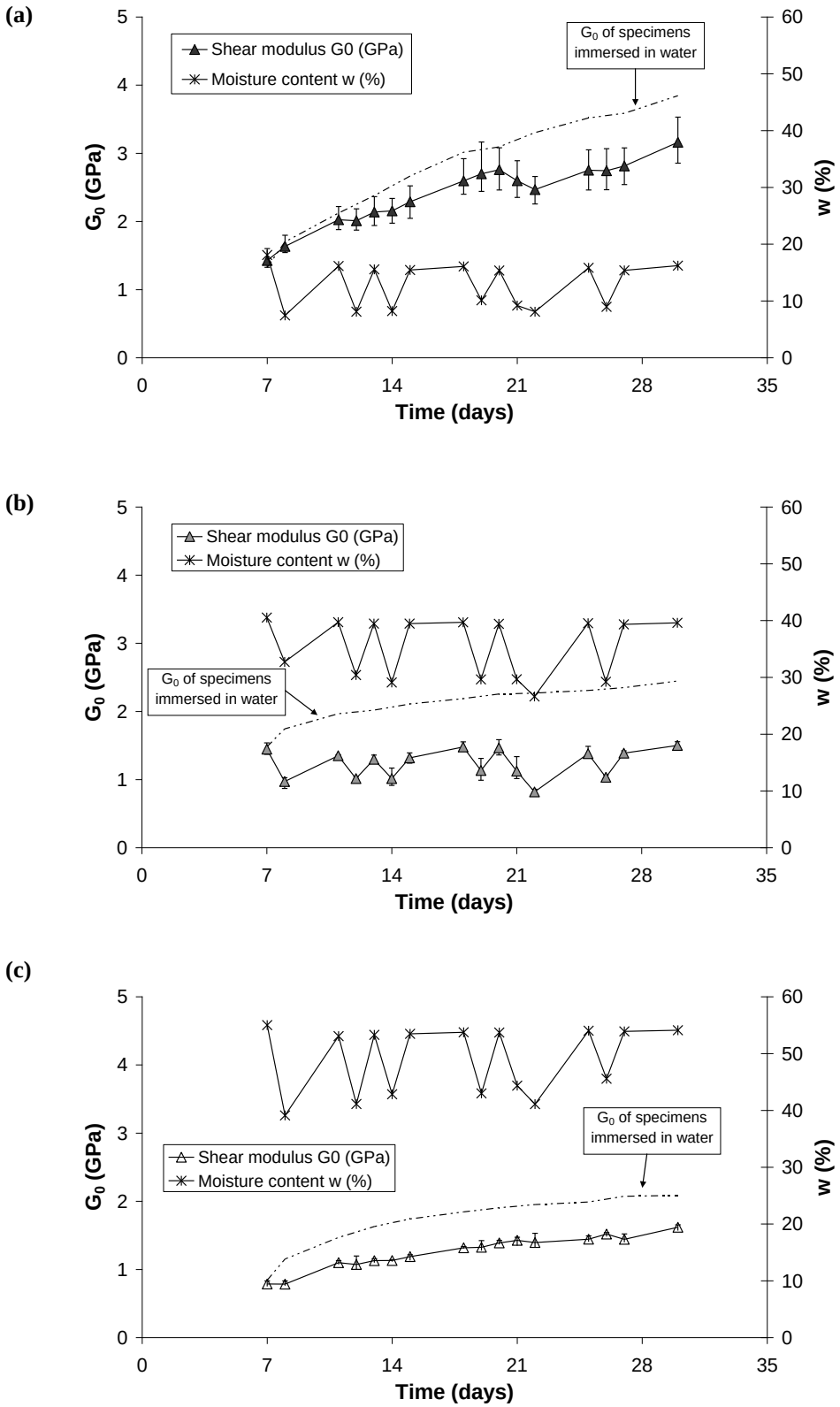

Figure 5-39 Small strain shear modulus G_0 and moisture content w versus time for specimens subjected to wetting and drying (a) FS200W20; (b) AS200W40; (c) AS300W57.

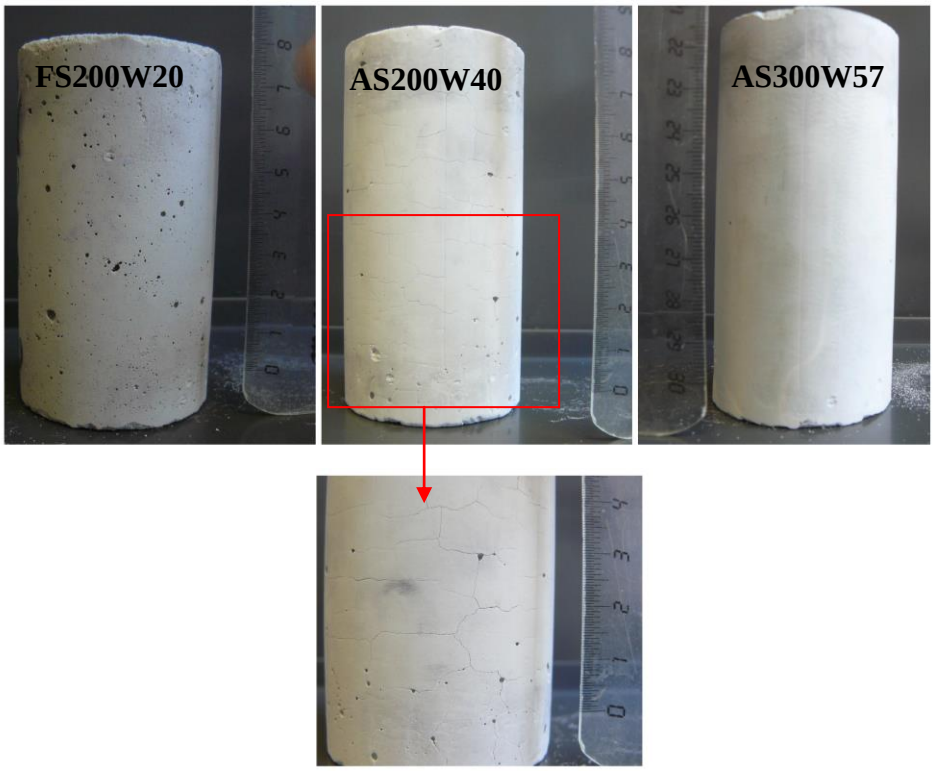

Figure 5-40 Specimens submitted to cycles of wetting and drying after 30 days.

5.2.4 Effects of continuous drying on small strain shear modulus

For the specimens of stabilised sand exposed to continuous drying (condition (3), Figure 2-7) after 7 days in water, stiffness G_0 remained generally constant up to 30 days (Figure 5-41 (a)). The stiffness of the sand specimens exposed to air after 30 days in water decreased sharply during the first few days of drying. (Figure 5-41 (a)). It stabilised at approximately 50% of its initial value after 17 days of drying (47 days after specimen preparation) and remained higher than the stiffness of the specimens dried after 7 days. No visible microcracks were formed during drying of the sand specimens.

The stiffness of the specimens of stabilised silt significantly decreased with time of drying (Figure 5-41 (b) and (c)). The rate of stiffness decrease is also higher during the first few days of drying. Microcracks appeared on the silt specimen surfaces after the first or second day of drying. These microcracks developed with time and lead to difficulties in the acceleration signal transmission during free-free resonance testing for the specimens placed in the climatic chamber after 7 days in water. The measurements were stopped after 11 days of drying (18 days after specimen preparation). Microcracks also appeared on the specimens of silt exposed to drying after 30 days but FFR testing was performed normally between 30 and 47 days pointing to the fact that prolonged curing in water increases the resistance to desiccation of fined grained soils treated with cement. Nevertheless, the final values of G_0 obtained on the specimens dried between 30 and 47 days are very low.

The 23 days of continuous drying (between 7 and 30 days) caused the specimens to shrink by -0.28 % for the treated sand, -2.79 % and -2.10 % for the silt mixes AS200W40 and AS300W57 respectively.

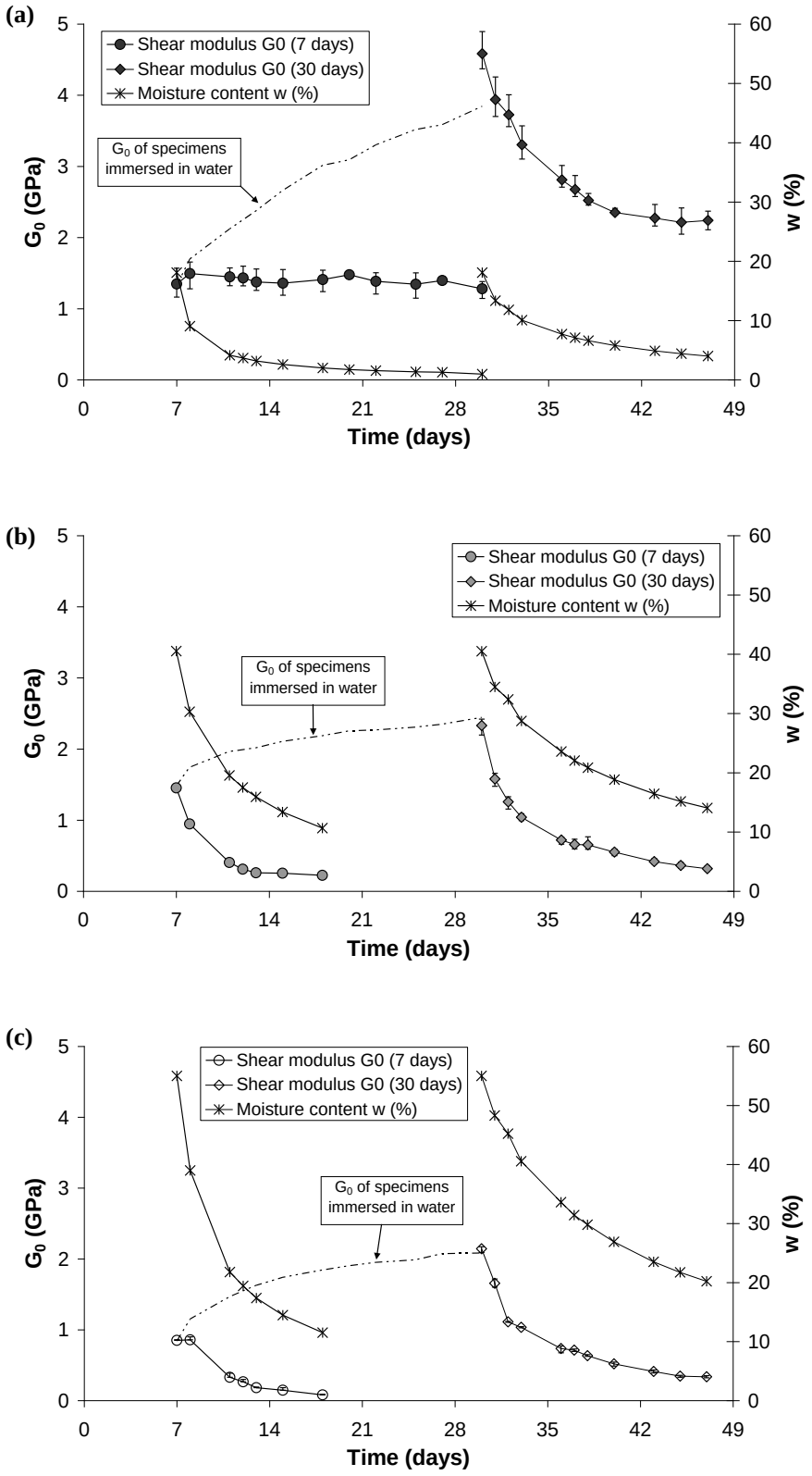

Figure 5-41 Small strain shear modulus G_0 and moisture content w versus time for specimens subjected to continuous drying (a) FS200W20; (b) AS200W40; (c) AS300W57.

5.2.5 Effects of curing conditions on strength and static stiffness

Typical stress-strain curves obtained from unconfined compressive strength tests on specimens of the 3 soil-cement mixes after different curing regimes and curing times are plotted in Figure 5-42. The derived values of unconfined compressive strength q_u, strain at failure ε_f, static stiffness E_{50} and stiffness to strength ratio E_{50}/q_u, are listed in Table 5-6 and compared in Figure 5-43.

For all mixes, the unconfined compressive strength q_u and static stiffness E_{50} of the specimens immersed in water between 7 and 30 days increased (Table 5-6). The E_{50}/q_u ratios are higher for the stabilised sand than for the treated silt. For both soils, E_{50}/q_u is slightly lower after 30 days. The same tendency is found for the small strain shear modulus to strength ratio G_0/q_u (Table 5-6). This confirms the results found for E_0 in Chapter 3. Strength increases more rapidly than stiffness between 7 and 30 days in soils treated with blastfurnace slag cement. These results differ from those obtained by Verástegui Flores et al. (2010). From tests on kaolin clay mixed with Portland and blast furnace slag cement at various dosages, they found that G_0 and compressive strength increase in equal proportions with curing time.

For all mixes (FS200W20, AS200W40 and AS300W57), the unconfined compression strengths measured after 30 days on the specimens subjected to cycles of wetting and drying were higher than the initial 7-day strength (Figure 5-43 (a)). This suggests that sufficient water remained present for hydration to continue during these cycles.
The static stiffness E_{50} of the sand (FS200W20) and the silt specimens treated with 20.7% cement (AS300W57) increased between 7 and 30 days despite the cyclic curing regime whereas E_{50} for the silt treated with 13.8% cement (AS200W40) remained close to the value measured on specimens after 7 days in water (Table 5-6).

After 23 days of continuous drying (between 7 and 30 days after mixing), the strength of the treated silt specimens of mix AS300W57 had increased while no variation in q_u was measured for the silt treated with 13.8% cement (mix AS300W57). The strength of the sand specimens dried between 7 and 30 days also increased compared to the 7-day strength.
After continuous drying between 7 and 30 days, E_{50} of the sand specimens was only slightly higher than after 7 days in water. A drastic decrease of E_{50} was measured after 30 days for both silt mixes after continuous drying (leading to E_{50}/q_u ratios of 37 and 24 for mixes AS200W40 and AS300W57 respectively). These low values of static E_{50} are related to the very high strains measured during unconfined compression tests, visible in Figure 5-42, and attributed to the observed microcracking as strain measurements were performed locally in the central part of the specimens. The initial part of the stress-strain curves, for which strain increases considerably at very low stress corresponds to the closing of the fissures. Once the gaps are closed, stress begins to increase with strain.

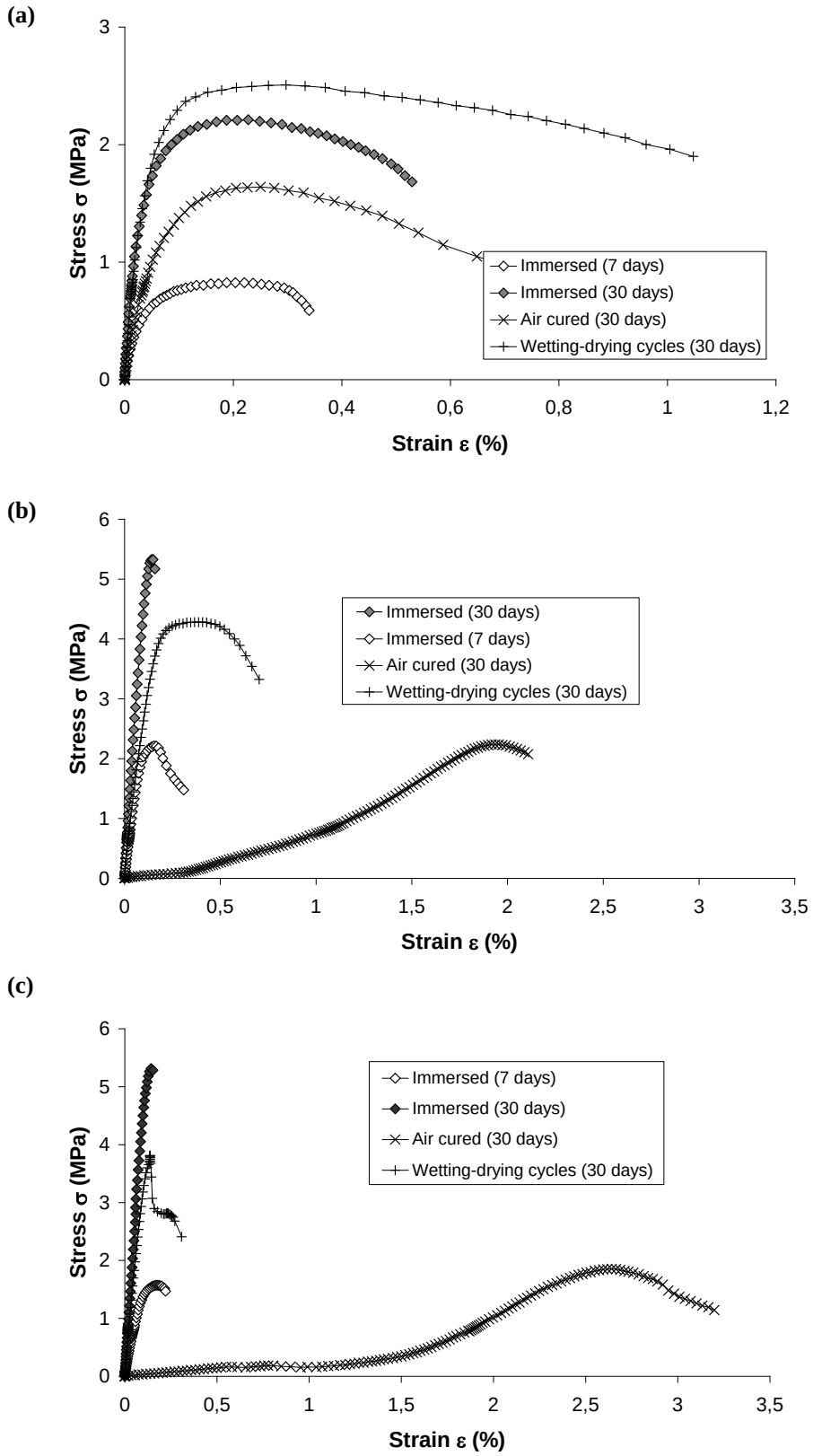

Figure 5-42 Typical stress-strain curves (a) FS200W20; (b) AS200W40; (c) AS300W57.

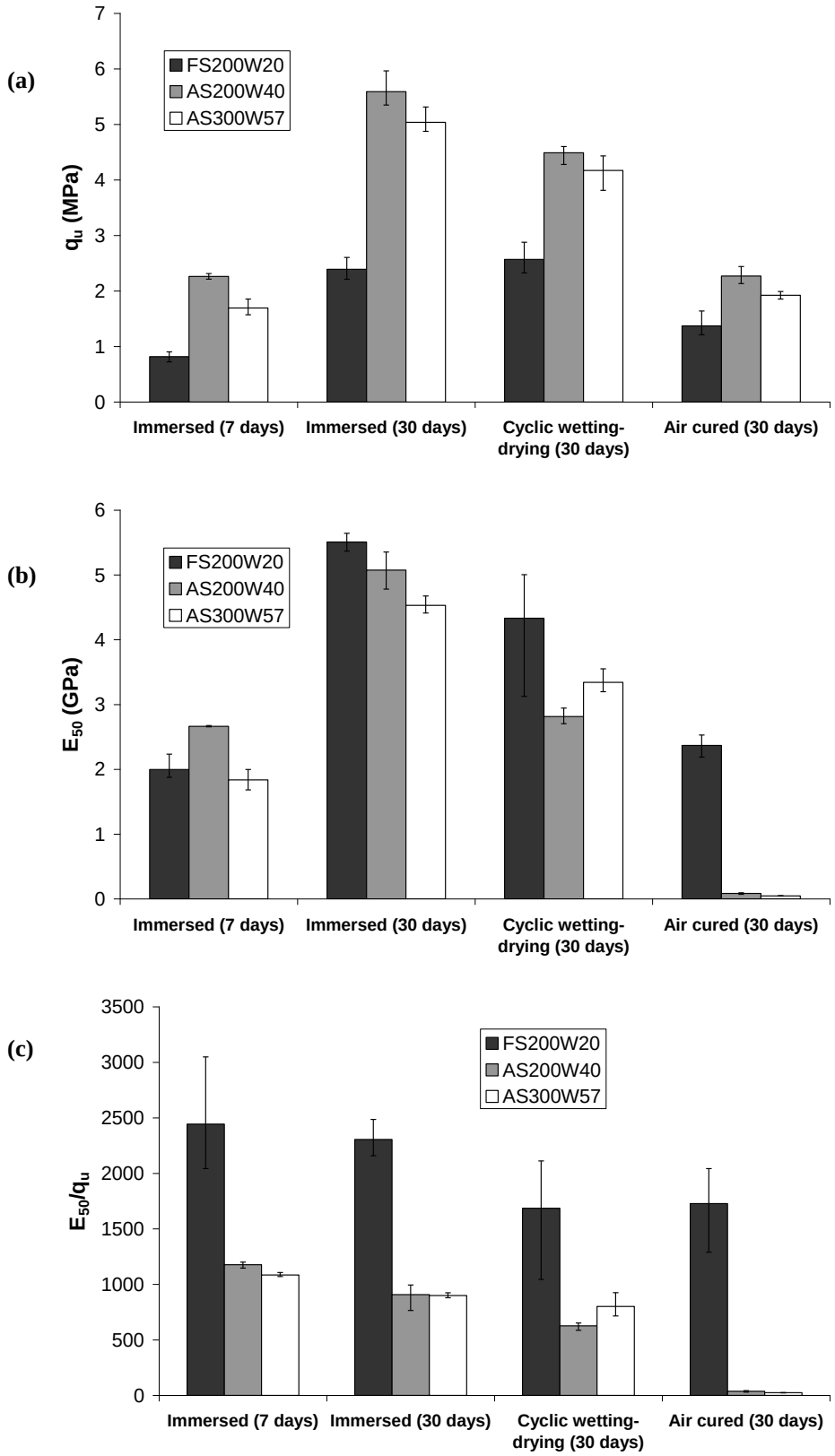

Figure 5-43 Effects of curing conditions on (a) unconfined compressive strength q_u; (b) static stiffness E_{50}; (c) E_{50}/q_u ratio.

Mix	Curing conditions	Relative difference in q_u (%) after 30 days	Relative difference in E_{50} (%) after 30 days	Relative difference in G_0 (%) after 30 days
FS200W20	**Relative difference between immersed and cyclic wetting-drying**	+8	-21	-22
	Relative difference between immersed and continuous air cured	-43	-57	-67
AS200W40	**Relative difference between immersed and cyclic wetting-drying**	-20	-45	-39
	Relative difference between immersed and continuous air cured	-59	-98	-91
AS300W57	**Relative difference between immersed and cyclic wetting-drying**	-17	-26	-22
	Relative difference between immersed and continuous air cured	-62	-99	-96

Table 5-8 Relative difference in strength and stiffness measured after 30 days due to cyclic wetting-drying and continuous drying compared to water-curing.

The effects of the different curing conditions on the static modulus E_{50} and on the small strain shear modulus G_0 are equivalent.

When comparing the variation in strength q_u and stiffness (E_{50} and G_0) after 30 days for specimens subjected to cyclic wetting-drying or continuous drying relative to the values determined after 30 days on specimens immersed in water (Table 5-8), it is evident that the adverse effects of the tested curing conditions are more pronounced:

- on silt than on sand,
- on stiffness than on strength.

5.2.6 Carbonation

Carbonation is a physico-chemical process that involves the diffusion of carbon dioxide through the pores of cementatious materials and the reaction with hydration products such as calcium hydroxide and calcium silicate hydrates.

The depth of carbonation in the treated soil specimens subjected to drying was determined on broken specimen fragments by spraying a solution of phenolphthalein in ethyl alcohol, which changes colour (from pink to colourless) and indicates the carbonated areas (Figure 5-44).

The depth of carbonation was measured by means of a calliper on freshly broken surfaces after compression tests.

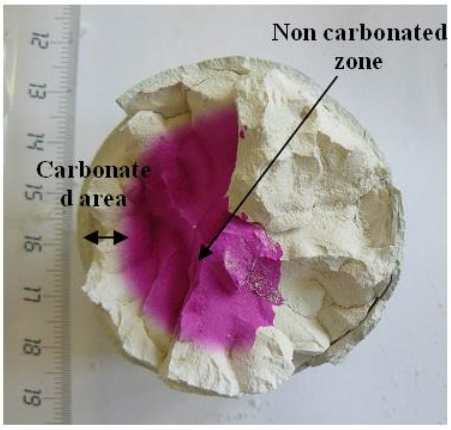

Figure 5-44 Carbonation depth of the treated soil specimens subjected to drying determined using a solution of phenolphthalein.

The results are given in Figure 5-45. The points with a carbonation depth of zero correspond to the curing time at exposure to air. The results on AS200W40-ac and AS300W57-ac (strengths are given in Figure 5-27) show that, in normal atmospheric conditions, carbonation is a slow process (less than 1 cm after 180 days) approximately proportional to the logarithm of time. Both the presence of moisture and carbon dioxide are required for carbonation to occur. The moisture content of the specimens placed in the climatic chamber at a temperature of 20 °C and a relative humidity of 65 % rapidly decreases. This partly explains the decrease in the rate of carbonation with time.

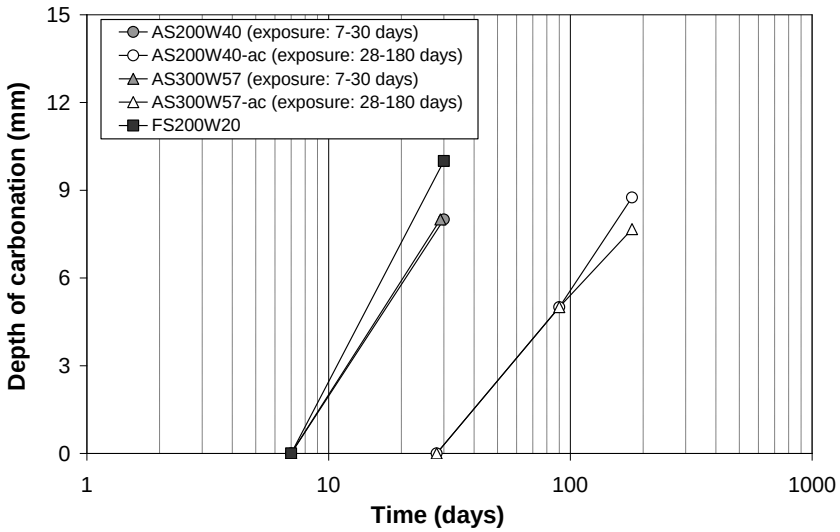

Figure 5-45 Depth of carbonation versus curing time.

The results also indicate that the rate of penetration of carbonation depends on the age of the specimens at the time of exposure to carbon dioxide. The final carbonation depth in the specimens dried between 7 and 30 days is very close to the depths measured on the specimens

dried between 28 and 180 days. The carbonation process appears to be slower in materials exposed to carbon dioxide after longer curing times.
No carbonation was observed in the specimens subjected to cyclic wetting and drying between 7 and 30 days (despite a total of 7 days of exposure to CO_2 during the cycles).

5.2.7 Discussion

For all three soil-cement mixes, three specimens were tested for each curing regime. The results obtained on both small strain stiffness measurements and unconfined compressive strength tests showed a satisfactory repeatability of the procedures used.

Free-free resonance testing was chosen to monitor G_0 as it is a simple and reliable test which has recently been successfully used on soils stabilised with hydraulic binders (Åhnberg and Holmen, 2011; Toohey and Mooney, 2012). The bender elements method is often used to monitor the small strain stiffness of stabilised soils in triaxial cells under confining pressures (for example Bahador and Pak, 2011). The use of this technique was not possible in the case of the present study as the shear modulus G_0 was monitored for a large number of soil-cement specimens on a daily basis during several weeks. Furthermore, the specimens were removed from different curing conditions immediately before testing and had to be replaced in those conditions shortly after. It is important to note that no confining pressure was applied to the specimens during testing.
Resonance testing is extensively used to monitor damage in concrete structures (Doebling et al., 1998). The tested specimens were assumed to remain homogeneous after the formation of cracks as the dimensions of the cracks were small compared to the size of the tested specimen and homogeneously distributed (Figure 5-40). The measured values of G_0 clearly illustrate the damage produced by drying to the specimens of stabilised silt and the evolution of this damage with time.

Indirect tensile strength tests, which are generally used to highlight the presence of damages or cracks in specimens of concrete, could not be performed here as the specimens of silt were extremely fragile after being submitted to drying.

The effect of drying on concrete is influenced by several factors such as cement type, water-cement ratio, properties and volume of aggregates, time of drying, environmental conditions, curing conditions and water content (Hewlett, 2003; Page and Page, 2007). Many experimental studies have demonstrated the impact of drying and desiccation on the mechanical properties of mature mortars and concretes (Burlion et al., 2005; Skoczylas et al., 2007; Yurtdas et al., 2004a, 2006, 2011). Desiccation provokes an increase in compressive strength (20% for mortars, Yurtdas et al., 2004b) whereas the elastic modulus decreases (by about 10 and 25 %). These effects are linked to different and competitive processes that occur during drying. The compression strength increases with desiccation due to the development of capillary suction. The reduction of elastic properties is caused by microcracks. These microcracks are induced by material heterogeneities (presence of aggregates) and differential shrinkage created by variations of water content between the core and extremities of samples.

These variations of moisture content induce stresses exceeding tensile strength. Similar observations on the effects of drying and desiccation have been made for untreated fine grained soils (Corte and Higashi, 1960; Kodikara et al., 2000). Microcracks generated by cyclic wetting–drying under unconfined conditions have been observed (Yesiller et al., 2000b; Tang et al., 2011b).

The drying imposed on the specimens in this study had an effect on both the soil and cement components and it is reasonable to assume that the processes described above for soils and concrete apply to soil-cement mixes.
The sand-cement mix serves as reference as the quartz grains composing the Fontainebleau sand are insensitive to water. Therefore, it can be assumed that the behaviour of the specimens of the sand-cement mix is predominantly governed by the effects of the curing conditions on the cement paste. Kaolin is sensitive to water. Drying had an effect on both the cement and the clay fraction of the silt-cement specimens. Treated sand specimens offered better resistance to drying than treated silt specimens (Table 5-8). This may be attributed to the difference in porosity and to the presence of water-sensitive clay minerals in the silt.

The cement hydration process was still ongoing in the case of specimens subjected to drying (cyclic or continuous) after 7 days of curing in water and this had an impact on the measured stiffness.
The shear modulus G_0 of the sand specimens (FS200W20) remained constant under continuous drying between 7 and 30 days whereas a rapid decrease in G_0 was observed for the two silt-cement mixes (Figure 5-41). Drying of the specimens kept in water for 30 days caused a noticeable decrease in stiffness for all three mixes.

A process countering the effects of drying seems to have taken place for the sand specimens subjected to continous drying between 7 and 30 days ((Figure 5-41 (a)). This effect is absent for the specimens of sand exposed to drying after 30 days in water as G_0 decreased after exposure to air. The constant G_0 of the sand specimens dried continuously after 7 days may be attributed to further hydration of the unreacted cement at least during the first days of exposure to air (Figure 5-41). The process appears to be comparable to autogeneous healing of concretes. Hydration of unreacted cement is one of many mechanisms involved in this phenomenon (Yang et al., 2011; Kan and Shi, 2012). For the silt mixes subjected to drying after 7 days, this countering effect may have been present but was rapidly surpassed by the formation of microcracks resulting in the measured decreases in G_0.

The data presented in this study for the silt-cement mixes suggests that the resistance to drying in soil-cement mixes (in terms of stiffness decrease) is not dependent on the value of initial stiffness and strength at the time of exposure to air as the specimens of mix AS300W57 which had lower initial mechanical properties after 7 days in water offered a better resistance to wetting/drying than the specimens of mix AS200W40 (microcracks appeared after first drying period). The higher resistance to wetting/drying of AS300W57 can be attributed to the higher cement content (despite the higher porosity).

For specimens cured in water, a significant proportion of the increase in stiffness and strength due to cement hydration occurs during the first 30 days. Therefore, the decrease in small strain stiffness observed for the specimens of all 3 mixes exposed to air after 30 days in water is assumed to be predominantly related to drying with no significant opposing effects due to cement hydration. In the conditions of this study, G_0 decreases almost linearly with the loss of water (degree of saturation), Figure 5-46.

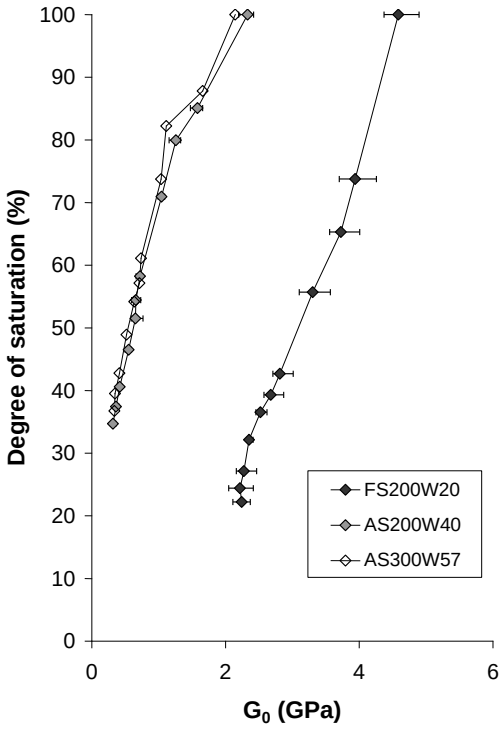

Figure 5-46 Decrease in G_0 with degree of saturation for specimens exposed to drying after 30 days in water.

The successive cycles of wetting and drying appear to have enhanced the resistance to drying of the specimens on which no microcracks were visible. The last cyclic drying periods imposed on the specimens of mixes FS200W20 and AS300W57 (Figure 5-39) had very little effect on G_0 and it is reasonable to assume that an additional period of drying at 30 days would have had a similar effect. On the contrary, the first days of drying of the specimens kept in water for 30 days caused a noticeable decrease in stiffness (Figure 5-41).

In the present study on the effects of drying, dessication and cracking are believed to be the predominant factors controlling the mechanical properties of treated soils. However, carbonation may also have an impact on strength and stiffness. In this case, it was not possible to isolate the effects of carbonation from drying.

It is important to note that the effects of drying on concretes and soils depend on the size of the specimen (Burlion et al., 2005; Lakshmikantha et al., 2012). The distribution of moisture in a specimen subjected to drying is a function of its dimensions. Moisture loss is slower in larger samples. On the contrary, there is a rapid variation of water content in small samples.

The specimen size of 50 x 100 mm was chosen for this study to easily detect the effects of drying on the mechanical properties of soil-cement mixes.

5.2.8 Conclusions on the influence of drying

Specimens of silt and sand stabilised in the laboratory with blast furnace cement were placed in different curing conditions (immersion in water, cycles of wetting and drying, air curing) after 7 days and 30 days. The small strain shear modulus G_0 was monitored using the free-free resonance (FFR) testing method and unconfined compression tests were performed to evaluate the strength q_u and static modulus E_{50}. The following conclusions, valid in the conditions tested in this study, can be drawn:

- An exponential function similar to the relation applied for strength can be used to estimate the increase with time of small strain shear modulus G_0 in cement-treated soils cured in water. Strength increases more rapidly than G_0 between 7 and 30 days.
- Treated sand specimens offer better resistance to drying than treated silt specimens. This is attributed to porosity and to the presence of water-sensitive minerals in the silt.
- As long as the periods of drying do not induce microcracking, the compressive strength and stiffness of treated soils submitted to cyclic wetting and drying before the cement hydration process is complete continues to increase. However, the measured strengths and stiffness are lower than for specimens cured in water indicating a disruptive effect of the imposed wetting-drying cycles on the mechanical properties.
- When specimens of treated sand are continuously dried after short curing times (7 days), a process appears to counter the negative effect of exposure to air on stiffness. The countering effect may also exist but is rapidly surpassed by the formation of microcracks in specimens of cement-treated silt under continuous drying. The cracks cause a rapid decrease in G_0.
- Prolonged curing in water (in this case 30 days in water) somewhat increases the resistance to desiccation. However, the collected data shows an approximately linear decrease in stiffness with decreasing degree of saturation for both tested soils.
- The tested curing conditions have similar effects on static modulus (E_{50}) and dynamic stiffness (G_0). The adverse effect of the curing conditions is more pronounced on stiffness than on strength.
- In normal atmospheric conditions, carbonation is found to be a slow process, approximately proportional to the logarithm of time, which depends on the age of the material at the time of exposure to CO_2.

5.3 Conclusions

The impact of chemical compounds on the long-term properties of soils stabilised with cement was studied in this chapter.

Although hardening of the soil-cement material occurred in all cases, the results show that sulfates, in the chosen concentration, have a negative effect on the long-term strength and stiffness of soils stabilised with Portland cement. The use of blastfurnace slag cement is found to be effective in preventing the potential deleterious effects of the tested compounds on the long-term mechanical properties. However, the mixing procedure used to study the effects of compounds in the laboratory can influence the results.

The curing conditions are also of great importance. Drying can have a significant impact on the characteristics of soils treated with cement. The results show that treated sand specimens offer better resistance to drying than treated silt specimens. For both types of soil, the negative effects of dessication are more pronounced on stiffness than on strength.

Special attention must be given to the mixing procedures used to study soil treatment with cement in the laboratory and the curing conditions must reproduce those existing in situ as closely as possible.

General discussion – Durability of soil-mix materials

The durability of a material in a particular environment can only be established over time. However, contractors are required to give indications regarding the duration of the service life of infrastructures.

With this in mind, a general approach based on durability indicators has been developed for concretes (AFGC, 2007; Baroghel-Bouny, 2008). Durability indicators are key material properties related to the resistance to a particular degradation mechanism. The general durability indicators for concrete, which are applicable to various degradation processes, include calcium hydroxide content, porosity, ion diffusion coefficients, and permeability (to gas and to liquid water). A system of classes of potential durability (PD) pertaining to a particular degradation mechanism is proposed for each durability indicator. The potential durability of a given concrete is assessed by comparing the measured values of durability indicators to selected class thresholds. Engineers and contractors can choose the constituents and design concrete mixtures for new structures on the basis of performance-related specifications linked to these durability indicators and classes.

Unlike concrete, the main constituent of soil-mix materials (the ground present on site) cannot be chosen based on durability specifications. The results presented in Chapter 3 and Chapter 4 clearly show that the type of soil has a major impact on the mechanical properties of stabilised soils.

The following table gives a non exhaustive list of potential factors affecting the general durability of soils treated with cement.

General factors affecting the durability of treated soils		High value	Low value
Factors related to the type of soil	Grain size distribution / fine content (% passing 80µm)	-	+
	Plasticity (PI or W_L)	-	+
Factors related to the binder (can be controlled)	Type of binder		
	Binder content C (% or kg/m^3)	+	-
	Moisture content W (%)	-	+
Potential durability indicators for soil mix material	Unconfined compressive strength (MPa)	+	-
	Density (kg/m^3)	+	-
	Porosity (%)	-	+
	Permeability (m/s)	-	+

+ : has a favourable effect on durability

- : has an adverse effect on durability

Table GD-1 General factors affecting the durability of treated soils and potential durability indicators.

Given past experience on concrete mixtures, it is reasonable to assume that materials with high strength and density, low porosity and permeability present high potential durability (Page and Page, 2007). These parameters could be used as general durability indicators for stabilised soils.

The values of potential durability indicators for soil-mix materials and some controlable factors on site are interrelated.

For example, the treated silt (AS and VSI) and sand (FS and VSA) mixes prepared in the laboratory showed that porosity and unit weight of soil-mix materials are directly correlated to moisture content (which can be controlled on site by modifying the cement-water ratio of the injected slurry). A decrease in moisture content increases both unit weight (Figure 3-11) and total porosity (Figure 3-12). Lower moisture contents also have a positive effect on strength as seen for Fontainebleau sand-cement mixes (Figure 3-18 and Figure 3-19). High binder contents increase the strength and durability of treated soils (Figure 1-24). The type of binder used also impacts the durability of soil-mix materials. The results presented in Chapter 5 prove the effectiveness of using blast furnace cement to prevent problems associated with the presence of deleterious compounds such as sulfates.

The direct correlation between potential indicators and controllable factors affecting the durability of treated soils (binder and water contents) suggests that is possible to optimise the durability-related properties (indicators) of soil-mix materials within the boundaries imposed by the soil conditions on site.

The tests conducted to study the effects of drying showed that treated sand specimens offered better resistance to drying than treated silt specimens due to porosity and the presence of kaolin in the silt.

The dosages used in deep mixing depend on the type of soil. A larger quantity of water is required in clays to obtain a sufficiently fluid soil-binder mixture compared to sands. Therefore, the porosity of treated clays is often greater than that of treated sands.
Highly plastic clays may be subjected to shrinking and swelling under certain curing conditions which could affect the durability.

Concerning these limitations imposed by the soil, a qualitative assessment of the durability of stabilised soils could be carried out based on information collected during the ground investigation performed on a site. In France, soils are classified based on two main criteria (LCPC-SETRA, 1992):

- grain size distribution (percentage smaller than 80µm),
- plasticity (Atterberg limits or methylene blue value).

Using porosity accessible to water as an indicator, trends of "increasing potential durability" for different soils from the classification in Figure GD-1 can be drawn (arrows) assuming:

- the porosity of soil-mix materials increases with increasing fine content of the initial soil,
- the porosity of treated fine grained soils decreases with plasticity index of the initial soil.

For a given treated soil, porosity is controlled by dosage (quantity of water added) and depends on the sampling method (higher porosities are measured in wet-grab samples).

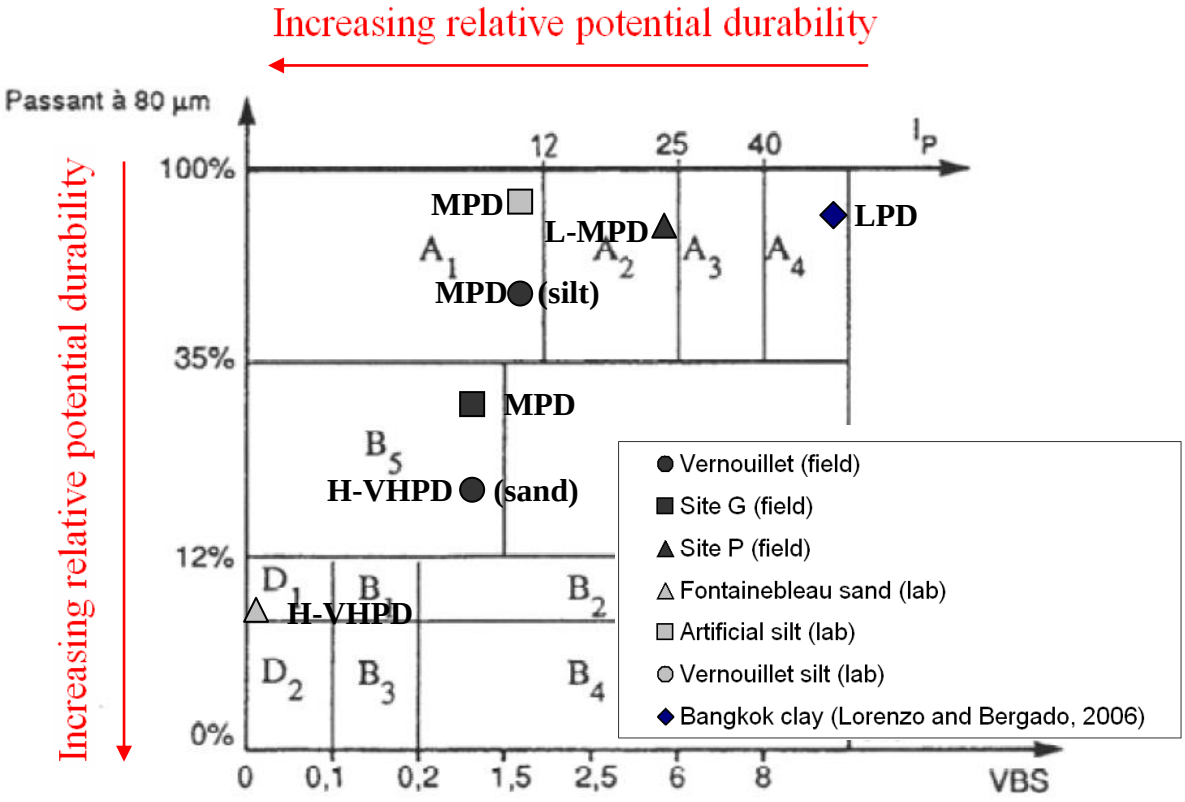

Figure GD-1 LCPC-SETRA(1992) soil classification system.

The total porosity data compiled in this study from soils treated in the laboratory and in situ can be used to propose thresholds for different general potential durability classes resembling those established for concrete (Figure GD-2). The classes range from "very low potential durability" (VLPD) for porosities greater than 85 % to "very high potential durability" (VHPD) for porosities lower than 25 %.

Figure GD-2 shows that a wide range of porosity values and different potential durability classes can be obtained for a same unconfined compressive strength depending on the type of soil, thus proving that mechanical characteristics alone are not sufficient to estimate the potential durability of treated soils. Less scatter in the relations between porosity and unit weight (Figure GD-3) or ultrasonic wave velocity (Figure GD-4) suggest that these parameters are more suitable to compare different potential durabilities.

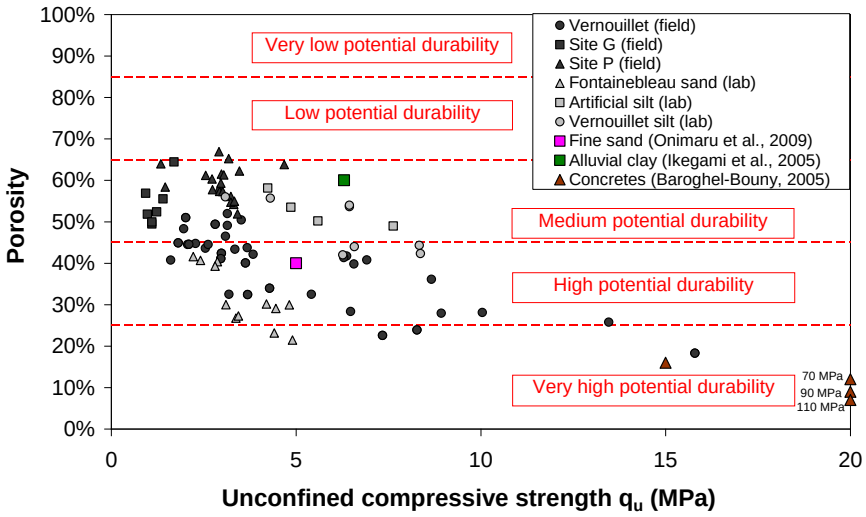

Figure GD-2 Classes of potential durability and experimental values of porosity for soil-cement samples at various ages versus unconfined compressive strength.

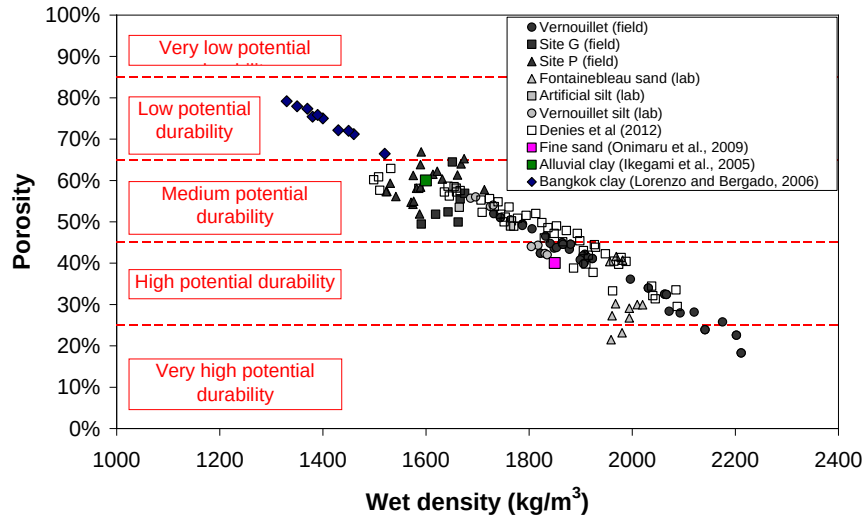

Figure GD-3 Classes of potential durability and experimental values of porosity for soil-cement samples at various ages versus wet density.

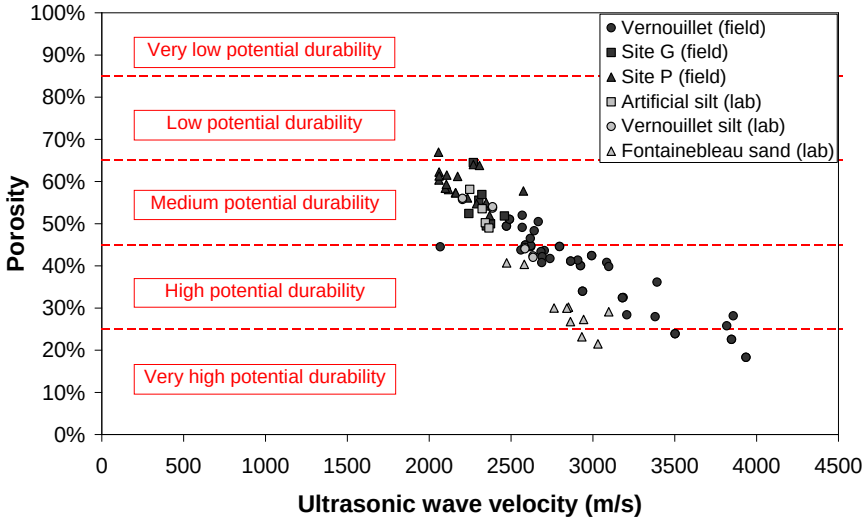

Figure GD-4 Classes of potential durability and experimental values of porosity for soil-cement samples at various ages versus ultrasonic wave velocity.

Most of the data from this study falls in the "medium to high potential durability" classes (M-HPD). The "low and very low potential durability" classes (L-VLPD) correspond to materials of very high porosity such as treated soft clays and peats (Lorenzo and Bergado, 2006; Figure GD-3). Materials with porosities close to those of concretes qualify as of "very high potential durability" (Baroghel-Bouny, 2005; Figure GD-2).
Treated Fontainebleau sand falls in "high to very high potential durability" classes whereas the artificial silt is classified in the "medium potential durability" category. The proposed classes are in agreement with the observations made on the effects of drying (i.e. the resistance of sand to drying is higher than that of treated silt).
The results on field samples from Vernouillet show that different potential durabilities can be obtained on a single site, even within a single column depending on the ground conditions (Figure GD-3).

Published data on the behaviour of existing soil mixing structures can be used to compare the proposed potential durability classes to actual long-term performances.

The stabilised fine sands studied by Onimaru et al. (2009, Figure 1-44) had an average wet density close to 1850 kg/m^3 and an average moisture content around 30 %. These values point to total porosities between 35 % (Figure 3-12) and 45 % (Figure 4-14). After 28 and 60 days of curing, the average compressive strength was around 5 MPa in the first 7 m below ground level (Figure 1-44). These treated fine sands fall in the "high potential durability" class in Figure GD-2 and Figure GD-3. The average compressive strength was 1.5 to 2 times higher after 8.5 years than the strengths measured after 28 and 60 days (Figure 1-44). Specific investigations were performed and no degradations of the material were observed at the boundary with the untreated soil (Onimaru et al., 2009).

Treated alluvial clay from the Port of Yokohama in Japan had an average wet density of around 1600 kg/m^3 and an average moisture content of approximately 65 % (Ikegami et al., 2005). A total porosity near 60 % can be estimated from these values (Figure 3-12 and Figure 4-14). The average strength after 3 months was 6.3 MPa (Figure 1-45). Twenty years later, the average strength had doubled (13.2 MPa). The stabilised alluvial clay falls in the "medium potential durability" category in Figure GD-2 and Figure GD-3. Weakening of the stabilised clay was observed by Ikegami et al. (2005) in a 30 to 50 mm thick zone near the exterior edge of the treated soil block (Figure 1-47).

The data from these two examples concur with the proposed durability classes. The long-term stability of treated materials of "medium to high potential durability" is verified in the environmental conditions of those two structures. Many years after treatment, strength was significantly higher than shortly after construction. Only minor external deteriorations were observed for the treated clay after 20 years.

The soils tested in this study and from the literature are added in Figure GD-1 (the positions were estimated for site G and site P) with an indication of the potential durability classes

based on porosity accessible to water. The data shows a reasonable agreement with the hypothesised trends in relative potential durability based on the classification of the intial soil.

The data collected in this research for soils treated in the laboratory and in situ indicates that it is possible to define a standardised framework for the assessment of the durability of soils treated by deep mixing. Durability indicators such as porosity accessible to water can be defined and linked to classes of potential durability.

For the construction of new deep mixing structures, performance-based specifications could be proposed according to the environmental conditions and the application.

The definition of these indicators, classes and specifications requires additional experimental data obtained on different soil-cement mixtures (in situ and laboratory) in different conditions. Furthermore, these specifications should be verified by field tests and numerical simulations. This is particularly challenging given the vast number of possible combinations of loading conditions (static loads, dynamic loads) and potential degradation mechanisms (mineralogy of the soil, external chemical attacks, drying, wetting and drying cycles, freezing and thawing cycles).

General conclusions

The present experimental work, part of the French RUFEX research project (Reinforcement and re-use of railway tracks and existing foundations), focused on the properties of soil-cement materials ("soil-mix materials") produced in the laboratory and in situ by wet deep mixing.

The aim of this research was to reach a better understanding of the properties of soil-mix materials and to assess potential factors affecting the durability of treated soils in order to optimise the soil mixing process.
The main objectives of the present study were:

(a) to examine the mechanical properties of soils stabilised in the laboratory in fresh and hardened states,

(b) to compare the results on soils mixed in the laboratory with the properties of soils treated in situ by wet deep mixing (cored and wet-grab samples),

(c) to study the durability of soil-cement mixtures against potential degradation mechanisms by:

- assessing the effectiveness of blastfurnace cement to counter the potential effects of certain chemical compounds on long-term strength and stiffness,
- considering the influence of drying on the properties of treated soils.

To reach these objectives, laboratory tests were performed on different treated soils at different curing times up to 360 days. The soils were mixed with varying quantities of cement and water in the laboratory. The testing program mainly consisted of unconfined compression tests with local strain measurements, indirect tensile strength tests and ultrasonic pulse wave velocity measurements. In addition, specimens of soils treated in situ were taken from four different test sites where soil-cement columns were installed by Soletanche Bachy using the wet deep mixing method.

The shear strength of fresh in situ soil-mix material measured almost immediately after mixing is significantly lower than the strength of the untreated soil due to the destructuration performed by the mixing tool. The yield stress of fresh soil-cement mixtures decreases as moisture content increases.
During the first 7 to 14 days after treatment, a decrease in water content occurs due to cement hydration for treated soils cured in endogenous conditions. Density in the fresh state is close to that of the hardened soil-cement material. The density and total porosity of soil-cement mixtures depend on the initial moisture content. The increase in porosity is approximately linear with moisture content. In general, wet density decreases linearly as moisture content increases. Wet density and porosity remain constant generally constant with time.

After mixing with cement, the strength and stiffness of treated soils progressively develop with curing time. Strength increases more rapidly than stiffness. Empirical correlations (exponential functions of time) based on data measured after short curing times (7 or 28 days) are found to provide reasonable estimates of long-term strength and stiffness growth.

The stress-strain behaviour of soils stabilised with cement is non-linear and stiffness significantly decreases with strain. Non-linearity depends on soil type. It appears to be more pronounced for treated sands than for treated silts. The stress-strain response of treated soils evolves with curing time from "soft soil-like" to "stiff soil/concrete-like" behaviour. Concrete-like behaviour is reached rapidly after 7 days.

The relations between strength, static modulus and dynamic modulus for soils mixed in situ are similar to those obtained for soils mixed in the laboratory:

- Empirical correlations based on strength and wave velocity are proposed to estimate the static modulus and dynamic modulus.
- The relationships between strength and static stiffness are approximately linear whereas non-linear relations are observed between strength and dynamic stiffness. Both compression and shear wave velocities increase non-linearly with strength.
- The dynamic modulus is higher than the static modulus. The dynamic-to-static modulus ratio E_0/E_{50} decreases with strength and curing time from values higher than 10 to a minimum close to 1.

The relations between strength and stiffness depend on soil type and sampling method:

- For a given strength, the static and dynamic stiffness of specimens of treated fine grained soils are lower than those of specimens of stabilised coarse grained soils. This is attributed to the combined effects of porosity and particle deformation.
- For the soils tested in this study, the static and dynamic stiffness of wet-grab samples are generally lower than the stiffness of cored specimens of similar strength. This is also attributed to higher porosity and fine content in wet-grab specimens due to the sampling procedure.

Field specimens contain inclusions of intact soil due to the in situ mixing process. Scatter in strength data of in situ treated soils is attributed to the heterogeneity and type of initial soil, variations in binder distribution, dosage, variations in execution parameters and to the presence of some soil inclusions. Lognormal distributions seem appropriate for the determination of characteristic strength values as reported in the literature. Comparisons between the results on cored specimens of in situ treated silt and the results on homogeneous laboratory specimens indicate that the influence of soil inclusions is strain dependent. The results show that the adverse effect of inclusions is more pronounced on strength than on stiffness.

Numerical analyses suggest that the mechanical parameters derived from tests performed on cored specimens of in situ deep mixed soils are representative of the behaviour of the material composing soil-mix columns.

The durability of soils stabilised with cement is an important concern for the design of permanent deep mixing structures.

The presence of three potential deleterious chemical compounds (calcium sulfate $CaSO_4$, sodium chloride NaCl and diesel) was studied to assess the durability of cement-mixed soils:

- The wet density, total porosity and permeability of treated soils are not affected by the addition of NaCl, $CaSO_4$ or diesel (in the concentrations chosen in this study).
- All the tested soil-cement specimens containing CaSO4, NaCl or diesel hardened and the strength and dynamic modulus of all mixes increased with time.
- However, $CaSO_4$ has an adverse effect on the strength and stiffness of sand treated with Portland cement (CEM I).
- The use of blastfurnace slag cement (CEM III) is found to be effective in preventing the potential deleterious effects of the tested compounds. However, microstructural investigations (scanning electron microscopy and mercury intrusion porosimetry) show that the mixing procedure used in the laboratory can influence the results.
- For all soil-cement mixes with chemical compounds, the relations between strength and stiffness remained valid.

Exposure to different curing conditions has a major effect on the characteristics of treated soils. Specimens of silt and sand stabilised in the laboratory with CEM III cement were placed in different conditions (cycles of wetting and drying, air curing) after 7 or 30 days in water. The small strain shear modulus was monitored using the free-free resonance (FFR) testing method and unconfined compression tests were performed to evaluate the strength and static modulus. The following conclusions can be drawn:

- The tested curing conditions (cycles of wetting and drying, air curing) generally have a disruptive effect on the mechanical properties of treated soils.
- The adverse effect of the exposure to air is more pronounced on stiffness than on strength. The effects on static modulus and dynamic shear modulus are similar.
- Treated sand specimens offer better resistance to drying than treated silt specimens.
- Prolonged curing in water (in this case 30 days in water) somewhat increases the resistance to desiccation. However, the collected data shows an approximately linear decrease in stiffness with decreasing degree of saturation for both tested soils exposed to drying after 30 days.
- In normal atmospheric conditions, carbonation occurs in treated soils exposed to air. Carbonation is found to be a slow process, roughly proportional to the logarithm of time, which depends on the age of the material at the time of exposure to CO_2.

The results concerning the effects of chemical compounds and curing conditions on the mechanical properties of treated soils indicate that a large number of internal and external factors must be taken into account to assess the durability of soil-mix materials.

However, the data gathered in this research shows that it is possible to define a general framework for the assessment of the durability of soils treated by deep mixing. Potential durability classes based on porosity accessible to water are proposed to compare different soil-cement mixtures and show a good agreement with data from the literature.

The following recommendations for the design of deep mixing projects can be formulated based on the results of this study:

- Local strain measurements should be used to determine the static modulus of treated soils.
- E_{50}/q_u ratios can be expected to be higher in coarse grained soils than in fine grained soils.
- Stiffness values determined on wet-grab samples taken at the surface during installation can be assumed slightly conservative (especially for soils with a high coarse fraction).
- Blast furnace slag cement (CEM III) can be used on sites where the tested chemical compounds are present in concentrations similar to those in this study.
- A preliminary assessment of potential durability can be made based on soil classification information collected during the ground investigation.
- For preliminary trials in the laboratory, special attention should be given to the mixing procedures used to study soil treatment with cement and the curing conditions should reproduce those existing in situ as closely as possible.
- Soils treated in the laboratory can be used for preliminary estimations of stiffness.
- The direct correlation between potential indicators and factors controllable during construction point to the possibility of optimising the durability-related properties (indicators) of soil-mix materials within the boundaries imposed by the soil conditions. Using porosity as a potential durability indicator, this can essentially be done by limiting the water content to the minimum possible value required for mixing.

Further research

Complementary experimental data obtained on different soil-cement mixtures (in situ and laboratory) in varying conditions are necessary to select appropriate durability indicators and to define classes associated to specific combinations of loading conditions (static, cyclic or dynamic) and potential degradation mechanisms.

The results from this study, combined with available data from the literature, highlight distinctive trends in terms of strength (compressive and tensile) and stiffness (static and dynamic), specific to soil-mix materials. The data could be used as an empirical database to estimate the characteristics of in situ deep mixed soils. However, relatively large scatter in the compiled data confirms that treated soils are complex materials, with variable mechanical properties that depend on multiple factors. Multi-criteria analyses could be carried out to obtain a quantitative assessment of the impact of these factors. Correlations established in certain conditions cannot be assumed to be systematically valid and must be verified.

Two binders were used in the laboratory. Recent studies have shown that many industrial by-products such as pulverised fuel ash can also provide suitable characteristics when blended with cement. In order to confirm the applicability of the properties and relations described in this research, the relations between strength and stiffness of soils treated with different binders should also be investigated.

Curing conditions can have a significant influence on the characteristics of soils treated with cement. Further research is required to better understand the processes involved. The resistance of soils stabilised by deep mixing to water circulation should be studied. In particular, the circulation of water containing potential deleterious compounds such as sulfates needs to be considered. In the case of drying, advanced laboratory tests such as suction measurements and quantitative methods for the description of crack patterns could be used.
The impact of carbonation on the properties of treated soils exposed to drying was not isolated in this study. Accelerated tests similar to those used for concretes could also be used to assess the effects of carbonation on strength and stiffness.

For deep mixing applications such as foundations and retaining walls, creep (i.e. the gradual increase in strain with time for a constant applied stress) of soil-mix materials is an important parameter which should be studied.

References

Åhnberg, H. (2006a). On yield stresses and the influence of curing stresses on stress paths and strength measured in triaxial testing of stabilised soils. Canadian Geotechnical Journal, 44, 54-66.

Åhnberg, H. (2006b). Consolidation stress effects on the strength of stabilised Swedish soils. Proceedings of the ICE - Ground Improvement, 10(1), 1-13.

Åhnberg, H., Johansson, S.E., Pihl, H. and Carlsson, T. (2003). Stabilising effects of different binders in some Swedish soils. Proceedings of the ICE - Ground Improvement, 7(1), 9-23.

Åhnberg, H., Johansson, S.-E., Retelius, A., and Ljungkrantz, C. (1995). Cement and lime for deep stabilisation of soils—a chemical/physical study of stabilisation effects (in Swedish). (No. 48): Swedish Geotechnical Institute, Linköping.

Åhnberg, H., and Johansson, S. E. (2005). Increase in strength with time in soils stabilised with different types of binder in relation to the type and amount of reaction products. Proceedings of the International Conference on Deep Mixing Best Practice and Recent Advances, Stockholm. Swedish Deep Stabilisation Research Center, Linköping, Sweden, Vol. 1, Vol. 1, 195-202.

Åhnberg, H. and Holmen, M. (2008). Laboratory determination of small-strain moduli in stabilized soils. In Burns, S. E., Mayne, P. W. and Santamaria, J. C. (Eds), Deformational Characteristics of Geomaterials (p. 291–297), Fairfax, VA: IOS Press.

Åhnberg, H. and Holmen, M. (2011). Assessment of stabilised soil strength with geophysical methods. Proceedings of the ICE - Ground Improvement, 164(3), 109-116.

ACI 318-05. (2005). Building code requirements for structural concrete and commentary. ACI Farmington Hills: Mich.

AFNOR. (1998). NF P94-068 Soils: investigation and testing. Measuring of the methylene blue adsorption capacity of à rocky soil. Determination of the methylene blue of à soil by means of the stain test.

AFNOR. (1999a). NF P94-100 Soils : investigation and testing - Lime and/or hydraulic binder treated materials - Test for determining the treatment ability of a soil.

AFNOR. (1999b). NF P 94-150-1 Essai statique de pieu isolé sous charge axiale Partie I – En compression.

AFNOR. (2000a). NF P 94-110-1, Essai pressiométrique Ménard.

AFNOR. (2000b). XP P94-105 Contrôle de la qualité du compactage Méthode au pénétromètre dynamique à énergie variable - Principe et méthode d'étalonnage du pénétromètre — Exploitation des résultats – Interprétation.

AFNOR. (2001). NF EN 197-1 - Ciment - Partie 1 : composition, spécifications et critères de conformité des ciments courants.

AFNOR. (2003a). NF EN 13286-41: Unbound and hydraulically bound mixtures - Part 41 : test method for the determination of the compressive strength of hydraulically bound mixtures.

AFNOR. (2003b). NF EN 13286-42: Unbound and hydraulically bound mixtures - Part 41: test method for the determination of the indirect tensile strength of hydraulically bound mixtures.

AFNOR. (2003c). EN 13286-43: Unbound and hydraulically bound mixtures - Part 43: Test method for the determination of the modulus of elasticity of hydraulically bound mixtures.

AFNOR. (2005). NF EN 14679 :2005-09 Exécution de travaux géotechniques spéciaux – Colonnes de sol traité.

Ajorloo, A., Mroueh, H., Lancelot, L. (2012). Experimental Investigation of Cement Treated Sand Behavior Under Triaxial Test. Geotechnical and Geological Engineering, 30(1), 129-143.

Alen, C., Baker, S., Ekström, J., Hallingberg, A., Svanand, V. and Sällfors, G. (2005). Test Embankments on Lime/Cement Stabilized Clay. Proceedings of the International Conference on Deep Mixing Best Practice and Recent Advances, Stockholm. Swedish Deep Stabilisation Research Center, Linköping, Sweden, Vol. 1, 213-220.

Al-Tabbaa, A., and Evans, C. (2003). Deep soil mixing in the UK: geoenvironmental research and recent applications. Land Contamination & Reclamation, 11, 1-14.

Al-Tabbaa, A. (2005). State of practice report - stabilisation/solidification of contaminated materials with wet deep soil mixing. Proceedings of the International Conference on Deep Mixing Best Practice and Recent Advances, Stockholm. Swedish Deep Stabilisation Research Center, Linköping, Sweden, 697-731.

Al-Tabbaa, A., Barker, P. and Evans, C. W. (2009). Innovation in soil mix technology for remediation of contaminated land. International Symposium on Soil Mixing and Admixture Stabilisation, 19-21 may, Okinawa, Japan.

Al-Tabbaa, A., and King, S. D. (1998). Time effects of three contaminants on the durability and permeability of a solidified sand. Environmental technology, 19(4), 401-407.

Andromalos, K. B. and Bahner, E. W. (2003). The Application of Various Deep Mixing Methods for Excavation Support Systems. Grouting and Ground Treatment, ASCE, Geotechnical Special Publication. 120, 515–526.

Asaka, A. and Abe, T. (2011). Non-destructive technique for assessing cement-treated ground Proceedings of the ICE - Ground Improvement, 164(3), 179 –187.

Asano, J., Ban, K., Azuma, K. and Takahashi, K. (1996). Deep Mixing Method of Soil Stabilisation Using Coal Ash. Proceedings, IS-Tokyo '96/2nd International Conference on Ground Improvement Geosystems, Tokyo, 1, 393-398.

ASTM. American Society for Testing and Materials (2005). D559-03 Standard Test Methods for Wetting and Drying Compacted Soil-Cement Mixtures.

ASTM American Society for Testing and Materials. (2006). C597-02 Standard test method for pulse velocity through concrete. ASTM, Easton.

Atkinson, J.H. (2000). Non-linear soil stiffness in routine design. Geotechnique, 50(5), 487–508.

Atkinson, J.H. and Sallfors, G. (1991). Experimental determination of soil properties. General Report to Session 1. Proceedings of the 10th ECSMFE, Florence, 3, 915-956.

Bahador, M. and Pak, A. (2011). Small-Strain Shear Modulus of Cement-Admixed Kaolinite, Geotechnical and Geological Engineering, 30(1), 163-171.

Bahner, E. W. and Naguib, A. M. (2000). Ground Improvement for Large Above Ground Tanks Using Deep Mixing. Proceedings of Sessions of Geo Denver 2000, 264-280.

Baker, S. (2000). Deformation Behaviour of Lime/Cement Column Stabilized Clay. Swedish Deep Stabilization Research Centre, Linköping, Report 7, 203.

Barnes, H.A. and Walters, K. (1995). The yield stress myth? Rheologica Acta, 24(4), *323-326.*

Barnes, H. A. (1999). The yield stress–a review or–everything flows? Journal of Non–Newtonian Fluids Mechanics, 81(1-2), 133–178.

AFGC. (2007). Concrete design for a given structure service life – durability management with regard to reinforcement corrosion and alkalisilica reaction. State-of-the-art and guide for the implementation of a predictive performance approach based upon durability indicators, AFGC Scientific and Technical Documents (AFGC, Paris, issue in French: 2004, issue in English:), 240 p.

Baroghel-Bouny, V. (2005). Nouvelle approche de la durabilité du béton. Indicateurs et méthodes. Techniques de l'Ingénieur C2245.

Baroghel-Bouny, V. (2008). Development of a global, performance and predictive approach of durability of (reinforced) concrete structures on the basis of durability indicators – results and perspectives. Characterization of the microstructure of concretes, study of their moisture and transport properties, assessment of free deformations and service life prediction (in French), LPC studies and researches, OA 63 (LCPC, Paris), 311 p.

Benhamou, L. and Mathieu, F. (2012). Geomix Caissons against liquefaction Proceedings of the International symposium of ISSMGE - TC211. Recent research, advances & execution aspects of ground improvement works. 31 May-1 June 2012, Brussels, Belgium, Vol. 3, 33-40.

Besq, A., Malfoy, C., Pantet, A., Monnet, P. and Righi, D. (2003). Physicochemical characterization and flow properties of some bentonite muds. Applied Clay Science, 23(5-6), 275–286.

Bhadriraju, V., Puppala, A. J., Madhyannapu, R. J., and Williammee, R. (2008). Laboratory Procedure to Obtain Well-Mixed Soil Binder Samples of Medium Stiff to Stiff Expansive Clayey Soil for Deep Soil Mixing Simulation. Geotechnical Testing Journal, 31(3), 225-238.

Bouazza, A., Kwan, P. S., and Chapman, G. (2004). Strength Properties of Cement Treated Coode Island Silt by the Soil Mixing Method. Proc. Geotechnical Engineering for Transportation Projects, ASCE press, 1421-1428.

Broms, B. (1999). Keynote lecture: Design of lime, lime/cement and cement columns. Proceedings of the International Conference on Dry Mix Methods for Deep Soil Stabilisation, 125-153.

Broms, B. (2004). Lime and lime/cement columns. In Moseley, M. P. and Kirsch, K. (Eds.), Ground Improvement (252-331), 2nd Edition. London: Spon Press Taylor & Francis Group.

Bruce, D. A., and Bruce, M. E. (2004). The Practitioner's Guide to Deep Mixing Grouting and Ground Treatment (GSP 120) Proceedings of 3rd International Specialty Conference on Grouting and Ground Treatment.

Bruce, D. A., Bruce, M. E. C. and DiMillio, A. F. (1998). Deep mixing methods: A global perspective. Civil Engineering, ASCE, 68(12), 38-41.

Bruce, D. A., Bruce, M. E. C. and DiMillio, A.F. (1999). Dry Mix Methods: A Brief Overview of International Practice. Dry Deep Mix Methods for Deep Soil Stabilization, Proceedings of the International Conference on Dry Deep Mix Methods for Deep Soil Stabilization, Ed. by H. Bredenberg, G. Holm, and B. Broms, Stockholm, Sweden, October 13-15, 15-25.

Bruce, D. A., Bruce, M. E. C. and DiMillio, A.F. (2000). Deep Mixing: QA/QC and Verification Methods. Grouting Sol Improvement, Geosystems Including Reinforcement. Proceedings of the 4th International Conference on Ground Improvement Geosystems. Finnish Geotechnical Society, Helsinki, Finland, June 7-9, 11-22.

Bruce, D. A., Bruce, M. E. C. and DiMillio, A.F. (2001). Deep Mixing Method: An International Overview of Technology, Testing and Product. Proceedings of the 15th International Conference on Soil Mechanics and Geotechnical Engineering, Istanbul, Turkey, August 27-31, Vol. 4.

Bruce, D. A., and Bruce, M. E. C. (2003). The Practitioner’s Guide to Deep Mixing. Grouting and Ground Treatment, Proceedings of the Third International Conference, Geotechnical Special Publication, 120, 475-488.

Burlion, N., Bourgeois, F. and Shao, J.F. (2005). Effects of desiccation on mechanical behaviour of concrete. Cement and Concrete Composites, 27, 367–379.

Butcher, A. P. (2005). The durability of deep wet mixed columns in an organic soil. Proceedings of the International Conference on Deep Mixing Best Practice and Recent Advances, Stockholm. Swedish Deep Stabilisation Research Center, Linköping, Sweden.

Cavey, J., Johnsen, L. F. and DiStas, J. (2004). Deep Soil Mixing for Foundation Support of a Parking Garage. Proceedings of GeoSupport Conference January 29–31, Orlando, Florida, USA.

CDIT. (2002). The Deep Mixing Method - Principle, Design and Construction. Coastal Development Institute of technology. Lisse: A. A. Balkema.

CEN (European Committee for Standardization). (2005a). ISO/TS 17892-1: Geotechnical investigation and testing - Laboratory testing of soil - Part 1 : determination of water content.

CEN (European Committee for Standardization). (2005b). ISO/TS 17892-4: Geotechnical investigation and testing - Laboratory testing of soil - Part 4 : determination of particle size distribution.

CEN (European Committee for Standardization) (2005c). ISO/TS 17892-10: Geotechnical investigation and testing - Part 10 : direct shear tests.

CEN (European Committee for Standardization) (2005d). ISO/TS 17892-12: Geotechnical investigation and testing - Laboratory testing of soil - Part 12: determination of Atterberg limits.

Chu, J., Varaskin, S., Klotz, U. and Mengé, P. (2009). Construction Processes, Proceedings of the 17th International Conference on Soil Mechanics and Geotechnical Engineering, 5-9 October 2009, Alexandria, Egypt, M. Hamza et al. (Eds.), IOS Press, Amsterdam, Vol. 4, 3006-3135.

Clayton, C. R. I. (2011). Stiffness at small strain: research and practice. Geotechnique, 61(1), 5–37.

Consoli, N. C., Cruz, C. R., Floss, M. F. and Festugato, L. (2010). Parameters Controlling Tensile and Compressive Strength of Artificially Cemented Sand. Journal of Geotechnical and Geoenvironmental Engineering, 136(5), 759-763.

Consoli, N. C., Foppa, D., Festugato, L., and Heineck, K. S. (2007). Key Parameters for Strength Control of Artificailly Cemented Soils. Journal of Geotechnical and Geoenvironmental Engineering,133(2), 197-205.

Corte, A. and Higashi, A. (1960). Experimental Research on Desiccation Cracks in Soil, Research Report 66: U.S. Army Snow Ice and Permafrost Research Establishment, Wilmette, Illinois.

Coussot, P., 1997, Mudflow Rheology and Dynamics, Balkema, Rotterdam.

Coussot, P. and Ancey, C. (1999). Rhéophysique des pâtes et des supensions, EDP Sciences.

Coussot, P., Proust, S. and Ancey.C. (1996). Rheological interpretation of deposits of yield stress fluids. Journal of Non-Newtonian Fluid Mechanics, 66(1), 55–70.

Cruz, R. B., Knop, A., Heineck, K. S. and Consoli, N. C. (2004) Encapsulation of a soil contaminated by hydrocarbons. Amélioration des sols en place. In Dhouib, Magnan et Mestat (ed.) Amélioration des sols en place. Paris : Presses de l'ENPC/LCPC.

Cuira, F., Costa d'Aguiar, S., Grzyb, A. Mosser, J.F., Guimond-Barrett, A. and Le Kouby, A. (2013). Modélisation numérique du comportement d'une colonne de soil-mixing Confrontation à un essai de chargement en vraie grandeur. Proceedings Proceedings of the 18th International Conference on Soil Mechanics and Geotechnical Engineering, Paris 2013.

Cuisinier, O., Le Borgne, T., Deneele, D. and Masrouri, F. (2011). Quantification of the effects of nitrates, phosphates and chlorides on soil stabilization with lime and cement. Engineering Geology, 117(3-4), 229-235.

Denies, N., Huybrechts, N., De Cock, F., Lameire, B., Vervoort, A., Van Lysebetten, G. and Maertens, J. (2012a). Soil Mix walls as retaining structures – Belgian practice. Proceedings of the International symposium of ISSMGE - TC211. Recent research, advances & execution aspects of ground improvement works. 31 May-1 June 2012, Brussels, Belgium, Vol. 3, 83-98.

Denies, N., Huybrechts, N., De Cock, F., Lameire, B., Vervoort, A., Van Lysebetten, G. and Maertens, J. (2012b). Soil Mix walls as retaining structures – mechanical characterization. International symposium of ISSMGE - TC211. Recent research, advances & execution aspects of ground improvement works. 31 May-1 June 2012, Brussels, Belgium, Vol. 3, 99-117.

Doebling, S.W., Farrar, C.R., and Prime, M.B. (1998). A Summary Review of Vibration-Based Damage Identification Methods, Shock and VibrationDigest, 30, 91–105.

Dupas, J. and Pecker, A. (1979). Static and Dynamic Properties of Sand Cement, Journal of Geotechnical Engineering Division, 105, 419–436.

Eurocode. (2006). Basis for Design. Comite European de normalisation (CEN), Brussels, Belgium.

EuroCode 2. (2005). Design of concrete structures. EN-1992-2, Comite European de normalisation (CEN), Brussels, Belgium; 2005.

EuroSoilStab. (2002). Development of Design and Construction Methods to Stabilise Soft Organic Soils. Design Guide Soft Soil Stabilisation. European Commission, Brussels, Belgium, CT97-0351. Project No. BE-96-3177, Brite-EuRam III. 95 pages.

Ekberg, A. and Paulsson, B. (2010). INNOTRACK Concluding technical report. International Union of Railways, Paris.

Escadeillas, G., and Hornain, H. (2008). Chapitre 12. La durabilité des bétons vis-à-vis des environnements chimiques aggressifs. In J.-P. OLLIVIER and A. VICHOT (Eds.), LA DURABILITÉ DES BÉTONS. Paris: Presses de l'école des Ponts et Chaussées.

Fardis, M., Papavassiliou, G. Abulnasr, L. Miljkovic, L. Rumm, R.J. Milia, F. Chaniotakis, E. and Frangoulis, D. (1994). Effect of clay minerals on the hydration of cement An NMR study. Advanced Cement Based Materials, 1(6), 243-247.

FHWA. (2000). An introduction to the Deep Soil Mixing Methods as Used in Geotechnical applications: Report from Geosystems for US Department of transportation Federal Highway Administration. FHWA-RD-99-138.

Futaki, M., Nakano, K., and Hagino, Y. (1996). Design Strength of Soil-Cement Columns as Foundation Ground for Structures, Proceedings, IS-Tokyo '96/2nd International Conference on Ground Improvement Geosystems, Tokyo, Vol. 1, 481–484.

Galaa, A. M., Thompson, B.D, Grabinsky, M. W. and Bawden, W. F. (2011). Characterizing stiffness development in hydrating mine backfill using ultrasonic wave measurements Canadian Geotechnical Journal, 48 (8), 1174-1187.

Ganne, P., Huybrechts, N., De Cock, F., Lameire, B., and Maertens, J. (2010). SOIL MIX Walls as Retaining Structures—Critical Analysis of the Material Design Parameters. Proceedings of the International Geotechnical Conference Geotechnical Challenges in Megacities, Vol. 3, Moscow, Russia, June 7–10, GRF, 991–998.

Goto, S., Tatsuoka, F., Shibuya, S., Kim, Y.S. and Sato, T. (1991). A simple gauge for local small strain measurements in the laboratory. Soils and Foundations, 31(1), 169-180.

Goto, T., Shimizu, K. and Chaen, T. (2000). Quality estimation of deep mixing columns by pile integrity tester. Proc. 4th GIGS, Helsinki, 31-38.

Harris, J.P., Sebesta, S., Scullion, T. (2004). Hydrated lime stabilization of sulfate-bearing vertisols in Texas. Transportation Research Record 1868, 31–39.

Hayashi, H., Nishikawa, J., Ohishi, K., and Terashi, M. (2003). Field observation of long-term strength of cement treated soils. Proceeding of the 3rd International Conference on Grouting and Ground Treatment. ASCE. New Orleans, USA, 598-609.

Hewlett, P. C. (2003). Lea's chemistry of Cement and Concrete (4th edition). Elsevier Ltd.

Hershel, W. M. and Bulkley, R. (1926). Measurement of consistency as applied to rubber-benzene solutions, Proc Amer Soc Testing Materials. 26(2).

Hilbrich, S. L. and Scullion, T. (2007). Rapid alternative for laboratory determination of resilient modulus input values on stabilized materials for AASHTO mechanistic-empirical guide, Transport Research Record, 2026, 62–69.

Hirabayashi, H., Yaguchi, H., Tokunaga, S., Shinkawa, N., Fujita, T., Inagawa, H. and Yasuoka, N. (2009). Laboratory Mixing Test on Cement Slurry Preparation, Specimen Preparatoin and Curing Temperature Proceedings of the International Symposium on Deep Mixing and Admixture Stabilisation, May 19-21, Okinawa.

Hird, C.C. and Chan, C.M. (2005). Correlation of shear wave velocity with unconfined compressive strength of cement-stabilised clay, Proceedings of the International Conference on Deep Mixing Best Practice and Recent Advances, Stockholm. Swedish Deep Stabilisation Research Center, Linköping, Sweden. Vol. 1, 79-85.

Holm, G. (1999). Keynote lecture: Applications of Dry Mix Methods for deep soil stabilization. Proceedings of the International Conference on Dry Mix Methods for Deep Soil Stabilisation, 3-13.

Holm, G. (2000). Deep Mixing. Soft Ground Technology, ASCE, Geotechnical Special Publication, 112, 105–122.

Holm, G., Andréasson, B., Bengtsson, P. E., Bodare, A. and Eriksson, H. (2002). Mitigation of track and ground vibrations by high speed trains at Ledsgard. Swedish Deep Stabilization Research Centre, Linköping, Report 10, 56.

Horpibulsuk, S., Miura, N. and Nagaraj, S., T. (2003). Assessment of strength development in cement-admixed high water content clays with Abrams' law as a basis. Geotechnique, 53(4).

Horpibulsuk, S., Katkan, W., Sirilerdwattana, W. and Rachan, R. (2006). Strength development in cement stabilized low plasticity and coarse grained soils: laboratory and field study. Soils and Foundations, 46(3), 351–366.

Horpibulsuk, S., Phojan, W., Suddeepong, A., Chinkulkijniwat, A. and Liu, M. D. (2012). Strength development in blended cement admixed saline clay. Applied Clay Science, 55, 44-52.

Hoyos, L. R., Puppala, A. J. and Chainuwat, P. (2004). Dynamic Properties of Chemically Stabilized Sulfate Rich Clay. Journal of Geotechnical and Geoenvironmental Engineering, 130(2), 153-162.

Hsi, H.-R. and Clifton, D. F. (1962) Flocculation of selected clays by various electrolytes: Clays and Clay Minerals, 9th Conf., Pergamon Press, N.Y., 269-276.

Hunter, D. (1988). Lime induced heave in sulfate bearing clay soils. Journal of Geotechnical Engineering 114, 150–167.

Ikegami, M., Ichiba, T., Ohnishi, K. and Terashi, M. (2005). Long-term properties of cement treated soil 20 years after construction. Proceedings of the 16th International Conference on Soil Mechanics and Geotechnical Engineering (Osaka), 1199-1202.

Janz, M. and Johansson, S.-E. (2002). The Function of Different Binding Agents in Deep Stabilization. Swedish Deep Stabilization Research Centre, Report 9.

Jardine, R. J., Symes, M. J. and Burland, J. B. (1984). The measurement of soil stiffness in the triaxial apparatus. Geotechnique, 34(3), 323–340.

Kan,L. L. and Shi, H.-S. (2012). Investigation of self-healing behavior of Engineered Cementitious Composites (ECC) materials, Construction and Building Materials, 29, 348-356.

Kamon, M. (1996). Effect of grouting and DMM regarding big construction projects and the 1995 Hyogoken-Nambu Earthquake. IS-Tokyo 1996. 5-21.

Kasali, G. and Taki, O. (2003). Design and Construction Aspects of Soil Cement Columns as Foundation Elements. Proceedings of 3rd International Specialty Conference on Grouting and Ground Treatment, 540-551.

Kawasaki, T., Niina, A., Saitoh, S. S., Y., and Honjyo, Y. (1981). Deep mixing method using cement hardening agent. Proc. of the 10th Internal Conference on Soil Mechanics and Foundation Engineering, 3, 721-724.

Khan, Z., Majid, A., Cascante, G., Hutchinson, D.J., and Pezeshkpour, P. (2006). Characterization of a cemented sand with the pulse-velocity method. Canadian Geotechnical Journal, 43(3), 294–309.

Kitazume, M., Nakamura, T., Terashi, M. and Ohishi, K. (2003). Laboratory tests on long-term strength of cement treated soil. Proceeding of the 3rd International Conference on Grouting and Ground Treatment. ASCE. New Orleans, USA, 586-597.

Kitazume, M. (2005). State of Practice Report: Field and laboratory investigation, properties of binders and stabilised soils. Proceedings of the International Conference on Deep Mixing Best Practice and Recent Advances, Stockholm. Swedish Deep Stabilisation Research Center, Linköping, Sweden.

Kitazume, M., Nishimura, S., Terashi, M. and Ohishi, K. (2009). International Collaborative Study Task 1: Investigation into Practice of Laboratory Mix Tests as Means of QC/QA for Deep Mixing Method. Proceedings of the Internation Symposium on Deep Mixing and Admixture Stabilisation, May 19-21, Okinawa.

Kodikara, J. K., Barbour, S. L. and Fredlund, D. G. (2000). Desiccation cracking of soil layers. Unsaturated soils for Asia. Proceedings of the Asian Conference on Unsaturated Soils, UNSAT-ASIA, Singapore, 18-19 May, 693-698.

Konstantelias, S., Ghataora, G. Brough, M. Stirlingand, A. and Madelin, K. (2002). Soil/Grout mixing auger trial at Leominster Herefordshire - A case study. Proceedings of the international conference on railway engineering, London, 3-4 July.

Lade, P.V., Liggio, C.D. and Yamamuro, J.A. (1998). Effects of non-plastic fines on minimum and maximum void ratio of sand. Geotechnical Testing Journal, 21, 336–347.

Lagaly. G. (1989). Principles of flow of kaolin and bentonite dispersions. Applied Clay Science, 4(2), 105–123.

Lakshmikantha, M. R., Prat, P. C. and Ledesma, A. (2012). Experimental evidence of size effect in soil cracking, Canadian Geotechnical Journal, 49(3), 264-284.

Larsson, S. (2003). Mixing Processes for Ground Improvement by Deep Mixing: KTH, Sweden.

Larsson, S. (2005). State of practice report - execution, monitoring and quality control. Proceedings of the International Conference on Deep Mixing Best Practice and Recent Advances, Stockholm. Swedish Deep Stabilisation Research Center, Linköping, Sweden,Vol. 2, 732-786.

Larsson, S., Rothhämel, M., and Jacks, G. (2009). A laboratory study on strength loss in kaolin surrounding lime-cement columns. Applied Clay Science, 44(1-2), 116-126.

LCPC-SETRA. (1992). GTR guide technique pour la réalisation des remblais et des couches de forme. Laboratoire Central des Ponts et Chaussées, Paris, France.

Lebon, S. P. (2005). Keynote lecture-New Methods in European Deep Mixing-A contractor's perspective on the developing challenges of execution. Proceedings of the International Conference on Deep Mixing Best Practice and Recent Advances, Stockholm. Swedish Deep Stabilisation Research Center, Linköping, Sweden.

Le Kouby, A., Bourgeois, E. and Rocher-Lacoste, F. (2008). Subgrade improvement method for existing railway lines – an experimental and numerical study. Electronic Journal of Geotechnical Engineering, 15, 461-494.

Le Runigo, B. Ferber, V., Cui, Y.-J., Cuisinier, O. and Deneele, D. (2011). Performance of lime-treated silty soil under long-term hydraulic conditions. Engineering Geology, 118(1–2), 20-28.

Löfroth, H. (2005). Properties of 10-year-old lime–cement columns. Proceedings of the International Conference on Deep Mixing Best Practice and Recent Advances, Stockholm. Swedish Deep Stabilisation Research Center, Linköping, Sweden,Vol. 1, 119–127.

Lorenzo, G. and Bergado, D. (2006). Fundamental Characteristics of Cement-Admixed Clay in Deep Mixing. Journal of Material in Civil Engineering, 18, 161–174.

Madhyannapu, R., Puppala, A. J., Nazarian, S. and Yuan, D. (2010). Quality Assessment and Quality Control of Deep Soil Mixing Construction for Stabilizing Expansive Subsoils, Journal of Geotechnical and Geoenvironmental Engineering, 136(1), 119-128.

Mair, R. J. (1993). Developments in geotechnical engineering research: applications to tunnels and deep excavations. Unwin Memorial Lecture 1992. Proceeding of the ICE, 97(1) : 27-41.

Mesbah H. A., Lachemi M. and Aitcin P.-C. (2002) Determination of elastic properties of high performance concrete at early ages. ACI Mater J, 99(1), 37–41.

Mishra, A., Ohtsubo, M., Li, L., Higashi, T., and Park, J. (2009). Effect of salt of various concentrations on liquid limit, and hydraulic conductivity of different soil-bentonite mixtures. Environmental Geology, 57(5), 1145-1153.

Mitchell, J. K. (1986). Practical problems from surprising soil behavior. Journal of the Geotechnical Engineering Division 112, 259–289.

Mitchell, J.K. and Dermatas, D. (1992). Clay soil heave caused by lime sulfate reactions. ASTM Standard Technical Publication, Innovation and Uses for Lime, STP 1135, 41–64.

Miura, N., Horpibulsuk, S. and Nagaraj, T.S., 2001. Engineering behavior of cement stabilized clay at high water content. Soil. Found. 41(5), 33–45.

Modmoltin, C. and Voottipruex, P. (2009). Influence of salts on strength of cement-treated clays. Ground Improvement, 162, 15–26.

Mosser, J-F. and Mathieu, F. (2011). SPRINGSOL Soil mixing avec outil ouvrant, Travaux, 885, 38-40.

Müller, M., Tyrach, J., Brunn, P.O., 1999, Rheological characterization of machine-applied plasters.ZKG Int 52.

Nagaraj, T. S., Miura, N., and Yamadera, A. 1998, Induced Cementation of Soft Clay. Proceedings of the International Symposium on Lowland Technology, Saga University, Japan, Institute of Lowland Technology, Saga, Japan, 267–278.

Nakamura, M., Matsuzawa, S., and Matsushita, M. (1982). Study of the agitation mixing of improvement agents (in Japanese). Proc. of the 17th Japan National Conference on Soil Mechanics and Foundation Engineering, 2, 2585-2588.

Namkoong W., Hwang E. Y., Park J. S. and Choi J.Y. (2002). Bioremediation of diesel-contaminated soil with composting. Environ Pollut, 119(1), 23-31.

Nazarian, S., Yuan, D. and Tandon, V. (1999). Structural field testing of flexible pavement layers with seismic methods for quality control, Transp. Res. Rec., 1654, 50–60.

Nishibayashi, K., Matsuo, T., Hosoya, Y. and Kohinata, T. (1988). Studies of getting low improving strength of deep mixing method for latter excavation (Part 2) – Investigation the method by model mixing tests. 23rd Annual Meeting, Japanese Society of Soil Mech. and Found. Engng., 2297-2300 (in Japanese).

Nishikawa, J., Tada, S. and Yamaguchi, S. (1996). Strength evaluation based on logging in ground stabilized by deep mixing method. Proc. of the IS-Tokyo´96, Tokyo, 649-652.

Onimaru, S., Suzuki, Y., Hijikata, K., Sugiyama, T., Isida, T. and Saitoh, S. (2009). Aging Effects of High Strength Improved Soil by Deep Cement Mixing Method. Proceedings of the Internation Symposium on Deep Mixing and Admixture Stabilisation, May 19-21, Okinawa.

Olsson, M., Edstamand, T. and Alén, C. (2008). Some experiences from full scale test embankments on floating lime-cement columns. Proceedings of the Second International workshop on Geotechnics of soft soils (Karstunen, M. and Leoni, M. (eds.)). London: Taylor and Francis, 77–85.

Osman, A. and Al-Tabbaa, A. (2009). Effect of cement-zeolite grouts on the durability of stabilised clays. In: XVII International Conference on Soil Mechanics and Geotechnical Engineering, 5-10-2009 to 9-10-2009, Alexandria, Egypt.

Page, C. L. and Page M. M. (2007). Durability of concrete and cement composites. Woodhead Publishing Ltd, Cambridge.

Panesar, D. K. and Shindman, B. (2011). Elastic properties of self consolidating concrete, Construction and Building Materials, 25(8), 3334-3344.

Pantet, A. and Monnet, P. (2007). Liquid–solid transition of kaolinite suspensions, Mechanics of Materials, 39(9), 819–833.

Perera, A. S. R., Al-Tabbaa, A., Reid, J. M., and Johnson, D. (2005). State of practice report UK stabilisation/solidification treatment and remediation, Part V: Long-term performance and environmental impact. Proceedings of the International Conference on Stabilisation/Solidification Treatment and Remediation, April, Cambridge, UK, 437-457.

Porbaha, A., Tanaka, H. and Kobayashi, M. (1998). State of the art in deep mixing technology: Part II. Applications. Proceedings of the ICE - Ground Improvement, 2, 125-139.

Porbaha, A. (1998). State of the art in deep mixing technology: Part I. Basic concepts and Overview. Proceedings of the ICE - Ground Improvement, 2(2), 81-92.

Porbaha, A., Shibuya, S. and Kishida, T. (2000). State of the art in deep mixing technology. Part III: geomaterial characterization. Proceedings of the ICE - Ground Improvement, 4(3), 91-110.

Porbaha, A. (2002). State of the art in quality assessment of deep mixing technology. Proceedings of the ICE - Ground Improvement, 6(3), 95-120.

Porbaha, A., Ghaheri, F. and Puppala, A.J. (2005). Soil cement properties from borehole geophysics correlated with laboratory tests, Proceedings of the International Conference on Deep Mixing Best Practice and Recent Advances, Stockholm. Swedish Deep Stabilisation Research Center, Linköping, Sweden, Vol. 1, 605-611.

Puppala, A.J., Kadam, R., Madhyannapu, R. and Hoyos, L. (2006). Small Strain Shear Moduli of Chemically Stabilized Sulfate Bearing Cohesive Soils. Journal of Geotechnical and Geoenvironmental Engineering, 132(3), 322-336.

Puppala, A., Intharasombat, N., & Vempati, R. (2005). Experimental Studies on Ettringite-Induced Heaving in Soils. Journal of Geotechnical and Geoenvironmental Engineering, 131(3), 325-337.

Puppala, A. J. and Porbaha, A. (2004). International perspectives on quality assessment of deep mixing. ASCE, Geotechnical Special Publication,124, 826-837.

Rabbi A. T., Kuwano, J., Deng, J. and Boon, T. W. (2011). Effect of Curing Stress and Period on the Mechanical Properties of Cement-mixed Sand, Soils and Foundations, 51(4), 651-661.

Rajasekaran, G., Murali, K. and Srinivasaragahvan, S. (1997). Effect of chlorides and sulfate on lime treated marine clays. Soils and Foundations, 37, 105–115.

Reiffsteck, P. (2007). Influence de la répartition granulométrique sur le comportement mécanique d'un sol. Bulletin de liaison des laboratoires routiers des Ponts et Chaussées, 268–269, 83–103.

Roussel, N. (2005). Steady and transient flow of fresh cement pastes, Cement and concrete research, 35(9), 1656–1664.

Rutherford, C. J., (2004). Design Manual for Excavation Support Using Deep Soil Mixing, M.S. Thesis, Texas A&M University, College Station, TX.

Ryan, C. R. and Jasperse, B. H. (1989). Deep Soil Mixing at Jackson Lake Dam. Proceedings of the ASCE 1989 Foundation Engineering Congress, Foundation Engineering: Current Principles and Practices, Evanston, Illinois.

Ryden, N., Ekdahl, U. and Lindh, P. (2006). Quality control of cement stabilised soils using on-destructive seismic tests, In Advanced testing of fresh cementitious materials, Lecture 34, 1–5. Stuttgart, Germany: Inst. fur Werkstiffe im Bauwesen Universiteit.

Saitoh, S., Nishioka, S., Suzuki, Y. and Okumura, R. (1996). Required strength of cement improved ground, Proceedings of the Second International Conference on Ground Improvement, Geosystems, Grouting and Deep Mixing, Tokyo, Japan, 481- 484.

Schatzmann., M., Bezzola, G. R., Minor, H.-E., Windhab E. J. and Fischer, P. (2009). Rheometry for large particulated fluids: analysis of the ball measuring system and comparison to debris flow rheometry, Rheologica acta, 48(7).

Shao, Y. Macari, E. J. and Cai, W. (2005). Compound Deep Soil Mixing Columns for Retaining Structures in Excavations. Journal of Geotechnical and Geoenvironmental Engineering, 131(11), 1370-1377.

Shibuya, S., Tatsuoka, F., Teachavorasinskun, S., Kong, X.J., Abe, F., Kim, Y-S. and Park, C-S. (1992). Elastic deformation properties of geomaterials. Soils and Foundations, 32(3), 26-46.

Shihata, S. A. and Baghdadi, Z. A. (2001). Long-Term Strength and Durability of Soil Cement. Journal of Materials in Civil Engineering, 13(3), 161-165.

Shinkawa, N., Nozu, M., and Inagaki, M. (2009). Long-Term Strength of Columns with DJM Method. Proceedings of the Internation Symposium on Deep Mixing and Admixture Stabilisation, May 19-21, Okinawa.

Skoczylas, F., Burlion, N. and Yurtdas, I. (2007). About drying effects and poro-mechanical behaviour of mortars. Cement and Concrete Composites, 29(5), 383-390.

Stawiński, J. Wierzchoś, J. and Garcia-Gonzalez, M.-T. (1990). Influence of Calcium and Sodium Concentration on the Microstructure of Bentonite and Kaolin. Clays and Clay Minerals, 38, 617-622.

Stewart, M. E., Navin, M. P. and Filz, G. M. (2004). Analysis of column-supported test embankment at the I-95 route 1 interchange. ASCE Geotechnical Special Publication Geotechnical Engineering for Transportation Projects, Geo-Trans 2004, 1337-1346.

Szymkiewicz, F. (2011). Evaluation des propriétés mécaniques du matériau Soil-Mixing (PhD Thesis). Paris: Université Paris-Est.

Szymkiewicz, F., Guimond-Barrett, A., Le Kouby, A. and Reiffsteck, P. (2012). Influence of grain size distribution and cement content on the strength and aging of treated sandy soils. European Journal of Environmental and Civil Engineering, 16(7), 882-902.

Szymkiewicz, F. (2011). Evaluation des propriétés mécaniques du matériau Soil-Mixing, PhD, Université Paris-Est.

Taki, O. and Yang, D. S. (1991). Soil-cement mixed wall technique. American Society of Civil Engineers, Proceedings, Geotechnical Engineering Congress, Denver, 298-309.

Tan, T. S., Goh, T. L., and Yong, K. Y. (2002). Properties of Singapore marine clays improved by cement mixing. Geotechnical Testing Journal, 25(4), 422–433.

Tang, A. M., Vu, M. N. and Cui, Y. J. (2011a). Effects of the maximum soil aggregates size and cyclic wetting-drying on the stiffness of a lime-treated clayey soil. Géotechnique, 61(5), 421-429.

Tang, C. S., Cui, Y. J., Shi, B., Tang, A. M. and Liu, C. (2011b). Desiccation and cracking behaviour of clay layer from slurry state under wetting-drying cycles. Geoderma, 166, 111-118.

Targan, Å., Olgun, A., Erdogan, Y., and Sevinc, V. (2002). Effects of supplementary cementing materials on the properties of cement and concrete. Cement and Concrete Research, 32(10), 1551-1558.

Tatsuoka, F., Kohata, Y., Uchida, K., and Imai, K. (1996). Deformation and Strength Characteristics of Cement-Treated Soils in Trans-Tokyo Bay Highway Project, Proceedings, IS-Tokyo '96/2nd International Conference on Ground Improvement Geosystems, Tokyo: Vol. 1, 453–459.

Tatsuoka, F., Uchida, K., Imai, K., Ouchi, T., and Kohata, Y. (1997). 'Properties of cement treated soil in Trans-Tokyo Bay Highway project. Ground Improvement, 1(1), 37–57.

Tattersall, G. H. and Banfill, P. F. G. (1983). The rheology of fresh concrete. Pitman.

Terashi, M., Tanaka, H., Mitsumoto, T., Niidome, Y., and Honma, S. (1980). Fundamental Properties of lime and cement treated soils (2nd report) (in Japanese): Report of the Port and Harbour Research Institute.

Terashi, M. (1997). Theme lecture: Deep mixing method - Brief state of the art. Proceedings of the 14th ICSMFE, Hamburg, 4, 2475-2478.

Terashi, M. (2003). The state of practice in deep mixing methods. Proceeding of the 3rd International Conference on Grouting and Ground Treatment. ASCE, New Orleans, 25-49.

Terashi, M. (2005). Keynote Lecture: Design of deep mixing in infrastructure applications. Proceedings of the International Conference on Deep Mixing Best Practice and Recent Advances, Stockholm. Swedish Deep Stabilisation Research Center, Linköping, Sweden.

Terashi, M., and Kitazume, M. (2009). Keynote lecture Current Practice and future perspective of QA/QC for Deep-Mixed ground. Proceedings of the Internation Symposium on Deep Mixing and Admixture Stabilisation, May 19-21, Okinawa.

Tokunaga, S., Miura, H. and Otake, T. (2005). Laboratory tests on effect of cement content on permeability of cement treated soils. Proceedings of the International Conference on Deep Mixing Best Practice and Recent Advances, Stockholm. Swedish Deep Stabilisation Research Center, Linköping, Sweden, Vol. 1, 397-402.

Toohey, N. M. and Mooney, M. A. (2012). Seismic modulus growth of lime-stabilised soil during curing, Géotechnique, 62(2), 161–170.

Topolnicki, M. (2004). In Situ Soil Mixing. In Moseley, M. P. and Kirsch, K. (Eds.), Ground Improvement (331-428), 2nd Edition. London: Spon Press Taylor & Francis Group.

Topolnicki, M. (2009). Design and execution practice of wet Soil Mixing in Poland. Proceedings of the Internation Symposium on Deep Mixing and Admixture Stabilisation, May 19-21, Okinawa.

Topolnicki, M. and Pandrea, P. (2012). Design of in-situ soil mixing. International symposium of ISSMGE - TC211. Recent research, advances & execution aspects of ground improvement works. 31 May-1 June 2012, Brussels, Belgium Vol.3, 309-319.

Verastegui Flores, R.D., Di Emidio, G., Van Impe, W., 2010. Small-strain shear modulus and strength increase of cement-treated clay. Geotechnical Testing Journal, 33(1), 62-71.

Vervoort, A., Tavallali, A., Van Lysebetten, G., Maertens, J., Denies, N., Huybrechts, N., De Cock, F. and Lameire, B. (2012). Mechanical characterization of large scale soil mix samples and the analysis of the influence of soil inclusions. International symposium of ISSMGE - TC211. Recent research, advances & execution aspects of ground improvement works. 31 May-1 June 2012, Brussels, Belgium, Vol. 3, 127-137.

Wang, W., Roy, A., Seals, R.K. and Metcalf, J.B. (2003). Stabilization of sulfate-containing soil by cementitious mixtures mechanical properties. Transportation Research Record, 1837, 12–19.

Wild, S., Kinuthia, J.M., Jones, G.I., Higgins, D.D., 1999. Suppression of swelling associated with ettringite formation in lime stabilized bearing clay soils by partial substitution of lime with ground granulated blastfurnace slag. Engineering Geology, 51, 257–277.

Xing, H., Yang, X., Xu, C., and Ye, G. (2009). Strength characteristics and mechanisms of salt-rich soil-cement. Engineering Geology, 103(1-2), 33-38.

Yang, Y., Yang, E.-H. and Li, V. C. (2011). Autogenous healing of engineered cementitious composites at early age, Cement and Concrete Research, 41(2), 176-183.

Yano, S., Tokunaga, S., Shima, M. and Manimura, K. (1996). Centralized control system of CDM Method. Grouting and Deep Mixing, Proceedings of IS-Tokyo'96, The Second International Conference on Ground Improvement Geosystems, Tokyo, May 14-17, 681-687.

Yesiller, N., Hanson, J.L. and Usmen, M.A. (2000a). Ultrasonic assessment of stabilized soils, ASCE Geotechnical Special Publication, 112, 170-181.

Yesiller, N., Miller, C. J., Inci, G. and Yaldo, K., (2000b). Dessication and cracking behavior of three compacted landfill liner soils. Engineering Geology, 57(1–2), 105–121.

Yilmaz, I. k., and Civelekoglu, B. (2009). Gypsum: An additive for stabilization of swelling clay soils. Applied Clay Science, 44(1-2), 166-172.

Yoshizawa, H., Okumura, R., Hosya, Y., Sumi, M. and Yamada, T. (1997). JGS TC Report: Factors affecting the quality of treated soil during execution of DMM. Proc. of the IS-Tokyo´96, 2nd Int. Conf. on Ground Improvement Geosystems, Tokyo, 1996, 2, 931-937.

Yurtdas, I., Burlion, N. and Skoczylas, F. (2004a). Triaxial mechanical behaviour of mortar: Effects of drying. Cement and Concrete Research, 34(7), 1131-1143.

Yurtdas, I., Burlion, N., and Skoczylas F. (2004b). Experimental characterisation of the drying effect on uniaxial mechanical behaviour of mortar. Mater. Struct. 37(3), 170–176.

Yurtdas, I., Burlion, N., Shao, J.-F. and Li, A. (2011). Evolution of the mechanical behaviour of a high performance self-compacting concrete under drying. Cement and Concrete Composites, 33(3), 380-388.

Yurtdas, I., Peng, H., Burlion, N. and Skoczylas, F. (2006). Influences of water by cement ratio on mechanical properties of mortars submitted to drying. Cement and Concrete Research, 36, 1286–1293.

Zhang, Z. and Tao, M. (2008). Durability of cement stabilized low plasticity soils, Journal of Geotechnical and Geoenvironmental Engineering, 134(2), 203-213.

Appendix A

Experimental programs

Soil	Mix	Binder	Cement content C		Moulding moisture content W (%)	Cement - water ratio C/W	Bentonite (kg/m^3)	Max. curing time	Curing conditions
			(%)	(kg/m^3)					
Fontainebleau Sand (FS)	FS200W20	CEM III	11.8	200	20.0	0.50	/	360	Endogenous
	FS200W20B50	CEM III	11.8	200	20.0	0.50	50	360	Endogenous
	FS200W35B50	CEM III	11.8	200	35.0	0.30	50	360	Endogenous
	FS-I-200W20	CEM I	11.8	200	20.0	0.50	/	180	Endogenous
	FS-I-200W15	CEM I	11.8	200	15.0	0.70	/	180	Endogenous
Artificial silt (AS)	AS300W57	CEM III	20.7	300	57.0	0.30	/	360	Endogenous
	AS200W40	CEM III	13.8	200	40.0	0.30	/	360	Endogenous

Table A-1 Composition of the soil-cement mixes prepared with artificial soils.

Soil	Simulated Vernouillet Column	Mix	Binder	Cement content C		Moulding moisture content W (%)	Cement - water ratio C/W	Bentonite (kg/m^3)	Max. curing time	Curing conditions
				(%)	(kg/m^3)					
Vernouillet sand (VSA)	X5	VSA346W29	CEM III	18.03	346.70	29.56	0.52	8.94	28	Endogenous
	X4	VSA249W17	CEM III	12.97	249.33	17.81	0.64	4.97	28	Endogenous
	C1	VSA230W14	CEM III	11.96	230.00	14.63	0.73	3.97	28	Endogenous
Vernouillet silt (VSI)	/	VSI300W57	CEM III	20.7	300	57.0	0.30	/	180	Endogenous
	X5	VSI346W50	CEM III	24.56	346.74	50.21	0.39	10.71	360	Endogenous
	X4	VSI248W35	CEM III	17.58	248.20	35.99	0.42	4.96	360	Endogenous
	C1	VSI236W31	CEM III	16.74	236.30	31.95	0.45	4.78	360	Endogenous

Table A-2 Composition of the soil-cement mixes prepared with natural soils from Vernouillet.

Test	Unconfined compression tests (*): with local strain measurements							Ultrasonic wave velocity measurements							Splitting tensile strength tests		Total porosity		Permeability	
Time (days)	**1**	**7**	**14**	**28**	**90**	**180**	**360**	**1**	**7**	**14**	**28**	**90**	**180**	**360**	**28**	**90**	**28**	**90**	**28**	**90**
FS200W20	3*	3*	3	3*	3	3*	3*	3	3	3	3	3	3	3	3	3	1	1	1	1
FS200W20B50		3	3	3	3	3*	3*		3	3	3	3	3	3	3	3	1	1		
FS200W35B50		3	3	3	3	3*	3*		3	3	3	3	3	3	3	3	1	1		
FS-I-200W20		3	3	3	3	3*			3	3	3	3	3		3	3	1	1		
FS-I-200W15		3	3	3	3	3*			3	3	3	3	3		3	3	1	1		
AS300W57	3*	3*	3	3*	3*	3*	3*	3	3	3	3	3	3	3	3		1	1	1	1
AS200W40	3*	3*	3	3*	3*	3*	3*	3	3	3	3	3	3	3	3	3	1	1	1	1
VSA346W29		3*		3*					3		3									
VSA249W17		3*		3*					3		3									
VSA230W14		3*		3*					3		3									
VSI300W57		3	3	3	3	3*			3	3	3	3	3	3			1			
VSI346W50		3	3	3	3	3*	3*		3	3	3	3	3	3	3		1			
VSI248W35		3	3	3	3	3*	3*		3	3	3	3	3	3	3		1			
VSI236W31		3	3	3	3	3*	3*		3	3	3	3	3	3	3		1			

Table A-3 Tests performed and number of specimens tested to investigate the characteristics of soils stabilised in the laboratory.

Soil	Mix	Binder	Cement content C (kg/m^3)	Moulding moisture content W (%)	Bentonite (kg/m^3)	Addition of chemical compound in the mix	Curing time (days)	Curing conditions
FS	FS200W35B50-diesel-endo	CEM III	200	35	50	Diesel (10g/kg)	360	Endogenous
	FS200W35B50-NaCl-endo	CEM III	200	35	50	NaCl (10g/kg)	360	Endogenous
	FS200W35B50-CaSO4-endo	CEM III	200	35	50	CaSO4, 2 H_2O (10g/kg)	360	Endogenous
	FS200W35B50-Imm	CEM III	200	35	50	/	360	Immersed
	FS200W35B50-CaSO4-Imm	CEM III	200	35	50	CaSO4, 2 H_2O (10g/kg)	360	Immersed (1g/LCaSO4)
	FS200W35B50-Imm-CaSO4	CEM III	200	35	50	/	360	Immersed (1g/LCaSO4)
	FS-I-200W15-CaSO4-endo	CEM I	200	15	/	CaSO4, 2 H_2O (10g/kg)	180	Endogenous
	FS-I-200W20-CaSO4-endo	CEM I	200	20	/	CaSO4, 2 H_2O (10g/kg)	180	Endogenous
AS	AS300W57-diesel-endo	CEM III	300	57	/	Diesel (10g/kg)	360	Endogenous
	AS300W57-NaCl-endo	CEM III	300	57	/	NaCl (10g/kg)	360	Endogenous
	AS300W57-CaSO4-endo	CEM III	300	57	/	CaSO4, 2 H_2O (10g/kg)	360	Endogenous
	AS200W40-diesel-endo	CEM III	200	40	/	Diesel (10g/kg)	360	Endogenous
	AS200W40-NaCl-endo	CEM III	200	40	/	NaCl (10g/kg)	360	Endogenous
	AS200W40-CaSO4-endo	CEM III	200	40	/	CaSO4, 2 H_2O (10g/kg)	360	Endogenous

Table A-4 Composition of the soil-cement mixes prepared with the artificial soils to investigate the effects of chemical compounds.

Test	Unconfined compression tests (*): with local strain measurements						Ultrasonic wave velocity measurements						Splitting tensile strength tests		Total porosity		Permeability	
Time (days)	7	14	28	90	180	360	7	14	28	90	180	360	28	90	28	90	28	90
FS200W35B50-diesel-endo	3*	3*	3*	3*	3		3	3	3	3	3							
FS200W35B50-NaCl-endo	3	3	3	3	3*	3*	3	3	3	3	3	3	3	3	1	1		
FS200W35B50-CaSO4-endo	3	3	3	3	3*	3*	3	3	3	3	3	3	3	3	1	1		
FS200W35B50-Imm		3	3	3	3	3		3	3	3	3	3	3	3	1	1		1
FS200W35B50-CaSO4-Imm		3	3	3	3	3		3	3	3	3	3			1	1		1
FS200W35B50-Imm-CaSO4		3	3	3	3			3	3	3	3				1	1		1
FS-I-200W15-CaSO4-endo	3	3	3	3	3*		3	3	3	3	3	3		3	1	1		
FS-I-200W20-CaSO4-endo	3	3	3	3	3*		3	3	3	3	3	3		3	1	1		
AS300W57-diesel-endo	3*	3*	3*	3*	3		3	3	3	3	3							
AS300W57-NaCl-endo	3*	3	3*	3*	3*	3	3	3	3	3	3	3	3		1	1	1	1
AS300W57-CaSO4-endo	3	3	3	3*	3*	3	3	3	3	3	3	3	3		1	1	1	1
AS200W40-diesel-endo	3*	3*	3*	3*	3		3	3	3	3	3							
AS200W40-NaCl-endo	3*	3*	3*	3*	3*	3	3	3	3	3	3	3	3	3	1	1	1	1
AS200W40-CaSO4-endo	3*	3*	3*	3*	3*	3	3	3	3	3	3	3	3	3	1	1	1	1

Table A-5 Tests performed and number of specimens tested to investigate the effects of chemical compounds.

Appendix B

Technical paper: Free–Free Resonance Testing of In Situ Deep Mixed Soils
Geotechnical Testing Journal, Vol. 36, No. 2, 2013

Geotechnical Testing Journal, Vol. 36, No. 2, 2013
Available online at www.astm.org
doi:10.1520/GTJ20120058

Antoine Guimond-Barrett,[1,2] *Elodie Nauleau,*[1] *Alain Le Kouby,*[1] *Anne Pantet,*[2] *Philippe Reiffsteck,*[1] *and François Martineau*[1]

Free–Free Resonance Testing of In Situ Deep Mixed Soils

REFERENCE: Guimond-Barrett, Antoine, Nauleau, Elodie, Le Kouby, Alain, Pantet, Anne, Reiffsteck, Philippe, and Martineau, François, "Free–Free Resonance Testing of In Situ Deep Mixed Soils," *Geotechnical Testing Journal*, Vol. 36, No. 2, 2013, pp. 1–9, doi:10.1520/GTJ20120058. ISSN 0149-6115.

ABSTRACT: This paper focuses on the use of free–free resonance testing (FFR testing) applied to the characterization of stabilized silt and sand specimens treated in situ by deep soil mixing. The aim of FFR testing is to measure the natural frequencies of free vibration of the tested specimen. Compression and shear wave velocities, seismic moduli and Poisson's ratio can be determined from these frequencies. Block samples were taken from soil–cement columns installed at a test site near Paris, France. Specimens of 100 by 50 mm (height to diameter ratio of 2) were cored from these blocks and submitted to FFR testing in the laboratory. The measured resonant frequencies were very repeatable for all specimens tested, validating the use of free–free resonance as a rapid testing method for the characterization of fairly heterogeneous stabilized soil specimens. It was found that both P-wave and S-wave velocities increase nonlinearly with unconfined compressive strength. A linear correlation between strength and dynamic stiffness was observed. Free–free resonance test results can be correlated with index parameters such as density and porosity and used for preliminary assessments of static stiffness as all these parameters varied linearly with measured wave velocities.

KEYWORDS: deep mixing, free-free resonance testing, stabilized soils, cement

Nomenclature

E_0 = seismic Young's modulus (MPa)
E_{50} = static secant deformation modulus at 50 % of maximum stress (MPa)
f_p = resonant frequency for compression waves (Hz)
f_s = resonant frequency for shear waves (Hz)
G_0 = seismic shear modulus (MPa)
L = length (m)
PI = plasticity index (%)
pl* = Menard pressure-meter limit pressure (MPa)
q_d = dynamic penetration resistance (MPa)
q_u = unconfined compressive strength (MPa)
t = travel time (s)
V = wave velocity (m/s)
V_p = compression wave velocity (m/s)
V_s = shear wave velocity (m/s)
w = moisture content (%)
w_L = liquid limit (%)
ν = Poisson's ratio
ρ = density (kg/m^3)

Manuscript received April 25, 2012; accepted for publication October 23, 2012; published online January 24, 2013.

[1]IFSTTAR, GER, 58, Boulevard Lefebvre F-75732 Paris Cedex 15, France.
[2]Université du Havre, LOMC, 53, Rue Prony, 76058 Le Havre Cedex, France.

Introduction

Deep mixing is a general term for a large number of techniques, in which binding agents are mechanically dispersed within the soil either in dry or slurry form using specially designed mixing tools (Porbaha 1998). Originally, the main purpose of deep soil mixing was to enhance the stability and reduce settlements of structures such as embankments on soft soils of low shear strength and very high moisture contents (CDIT 2002). Nowadays, improving the strength and deformation properties as well as the permeability of very soft soils by deep soil mixing is a commonly used stabilization method. Lime and cement are the most frequently used binders. There is an increasing interest in the use of this technique not only for soil stabilization but also to construct temporary and permanent foundation/structural (load bearing) elements and excavation retaining walls (Ganne et al. 2010; Shao et al. 2005). The properties and types of soils encountered for these new applications of deep soil mixing differ greatly from those found in soft soil stabilization projects, i.e., they have higher strengths and lower deformation characteristics. A large number of factors are known to influence the strength and deformation properties of the treated soils (Terashi 1997). These factors are mainly related to the characteristics of the binder (type, amount), the soil conditions (soil type, moisture content, and organic content), the mixing conditions (degree of mixing) and the curing conditions.

In general, the strength of in situ stabilized soils is evaluated by means of unconfined compressive strength tests. In addition to these tests, nondestructive geophysical methods may be used. Seismic-based testing procedures have been utilized to assess the

dynamic modulus of laboratory specimens (Nazarian et al. 1999; Hoyos et al. 2004; Puppala et al. 2006; Ryden et al. 2006; Hilbrich and Scullion 2007; Åhnberg and Holmen 2008; Rabbi et al. 2011) and offer promising perspectives in terms of quality assessment and quality control of stabilized soils (Madhyannapu et al. 2010). Bhadriraju et al. (2008) subjected in situ wet grab samples to strength and small strain stiffness tests (using bender elements) in the laboratory. They found a good agreement between test results from field cores and laboratory fabricated specimens. The investigation of small strain stiffness may be of interest in projects associated with vibration problems such as liquefaction mitigation but also to verify that satisfactory design strengths have been reached after treatment. To estimate strength properties based on measured dynamic parameters, empirical relations with unconfined compressive strength are necessary.

Different studies have been published relative to the use of free–free resonance testing (FFR testing) on homogeneous laboratory specimens of rather low strengths. Åhnberg and Holmen (2011) have investigated the use of resonant column free–free testing on different types of soils of high moisture contents (over 40 %) stabilized in the laboratory with cement and lime. They demonstrated the usefulness of this method by proposing empirical correlations between compression wave velocity, shear wave velocity, and unconfined compressive strength. Toohey and Mooney (2012) analyzed the growth in seismic modulus with curing time up to 28 days for soils stabilized with lime in the laboratory. One of the main advantages of FFR tests is that they can be executed very rapidly on specimens of different dimensions.

This paper focuses on FFR testing applied to the characterization of soils stabilized in situ by deep soil mixing with cement.

The main objectives of the present study are:

(a) to investigate the use of FFR testing on relatively heterogeneous soil specimens of intermediate to high strength obtained from block samples of in situ deep mixing columns,
(b) to determine the wave velocities and dynamic moduli of the stabilized soils tested, and
(c) to explore possible correlations with strength and static deformation modulus but also with index properties, such as density and porosity.

Experimental Details and Procedures

Ground Conditions at the Test Site and Column Installation Procedure

Soil–cement columns were installed by deep mixing at a test site located near the river Seine in Vernouillet (Yvelines), France, approximately 35 km northwest of Paris (Guimond-Barrett et al. 2012). A preliminary site investigation was carried out to determine the ground conditions at the test site. The ground investigation consisted of trial pits (dug down to approximately 2 m), dynamic penetration tests and boreholes drilled down to depths of 6 and 9 m. Pressure-meter tests were performed at different depths in each borehole. The ground investigation revealed that the site was covered by a 0.5 -m-thick layer of fill consisting of dark greyish brown sandy gravel, overlaying a 3 -m-thick layer of brownish beige clayey silt. An average penetration resistance of 4 MPa and pressure-meter limit pressures between 0.70 and 1.70 MPa were measured in this silt layer. Underlaying the clayey silt are old alluvium deposits of the river Seine, which may be described as dense brownish orange gravelly sand. This sand is present down to a depth of at least 9 m below ground level. The average dynamic penetration resistance in this layer is 16 MPa. Pressure-meter limit pressures greater than 2.40 MPa were measured. No groundwater was encountered during the site investigation. Soils sampled from the trial pits were characterized in the laboratory by moisture content measurements (CEN ISO/TS 17892-1 2005), grain size distribution analyses (CEN ISO/TS 17892-4 2005), methylene blue value tests (AFNOR NFP94-068 1998), and Atterberg limits (CEN ISO/TS 17892-12 2005). The drained shear strength parameters were determined by direct shear box tests (CEN ISO/TS 17892-10 2005). The geotechnical properties of the silt and sand from the Vernouillet test site are summarized in Table 1.

Soil–cement columns were installed down to the gravely sand layer at a depth of 5 m using a mixing tool equipped with two mixing blades. Soil mixing was carried out by the wet method: the binder was mixed with water forming a slurry before it was added into the soil. The slurry was injected during the penetration (downward) phase. Depending on the column, the penetration speeds varied between 10 and 25 ms per hour (m/hr) and the tool rotation speed was between 70 and 160 rpm. The blade rotation number is defined by (EN14679 2005):

$$T = M \times \frac{N}{V} \tag{1}$$

where T is the blade rotation number per meter, M is the total number of mixing blades, N is the rotational speed of the blades (rpm), and V is the penetration rate in meters per minute (m/min).

The blade rotation number for the columns in Vernouillet was between 700 and 1500 rotations per meter. The binder used was a slag cement containing 85 % of ground granulated blast furnace slag (CEM III/C). Bentonite was added to stabilize the cement grouts. The cement factors (mass of dry binder per cubic meter of soil) tested varied between 200 and 400 kg/m^3. It is important to note that these cement contents represent the amount of binder injected into the columns by the operators. The actual binder contents are probably slightly lower as approximately 30 % of spoil returns to the surface during mixing operations.

TABLE 1—*Summary of soil characteristics.*

Strata	Silt	Gravelly sand
Thickness (m)	3	>5.5
Moisture content w (%)	11.9 to 19.7	5 to 7.6
% passing 80 μm	72.5	17.9
Methylene blue value MBV	1.38	0.71
Atterberg limits		
w_L (%)	30	/
PI (%)	10	/
Dynamic penetration resistance q_d (MPa)	4	16
Pressuremeter limit pressure pl* (MPa)	0.70 to 1.70	>2.40
Cohesion (kPa)	2	0
Friction angle (°)	27	37

Five columns were excavated with a 20-ton mechanical excavator approximately 6 months after construction to check that the full strength had been reached. The columns were found to be well mixed with some inhomogeneities visible.

The first three meters of the columns generally consisted of treated silt. Centimetric inclusions of beige/brown soil were visible in a matrix of mixed soil–cement. The central/axial part of the column section appeared to be more homogeneous and concentrated in slurry. The lower part of the columns consisted of stabilized sand down to 5 m. The mixture produced was visually homogeneous with no unmixed soil inclusion pointing to the fact that it is easier to obtain well mixed soil–cement columns in coarse-grained soils than in fine-grained soils. Block samples were taken from the upper silt and lower sand parts of the five excavated columns for FFR testing in the laboratory and to determine the mechanical properties of the soil-mix material. Cylindrical specimens of approximately 100 by 50 mm (height to diameter ratio of 2) were cored from these blocks and stored standing in full contact in tap water at 20°C. Their extremities were cut and smoothed. The specimens were then measured, weighted, and tested.

Testing Procedures

Free–Free Resonance Testing (FFR Testing)—The aim of FFR testing is to measure the natural frequency of free vibration of the tested specimen. To perform the free–free resonant column tests, the compression and flexural signals were measured by two 6-mm-diameter accelerometers with a frequency range of 1 to 17 kHz.

Three different methods of excitation and recording were considered:

- Method 1: longitudinal excitation/longitudinal and flexural recording.
  The specimens were subjected to a longitudinal (compressive) excitation produced by a metal ball falling from a constant height guided by a plastic tube on the upper extremity of the specimen (Fig. 1(*a*)). The specimens were placed vertically in equilibrium on one of the accelerometers to measure the resonant frequencies associated with compressive wave propagation (Figs. 1(*a*) and 1(*b*)). This was only possible because of the relatively high strength of the tested specimens. A rubber base with a wooden core was used to hold the accelerometer vertically and to isolate the specimen from surrounding vibrations. In addition, a second accelerometer was secured on the lateral surface of the specimen using an elastic band to study the flexural response out of the longitudinal excitation (Fig. 1(*b*)).
- Method 2: flexural excitation (with a falling metal ball) and recording.
  The specimens were placed horizontally on a sheet of foam to measure the resonant frequency associated with shear wave propagation (Fig. 1(*c*)). The specimens were subjected to flexural excitations produced by the same metal ball falling from a constant height on the lateral surface of the specimen (Fig. 1(*d*)).

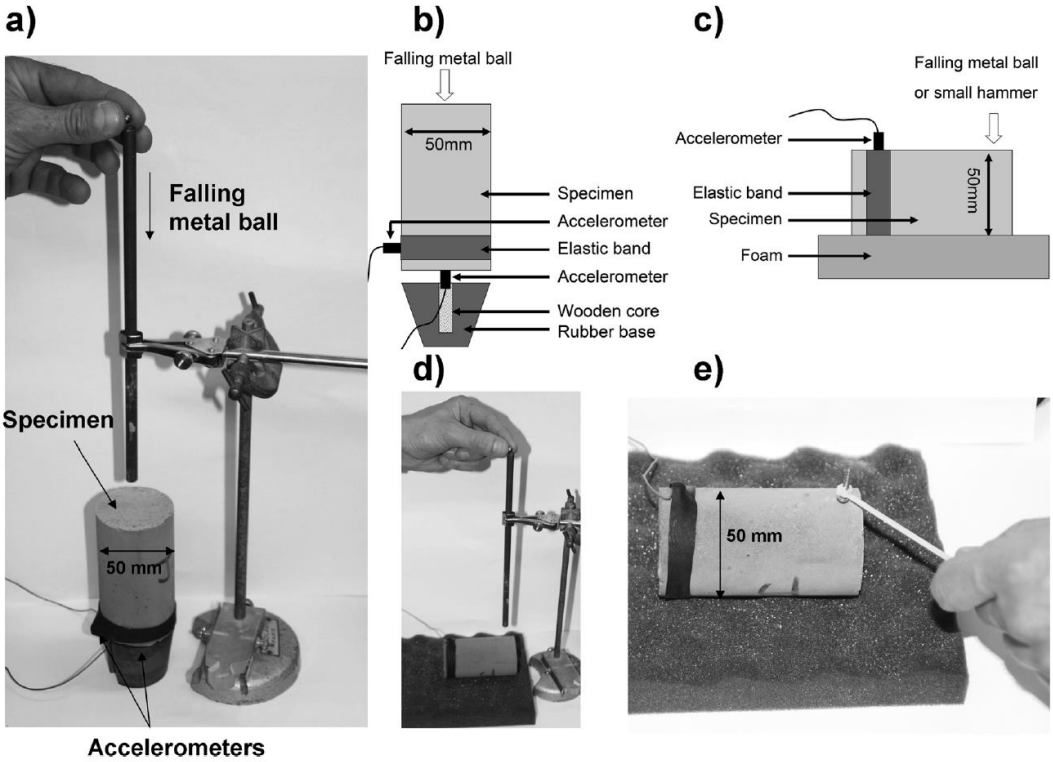

FIG. 1—*FFR testing: (a) setup for longitudinal excitation/longitudinal and flexural recording with impulses produced by a falling metal ball; (b) schematic drawing of the setup for longitudinal excitation/longitudinal and flexural recording; (c) schematic drawing of the setup for flexural excitation and recording; flexural excitation and recording with impulses produced by (d) a falling metal ball; and (e) a small hammer.*

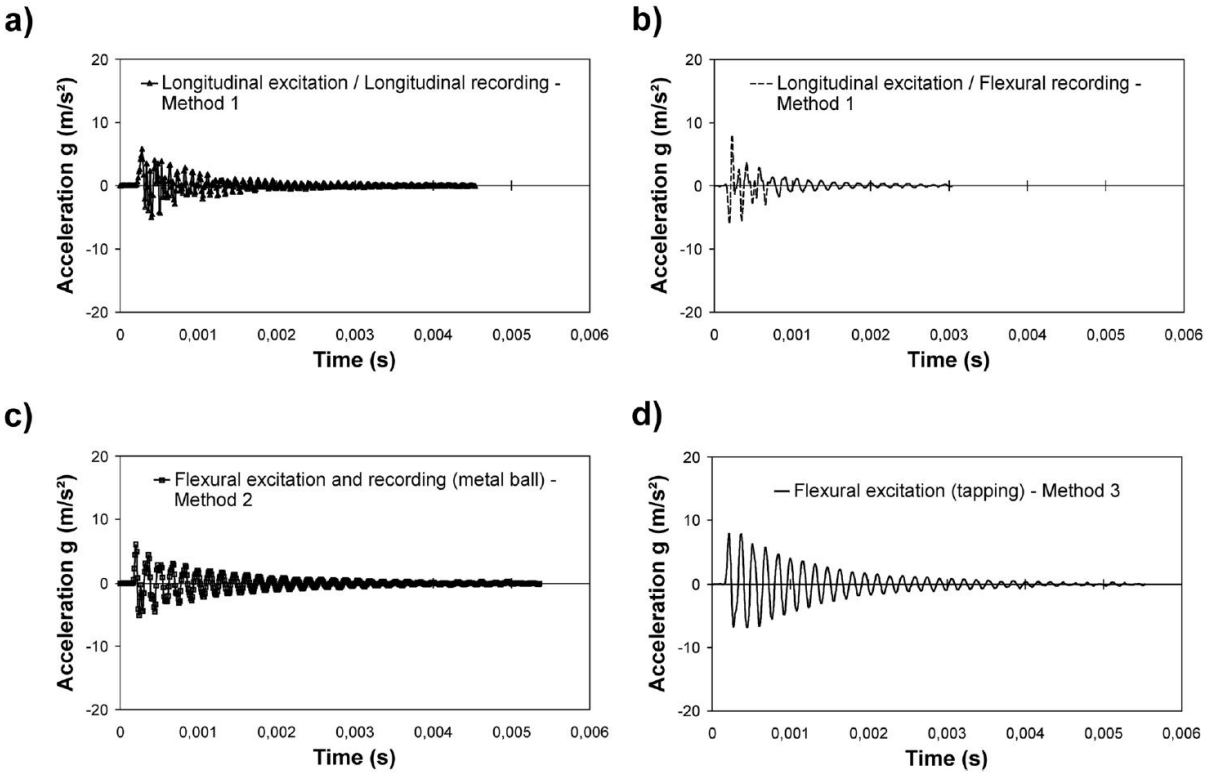

FIG. 2—*Typical FFR time histories for specimens of stabilized silt using different solicitation and recording methods.*

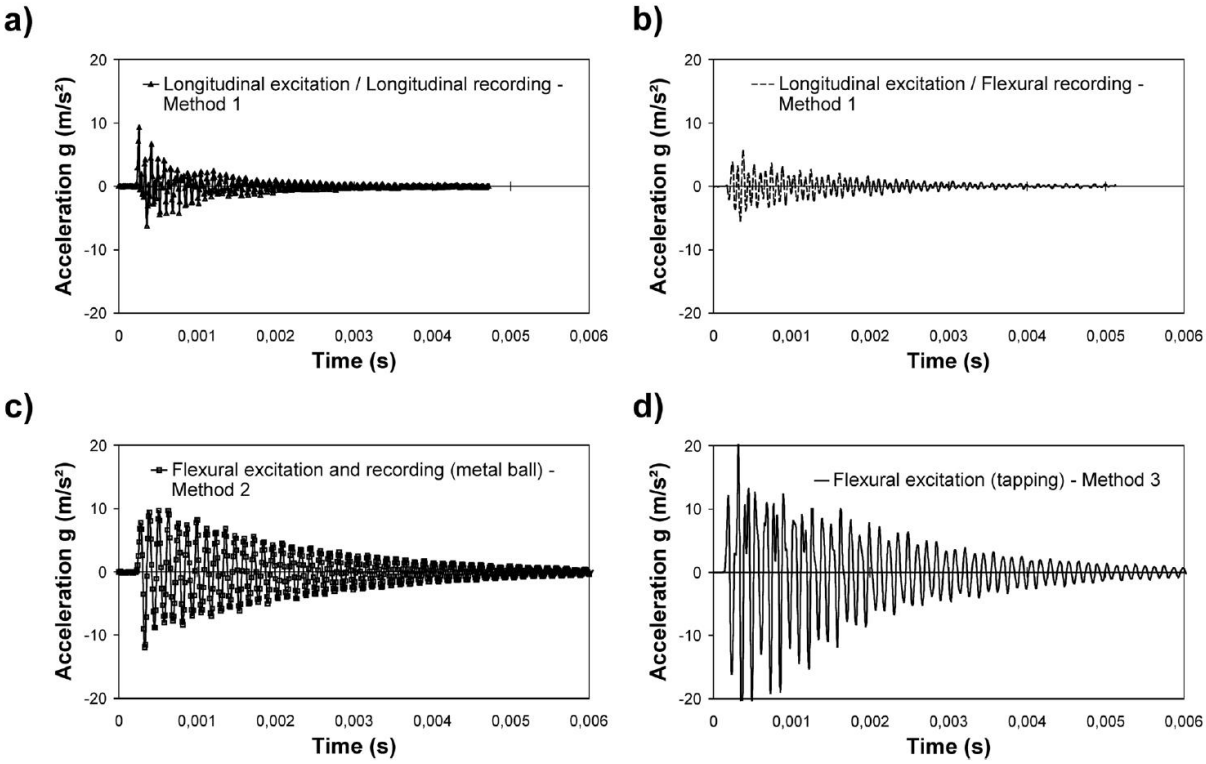

FIG. 3—*Typical FFR time histories for specimens of stabilized sand using different solicitation and recording methods.*

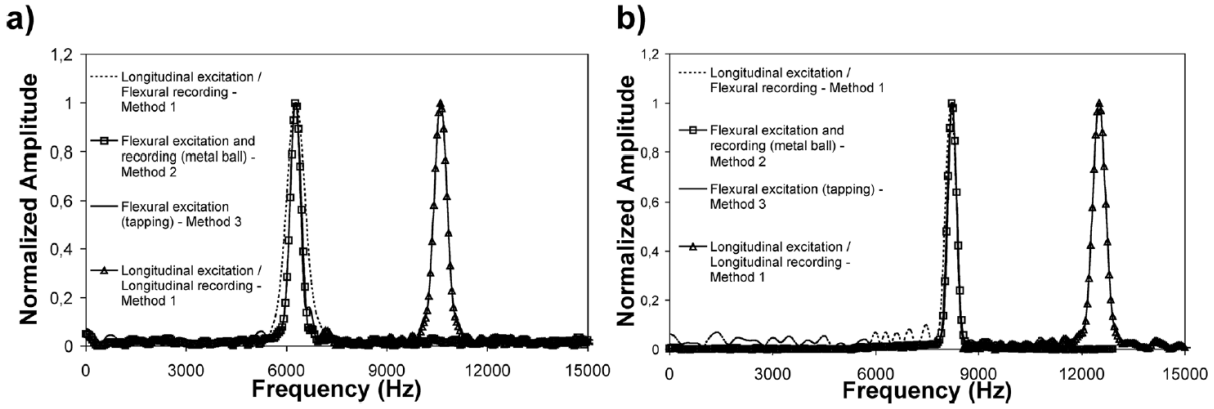

FIG. 4—*Typical FFR frequency domains for flexural and longitudinal excitations for specimens of (a) stabilized silt, and (b) sand.*

- Method 3: flexural excitation (with a small hammer) and recording.

To investigate the use of FFR testing on relatively heterogeneous soil specimens and to check the repeatability of the measured signal, the specimens were also subjected to flexural excitations produced by tapping the specimen with a small hammer (Fig. 1(*e*)).

For these two flexural solicitations (methods 2 and 3), the shear acceleration signal was recorded by an accelerometer placed on the lateral surface at the other extremity of the specimen. Method 3 is similar to the excitation technique used by Åhnberg and Holmen (2011) on treated soils of low strength.

The following relationships are used to determine the shear wave and compression wave velocities from the resonant column free–free tests:

$$V_s = 2 \times L \times f_s \tag{2}$$

$$V_p = 2 \times L \times f_p \tag{3}$$

where V_s is the shear wave velocity, V_p is the compression wave velocity, L is the specimen length, f_s, and f_p are the resonant frequencies for shear waves and compression waves, respectively. The wavelength is assumed to be equal to twice the length of the specimen during free vibration for specimens with free ends and with a length-to-diameter ratio of about 2 or more (Ryden et al. 2006).

The small-strain seismic compression (E_0) and shear (G_0) moduli can be calculated from the wave velocities knowing the specimen's mass density (ρ) using the following equations (Nazarian et al. 1999):

$$E_0 = \rho \times V_p^2 \tag{4}$$

$$G_0 = \rho \times V_s^2 \tag{5}$$

Based on Eqs (4) and (5), and assuming homogeneous, isotropic, linear elasticity, the Poisson's ratio can be determined from the computed values of E_0 and G_0 by the following relation:

$$\nu = \frac{E_0}{2G_0} - 1 \tag{6}$$

The free vibration acceleration time records collected by both accelerometers were stored in a computer. The time domain signals were digitized using 2048 points and a sampling time interval of 10 μs. Frequency domain analysis was performed on the free vibration through fast Fourier transforms (FFT). No stacking

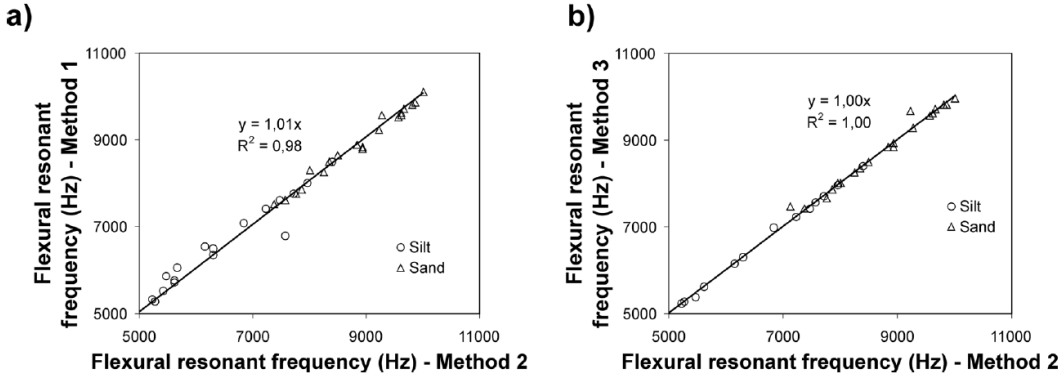

FIG. 5—*Calculated resonant frequencies: (a) flexural excitation produced by a falling metal ball (method 2) versus longitudinal excitation (method 1), and (b) flexural excitation (method 2) versus flexural excitation using a small hammer (method 3).*

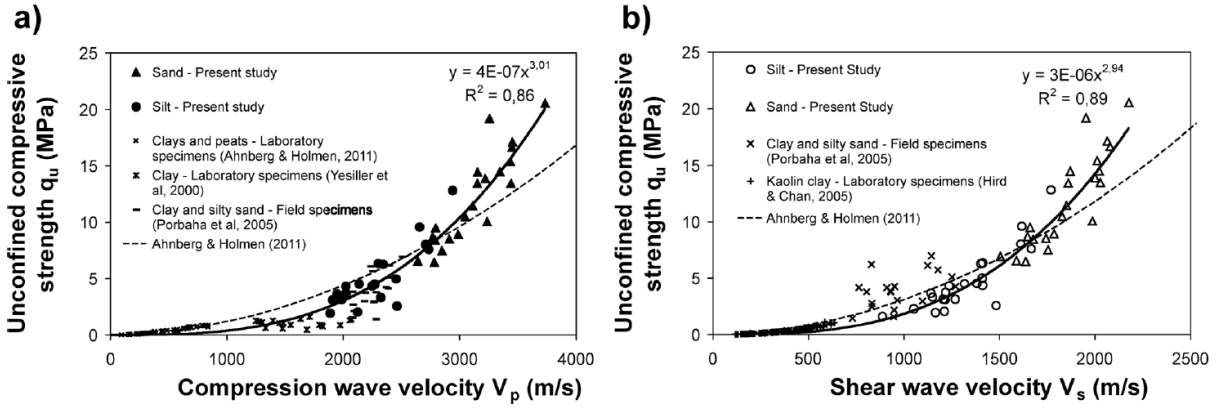

FIG. 6—*(a) Unconfined compressive strength q_u versus compression wave velocity V_p, and (b) Unconfined compressive strength q_u versus shear wave velocity V_s.*

of repeated signals was performed and no filters were used to eliminate background noise before applying the FFT.

Typical time records for both silt and sand specimens are presented in Fig. 2 and Fig. 3, respectively. The corresponding frequency domains are shown in Fig. 4.

Unconfined Compressive Strength Tests and Static Deformation Modulus Measurements—After the FFR tests, unconfined compression tests were performed on the specimens to evaluate their strength (q_u). The tests were conducted in accordance with standard EN13286-41 (2003). The vertical load was statically applied at a constant displacement rate of 1.5 mm/min. The longitudinal strains were measured locally in the central part of the specimen by three LVDTs offset by 120° supported by two rigid rings. Each ring was attached on the wall of the specimen by three screws as described in standard EN13286-43 (2003). The E_{50} modulus was calculated from the stress–strain curves as the secant modulus at a stress equal to half the maximum strength.

Porosity Measurements—The total porosity of some specimens was determined by hydrostatic weighing after saturation under vacuum for 24 h and by the measurement of the loss of water under controlled drying by heating to 105°C.

Experimental Results and Analyses

In general, the accelerations measured for the specimens of treated silt (Fig. 2) were lower than those measured for the treated sand specimens (Fig. 3). The resonant frequencies associated with compression wave propagation (longitudinal recording) were higher than the flexural resonant frequencies (flexural recording) (Fig. 4). Flexural frequency response was very repeatable for all samples when comparing the results obtained by impulses produced by the falling metal ball (method 2) and by the small hammer (method 3) (Fig. 5(*b*)). For the specimens tested in this study, it was possible to simultaneously measure from a single compressive impulse both compressive and flexural signals. When a longitudinal impulse was applied to the specimens by the falling metal ball (method 1), a flexural signal was recorded by the accelerometer placed horizontally on the side of the specimens (Fig. 2(*b*) and Fig. 3(*b*)). The flexural resonant frequencies recorded from longitudinal excitations are found to be in good agreement with the results obtained from flexural impulses. This is illustrated in

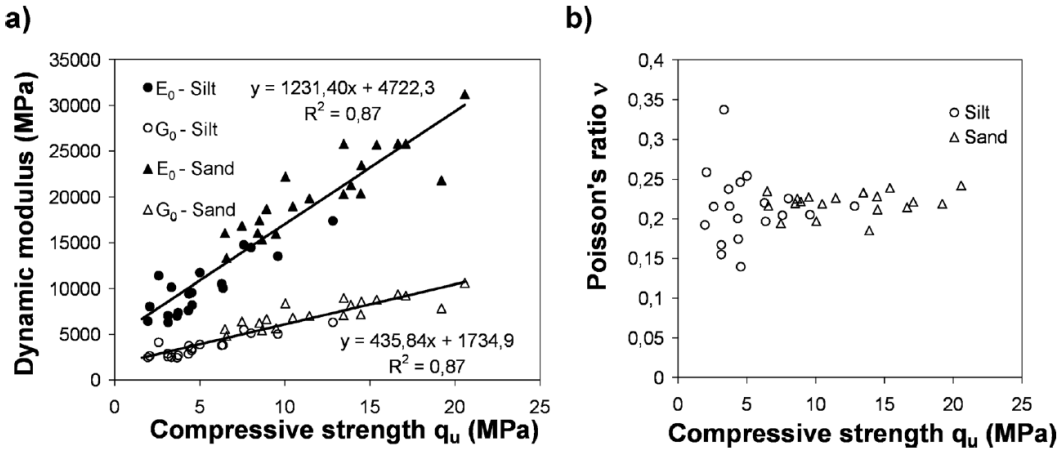

FIG. 7—*(a) Dynamic moduli E_0 and G_0 versus unconfined compressive strength q_u, and (b) Poisson's ratio ν versus unconfined compressive strength q_u.*

Figs. 5(*a*) and 5(*b*) as almost identical shear resonant frequencies were determined by all three testing methods, validating the use of free–free resonance testing applied to fairly heterogeneous soil specimens. This would certainly not be possible for specimens of lower strengths. The amplitudes of the flexural signals measured with longitudinal excitations (Fig. 2(*b*) and Fig. 3(*b*)) were often smaller than with flexural solicitation methods (Figs. 2(*c*) and 2(*d*), and Figs. 3(*c*) and 3(*d*)). However, the results show that the resonant frequency is not influenced by the amplitude.

Correlation With Unconfined Compressive Strength

Figures 6(*a*) and 6(*b*) present the shear and compression wave velocities evaluated from free–free resonance tests versus unconfined compressive strength. For both types of soil, the wave velocities increase with strength. The unconfined compressive strength of the stabilized silt specimens generally varied between 2 and 5 MPa with some specimens of higher strength. The P-wave and S-wave velocities were between 1800 and 2500 m/s and between 1000 and 1500 m/s, respectively. The dispersion in unconfined compression strength within the population of silt specimens can be related to the heterogeneity of the initial soil, variations in binder distribution, variations in the column execution parameters (different sets of parameters were tested), and to the presence of some unmixed soil inclusions.

The specimens of stabilized sand were of higher strength, which explains the higher amplitudes measured in the free–free resonance tests. The unconfined compressive strength of most specimens varied between 5 and 20 MPa with P-wave velocities between 2500 and 3500 m/s and S-wave velocities between 1500 and 2000 m/s.

The wide range of strengths measured for the sand specimens can be linked to similar factors as those mentioned above for the silt specimens. The very high strengths can largely be attributed to the heterogeneity of the initial alluvial sand layer which contains lenses of gravel that are responsible for the q_u values greater than 15 MPa. These heterogeneities in the soil were observed during the coring of the block samples.

Data on stabilized soils of similar high strengths are scarce in the literature. Some published results of shear wave and compression wave velocity measurements performed in the laboratory and in situ by different methods on different types of soils, stabilized with different binders, with strengths up to 5 MPa were added to Fig. 6 (Yesiller et al. 2000; Hird and Chan, 2005; Porbaha et al. 2005; Åhnberg and Holmen 2011). The results from this study, combined with data from the literature, clearly show that nonlinear relations exist between wave propagation velocities and unconfined compressive strength, for strengths in the range of 0 to 20 MPa.

Based on tests performed on specimens of maximum strength approximately 1 MPa, Åhnberg and Holmen (2011) proposed empirical relations (polynomial equations) to estimate q_u from V_s and V_p. Although these correlations were established based on results obtained on soft stabilized soils, when extrapolated to higher strengths, they provide a reasonably good agreement with the data collected in the present study. However, it appears that power law relationships provide a better fit for the stabilized silt and sand specimens having strengths greater than 2 MPa. It is interesting to note that the exponent, very close to 3, is consistent for both compression and shear wave velocities. Nevertheless, the power law relations seem to underestimate the strength in the lower wave velocity range.

Dynamic Moduli and Poisson's Ratio

The seismic compression and shear moduli E_0 and G_0, calculated from Eqs 4 and 5, are plotted versus unconfined compressive strength in Fig. 7(*a*). In the range of strengths tested, both E_0 and G_0 increase linearly with strength. The relation appears to be valid for both soil types.

The ratio of compression modulus E_0 to shear modulus G_0 varies between 2.4 and 4.1 for the treated silt. This ratio is less variable for the stabilized sand specimens between 2.6 and 2.9. Consequently, the Poisson's ratio calculated from Eq 6 is more variable in the silt (Fig. 7(*b*)). It appears to be relatively constant for the sand at approximately 0.22.

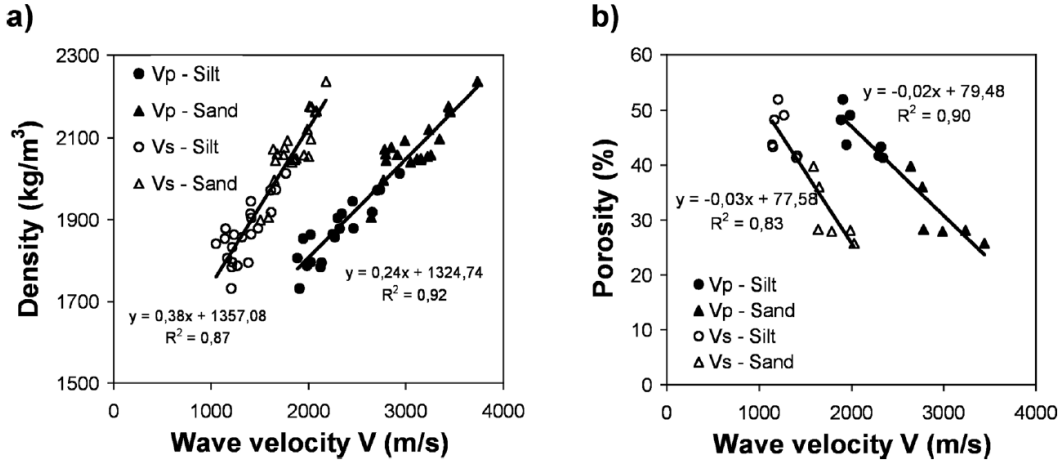

FIG. 8—*(a) Density versus wave velocity, and (b) porosity versus wave velocity at a curing time of 6 months.*

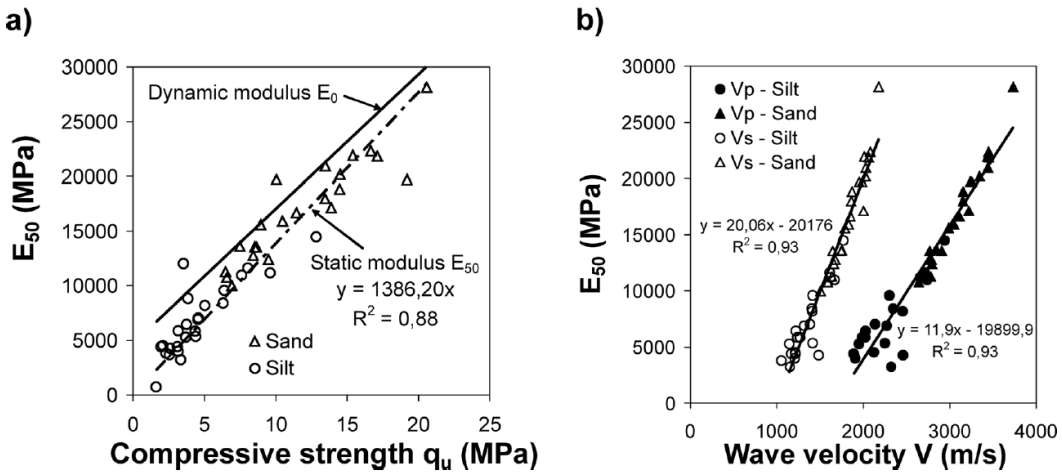

FIG. 9—*(a) Static secant modulus E_{50} versus unconfined compressive strength q_u, and (b) Static secant modulus E_{50} versus wave velocity.*

Correlation With Density and Porosity

The specimens of stabilized silt cored from the block samples of soil mix columns had a density of 1800 to 2000 kg/m^3. The porosities in the silt were between 40 % and 55 %. The density of the sand specimens varied between 2000 and 2300 kg/m^3 with porosities of 25 to 40 %. For both soils tested, P-wave and S-wave velocities increase linearly with density (Fig. 8(*a*)) and decrease with porosity (Fig. 8(*b*)). It is important to note that all specimens were tested after the same curing period of 6 months. Correlations with porosity and density are obviously dependent on curing time.

Relation With Static Deformation Modulus

There are few published studies on correlations between static deformation properties and S-wave and P-wave velocities. The propagation of shear and compression waves occurs along the fastest pathway in the stabilized soil specimen and can therefore be assumed to strongly correlate to static stiffness as these parameters are influenced by similar factors, such as porosity, microstructure, and particle bonding (Larsson 2005). The ratio of static secant modulus E_{50} to unconfined compressive strength q_u for the specimens considered in this study is close to 1400 (Fig. 9(*a*)). This ratio is higher than the majority of the results published in the literature for stiffness calculated based on external strain measurements. Strain measurements between end-platens during unconfined compressive strength tests usually considerably underestimate the stiffness (Goto et al. 1991; Shibuya et al. 1992; Tan et al. 2002). The stiffness calculated here is similar to those reported by Ganne et al. (2010) on soil–cement specimens using similar local strain measurements. The static E_{50} modulus is slightly lower than the seismic modulus E_0 (Fig. 9(*a*)). This can be explained by the nonlinear behavior of soil stiffness with strain (Atkinson 2000). The strains generated by the passage of a shear wave are generally less than 0.001 %. The static E_{50} moduli were calculated for strains of around 0.03 %. Figure 9(*b*) shows that both compression and shear wave velocities correlate linearly with E_{50}. Again, this correlation appears to be valid for both soil types tested although larger scatter is clearly visible in the results for the silt specimens. This scatter can probably be attributed to the presence of inclusions of untreated silt.

Conclusions

In this paper, specimens of silt and sand stabilized in situ by deep soil mixing were submitted to free–free resonance testing in the laboratory. The following conclusions can be drawn:

- The measured resonant frequencies were very repeatable for all specimens tested, validating the use of free–free resonance tests as a rapid testing method for the characterization of fairly heterogeneous stabilized soil specimens.
- The P-wave and S-wave velocities of the stabilized silt specimens generally varied between 1800 and 2500 m/s and between 1000 and 1500 m/s, respectively, for unconfined compressive strengths of 2 to 5 MPa. The specimens of stabilized sand were of higher strength (between 5 and 20 MPa) with P-wave velocities between 2500 and 3500 m/s and S-wave velocities between 1500 and 2000 m/s.
- Both P-wave and S-wave velocities increase nonlinearly with strength. A linear correlation between strength and dynamic stiffness was observed.
- Free–free resonance test results can be correlated with index parameters such as density and porosity but also used for preliminary assessments of static stiffness as all these parameters varied linearly with measured wave velocities.

Acknowledgments

This study was carried out as part of the RUFEX research project which focuses on the reinforcement and re-use of existing railway track and building foundations by deep soil mixing. The installation of the soil–cement columns was performed by Soletanche Bachy. The writers would like to thank Sonia Fanelli and Frank Guirado of IFSTTAR for their help with the laboratory tests.

References

AFNOR, EN13286-41, 2003, "Unbound and Hydraulically Bound Mixtures—Part 41: Test Method for the Determination of the Compressive Strength of Hydraulically Bound Mixtures," La Plaine Saint Denis Cedex, France.

AFNOR, EN13286-43, 2003, "Unbound and Hydraulically Bound Mixtures—Part 43: Test Method for the Determination of the Modulus of Elasticity of Hydraulically Bound Mixtures," La Plaine Saint Denis Cedex, France.

AFNOR, EN14679, 2005, "Execution of Special Geotechnical Works—Deep Mixing," La Plaine Saint Denis Cedex, France.

AFNOR, NFP94-068, 1998, "Soils: Investigation and Testing. Measuring of the Methylene Blue Adsorption Capacity of à Rocky Soil. Determination of the Methylene Blue of a Soil by Means of the Stain Test," La Plaine Saint Denis Cedex, France.

Åhnberg, H. and Holmen, M., 2008, "Laboratory Determination of Small–Strain Moduli in Stabilized Soils," *Deformational Characteristics of Geomaterials*, S. E. Burns, P. W. Mayne, and J. C. Santamaria, Eds., IOS Press, Fairfax, VA, pp. 291–297.

Åhnberg, H. and Holmen, M., 2011, "Assessment of Stabilised Soil Strength With Geophysical Methods," *Proc. Inst. Civ. Eng. Ground Improv.*, Vol. 164, No. 3, pp. 109–116.

Atkinson, J. H., 2000, "Non-Linear Soil Stiffness in Routine Design," *Géotechnique*, Vol. 50, No. 5, pp. 487–508.

Bhadriraju, V., Puppala, A. J., Madhyannapu, R. J., and Williammee, R., 2008, "Laboratory Procedure to Obtain Well-Mixed Soil Binder Samples of Medium Stiff to Stiff Expansive Clayey Soil for Deep Soil Mixing Simulation," *Geotech. Test. J.*, Vol. 31, No. 3, pp. 225–238.

CDIT, Coastal Development Institute of Technology, 2002, *The Deep Mixing Method—Principle, Design and Construction*, A.A. Balkema, Lisse, The Netherlands, p. 123.

CEN, ISO/TS 17892-1, 2005, "Geotechnical Investigation and Testing—Laboratory Testing of Soil—Part 1: Determination of Water Content," European Committee for Standardization, Brussels, Belgium.

CEN, ISO/TS 17892-4, 2005, "Geotechnical Investigation and Testing—Laboratory Testing of Soil—Part 4: Determination of Particle Size Distribution," European Committee for Standardization, Brussels, Belgium.

CEN, ISO/TS 17892-10, 2005, "Geotechnical Investigation and Testing—Part 10: Direct Shear Tests," European Committee for Standardization, Brussels, Belgium.

CEN, ISO/TS 17892-12, 2005, "Geotechnical Investigation and Testing—Laboratory Testing of Soil—Part 12: Determination of Atterberg Limits," European Committee for Standardization, Brussels, Belgium.

Ganne, P., Huybrechts, N., De Cock, F., Lameire, B., and Maertens, J., 2010, "SOIL MIX Walls as Retaining Structures—Critical Analysis of the Material Design Parameters," *Proceedings of the International Geotechnical Conference Geotechnical Challenges in Megacities*, Vol. 3, Moscow, Russia, June 7–10, GRF, pp. 991–998.

Goto, S., Tatsuoka, F., Shibuya, S., Kim, Y. S., and Sato, T., 1991, "A Simple Gauge for Local Small Strain Measurements in the Laboratory," *Soil. Found.*, Vol. 31, No. 1, pp. 169–180.

Guimond-Barrett, A., Mosser, J.-F., Calon, N., Reiffsteck, P., Pantet, A., and Le Kouby, A., 2012, "Deep Mixing for Reinforcement of Railway Platforms with a Spreadable Tool," *Proceedings of the International Symposium on Ground Improvement IS-GI,* Vol. 3, Brussels, Belgium, May 31 and June 1, pp. 169–178.

Hilbrich, S. L. and Scullion, T., 2007, "Rapid Alternative for Laboratory Determination of Resilient Modulus Input Values on Stabilized Materials for AASHTO Mechanistic-Empirical Guide," *Transp. Res. Rec.*, No. 2026, pp. 62–69.

Hird, C. C. and Chan, C. M., 2005, "Correlation of Shear Wave Velocity With Unconfined Compressive Strength of Cement-Stabilised Clay," Proc. Int. Conf. on Deep Mixing Best Practice and Recent Advances, Vol. 1, Stockholm, Sweden, pp. 79–85.

Hoyos, L. R., Puppala, A. J., and Chainuwat, P., 2004, "Dynamic Properties of Chemically Stabilized Sulfate Rich Clay," *J. Geotech. Geoenviron. Eng.*, Vol. 130, No. 2, pp. 153–162.

Larsson, S., 2005, "State of Practice Report—Execution, Monitoring and Quality Control," *Proceedings of the International Conference on Deep Mixing Best Practice and Recent Advances*, Vol. 2, Stockholm, Sweden, pp. 732–786.

Madhyannapu, R., Puppala, A. J., Nazarian, S., and Yuan, D., 2010, "Quality Assessment and Quality Control of Deep Soil Mixing Construction for Stabilizing Expansive Subsoils," *J. Geotech. Geoenviron. Eng.*, Vol. 136, No. 1, pp. 119–128.

Nazarian, S., Yuan, D., and Tandon, V., 1999, "Structural Field Testing of Flexible Pavement Layers With Seismic Methods for Quality Control," *Transp. Res. Rec.*, No. 1654, pp. 50–60.

Porbaha, A., 1998, "State of the Art in Deep Mixing Technology: Part I. Basic Concepts and Overview," *Proc. Inst. Civ. Eng. Ground Improv.*, Vol. 2, No. 2, pp. 81–92.

Porbaha, A., Ghaheri, F., and Puppala, A. J., 2005, "Soil Cement Properties from Borehole Geophysics Correlated With Laboratory Tests," *Proceedings of the International Conference on Deep Mixing Best Practice and Recent Advances*, Vol. 1, Stockholm, Sweden, pp. 605–611.

Puppala, A. J., Kadam, R., Madhyannapu, R., and Hoyos, L., 2006, "Small Strain Shear Moduli of Chemically Stabilized Sulfate Bearing Cohesive Soils," *J. Geotech. Geoenviron. Eng.*, Vol. 132, No. 3, pp. 322–336.

Rabbi A. T. M. Z., Kuwano, J., Deng, J., and Boon, T. W., 2011, "Effect of Curing Stress and Period on the Mechanical Properties of Cement-Mixed Sand," *Soil. Found.*, Vol. 51, No. 4, pp. 651–661.

Ryden, N., Ekdahl, U., and Lindh, P., 2006, "Quality Control of Cement Stabilised Soils Using On-Destructive Seismic Tests," *Advanced Testing of Fresh Cementitious Materials, Lecture 34*, Inst. fur Werkstiffe im Bauwesen Universiteit, Stuttgart, Germany, pp. 1–5.

Shao, Y., Macari, E. J., and Cai, W., 2005, "Compound Deep Soil Mixing Columns for Retaining Structures in Excavations," *J. Geotech. Geoenviron. Eng.*, Vol. 131, No. 11, pp. 1370–1377.

Shibuya, S., Tatsuoka, F., Teachavorasinskun, S., Kong, X. J., Abe, F., Kim, Y-S., and Park, C-S., 1992, "Elastic Deformation Properties of Geomaterials," *Soil. Found.*, Vol. 32, No. 3, pp. 26–46.

Tan, T. S., Goh, T. L., and Yong, K. Y., 2002, "Properties of Singapore Marine Clays Improved by Cement Mixing," *Geotech. Test. J.*, Vol. 25, No. 4, pp. 422–433.

Terashi, M., 1997, "Theme Lecture: Deep Mixing Method—Brief State of the Art," *Proceedings of the 14th ICSMFE*, Hamburg, Germany, September 6–12, pp. 2475–2478.

Toohey, N. M. and Mooney, M. A., 2012, "Seismic Modulus Growth of Lime-Stabilised Soil During Curing," *Géotechnique*, Vol. 62, Issue 2, pp. 161–170.

Yesiller, N., Hanson, J. L., and Usmen, M. A., 2000, "Ultrasonic Assessment of Stabilized Soils," *Report No. 112*, ASCE Geotechnical Special Publication, Reston, VA, pp. 170–181.

Appendix C

Predicted values of q_u for the treated silt and sand-cement mixes calculated for different curing times

Mix	Time (days)	Predicted q_u from 28-day strength (MPa)	$\%q_{u28}$	Predicted q_u from 7-day strength (MPa)	$\%q_{u7}$
AS300W57	7	2.19	8.51	2.02	0.00
	28	4.23	0.00	4.12	-2.63
	90	5.67	16.61	5.65	16.33
	180	6.31	1.69	6.35	2.37
	360	6.81	-9.28	6.90	-8.10
AS200W40	7	2.69	21.11	2.22	0.00
	28	5.59	0.00	5.23	-6.43
	90	7.72	1.19	7.63	0.06
	180	8.70	17.34	8.78	18.42
	360	9.46	-9.22	9.69	-7.05
VSI300W57	7	1.39	76.71	0.79	0.00
	14	2.22	15.59	1.59	-16.83
	28	3.09	0.00	2.63	-14.73
	90	4.40	2.17	4.50	4.44
	180	5.01	-4.70	5.48	4.16
VSI346W50	7	2.48	9.78	2.26	0.00
	14	3.74	-0.12	3.55	-5.21
	28	5.00	0.00	4.89	-2.31
	90	6.82	5.74	6.87	6.55
	180	7.64	-3.53	7.79	-1.68
	360	8.29	1.29	8.51	4.08
VSI248W35	7	3.05	-10.80	3.41	0.00
	14	4.78	7.84	5.15	16.05
	28	6.58	0.00	6.88	4.53
	90	9.25	10.94	9.37	12.43
	180	10.49	-9.46	10.51	-9.29
	360	11.46	-6.31	11.39	-6.88
VSI236W31	7	2.62	-29.39	3.72	0.00
	14	4.37	-13.30	5.42	7.62
	28	6.26	0.00	7.08	13.08
	90	9.20	10.02	9.42	12.63
	180	10.61	-10.52	10.47	-11.70
	360	11.73	-9.56	11.28	-13.05

Table C-1 Predicted values of q_u for the silt-cement mixes calculated for different curing times.

Mix	Time (days)	Predicted q_u from 28-day strength (MPa)	$\%q_{u28}$	Predicted q_u from 7-day strength (MPa)	$\%q_{u7}$
FS200W20	7	1.40	6.08	1.32	0.00
	28	3.10	0.00	3.00	-3.34
	90	4.42	-0.64	4.32	-2.89
	180	5.04	0.88	4.95	-1.01
	360	5.53	-0.27	5.44	-1.85
FS200W20B50	7	2.82	-8.91	3.09	0.00
	28	4.20	0.00	4.39	4.43
	90	5.01	4.07	5.12	6.31
	180	5.35	-8.00	5.42	-7.42
	360	5.60	-4.34	5.65	-3.64
FS200W35B50	7	1.54	4.15	1.48	0.00
	28	2.41	0.00	2.37	-2.04
	90	2.95	2.55	2.91	1.35
	180	3.17	2.77	3.14	1.89
	360	3.34	0.07	3.32	-0.55
FS-I-200W20	7	2.76	-1.73	2.81	0.00
	28	3.37	0.00	3.38	0.25
	90	3.69	7.16	3.67	6.71
	180	3.81	-4.12	3.78	-4.75
FS-I-200W15	7	3.54	6.46	3.32	0.00
	28	4.41	0.00	4.29	-2.72
	90	4.86	-0.90	4.80	-2.10
	180	5.04	-4.12	5.00	-4.73
VSA346W29	7	/	/	2.46	0.00
	28	/	/	3.75	-0.09
VSA249W17	7	/	/	4.02	0.00
	28	/	/	6.87	-0.20
VSA230W14	7	/	/	5.76	0.00
	28	/	/	8.18	-0.04

Table C-2 Predicted values of q_u for the sand-cement mixes calculated for different curing times.

Reference	Soil type	Cement type	Cement content	Water content	Max curing time (days)	s_7	R^2
Szymkiewicz (2011)	Argile du Puy	CEM III	26.7%	70%	90	1.11	0.73
			17.5%	70%	90	1.62	0.96
			11.5%	70%	90	2.51	0.92
			33.5%	80%	90	1.47	0.98
			17.5%	80%	90	2.21	0.93
Horpibulsuk et al. (2003)	Bangkok clay	Portland cement	20%	80%	170	1.24	0.95
			15%	80%	170	1.21	0.89
			12.5%	80%	170	1.01	0.82
			10%	80%	170	1.20	0.95
			7.5%	80%	170	0.69	0.95
	Ariake clay	Portland cement	20%	106%	180	0.95	0.98
			20%	130%	120	1.05	1.00
			20%	160%	180	1.18	0.97
			15%	130%	180	1.03	0.99
			15%	160%	180	1.08	0.99
			10%	106%	180	1.09	0.99
			10%	130%	180	1.03	0.99
	Bangna Bangpakong clay	Portland cement	17.2%	99.5%	28	1.00	1.00
			20.7%	99.5%	28	0.75	1.00
			27.6%	99.5%	28	0.85	1.00
			34.5%	99.5%	28	1.22	1.00
Lorenzo et al. (2004)	Bangkok clay	Portland cement	10%	100%	28	0.95	1.00
			10%	130%	28	1.45	0.97
			10%	160%	28	1.35	0.84
Chew et al. (2004)	Singapore marine clay	Portland cement	5%	120%	28	1.55	1.00
			10%	120%	28	1.56	1.00
			20%	120%	28	1.35	1.00
			30%	120%	28	1.23	1.00
			40%	120%	28	1.35	1.00
			50%	120%	28	0.86	1.00

Table C-3 Values of the empirical parameter s7 for soil-cement mixes from the literature.

Appendix D

Predicted values of E_0 for the treated silt and sand-cement mixes calculated for different curing times

Mix	Time (days)	Predicted E_0 from 28-day stiffness (MPa)	$\%E_{28}$	Predicted E_0 from 7-day stiffness (MPa)	$\%E_7$
AS300W57	7	5719.85	3.86	5507.00	0.00
	28	6986.23	0.00	6931.11	-0.79
	90	7632.28	1.82	7673.19	2.37
	180	7885.78	-3.07	7966.99	-2.07
	360	8070.09	-0.04	8181.51	1.34
AS200W40	7	6715.54	2.30	6564.54	0.00
	28	8039.96	0.00	7938.17	-1.27
	90	8706.11	5.61	8633.98	4.73
	180	8965.93	-0.27	8906.18	-0.93
	360	9154.31	-1.36	9103.82	-1.90
VSI300W57	7	4820.08	5.70	4560.05	0.00
	14	5547.67	1.16	5404.39	-1.45
	28	6127.52	0.00	6094.17	-0.54
	90	6813.63	-0.78	6928.05	0.89
	180	7086.08	-2.20	7264.18	0.26
VSI346W50	7	5215.87	-8.49	5700.01	0.00
	14	6217.96	-4.79	6579.68	0.75
	28	7040.69	0.00	7282.46	3.43
	90	8039.55	-2.20	8115.81	-1.27
	180	8443.39	-0.55	8447.23	-0.50
	360	8741.13	-0.06	8689.72	-0.65
VSI248W35	7	6527.63	-4.52	6836.88	0.00
	14	7691.11	2.71	7915.15	5.70
	28	8636.90	0.00	8778.73	1.64
	90	9775.39	-2.79	9804.96	-2.50
	180	10232.93	-2.71	10213.71	-2.90
	360	10569.33	-5.82	10512.98	-6.32
VSI236W31	7	6694.67	-11.42	7557.66	0.00
	14	8074.92	-4.53	8775.27	3.75
	28	9219.41	0.00	9752.87	5.79
	90	10620.90	-0.02	10917.09	2.77
	180	11190.90	-5.49	11381.49	-3.89
	360	11612.33	-0.93	11721.75	0.00

Table D-1 Predicted values of E_0 for the silt-cement mixes calculated for different curing times.

Mix	Time (days)	Predicted E_0 from 28-day strength (MPa)	$\%E_{28}$	Predicted E_0 from 7-day strength (MPa)	$\%E_7$
FS200W20	7	8058.22	12.75	7147.03	0.00
	28	12637.81	0.00	12264.36	-2.96
	90	15420.46	-3.26	15572.39	-2.31
	180	16596.81	-0.37	17008.59	2.10
	360	17482.39	0.09	18103.37	3.65
FS200W20B50	7	10863.86	-5.80	11532.69	0.00
	28	13269.15	0.00	13332.25	0.48
	90	14496.21	6.71	14215.15	4.64
	180	14977.68	-2.21	14555.91	-4.97
	360	15327.75	1.66	14801.77	-1.83
FS200W35B50	7	8264.68	-0.81	8332.55	0.00
	28	9994.06	0.00	9975.88	-0.18
	90	10870.08	0.04	10802.43	-0.58
	180	11212.78	1.06	11124.80	0.27
	360	11461.60	3.34	11358.55	2.41
FS-I-200W20	7	11932.05	-3.54	12369.42	0.00
	28	13453.35	0.00	13466.80	0.10
	90	14186.57	0.90	13982.64	-0.55
	180	14467.43	2.80	14178.16	0.75
FS-I-200W15	7	11958.58	-3.73	12421.65	0.00
	28	14033.52	0.00	13935.52	-0.70
	90	15062.45	0.42	14662.56	-2.24
	180	15461.36	2.76	14940.63	-0.70
VSA346W29	7	/	/	16940.48	0.00
	28	/	/	19979.49	-0.26
VSA249W17	7	/	/	14604.57	0.00
	28	/	/	18017.34	0.17
VSA230W14	7	/	/	16940.48	0.00
	28	/	/	19979.49	-0.24

Table D-2 Predicted values of E0 for the sand-cement mixes calculated for different curing times.

Appendix E

X-ray diffraction analyses

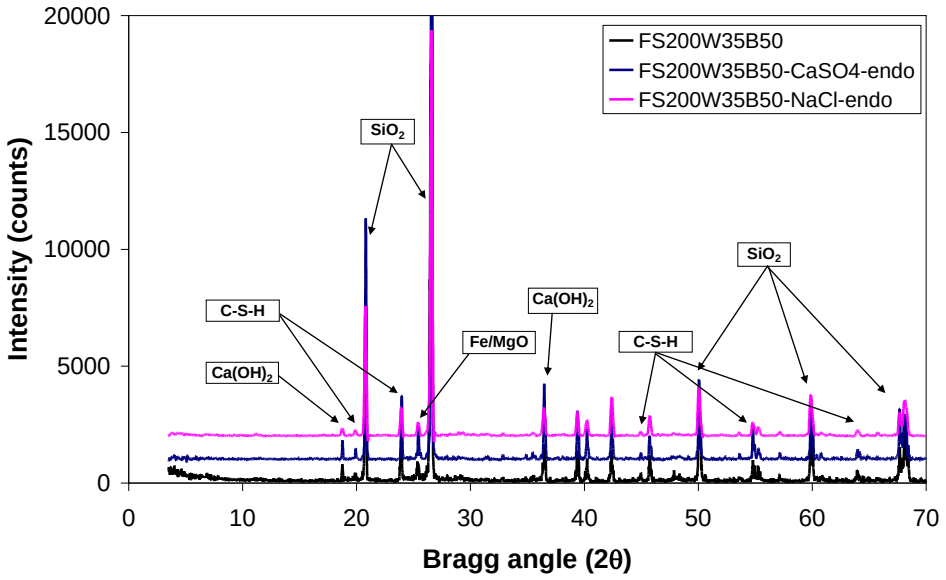

Figure E-1 Effect of CaSO4 and NaCl on X-ray diffraction patterns of Fontainebleau sand-CEM III cement mixes.

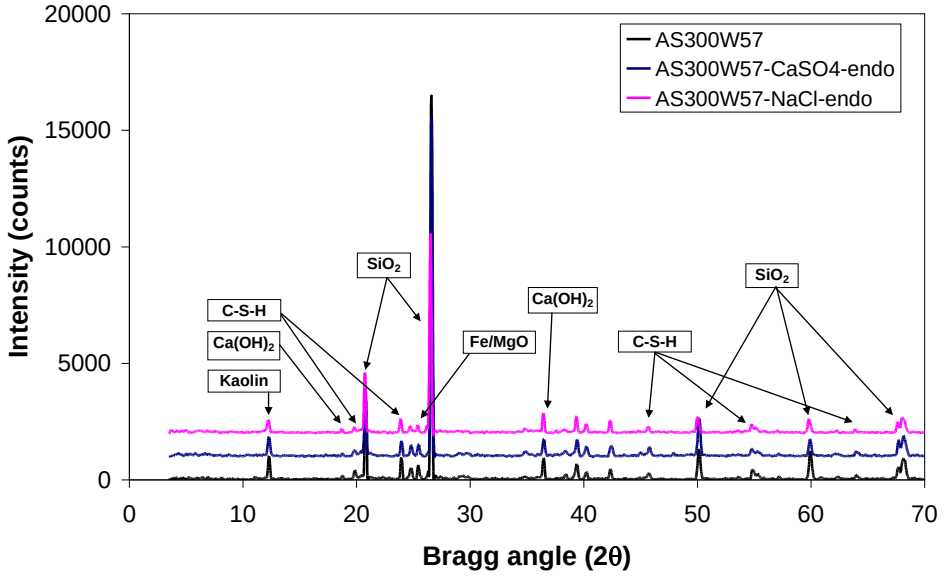

Figure E-2 Effect of CaSO4 and NaCl on X-ray diffraction patterns of artificial silt-CEM III cement mixes.